Cell fate commitment during nervous system establishment: from stem cells to neurons

Author: Eleni Chrysostomou

Supervisor: Prof Uri Frank

Centre for Chromosome Biology,

Discipline of Biochemistry,

School of Natural Sciences,

National University of Ireland Galway

Thesis submission: March 2020

A thesis submitted in partial fulfilment of the requirements of National University of Ireland, Galway for the degree of Doctor of Philosophy

Table of contents

Acknowledgements

First of all, THANK YOU URI! Thank you for all the patience, support and your amazing mentorship. Thank you for encouraging me to keep going during the dark days when I was frustrated, crying in your office, and angry with failed experiments. Thank you for being there guiding me through this amazing journey. I couldn't have asked for a better mentor.

Cheers and a huge thank you to the amazing people I met in the lab. I can't imagine what this journey would be without you guys. Thank you, Tim, Hakima, James, Emma, Liam, Brian, Feb, Anna, Seb, Kate and all past and current members in Uri's lab Miguel, Aine and Helen.

Of course, I could not have done this without your support mom. You 've always been there supporting me and believing in me, even in times I didn't believe in myself. Τα καταφέραμε μάμι μου!

I would also like to thank the CCB crew and the members of my GRC committee for their constructive input all these years, and all the brilliant collaborators I had the pleasure working with. Special thanks to Dr Shirley Hanley and the Flow Cytometry core facility, and to Dr Kerry Thompson and the Centre for Microscopy and Imaging for their invaluable contribution and guidance.

Que sera sera…

List of abbreviations

APS: Ammonium Persulfate

ASW: Artificial Sea Water

BSA: Bovine Serum Albumin

DEPC: Diethyl Pyrocarbonate

DPF: Days Post Fertilisation

EDTA: Ethylenediaminetetraacetic Acid

EdU: 5-Ethynyl-2'Deoxyuridine

ESCs: Embryonic Stem Cells

FACS: Fluorescence-Activated Cell Sorting

FC: Flow Cytometry

FISH: Fluorescence *In Situ* Hybridisation

HPD: Hours Post Decapitation

HPF: Hours Post Fertilisation

IF: Immunofluorescence

IFC: Imaging Flow Cytometry

ISH: *In Situ* Hybridisation

LB: Lysogeny Broth

MOPS: 3-(N-morpholino) Propanesulfonic Acid

NPCs: Neural Progenitor Cells

ON: Overnight

PBS: Phosphate Buffered Saline

PBSTx: Phosphate Buffered Saline with 0.3% Triton X-100

PCR: Polymerase Chain Reaction

PFA: Paraformaldehyde

PTW: Phosphate Buffered Saline with 0.1% Tween20

RT: Room Temperature

SABER FISH: Signal Amplification By Exchange Reaction Fluorescence *In Situ* Hybridisation

SDS: Sodium Dodecyl Sulfate

SDS-PAGE: Sodium Dodecyl Sulfate Polyacrylamide Gel Electrophoresis

SSC: Saline Sodium Citrate

TBS: Tris-Buffered Saline

TBST: Tris-Buffered Saline with 0.05% Triton X-100

TEA: Triethylamine

TF: Transcription Factor

Abstract

Members of the early-branching metazoan phylum of Cnidaria are well-recognized as a sister group to bilaterians making them an ideal candidate to study the evolution of the eumetazoan nervous system. I began to unravel the neurogenesis transcriptional network in *Hydractinia* by generating transgenic reporter animals expressing fluorescent proteins under the control of neurogenesis-related genes, and a *Piwi1* reporter line that marks stem cells. By generating these lines, I was able to trace neuronal cells and their precursors to study their fate in regeneration. Tracing of individual differentiated neurons showed that the injured nervous system is re-established by *de novo* neurogenesis rather than by migration/proliferation of existing neurons. Using *Piwi1, SoxB2* and *Rfamide* reporter lines, I was able to apply fluorescence-activated cell sorting (FACS) to sort cells along the neurogenesis pathway for subsequent RNA sequencing. In addition, these lines where further analyzed using imaging flow cytometry by focusing on the level of the transgene expression and morphology of the cells. Working with our animal model, is a novel opportunity to shed light on neural lineage specification markers as well as understanding how commitment of cells to a certain lineage is established.

In addition, the role of SoxB genes during embryonic development seems to be more complex than originally thought. *SoxB1* knockdown affected many lineages as it is expressed in stem cells, whereas *SoxB2* knockdown affected specifically the neuronal lineage as it is expressed in neural progenitor cells with a preference to distinct neuronal subtypes. Along with over-expression studies, *SoxB1* seems to act in a similar manner with the mammalian *Sox2* as it is required for cells to remain in a pluripotent state. These data provide an insight into a potentially conserved role of SoxB genes between bilaterians and cnidarians.

Declaration

This thesis has not been submitted in whole, or in part, to this or any other University for any other degree and is, except where otherwise stated, the original work of the author.

This study was funded by an SFI Principal Investigator award (grant number 11/PI/1020), by a Wellcome Trust Investigator award (grant number 210711/Z/18/Z), and by CURAM – SFI Centre for Research in Medical Devices, awarded to my supervisor.

Signed: _____

Eleni Chrysostomou, March 2020

Chapter 1: Introduction

1.1 The Phylum Cnidaria

1.2 Main cnidarian model systems

1.3 *Hydractinia* as an animal model

1.4 Life cycle

1.5 Body plan and cellular composition

1.6 Evolution of the nervous system

1.7 SoxB family of transcription factors

1.8 Evolution of animal regeneration

1.9 Project aims

1.1 The Phylum Cnidaria

The early-branching metazoan phylum, Cnidaria, is a well-supported sister group to bilaterians and comprised by the commonly known sea anemones, reef-forming and soft corals, jellyfish, the freshwater *Hydra*, and marine hydroids (Figure 1.1). This diverse group is the oldest eumetazoan phylum and contains over ≈11,000 described species, predominantly living in marine environments and along with the phyla Ctenophora, Placozoa, and Porifera, are considered as the early diverging/basal animals (Hejnol *et al.*, 2009; Pick *et al.,* 2010; Zapata *et al.*, 2015).

The phylum Cnidaria is divided into two major clades: Medusozoa and Anthozoa (Bridge *et al*., 1995). The Anthozoa contains the Hexacoralia (e.g. sea anemones and stony corals) and Octocoralia (e.g. soft corals, gorgonians, sea pens) clades. The Medusozoa clade is much more diverse. It is divided into four subgroups, including some ≈3,700 described species: Hydrozoa (hydromedusae, hydroids, siphonophores), Cubozoa (box jellies), Scyphozoa (true jellyfish) and Staurozoa (stalked jellyfish) (Cartwright *et al*., 2007; Daly *et al*., 2007; Zapata *et al.,* 2015).

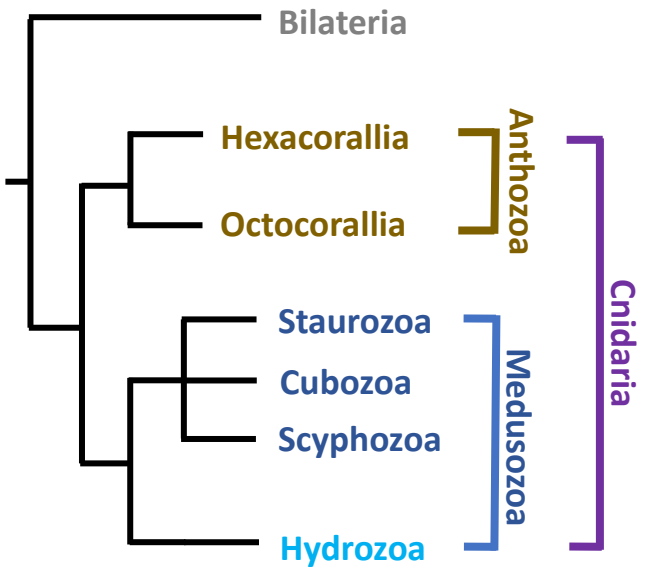

Figure 1.1. Simplified phylogenetic relations between the cnidarian sub-clades and Bilateria.

All cnidarians are diploblastic organisms; they develop from only two embryonic germ layers, ectoderm and endoderm, and lack a mesoderm. Postembryonic cnidarians have a body wall consisting of two epithelial layers, an outer epidermis and inner gastrodermis, separated by an extracellular matrix known as mesoglea (Salvini-Plawen, 1978). The adult epithelial layers

are not direct descendants of the two embryonic germ layers, at least in some cnidarians (Gahan *et al*., 2016; Steinmetz *et al*., 2017). The body plans of cnidarians are diverse, as well as their life cycles and morphologies. Cnidarians are often characterized as "simple" animals due to presumed simplicity based on lack of knowledge of their biology. Cnidarians are morphologically simpler than most bilaterians, but their complexity is probably underestimated. They are described as having radial symmetry but only a subset of the phylum's species exhibits this trait. Depending on the clade or individual species within the phylum, some have bilateral symmetry or directional asymmetry (Hyman, 1940; Manuel, 2009).

Despite their body plan differences, cnidarians have a single opening on one side of the animal which acts both as mouth and anus and generally is surrounded by tentacles bearing nematocytes (Technau and Steele, 2011). Members of the Cnidaria exhibit a variety of cell types found in all animals such as epithelial cells, sensory and ganglionic nerve cells, gland cells, and muscle cells. The shared characteristic of all cnidarians is the presence of a phylum-defining intracellular structure called the cnidae with the most diverse and universal cnidae being the nematocysts (also called stinging structures). Nematocysts are extrusive organelles mostly used for predation and defense, as well as for adhesion, by excreting a mixture of toxic substances located in the nematocyst capsules (Holstein, 1981; Tardent and Holstein, 1982).

Cnidarian species display two main life cycle patterns and considerable variation is present within these modes. Most cnidarians are capable of sexual reproduction and, in some cases, they can also asexually reproduce through budding and/or colony formation (Collins, 2002). The life cycle of medusozoans is rather complex as they can reproduce both sexually and asexually by an alternation between an asexual polyp and a free-living sexual medusa stage although variations with this rule are common. Anthozoans' reproduction is also sexual and asexual, but they lack a medusa stage altogether (Technau and Steele, 2011). The medusa stage is believed to have been lost and gained multiple times in different lineages of Medusozoa and for that reason certain medusozoans do not exhibit the medusa stage, like *Hydractinia.* In this case, the medusa stage is reduced and remains attached to the polyp, serving as gonads (Plickert *et al*., 2012).

1.2 Main cnidarian model systems

Cnidarians have been utilized for many decades now to study key aspects in evolutionary biology, from nervous system evolution to the formation of germ layers, to symbiosis.

Well-studied cnidarians including species from both the Anthozoa and Hydrozoa clades, such as *Nematostella vectensis* and *Acropora* spp., and *Hydra* spp. and *Hydractinia* spp., respectively. *N. vectensis*, one of the most commonly used cnidarian models, is the first member of its phylum whose genome has been sequenced (Putnam *et al*., 2007). It exhibits a typical anthozoan life cycle – from embryo to larva to adult polyps (Fritzenwanker and Technau, 2002). Due to its ease of maintenance and culture, and the great experimental accessibility, *N. vectensis* has been greatly utilised as a developmental model system (Genikhovich and Technau, 2009). On the other hand, *Acropora* – a major contributor to the Australian Great Barrier Reef – can provide insights into the diversification within the anthozoan clade, and is useful for the study of the formation of calcified skeletons and intracellular symbiosis; both being essential for the formation of coral reefs (Shinzato *et al*., 2011; Ball *et al*., 2002).

Within the hydrozoan clade, the freshwater polyp *Hydra* has been the major player for centuries, and classical studies regarding asexual budding, regeneration and tissue grafting experiments have been first described by the Swiss scholar Trembley back in the 1700s (Trembley, 1744; Glauber *et al*., 2010). *Hydra* can reproduce both asexually by budding of new polyps, and sexually by shedding gametes. Its polyps are dioecious (separate sexes) or hermaphroditic depending on the species and/or strains which makes it an excellent candidate to study embryogenesis and gametogenesis (Miller *et al*., 2000; Technau *et al*., 2003). For many years, transgenesis was not feasible in this animal or indeed in any other cnidarian; a lack that impeded the understanding of biological mechanisms and processes. After long-term efforts, the first stable transgenic reporter line was reporter in 2006 (Wittlieb *et al*., 2006) and since then many studies have been published describing the tracking of cell fate, manipulation of genes by overexpression/knockdown, as well as sorting of cells for downstream applications (Juliano *et al*., 2014; Khalturin*, et al*., 2007; Siebert *et al*., 2008; Hemmrich *et al*., 2012; Nishimiya-Fujisawa and Kobayashi, 2012).

Both *Hydractinia* species – *Hydractinia echinata* and *Hydractinia symbiolongicarpus* – have been established models for versatile applications such as developmental biology, allorecognition, reproduction and environmental studies for over a century. As a typical hydrozoan representative, *Hydractinia* – like *Hydra* – offers a unique opportunity to study

neurogenesis, axial patterning, regeneration, and stem cell biology (Frank *et al*., 2001). A more detailed description of *Hydractinia* as an animal model follows in the next section (section 1.3).

1.3 *Hydractinia* as a model organism

Hydractinia, a colonial marine hydroid can be described as a great representative of the Cnidaria phylum and an excellent animal model to study cell and developmental biology, as its utility let to the assembly of the very first concepts and terms in biology, including the characterisation of stem and germ cells (Weismann, 1883).

More than 30 *Hydractinia* species have been described to date with two North Atlantic ones – the European *Hydractinia echinata* and the American *H. Symbiolongicarpus* – being intensively utilised to study allorecognition, stem cells, and developmental biology (Frank *et al*., 2001). The closely related species *Podocoryna carnea* (previously known as *Hydractinia carnea*) has been of special interest as its life cycle includes a medusa stage. *Podocoryna* is also used as an animal model for regeneration studies through trans- and de-differentiation (Schuchert, 2011).

In its nature habitat, *Hydractinia* inhabits the shells of hermit crabs with each adult colony having four main types of polyps: feeding (gastrozooids) and sexual (gonozooids) polyps, and the less frequent ones dactylozooids and tentaculozooids (Frank *et al*., 2001). In *Hydractinia* colonies, the sexes are always separated and genetically determined (Nicotra M., unpublished data).

What makes *Hydractinia* an attractive model for studying fundamental questions in the field of evolutionary and developmental biology is its easy culture in laboratory settings and broad technique toolbox currently available. It is cultivable in the lab and all the life stages are accessible for manipulation: from zygote to adult feeding and sexual polyps (Plickert *et al*., 2012). Since the generation of stable transgenic lines is feasible (Künzel *et al*., 2010), cell-fate studies can provide insights into how cells commit to certain lineages as well as their fate in both embryogenesis and regeneration contexts (Bradshaw *et al*., 2015). In addition, molecular tools are available for other mis-expression studies including RNA interference (Millane *et al*., 2011; Flici *et al.,* 2017), short-hairpin RNA interference (DuBuc *et al*., 2020; this thesis), morpholino injections (Kanska and Frank, 2013), mRNA and plasmid injections for over- and ectopic expression studies (Duffy *et al*., 2010). CRISPR/Cas9-mediated mutagenesis protocols are also available for this animal model (Gahan *et al*., 2017; Sanders *et al*., 2018). Flow cytometric analysis has been recently made available along with sorting of distinct cell populations in order to start understanding the transcriptional regulatory network of certain cell lineages (DuBuc *et al*., 2020; this thesis).

In addition to *Hydractinia'*s many technical benefits, this animal model also offers an advantage as a model system from a biological point of view. It can be used in comparative studies as its genome encodes more homologous to vertebrate genes than other classical animal models such as *C. elegans* and *Drosophila* (Kortschak et al., 2001; Soza-Ried et al., 2010; Technau and Steele, 2011), indicating a conserved gene inventory of all major signaling pathways used in animal developmental control.

Moreover, *Hydractinia,* as a clonal animal, does not sequester a germ line during embryogenesis (DuBuc *et al*., 2020). Instead, adult stem cells contribute to both somatic tissues and gametes continuously. This property makes this animal an attractive model system to study germ cell specification and the evolution of bilaterian sequestered germ lines. Also, the fact that *Hydractinia*, like all cnidarians, are diploplastic animals meaning that they have only endoderm and ectoderm, makes is an ideal candidate to study the evolution of mesoderm layer evolutionary origin.

These few examples showcase the value of *Hydractinia* as an excellent animal model to study evolutionary and developmental biology.

1.4 Life cycle

Hydrozoan cnidarians have a complex life cycle with two dominant life stages: polyp and medusa. In *Hydractinia,* the medusa stage is rudimentary reduced to sessile gonophores. The sexes are separated and both sexes release gametes daily into the water in a light-induced spawning act (Kraus *et al.,* 2014). Following fertilization, the zygotes develop within 2-3 days into a planula larva that can be induced to metamorphoses to primary polyps – this process usually takes one day. Primary polyps are the founders of new colonies and secondary polyps are then generated by budding from interconnected stolons (gastrovascular tubes) (Fig. 1.2A), and within 2-3 months, the colony will be sexually mature and ready to spawn. Each colony is either female or male – both sexes are not present within the same colony (Fig. 1.2B-D). The stolonal tissue, covered by a chitinous periderm, is responsible for the distribution and exchange of nutrients and cells between polyps of the same colony as well as for defense purposes in order to avoid fusion of two colonies that do not share the same allorecognition alleles through active rejection – a process that resembles tissue rejection in organ transplantation (Shenk, 1991; Powell *et al*., 2007; Nicotra *et al*., 2009).

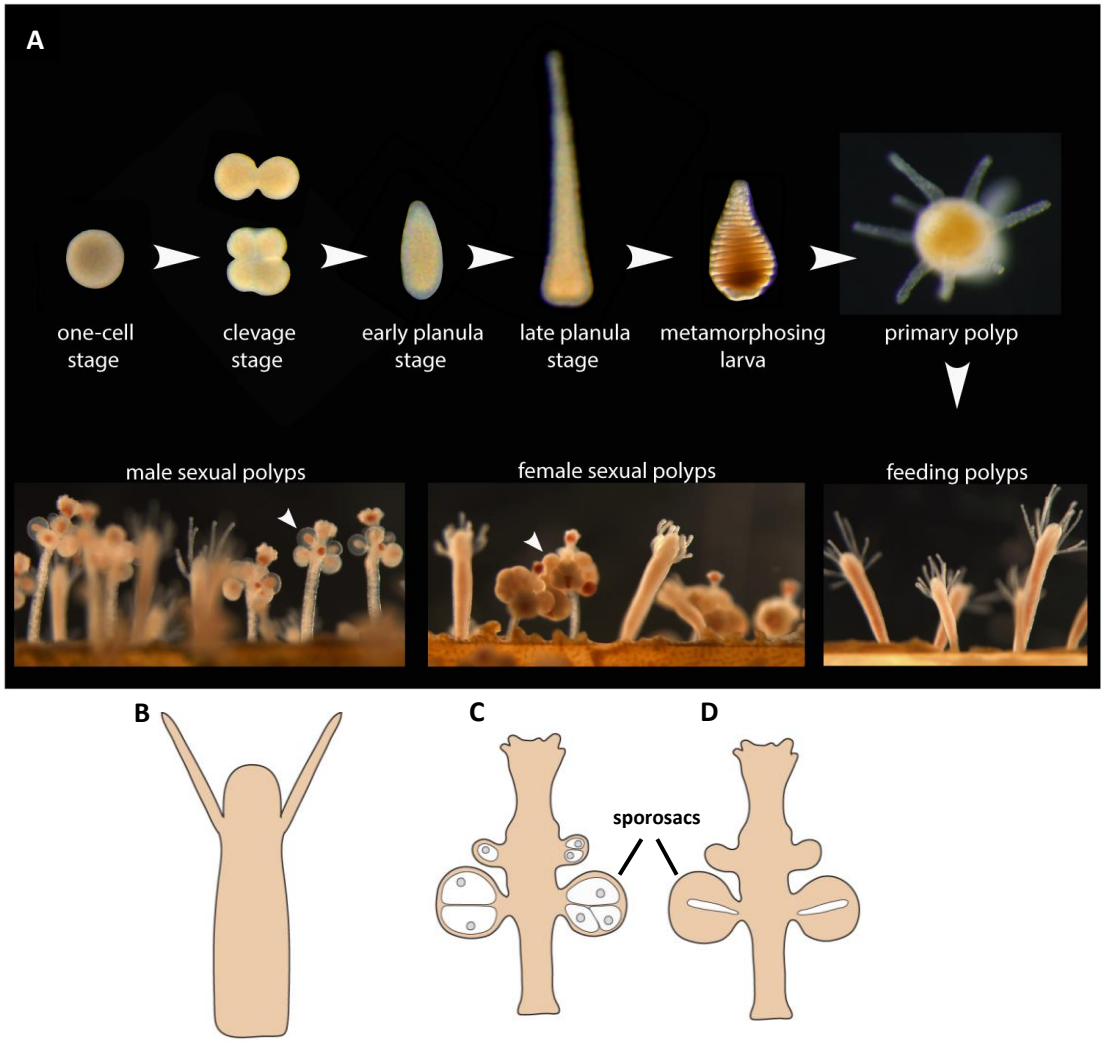

Figure 1.2. (A) Life cycle of *Hydractinia* and morphology of the (B) feeling polyp, (C) female sexual polyp, and (D) male sexual polyp. Hydractinia reproduces clonally and sexually daily. Sexual reproduction involves many stages beginning with multiple cleavage stages followed by the establishment of fully developed larva. Upon metamorphosis induction, the larva will rearrange its body plan resulting into a primary polyp. Within a few months, this primary polyp will asexually reproduce to generate a sexually mature colony, including either female or male sexual polyps.

One of the most intriguing features of nearly all cnidarians is the ability to metamorphose. Metamorphosis derives from the Greek word μεταμόρφωσις (metamórphosis) which describes the transition from one morphe (μορφή) to another, in this case, from larval to adult tissue. During this process, the planula larvae, upon the receival of appropriate internal and external stimulation, can completely re-arrange its tissue architecture and give rise to a different structure from the original one, the primary polyp. It has been previously described that this process is depended on the presence of bacteria which provide the external signals required (Müller, 1973; Müller *et al*., 1976). This bacterial inducer stimulates GLWamide^{+} sensory neurons located at the aboral end of the larva and causes the activation of a signal transduction cascade and ultimately the release of the neuropeptide GLWamide. This neuropeptide diffuses posteriorly and acts as a hormone and triggers and synchronises metamorphosis in the entire larva by acting as the internal signal (Schmich *et al*., 1998; Leitz, 1998).

It has been well documented by Seipp and colleagues (2001; 2010) that apoptosis has a fundamental role during the process of metamorphosis by eliminating cells that are no longer needed (larval posterior end and anterior cap) before reaching a distinct turning point which is followed by a subsequent development of adult features. Distinct neuronal subtypes, such as GLWamide- and RFamide- expressing neurons, are subject to apoptosis during metamorphosis and hence, a *de novo* establishment of the adult nervous system is required by proliferation and commitment of stem cells to the neural lineage.

1.5 Body plan and cellular composition

The body plan of *Hydractinia* is rather simple. The adult polyp is composed of two myoepithelial layers – gastrodermis and epidermis – with several other cell types positioned in the interstitial spaces. These include stem cells, neurons, nematocytes, and gland cells (Figure 1.3) (Plickert *et al*., 2012). Even though the nervous system of *Hydractinia* has been considered relatively simple for many years, recent evidence including the study by Flici and colleagues (2017) and this thesis, suggest a much more anatomically complex system. A detailed description of the structure and composition of the nervous system follows in the section 1.6.

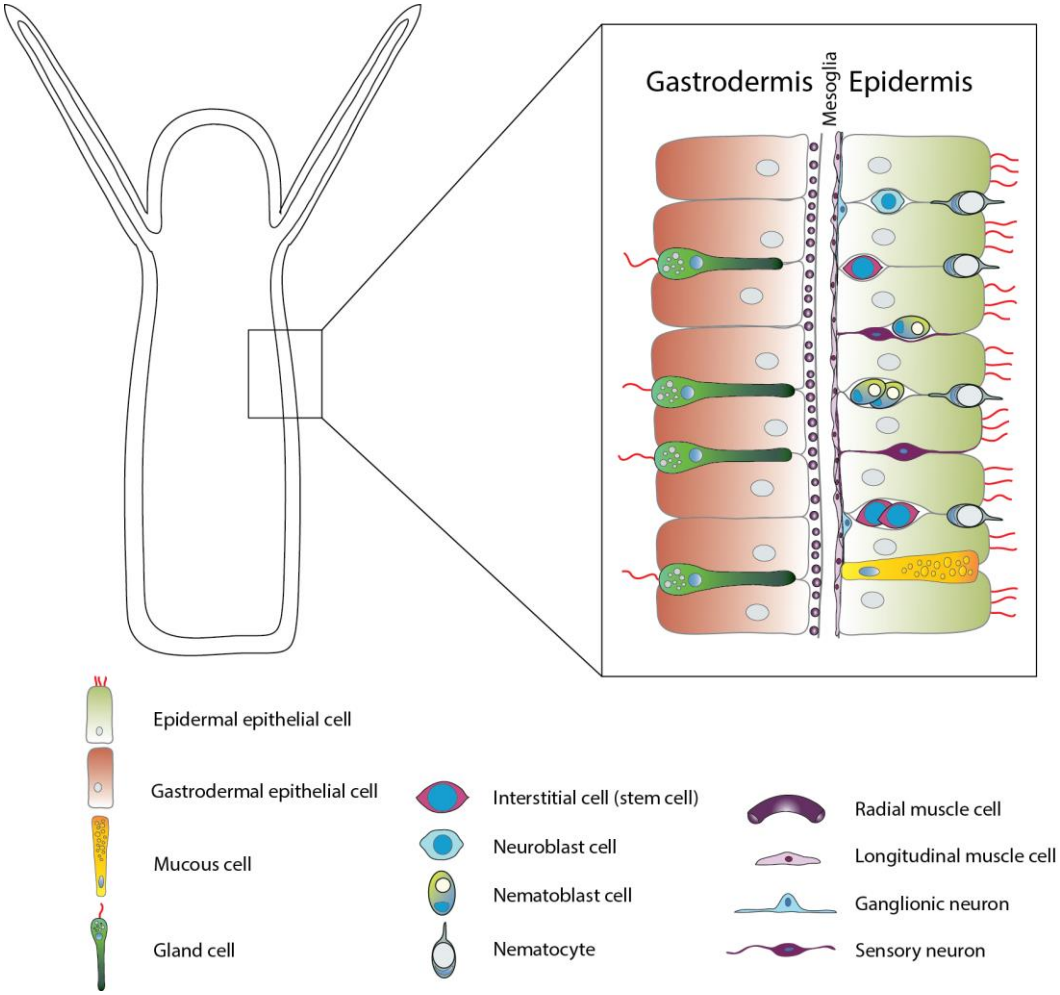

Figure 1.3. Schematic representation of *Hydractinia* body plan in the adult stage. Polyps are composed by two epithelial layers separated by an extracellular matrix-like layer, named mesoglea. In the epidermal layer, proliferative cells such as stem cells (i-cells), nematoblasts and neuroblasts are located in the interstitial spaces. In this layer, other cell types are found such as neuronal cells, nematocytes and mucous cells. In the gastrodermal layer, gland cells are found as well as muscle cells.

One of the main characteristic features of hydrozoans is the presence of a population of stem cells residing primarily in the interstitial spaces (interstitial cells; i-cells) of the epidermal epithelial layer. As a population, i-cells remain pluripotent throughout the organism's life and constantly express genes whose bilaterian homologues are well known for their involvement in both stem and germ cell biology (Bradshaw *et al*., 2015; Plickert *et al*., 2012; Frank *et al*., 2009; Gahan *et al*., 2016). Up until now, there has been no clear distinction between stem and germ cells as classic markers for either population, like *Vasa*, *Nanos1* and *Pl10*, are expressed in both subsets (Künzel *et al*., 2010). Recently, DuBuc *et al*. (2020) demonstrated that transcription factor AP2 acts as a molecular switch to commit adult stem cells (i-cells) to the germ cell fate.

So far, i-cells have only been found in hydrozoans and *Hydra* and *Hydractinia* are the two genera in which most investigations have been made (Bode, 1996; Bosch *et al*., 2010; David, 2012; Weismann, 1883; Müller *et al*., 2004; Künzel *et al*., 2010; Millane *et al*., 2011; Bradshaw *et al*., 2015). In the adult *Hydra* polyp, there are three distinct cell lineages responsible for its homeostatic maintenance - epidermal epithelial, gastrodermal epithelial, and interstitial lineage. The two epithelial lineages, although not classical stem cells, being already differentiated epithelia-muscle cells, preserve the self-renewal capacity and can be described as mitotic unipotent stem cells (David, 2012). On the other hand, the interstitial stem cell lineage contains continuously proliferative multipotent stem cells, which provide an inexhaustible source for the replacement of all other cell types, including germ cells (David and Murphy, 1977; Bosch and David, 1987, Bode *et al*., 1987; Nishimiya-Fujisawa and Kobayashi, 2012).

In *Hydractinia*, by contrast, epithelial cells do proliferate but are probably derived at least partly from i-cells that also give rise to all other somatic cells and germ cells (Duffy *et al*., 2010; Müller *et al*., 2004). During embryogenesis, i-cells first arise in the gastrodermis and upon metamorphosis they migrate to the epidermis (Emma McMahon, 2018). In the adult polyp, they are found in a band-like zone in the lower half of the body column primarily in the epidermis and upon wound healing or head regeneration they are able to migrate to the injury site and form a blastema in order to re-establish the missing tissue. On the other hand, i-cells in stolonal tissue are more ubiquitously distributed (Bradshaw *et al*., 2015). *Hydractinia* i-cells express a variety of markers depending on the sub-population in question. For instance, genes like Piwi and Vasa (Bradshaw *et al*., 2015; Rebscher *et al*., 2008) are expressed in i-cells responsible for self-renewal and stem cell maintenance whereas *Nanos2*

is implicated in the neural lineage commitment (Kanska and Frank, 2013). However, since several i-cell-defined genes are expressed by multiple distinct sub-populations, comparable to the planarian neoblasts (Van Wolfswinkel *et al*., 2014; Adler and Sanchez Alvarado, 2015), the need for more definitive molecular markers for various i-cell subsets are highly needed as well as markers for populations further down the commitment path to start understanding how the stem cells in *Hydractinia* behave and define multiple lineages.

1.6 Evolution of the nervous system

Even though many aspects regarding the development of the nervous system have been intensively studied in the past decades, its evolutionary origins are still not well understood. Restricted phylogenetic representation and studies based mostly on standard model organisms contributed to the lack of a viable theory regarding the ancestral development of the nervous system.

The positioning of Cnidarians as a sister group to Bilateria makes them an ideal candidate to study the evolution of eumetazoan nervous system and to reconstruct the cnidarian/bilaterian ancestor (Hejnol *et al*., 2009; Pick *et al*., 2010). However, the origin of the nervous system is a controversial topic. While cnidarians have nerve nets, no neurons have been found in placozoans and sponges – the closest outgroup to cnidarian-bilaterian ancestor (Galliot *et al*., 2009; Galliot and Quiquand, 2011; Marlow and Arendt, 2014; Moroz *et al*., 2014). However, a recent study on the placozoa *Trichoplax* showed that these animals do express *Elav* (DuBuc *et al*., 2019), which is a broad neuronal marker in the sea anemone *Nematostella* (Marlow *et al*., 2009; Kelava *et al.*, 2015). This, however, neither confirm nor rejecting the existence of neuronal populations in these animals.

Regardless of that, it is well accepted that bilaterian and cnidarian nervous systems are homologous. Based on that, many questions can be addressed regarding the structure and molecular determinants of the nervous systems. For example, how patterning and cell commitment is facilitated, how the nervous system is organized, and what genes and pathways are involved in such processes.

In most animals, neural progenitors arise within the context of the epithelial ectoderm layer, once internalization of embryonic cells destined to produce the inner organs is established. In cnidarians, endodermal cells also acquire the potential to form neural cells (Nakanishi *et al*., 2012). Neurogenesis in bilaterians is followed by the separation of neural cells from the epithelial ectoderm and then by migration, proliferation and differentiation (Hartenstein and Stollewerk, 2015).

The neurogenic potential can be spread out over the entire ectoderm which results in the formation of a more generalized neurogenic ectoderm (nerve plexus - found in Cnidarians), whereas when the potential is restricted to a specific region (neuroectoderm), a CNS is formed (Richards and Rentzsch, 2014). Neural precursors can directly differentiate as neurons or give rise to “stem-cell-like” progenitors which can divide asymmetrically (self-

renewal and a second daughter cell that is committed to neural differentiation) (Noctor *et al.*, 2004; Kowalczyk *et al*., 2009). Then, neural progenitors can either be internalized via ingression, invagination or delamination, or remain integrated within the neuroepithelium surface (Fig. 1.4).

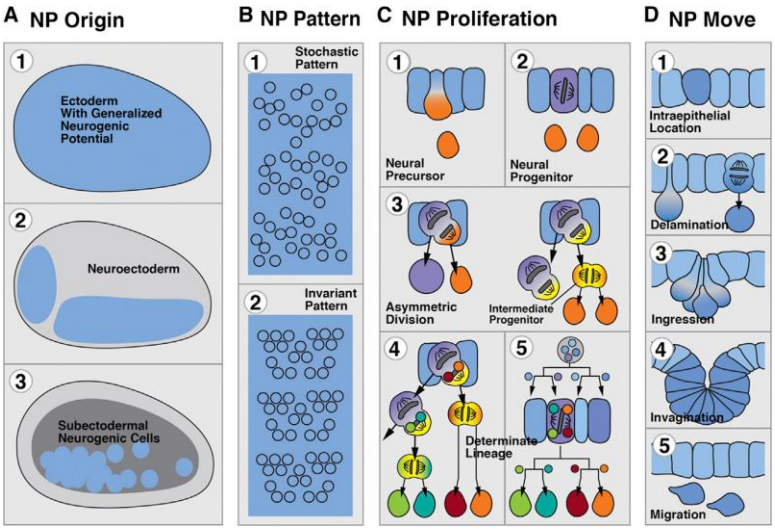

Figure 1.4. Schematic representation of the basic steps in neurogenesis. Cells first acquire neurogenic potential (A), then neural progenitors will pattern themselves in various ways (B), proliferate (C), and migrate (D). Figure adapted from Hartenstein and Stollewerk (2015). Neurogenesis begins when ectodermal cells (also endodermal cells in cnidarians) acquire the neurogenic potential. Following, neural progenitors or precursors arise within the particular domain (neurogenic ectoderm or endoderm) and pattern themselves stochastically or invariant depending on the animal. Afterwards, neural progenitor cells will either directly differentiate to neurons or give rise to proliferating neural progenitors which in turn they can asymmetrically self-renew. Finally, neural progenitors will either remain integrated within the neuroepithelium or internalise by delamination, ingression, or invagination (Hartenstein and Stollewerk, 2015).

Cnidarians do not present a central nervous system (CNS) like bilaterians. Instead, they have structurally a much simpler system, yet with a considerable degree of functional complexity. The nerve net is composed by sensory and ganglionic neurons whose processes are interspersed among the epithelial cells of both epidermis and gastrodermis (diffused nervous system). Several cnidarian species present some degree of regionalization of the neural structure (Watanabe *et al*., 2009). For instance, regionalization can be characteristically seen in the medusozoans which incorporate an eye-bearing sensory system. All the aforementioned cell types are derived from stem cell populations lodged in interstitial spaces of epithelia, and hence named interstitial cells (i-cells). I-cells do not only give rise to sensory neurons, nematocytes and ganglion cells, but also give rise to germline cells and multiple secretory cell types (Khalturin *et al*., 2007).

For instance, *Hydra*, a freshwater polyp and a typical example of the structural simplicity of this animal family, has at least three neuronal cell types: sensory and ganglionic neurons, and nematocytes. The later one exhibits mechanosensory functions with a great level of complexity, underlying the usefulness of this Phylum in understanding fundamental processes in a less complex environment (David *et al*., 2008).

As mentioned above, the cnidarian nervous system has a basiepithelial nerve plexus form; neurons and their processes form part of the epithelium as they are located between the apical junctions of the epithelium and the basement membrane (Hartenstein and Stollewerk, 2015). However, some members of this family present condensed neurites and neuronal cell bodies to form circular or linear tracts; features seen in bilaterian animals (Koizumi *et al*., 2004).

Cnidarian nervous systems are highly peptidergic. Classical neurotransmitters that have been long studied in higher eukaryotes are also involved in cnidarian neurotransmission (Kass-Simon and Pierobon, 2007). In brief, neurotransmission is the process by which neurotransmitters (signaling molecules – including peptides) are released by a neuron and bind and activate receptors from another neuron (Takahashi and Takeda, 2015). Neuropeptides are derived from nerve cells and range from as short as three amino acids (Nillni *et al*., 1996) to as long as 70 amino acids (Truman, 1992), whereas neuropeptide receptors belong primarily to the family of G protein-coupled receptors (Fujisawa and Hayakawa, 2012).

To date, three major neuropeptide families have been well characterized in cnidarians: FMRFamide-like peptides (FLPs), GLWamides, and PRXamide peptides.

The most extensively studied among all classes (Anthozoa, Cubozoa, Scyphozoa and Hydrozoa) is the FLP family (Grimmelikhuijzen *et al*., 1991; Anderson *et al*., 2004; Grimmelikhuijzen *et al*., 1985). The FMRFamide peptide is composed of four amino acid residues with C-terminal amidation and it was first isolated from the cerebral ganglion of the clam *Macrocallista nimbosa* (Price and Greenberg, 1977a; 1977b). FLPs are further subdivided into two groups: FMRFamide-related peptides (FaRPs) which contain N-terminal extensions of the C-terminal FMRFamide or FLRFamide code sequences (Price and Greenberg, 1989), and FLPs which include all peptides with the RFamide sequence only (18). In *Hydra* and *Hydractinia* polyps, FMRFamide-positive neurons can be found in the epidermis around the mouth opening, whereas RFamide-positive ganglion cells are located at the head

region, peducle (in *Hydra*) and tentacles (Grimmelikhuijzen *et al*., 1985; Grimmelikhuijzen *et al*., 1991; Koizumi *et al*., 1992).

Another NP family, the GLWamide-s, has been demonstrated to be expressed in cnidarians, especially in *Hydra* and *Hydractinia* (Schmich *et al*., 1998). GLWamides have characteristic structural features in their N- and C-terminal regions. For instance, most of the peptides belonging to this family share a GLWamide motif at their C-termini (Takahashi and Takeda, 2015).

The third class of neuropeptides in cnidarians has been studied in a much less extend compared to the other two families. PRXamide peptides are generally divided in three subgroups: Pheromone biosynthesis activating neuropeptides (Raina *et al*., 1989), small cardioactive neuropeptides (Morris *et al*., 1982; Lloyd *et al.,* 1987), and antho-RPamide and related peptides (Carstensen *et al*., 1992). So far, PRXpeptides have only been identified in *Hydra magnipapillata* (Hym-355; Takahashi *et al*., 2000) and in *Anthopleura elegantissma* (Antho-RPamide; Carstensen *et al*., 1992), and both of them share homology with members of the last group (antho-RPamide and related peptides).

Generally, FLPs have various roles in muscle contraction, feeding, sensory activity, metamorphosis, and larval movement. On the other hand, GLWamides have roles in planula migration, oocyte maturation and spawning, as well as in metamorphosis and in muscle contraction. Hym-355 which belongs to the PRXamide peptide family enhances neuronal differentiation, along with muscle contraction, oocyte maturation and spawning (Takahashi and Takeda, 2015).

Both GLWamide- and FMRFamide-positive neurons seem to play a significant role in the regulation of metamorphosis induction as they directly receive environmental cues (Müller, 1969). The two NP families are also involved in the regulation of the creeping behavior of planula towards a light source. Phototaxis was suppressed or promoted by the exogenously administration of RFamide or LWamide peptides, respectively (Katsukura *et al*., 2004).

Neurosecretory cells in vertebrates form a distinct population of nerve cells and release NPs anywhere along the cell body and neurites, as well as at the synapses, whereas in the cnidarian nervous system the distribution of synaptic vesicles is limited at the synapses (Hartenstein, 2006; Westfall, 1987). Furthermore, synaptic connections in cnidarians can be established between ganglionic neurons and between sensory and epithelial muscular cells (Westfall, 1973; Kinnamon and Westfall, 1982). Hence, the synapse-restricted secretion of

NPs may serve as a directed signal transmission rather than a generalized undirected neurosecretion.

The regulation of neural differentiation and cell type specification by neurogenic transcription factors seems to be conserved between Bilateria and Cnidaria, but the molecular nature of the neural inducers in the cnidarians is still not specified. For instance, the bone morphogenetic protein (BMP) signaling is involved in the triggering of regionalized neurogenesis in Bilateria (Levine and Brivanlou, 2007). Recent studies using *Nematostella* did show asymmetric expression of *BMP2/4* and its antagonist *Chordin* around the blastopore lip at the gastrula stage, whereas in bilaterians Chordin antagonizes Bmp activity on the opposite side of the dorsal-ventral axis (Rentzsch *et al*., 2006).

Transcriptional regulators are essential for guiding cells to a specific identity. SoxB transcription factors are central in neurodevelopment. Their presence or absence determines whether a neural precursor cell will self-renew or differentiate into a specialized cell. Furthermore, they maintain the neuroectoderm in a proliferative state as they provide neurogenic potential but at the same time inhibit neural differentiation (Sasai, 2001; Elkouris *et al*., 2011). More specific, the expression of SoxB factors is under the control of various signaling pathways, notably the BMP/BMP antagonist and the Wnt pathways (Mizuseki *et al*., 1998; Niehrs, 2010). In mammals, 20 Sox proteins have been identified and classified into groups (SoxA-SoxH) based on the degree of amino acid identity within the HMG (high mobility group)-box (Reiprich and Wegner, 2015). In cnidarians, specifically in Anthozoa and Hydrozoa, an almost complete set of homologous genes that have critical roles in bilaterian neurodevelopment (neurogenesis, neuronal specification and network formation) has been described. Among them are the proneural basic helix loop helix (bHLH) factors, SoxB genes, zinc-finger protein genes, and neuron specific RNA binding proteins (RBPs) (Watanabe *et al*., 2009).

The fact that Cnidaria possess an almost complete set of such genes implicated in bilaterian neurodevelopment with a relatively morphological simple nervous system, makes this phylum ideal to study cellular and developmental processes that establish and maintain a nervous system. In *Hydractinia*, nervous system development and cell commitment to the neural fate has not been fully characterised.

1.7 SoxB family of transcription factors

As briefly mentioned in the previous section, the Sox family of transcription factors (TFs) are versatile regulators of stem and progenitor cell fate with a central role in neurodevelopment.

Studies focused on this superfamily began with the discovery of the mammalian testis-determining factor *Sry* (Gubbay *et al.,* 1990; Sinclair *et al*., 1990). They identified the protein domain, now called high-mobility-group (HMG) which binds DNA in a sequence-specific manner and based on the amino acid similarity ($\geq$ 50%) to this domain of Sry, other Sox proteins were identified. In total, 20 Sox genes have been identified in humans and mice (Schepers *et al*., 2002). Sox proteins sharing $\geq$ 80% similarity in the HMG domain are divided into different subgroups: SoxA-H (Wegner, 2010).

Members from the same Sox group share biochemical properties and overlapping functions whereas Sox TFs from different groups have distinct biological functions despite the same protein consensus motif. Sox factors can achieve target gene selectivity through differential affinity for distinct flanking sequences next to consensus *Sox* sites through post-translational modifications, homo- or heterodimerization among Sox proteins, or through interaction with other co-factors (Wegner, 2010).

Sox TFs are well recognized as master regulators in many developmental and physiological processes by facilitating cell-type specific genetic programs both in stem and progenitor cells as well as in highly specialized cell types (Kamachi and Kondoh, 2013). Members of the Sox TF family are conserved along the animal kingdom (Fig. 1.5), and of great interest is the group B of the Sox family as they regulate neural progenitors from early development and they are implicated in nervous system development (Sarkar and Hochedlinger, 2013).

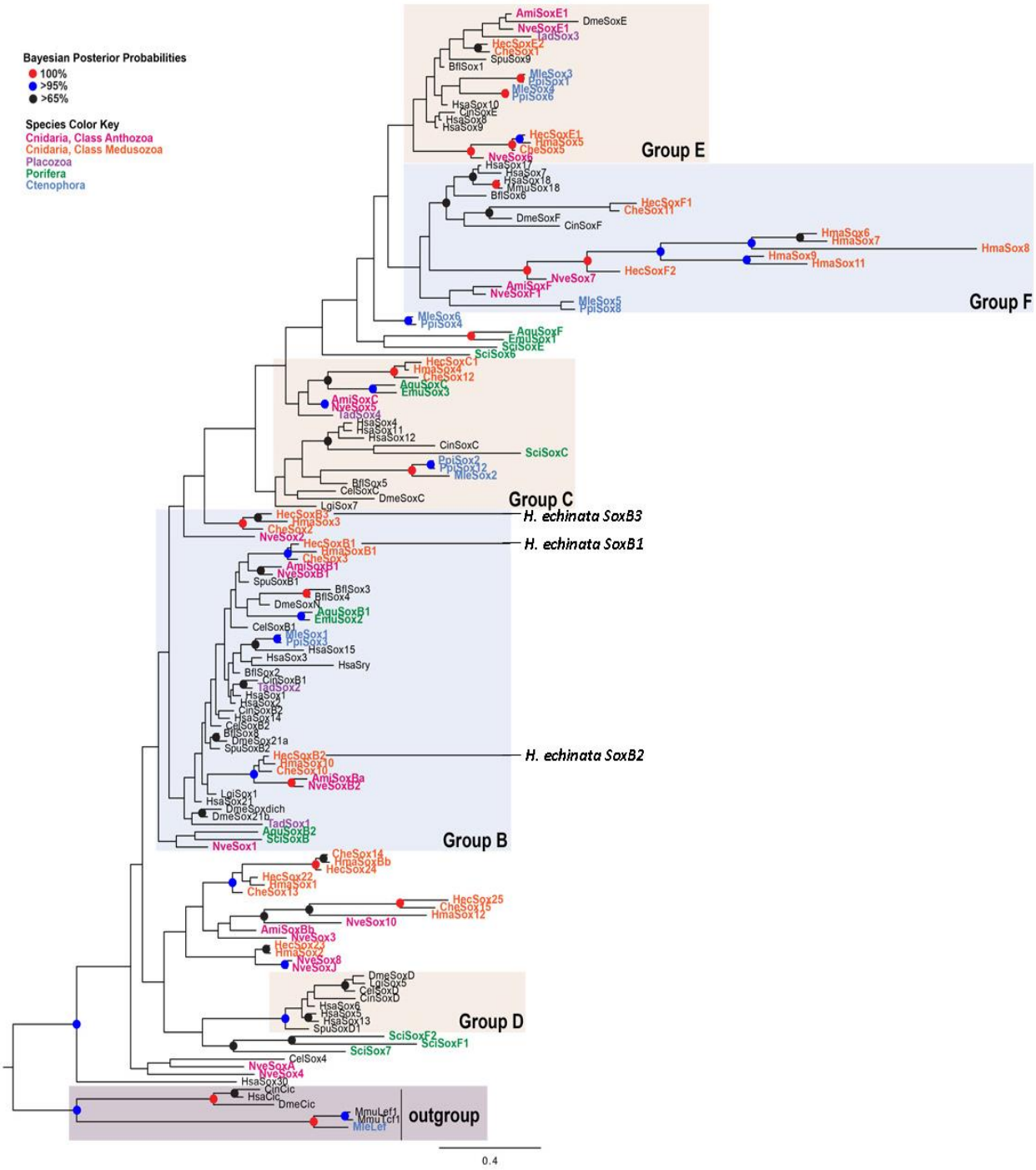

Figure 1.5. Phylogenetic analysis of Sox HMG domains. Image adapted from Flici *et al* (2017). 12 Sox-like sequences were identified in Hydractinia. Eight of these sequences belonged to groups B, C, E and F, whereas the remaining four sequences were unstable in their placement on the tree falling either at the base of the tree (not in known groups) or within group B. Species are abbreviated as following: Ami, *Acropora millepora*; Aqu, *Amphimedon queenslandica*; Bfl, *Branchiostoma floridae*; Cel, *Caenorhabditis elegans*; Cin, *Ciona intestinalis*; Che, *Clytia hemisphaerica*; Dme, *Drosophila melanogaster*; Emu, *Ephydatia muelleri*; Hec, *Hydractinia echinata*; Hma, *Hydra magnipapillata*; Hsa, *Homo sapiens*; Lgi, *Lottia gigantea*; Mle, *Mnemiopsis leidyi*; Mmu, *Mus musculus*; Nve, *Nematostella vectensis*; Ppi, *Pleurobrachia pileus*; Sci, *Sycon ciliatum*; Spu, *Strongylocentrotus purpuratus*; Tad, *Trichoplax adhaerens*.

Vertebrate SoxB TFs are subdivided into two subgroups, SoxB1 (Sox1, Sox2, Sox3) and SoxB2 (Sox14, Sox21) with roles in self-renewal and pluripotency maintenance (Sarkar and Hochedlinger, 2013), and in neural differentiation, respectively (Graham *et al*., 2003). The effect of Sox2 on self-renewal and differentiation of embryonic stem cells (ESCs) is highly dosage-dependent suggesting that its expression needs to be in equilibrium with other co-factors in order to maintain a pluripotency state (Kopp *et al*., 2008). Based on numerous studies, Sox2 acts in a cooperation with other TFs that are also dosage-sensitive, such as Nanog and Oct4, in order to maintain regulatory networks responsible for self-renewal while repressing differentiation programs in ESCs (Boyer *et al*., 2006; Chen *et al*., 2008; Kim *et al*., 2008; Orkin and Hochedlinger, 2011). For instance, Sox2 and Oct4 closely collaborate to each other to efficiently bind to DNA and recruit other cofactors for gene activation (Tomioka *et al*., 2002; Masui *et al.*, 2007). On the other hand, Sox TFs can act opposing to each other's function. For example, Sox17 (SoxF group) antagonizes Sox2 function by repressing target genes and this action is partly accomplished by displacing Nanog from silenced Nanog/Sox2 targets resulting in their transcriptional activation (Niakan *et al*., 2010). Sox2 also has a role in ectoderm development by determining early neural lineage specification in the embryo. This regulation of cell fate commitment by Sox2 is achieved by antagonizing other factors such as Tbx6 which is a regulator of presomitic mesoderm development (Takemoto *et al*., 2011).

Based on the above examples and many more additional studies, it is well recognized that Sox2 determines cell fate by antagonizing directly or indirectly TFs of alternative lineages in a highly cell type and developmental stage specific manner. Another example is how Sox2 biases cells multipotent optic cup progenitors towards a neurogenic fate by antagonizing Pax6. When *Sox2* was ablated, these cells were biased towards a non-neurogenic epithelium fate (Pax6-driven fate), supporting this notion (Matsushima *et al*., 2011).

Apart from its role during embryogenesis, Sox2 is also a key regulator of central and peripheral nervous system (CNS, PNS) development, by controlling proliferation and differentiation of neural stem cells (Pevny and Nicolis, 2010). *Sox2* expression overlaps with that of the other two SoxB1 TFs, namely *Sox1* and *Sox3* in the CNS and PNS (Bylund *et al*., 2003). It has also been reported that *Sox2* expression is not only important in maintaining stem cells and progenitors, but also for the differentiation of neuronal subsets such as GABAergic neurons in cortex and olfactory bulb (Cavallaro *et al*., 2008). Defining the mechanisms by which the same TFs regulate both neural progenitor maintenance and cell

differentiation within the same lineage will provide insights into the molecular mechanisms responsible for such various outcomes.

However, not only members of the SoxB1 family are responsible for stem and progenitor cell maintenance. Most Sox TFs are expressed in various types of stem and progenitor cells or tissues. For example, Sox9 (SoxE) is expressed in stem and progenitor cells in the adult intestine, exocrine pancreas and liver under both homeostatic and injury conditions (Furuyama *et al*., 2011). Another example from the SoxF group, Sox17 is required for fetal and neonatal hematopoietic stem cell maintenance but it is dispensable in adult hematopoiesis (Kim *et al.,* 2007).

Like in many other Sox factors, *Sox2* expression is positively or negatively regulated by different extracellular and intracellular modulators in adult and pluripotent stem cells. Major signaling pathways control Sox2 TF expression levels during embryonic development, tissue homeostasis and regeneration in a context-dependent manner. For instance, Wnt signaling positively regulates *Sox2* expression in the endodermal progenitors of the developing taste buds, derived from progenitor cells of the pharyngeal endoderm, causing their differentiation in the expense of keratinocytes (Okubo *et al.*, 2006). On the other hand, *Sox2* upregulation by Fgf signaling on calvarian osteoblast progenitors leads to Wnt signaling inhibition as Sox2 is physically associated with beta-catenin (Mansukhami *et al*., 2005). Furthermore, Sox2 itself can modulate these signals by directly activating or repressing key regulators of such major pathways.

Furthermore, activation of Sox2 by extracellular signaling is followed by intracellular interactions with other core pluripotency factors, cell cycle regulators, miRNAs, and activating and repressive chromatin regulators to control gene expression which in turn balances self-renewal and/or differentiation in pluripotent cells (Sarkar and Hochedlinger, 2013).

Sox gene family members exert key roles during development and beyond (Fig. 1.7) and any developmental disorders arising due to SOX mutations are referred to as SOXopathies, just as RASopathies which are due to mutations in components of the Ras/MAPK pathway (Angelozzi and Lefebvre, 2019; Tajan *et al*., 2018). To date, SOXopathies have only been related to half of the Sox gene family (10 out of 20). Most SOXpathies are rare developmental disorders and the mutations underlining them are generally *de novo*, heterozygous and inactivating (loss of function) revealing gene haploinsufficiency (Angelozzi and Lefebvre,

2019). These mutations are predominantly found in the DNA-binding domain HMG box which mediates DNA binding, nuclear trafficking, protein-protein interactions and other crucial functions (Gubbay *et al.,* 1990; Sinclair *et al*., 1990), and result in various developmental defects.

To date, most of the SOXopathies reported are regarding distinct *SRY* mutations. This is probably because *SRY* is a master determinant of sex determination and is present in only one copy, thus it has no other SoxA gene to share its function with. Most mutations identified in this gene cause XY sex reversal and since its only functional domain is the HMG domain, most of the alterations are found within these residues (Berta *et al.,* 1990; Berkovitz *et al*., 1992; Harley *et al*., 2003).

Furthermore, *SOX2* heterozygous loss-of-function mutations were reported to cause developmental delay, learning difficulties and a range of craniofacial and genital disorders (Kelberman and Dattani, 2007; Slavotinek, 2018). In addition, *SOX2* homozygous deletion in mice resulted in early embryogenesis death due to failure to form pluripotent epiblast (Zhang and Cui, 2014). Another example of the vital importance of these genes is the SoxF group. Members of this group (*Sox7, Sox17, Sox18*) encode transcriptional activators central to several developmental processes such as cardiogenesis, vasculogenesis, and angiogenesis (Lilly *et al*., 2017; Francois *et al*., 2010; Seguin *et al.*, 2008; Lange *et al*., 2014; Pennisi *et al*., 2000). Mutations identified in these genes resulted in a range of developmental abnormalities such as hypotrichosis-lymphedema-telangiectasia syndrome and congenital anomalies of the kidney and urinary tract (Irrthum *et al*., 2003; Gimelli *et al*., 2010).

Apart from germline SOX mutations (SOXopathies), dysregulations of SOX genes have been also involved in at least one tumor type (Grimm *et al*., 2019). Since Sox factors are key regulators of cell fate, increased or decreased activities of these genes can cause drastic changes in cell stemness, survival, proliferation and differentiation. Their dysregulation can occur at any level: genetic, epigenetic, transcriptional, translational and post-translational.

In addition to vertebrates, Sox TFs have been well studied in bilaterian invertebrates (Bowles *et al*., 2000). Based on phylogenetic analysis, *Drosophila* has two SoxB-like proteins: SoxNeuro (SoxB1-like) and Dichaete (SoxB2-like), and both proteins are involved in the regulation of neurodevelopment with a partial redundancy in their function (Buescher *et al*., 2002; Ferrero *et al*., 2014).

However, Sox genes are conserved throughout the animal kingdom and surprisingly diverse in non-bilaterian animal lineages such as ctenophores, sponges, placozoans and cnidarians (Schnitzler *et al.,* 2014). Sox-like genes are present in the unicellular choanoflagellate *Monosiga brevicollis* (King *et al*., 2008) suggesting that the origin of Sox proteins predates multicellularity. However, studies based on phylogenetic analyses support the hypothesis that true Sox genes arose at the base of the animals and that four major Sox groups (B, C, E and F) were fully diversified in ctenophores as shown in Fig 1.6 (Schnitzler *et al*., 2014; Larroux *et al*., 2006; Fortunato *et al*., 2012; Jager *et al*., 2006; Jager *et al*., 2008; Hejnol *et al*., 2009; Dunn *et al*., 2008; Ryan *et al*., 2013). Based on the findings presented by Schnitzler and colleagues (2014), not true Sox genes are the ones whose sequences always clustered outside the Sox gene family with outgroup sequences. This evolutionary hypothesis suggests that Sox TFs diversified early and remained relatively stable throughout animal evolution.

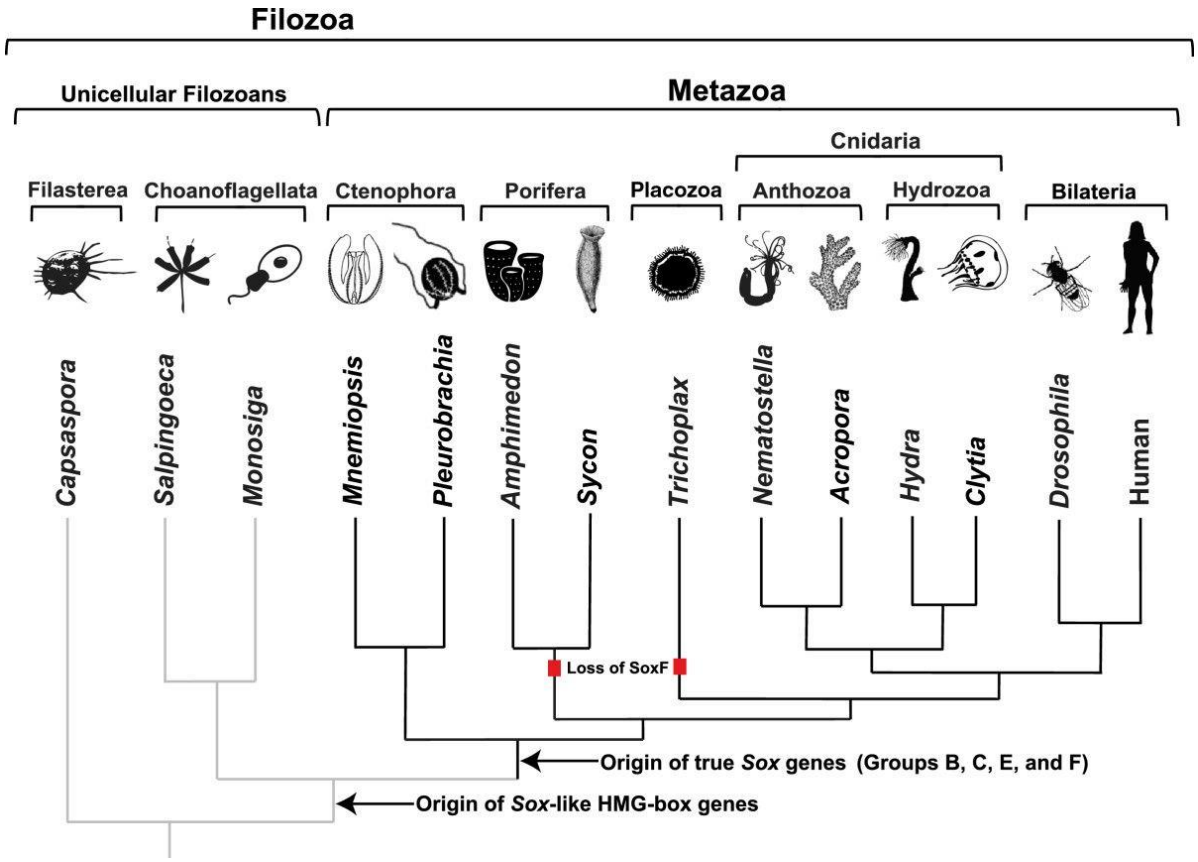

Figure 1.6. Evolutionary history of Sox transcription factor family. Image obtained from Schnitzler *et al*., 2014. Sox genes are diverse in non-bilaterian animal lineages such as ctenophores, sponges, placozoans and cnidarians. True Sox genes arose at the base of the animals, whereas Sox-like genes are present even earlier, at unicellular organisms such as Choanoflagellata. In addition, SoxF group seemed to be lost in Porifera and Placozoa.

In cnidarians, Sox genes have been identified in several animals including *Hydractinia* spp. (Flici *et al*., 2017), *Nematostella vectensis* (Richards and Rentzsch, 2014, 2015; Watanabe *et al*., 2014), *Clytia hemishpaerica* (Jager *et al*., 2011), *Hydra magnipapillata* (Chapman *et al*., 2010; Jager *et al.,* 2006), and *Acropora millepora* (Shinzato *et al.,* 2008). So far, the functional roles of SoxB TFs were only studied in *Hydractinia* and *Nematostella*.

The first evidences for the existence of dedicated neural progenitor cells (NPCs) able to strictly generate multiple neural cells types outside the Bilateria came from the anthozoan cnidarian *Nematostella* (Richards and Rentzsch, 2014). Based on this study, the three major neuronal types in cnidarians, namely sensory and ganglionic neurons and nematocytes, are derived from *NvSoxB(2)*-expressing cells, but it is unclear whether NPCs are a homo- or heterogeneous NPC population. One possibility is that sensory and ganglionic neurons are derived from a subpopulation of *NvSoxB(2)*-expressing cells and nematocytes from another one as, at least on the molecular and morphological level, these neuronal populations differ from each other – sensory/ganglionic neurons vs nematocytes (Marlow *et al*., 2009; Nakanishi *et al.*, 2012).

In addition, these NPCs displayed asymmetric cell cycle behavior suggesting differential self-renewal and/or adaptation of distinct fates within *NvSoxB(2)*$^{+}$ lineages. These observations are in line with mammalian and *Drosophila* studies in which changes in the length of cell cycle phases denote changes in the future trajectories of these NPCs (Takahashi *et al*., 1995; Calegari *et al*., 2005; Bowman *et al*., 2008; Bayraktar *et al*., 2010). Moreover, the absolute numbers of *NvSoxB(2)*$^{+}$ cells in the ectoderm did not change from blastula to planula stages. This observation favors a scenario in which NvSoxB(2) promotes and/or stabilizes NPC fate. This is in line with previous studies describing the neural potential of ectodermal cells by characterizing the expression of other Sox genes, namely *NvSoxB(1), NvSox1* and *NvSox3* (Magie *et al*., 2005). Furthermore, a study from the same group (Richards and Rentzsch, 2015) also demonstrated that Notch signaling, a key regulator of neural progenitors' maintenance, regulates NPCs in Nematostella along with NvSoxB(2) via parallel and yet interacting mechanisms. In brief, Notch signaling regulates neurogenesis by maintaining NPCs in an undifferentiated state. It does so by inducing the expression of bHLH genes of the Hes family which in turn act as repressors of proneural bHLH genes (Bertrand *et al*., 2002).

Unlike *Nematostella*, neurogenesis in hydrozoans like *Hydra* and *Hydractinia,* is of endodermal origin (Martin, 1988; Jager *et al*., 2011; Kanska and Frank, 2013; Gahan *et al*., 2016). Based on a phylogenetic analysis of *Sox* HMG domains (Flici *et al*., 2017), 12 Sox-like

sequences were identified in *Hydractinia*. Eight of these sequences belonged to groups B, C, E and F, whereas the remaining four sequences were unstable in their placement on the tree falling either at the base of the tree (not in known groups) or within group B. Unlike the subgrouping of SoxB genes in vertebrates into SoxB1 and SoxB2 subgroups, *Hydractinia* SoxB genes failed to further resolve their subgrouping within this cluster.

Hydractinia has three SoxB genes, namely *SoxB1*, *SoxB2*, and *SoxB3*, and all of them are expressed throughout the animal's life. The study was primarily focused on *SoxB2* and *SoxB3* and the data were in the line the scenario in which *SoxB2* is expressed in NPCs and *SoxB3* in post-mitotic cells committed to become neurons/nematocytes. This suggests a similar mode of action during neurogenesis between anthozoans and hydrozoans (Richards and Rentzsch, 2014, 2015). In addition, this study also showed that *SoxB2* and *SoxB3* positively regulate neurogenesis during development, tissue homeostasis, and regeneration with these two genes being in part functionally redundant.

Despite the extensive work done on *SoxB2* and *SoxB3* in *Hydractinia*, little is known about the third member of SoxB family: *SoxB1*. Since *SoxB2* and *SoxB3* seem to be expressed sequentially based on their functions with the former expressed in NPCs and the latter in differentiating/differentiated neurons and nematocytes, it can be hypothesized that *SoxB1* acts upstream of these two and has a conserved role with mammalian *Sox2*. The majority of the work presented in this thesis will try to further elucidate the roles of these three SoxB genes during embryonic neurodevelopment and adult nervous system regeneration and test the hypothesis regarding their sequential expression.

1.8 Evolution of animal regeneration

Regeneration, in simple terms, is the identical or largely similar restoration of any lost body part and can occur at multiple levels; cellular (e.g. regrowth of severed nerve axon), tissue (e.g. growth of epidermis covering a wound), organ (e.g. liver and lens), structure (e.g. limb regeneration in salamander), and whole-body regeneration (e.g. cnidarians and planarians) (Fig. 1.7). Many fundamental questions regarding this fascinating branch of developmental biology remain unexplored or partially answered. One of the oldest questions about regeneration is whether this property is an ancestral characteristic that is a general trait among animals or whether it is a set of specific adaptations acquired by certain taxa in order to face different circumstances. However, some phenomena complicate even more the evolutionary history of regeneration as they are named "regeneration" but might have arisen independently. The main reason for the slow advancement of this field was the inability to carry out genetic studies in species with various regeneration potential, but fortunately with the advancement of methodologies and expansion of the genetic toolbox, such studies are becoming feasible nowadays.

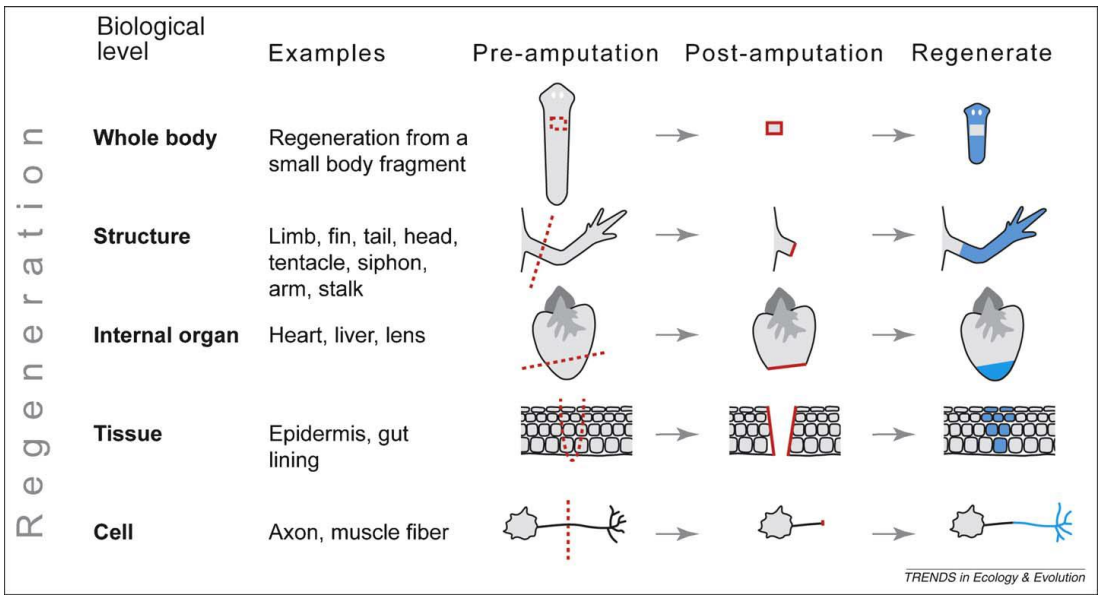

Figure 1.7. Regeneration occurs at multiple levels: whole-body, structure, internal organ, tissue, and cell regeneration. Image adapted from Bely and Nyberg (2009).

During regeneration many processes are employed such as rearrangement of pre-existing tissues, use of adult somatic cells, and trans-differentiation or de-differentiation of cells. Many processes can be used within the same animal and different modes are often employed in closely related taxa (Sanchez Alvarado and Tsonis, 2006; Bradshaw *et al*., 2015).

Regeneration was originally classified by T. H. Morgan into two major groups. Animals that achieve regeneration through morphallaxis – a mechanism involving no or limited cell proliferation, where new structures are formed by remodeling existing tissue. The other regeneration mode is known as epimorphosis – a mechanism involving cell proliferation (Morgan, 1901). The processes of morphallaxis and epimorphosis are not mutually exclusive with various taxa often using both to re-establish missing tissues (Sanchez Alvarado, 2000; Bradshaw *et al*., 2015).

Regeneration through epimorphosis can be further divided into two groups: blastemal and non-blastemal regeneration. During the former, specialized structures (regeneration blastema) can be formed within hours or days post amputation. It is composed of an outer layer which covers the wound site, and a second cell population that proliferate and accumulate beneath the first layer (Sanchez Alvarado and Tsonis, 2006). For example, during regeneration, planarians go through both morphallaxis and epimorphosis. They first close the wound by cells already present in the injury site and the second population of cells reside within the blastema are derived from migration and proliferation of neoblasts – pluripotent stem cells (Reddien and Sanchez Alvarado, 2004; Guedelhoefer and Sanchez Alvarado, 2012). Non-blastemal epimorphic regeneration occurs through trans-differentiation, de-differentiation, and proliferation of already existing stem cells present in the injured tissue (Jopling *et al*., 2011; Tanaka and Reddien, 2011). This phenomenon is observed during retina and lens regeneration in newts (Call *et al.,* 2005).

The earliest studies documenting extensive regeneration potential are dated more than 200 years ago on the freshwater solitary polyp *Hydra vulgaris* by Abraham Trembley (Lenhoff and Lenhoff, 1986). Since then, *Hydra* has been considered as one of the classical models to study regeneration. *Hydra* employs a combination of morphallaxis and epimorphosis to regenerate (Chera *et al*., 2009), and it has been shown that any fragment that holds at least a few hundred epithelial cells can regenerate into a full-size animal, as epithelial cells are considered as stem cells. However, epimorphic regeneration in Hydra is incomplete since not all cell types are regenerated. Another interesting property of *Hydra* is its unique ability to reform a whole animal by aggregation of dissociated cells (Gierer *et al.,* 1972; Galliot and Schmid, 2002; Holstein *et al*., 2003; Bode, 2009). This phenomenon could lead to a more in-depth understanding of the molecular basis of *de novo* organizer formation.

Another interesting side of regeneration is whether it should be treated as a distinct evolutionary phenomenon or associated with other developmental modes such as

embryogenesis, asexual reproduction, and growth. Studies suggest that regeneration can only be initiated by an unpredictable injury, leaving a wounded multicellular stump, and it also involves regeneration-specific features such as regeneration-specific gene expression (Brockes and Kumar, 2008; Lengfeld *et al*., 2009). Also, regeneration has a unique phylogenetic distribution unlike other developmental phenomena such as asexual reproduction and embryogenesis. It occurs only in a subset of animals unlike embryogenesis which is ubiquitous, and regeneration can be lost in asexually reproducing groups despite their close evolutionary links (Bely and Wray, 2001; Lengfeld *et al*., 2009).

A recent study from Warner *et al* (2019) suggests regeneration is a partial redeployment of the embryonic gene network using the anthozoan cnidarian *Nematostella vectensis.* By employing this unique whole-body regeneration animal model, they showed that the regenerative program partially reuses elements from the embryonic gene network at the transcriptomic level. They also identified regeneration specific modules driving cellular events unique to regeneration. This is the first study regarding cnidarian regeneration that shows this overlap in gene networks between embryonic and regenerative states. In order to start understanding this exciting side of regeneration and answer fundamental questions, further studies from various clades that have, or not regenerative capacities are needed for comparisons.

Nematostella also serves an excellent comparative system for regeneration. Following bisection through the oral-aboral axis, both halves of this animal can fully regenerate into normal polyps (Reitzel *et al*., 2007; Trevino *et al*., 2011; Bossert *et al*., 2013). Unlike *Hydra*, this anthozoan does not appear to have i-cells, and therefore cell proliferation is required in order to complete the regenerative process (Passamaneck and Martindale, 2012). Interestingly, wound healing acts as initiator of regeneration where the onset of proliferation serves as a transition between wound healing and a regenerative response (DuBuc *et al*., 2014).

Hydractinia offers a great comparative system for regenerative studies. I-cells are located in the lower part of the body column and upon decapitation, they are able to migrate to the injury site in order to form a blastema and regenerate the missing head region, like planarians (Gahan *et al.*, 2016; Reddien and Sanchez Alvarado, 2004). Bradshaw *et al*. (2015) demonstrated that decapitation was followed by a wound healing process without requiring any cell proliferation. Instead, i-cells started migrating to the injury site within the first 4-6 hours post decapitation from the body column and proliferated during migration and locally

to form a blastema. Full re-establishment of the missing head region was done within 2-3 days post decapitation (Fig. 1.8). Unlike oral injury, aboral wound closure did not resulted in a blastema formation but instead polyps transformed into stolonal tissue and then budded new polyps. This suggests that distinct mechanisms govern oral and aboral regeneration in *Hydractinia*.

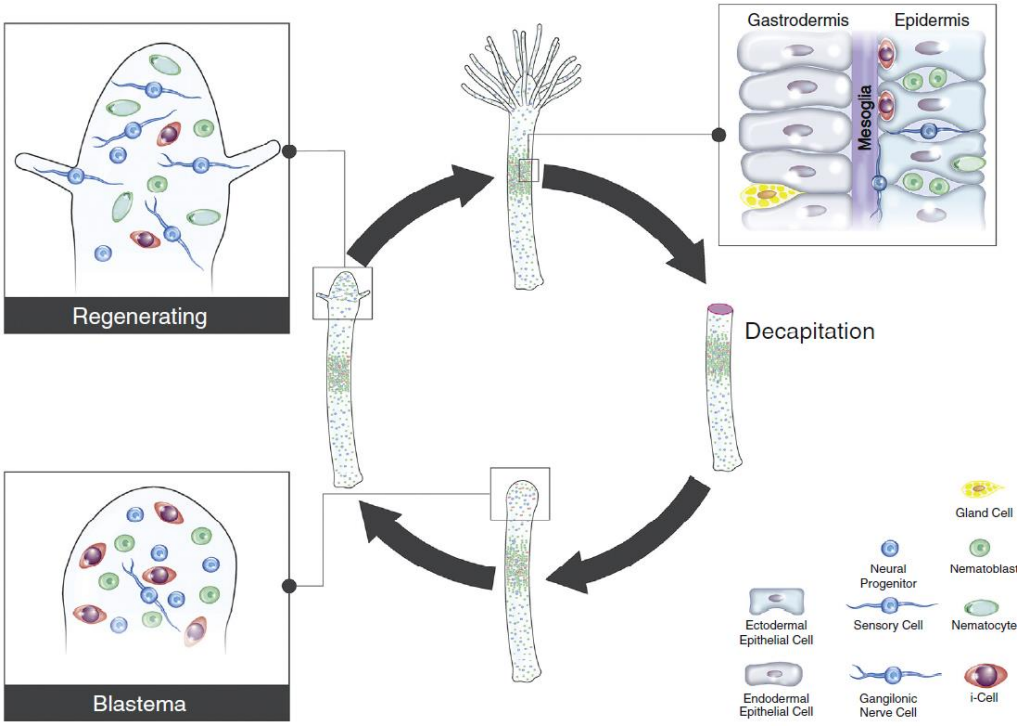

Figure 1.8. Overview of head regeneration in *Hydractinia*. Image adopted from Gahan *et al.* (2016). Head regeneration is a short process that lasts two to three days. Upon decapitation, wound closure is completed within a few hours, which in turn is followed by the migration of i-cells to the injury site. Migrating i-cells will form a blastema which is able to provide cells to the re-establishment of the missing head region.

The mechanisms governing animal regeneration can be species-specific but also tissue-specific within a single species. With the development of transgenesis and other tools in *Hydractinia*, a new window of opportunities becomes available to study *in vivo* cell migration during development and regeneration. These studies will facilitate the understanding of cell dynamics during injury/decapitation and further contribute to the general picture of the evolution of animal regeneration.

1.9 Project aims

Hydractinia and all the members of the phylum Cnidaria are recognized as sister group to bilaterians and one of the extant, Eumetazoa exhibiting nervous system. This makes cnidarians excellent candidates to study the evolution of the nervous system. The general objective of my PhD project was to study cell fate commitment during nervous system establishment in both embryogenesis and regeneration contexts with an emphasis on SoxB genes.

To start understanding how the nervous system is formed and arranged in this animal, my first aim was to determine the composition and structure of the nervous system with previously established markers both in embryonic and adult stages. This in-depth characterisation was lacking for *Hydractinia*, whereas for other cnidarians such as *Hydra* and *Nematostella*, this analysis has already been done. By having such characterisation in another cnidarian, more comparative studies regarding the evolution of the nervous system would be feasible in the feature.

Since my general objective was to study embryogenesis with an emphasis on SoxB genes, I aimed to identify their roles during embryonic neurogenesis, as well as during nervous system regeneration. A previous study regarding this family of genes was performed in *Hydractinia* but the focus was mostly on *SoxB2* and *SoxB3* with a greater emphasis in the adult neurogenesis as positive regulators of this process. For that reason, I wanted to understand the contribution of all three SoxB genes primarily in embryonic neurogenesis as well as the role of *SoxB1* in adult neurogenesis.

Furthermore, I was interested to reveal the transcriptional profile along the neuronal lineage by utilizing transgenic reporter animals. For that, I wanted to find a reliable and reproducible technique to achieve that aim. Since flow cytometry was an incredible way to achieve my goal, I wanted to establish this essential technique in *Hydractinia* and utilize it to identify the transcriptional profile of certain cell populations along the neuronal lineage.

In more detail, the specific aims of my project were:

1. Determine the composition of *Hydractinia* nervous system:
    a. During embryogenesis
    b. In adult stages
2. The roles of SoxB transcription factors in development and regeneration:
    a. Spatial and temporal expression of SoxB genes
    b. Cell fate commitment during nervous system regeneration
    c. Roles of SoxB genes during development
    d. Role of *SoxB1* in adult stage
3. Transcriptional profiling along the neural lineage:
    a. Decipher distinct cell populations based on flow cytometric profiling
    b. Explore gene expression patterns in different stages of the neural lineage

Chapter 2: Materials and Methods

2.1 Animal care

2.1.1 Culture and metamorphosis

2.1.2 Microinjection

2.1.3 Polyp manipulation

2.2 Generation of SoxB1/B2/B3 transgenic reporter animals

2.2.1 Plasmid design overview

2.2.2 *SoxB1::tdTomato::SoxB1* reporter line

2.2.3 *SoxB2::GFP::SoxB2* reporter line

2.2.4 *SoxB3::mScarlet::SoxB3* reporter line

2.2.5 PCR and gel DNA extraction

2.2.6 Restriction digest-based cloning

2.2.7 Bacterial production, transformation and culture

2.2.8 Plasmid extraction

2.2.9 Genomic DNA extraction and RNA extraction for cDNA synthesis

2.3 Cellular staining

2.3.1 Immunofluorescence (IF) staining

2.3.2 Nematocyte staining

2.3.3 EdU staining of cycling cells

2.4 *In situ* hybridization

2.4.1 SoxB coding sequences cloning

2.4.2 RNA probe synthesis (for FISH)

2.4.3 Double FISH protocol (for FISH)

2.4.4 FISH buffers and solutions (for FISH)

2.4.5 DNA probe synthesis (for SABER FISH)

2.4.6 SABER FISH protocol

2.4.7 Buffers and solutions (for SABER FISH)

2.5 Gain and loss of function approaches

2.5.1 Short-hairpin RNA interference

2.5.2 RNA interference

2.5.3 Over-expression constructs

2.6 In-vivo imaging

2.7 Flow cytometric techniques

2.7.1 Tissue dissociation

2.7.2 Flow cytometry

2.7.3 Imaging flow cytometry

2.7.4 Fluorescence-activated cell sorting (FACS) and RNA extraction

2.7.5 Cell cycle analysis

2.8 Protein detection by Western blotting

2.8.1 Protein extraction

2.8.2 Gel preparation and gel transfer

2.8.3 Coomassie staining

2.8.4 Antibody staining

2.9 Antibody production

2.9.1 Protein expression, induction and extraction

2.9.2 Soluble Vs insoluble protein expression

2.9.3 Antibody production

2.1 Animal care

2.1.1 Culture and metamorphosis

For the purposes of the present study, the marine hydroid *Hydractinia symbiolongicarpus* was used as an animal model. In the wild, *H. symbiolongicarpus* is found on the hermit crab shell and under laboratory conditions, stable clones were grown on glass microscope slides and cultured at 20-22°C in artificial seawater under a 14:10 light:dark cycle regime. They were fed four times a week with freshly hatched *Artemia nauplii* and once a week with oysters (pureed when fresh and then stored frozen in aliquots).

Spawning takes place approximately one and a half hours after light induction by the release of gametes (sperm and oocytes) in a water column. Once collected, the embryos can be stored in 4°C for up to 4 hours to halt their development and provide a wider timeframe for injections.

Once the embryo reaches the planula larval stage, metamorphosis is be induced by a 3-4 hours incubation in 1:5 580mM CsCl:ASW. Once metamorphosing larvae fully retract, they are place in the desired substrate to settle and form a new colony. The same workflow is also applied for microinjected embryos (transgenesis).

2.1.2 Microinjection

For plasmid or shRNAi injections, the embryos were placed in a 35mm petri dish with a 100µm plankton net attached. Generally, plasmids were injected at 3-4µg/µl concentration eluted in nuclease-free water. For shRNAi injection concentrations see section 2.5. Injection needles were prepared from glass capillaries with filament (Narishige; GD-1) using a pulling machine. For shRNAi injections, fluorescent Dextran was mixed to 1:20 ratio in order to select the injected embryos. For all the types of injections, 400 mM KCl was mixed with the injectable product to 1:5 ratio.

2.1.3 Polyp manipulation

In order to remove sexual or feeding polyps from the colony, the whole slide was placed in 4% $MgCl_2$ (prepared in 1:1 ASW:diH_2O) for 10-15min. For regeneration experiments, individual polyps were decapitated by a transverse cut right below the tentacle base and further used for various experiments.

2.2 Generation of SoxB1/B2/B3 transgenic reporter animals

2.2.1 Plasmid design overview

For the generation of SoxB1/B2/B3 reporter lines, tdTomato, GFP and mScarlet fluorescent proteins were expressed under both the 5' and 3' genomic control elements of the three genes respectively (Fig. 2.1). All the primers designed and used can be found in Appendix A, and sequences used in Appendix B.

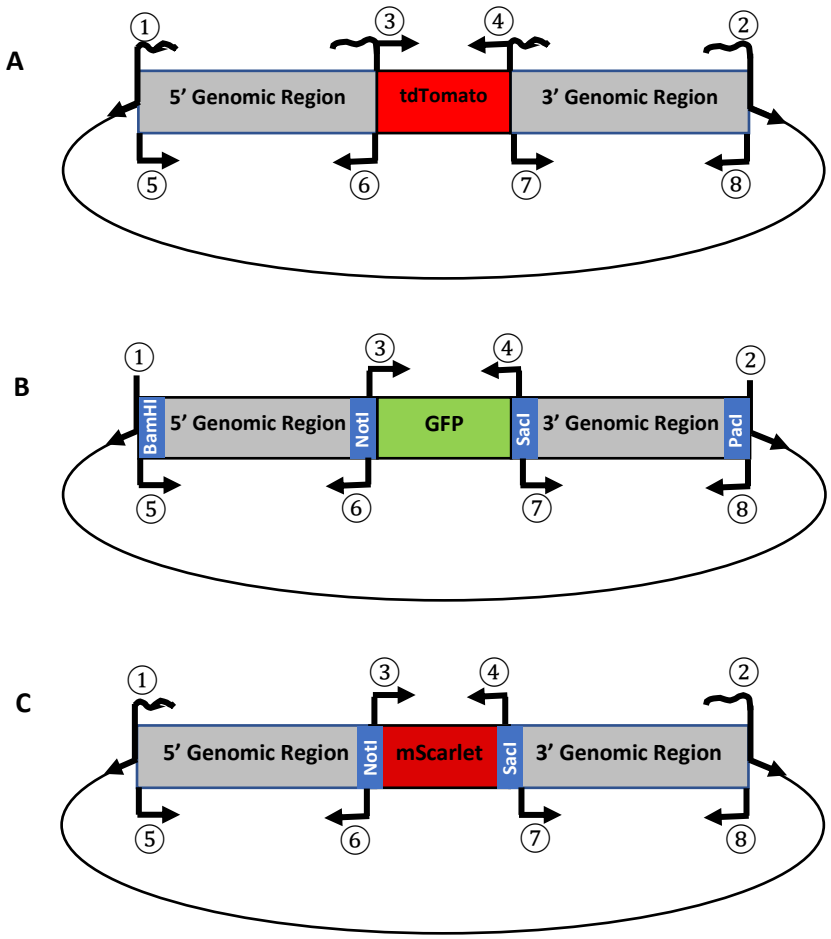

Figure 2.1. Schematic of SoxB1 (A), SoxB2 (B) and SoxB3 (C) plasmid constructs for the generation of transgenic reporter lines. Numbers indicate the primers used (Appendix A).

2.2.2 SoxB1::tdTomato::SoxB1 reporter line

Gibson assembly-based cloning was utilized to generate this construct. Forward and reverse PCR primers were designed with 20-25bp overhangs on both the backbone and the fluorescent protein to match the 5' and 3' genomic regions. Both upstream and downstream genomic regions of *Hydractinia SoxB1* coding sequence were cloned without any overhangs. The assembly was carried out in two phases. First, the promoter, tdTomato and terminator

were assembled by using 100ng from each fragment, 2x Gibson master mix (NEBuilder HiFi DNA Assembly Master Mix; E2621) and nuclease-free water to a final reaction volume of 10µl. The reaction mixture was then incubated for one hour at 50°C. The resulted fragment was used as a PCR template to confirm the assembly. Upon confirmation, the cassette was used in the second phase in which it was mixed with the cloned backbone containing the overhangs along with 2x Gibson master mix and nuclease-free water and incubated at 50°C for one hour as well. Correct assembly was confirmed by both PCR and sequencing. The resulted plasmid was transformed into chemically competent bacteria as described in section 2.2.7 and plasmid is extracted as described in section 2.2.8.

2.2.3 *SoxB2::GFP::SoxB2* reporter line

This construct was generated by restriction digest-based cloning. First, primers were designed to clone the genomic regions upstream and downstream of *Hydractinia SoxB2* coding sequence. The *β-tubulin*::GFP::*β-tubulin* was used as a template for the generation of this reporter construct and primers with overhanging restriction sites where designed to clone out both the promoter and the terminator if this line. First, the SoxB2 5' genomic region was inserted in the construct (*SoxB2*::GFP:: *β-tubulin*) and after confirmation of the insertion, the 3' genomic region was replaced as well by the 3' SoxB2 genomic region (*SoxB2::GFP::SoxB2*) by restriction digest-based cloning (see section 2.2.6). The plasmid was then transformed into chemically competent bacteria (see section 2.2.7 and 2.2.8).

2.2.4 SoxB3::mScarlet::SoxB3 reporter line

The SoxB3 reporter line was generated by Gibson assembly-based cloning. Like SoxB1 reporter line, PCR primers were designed to clone both the upstream and downstream genomic regions of *Hydractinia SoxB3* coding sequence without any overhangs. The construct was originally designed to contain GFP and for reasons mentioned later, GFP was replaced by mScarlet. Primers were also designed with 20-30bp overhangs on both the backbone and GFP to flank the 5' and 3' genomic region fragments. For both SoxB1 and SoxB3 lines the same assembly strategy was followed (see section 2.2.2). In order to replace GFP with mScarlet, primers were designed with overhanging restriction sites for both the vector and the fluorescent protein. The resulted fragments were ligated (see section 2.2.6) and the resulted vector was transformed into chemically competent bacteria (see section 2.2.7 and 2.2.8).

2.2.5 PCR and gel DNA extraction

Two main approaches were used for PCR purposes: Phusion High-Fidelity DNA Polymerase (Thermo Fisher Scientific; F530), and MyTaq DNA Polymerase (BioLine; BIO-21101). Phusion approach was used for all cloning PCRs and Mytaq approach mostly for insert confirmation PCRs as per manufacture's guidelines. All PCR products were ran on 1% agarose gels (Fisher; BP1356) for 25-20min at 100V and visualized using the FluorChem FC2 Imager. Gel DNA extraction of the desired bands was carried out by using Nucleospin Gel and PCR clean-up kit as per manufacturer's instructions (Macherey-Nagel; 740609.50). The eluted DNA concentration and purity was measured by NanoDrop spectrophotometer.

2.2.6 Restriction digest-based cloning

After successful PCR and gel DNA extraction, the desired fragments (backbone and inserts) were digested with the appropriate restriction enzymes by using 100ng of the backbone fragment and either equimolar or 3x molar excess of the insert fragment along with 0.5-1µl of each restriction enzyme, and 10x reaction buffer and nuclease-free water to a final reaction volume of 20µl. The reaction mixtures were placed at a 37°C water bath for one hour followed by a 20min heat inactivation phase at 80°C. The reaction mixtures were then placed in room temperature (RT) to gradually cool down. Ligation was then carried out by adding 0.7µl T4 DNA ligase 5U/µl (Thermo Fisher Scientific; EL0011) and 2.3µl 10x T4 DNA ligase buffer. The ligation could be achieved by either a 60min incubation at RT or overnight (ON) at 4°C.

2.2.7 Bacterial production, transformation and culture

Chemically competent XL1 Blue *Escherichia coli* (*E. coli*) bacteria must be first made along with LB broth and agar without antibiotics and autoclaved. Once all the materials needed were prepared, bacteria taken from the stock sample were mixed with LB broth, spread on agar plates and incubated ON at 37°C. The following day, individual colonies were selected and grown without any antibiotics in 5ml of broth ON at 37°C along with the necessary controls. The 5ml bacterial culture was then inoculated in 300ml of LB broth and allowed to grow at a 37°C incubator for ~2-3hours until an OD600 of 0.35-0.40 is reached. Once the optical density was at the desired level, the media was aliquoted in 50ml pre-chilled tubes and centrifuged for 10min at 3500RPM at 4°C. The supernatant was then discarded, and

pellets were resuspended in 5ml of pre-chilled sterile-filtered 0.1M $CaCl_2$ and left on ice for 10min. Bacterial resuspensions were centrifuged again at 3500RPM for 10min at 4°C and resuspended in 1ml of pre-chilled sterile-filtered 14% glycerol / 0.1M $CaCl_2$. Chemically competent bacteria were then aliquoted into pre-chilled 1.5ml tubes and stored at 80°C for future use.

Chemically competent XL1 Blue bacterial transformation was achieved by adding either the ligation mixture (from section 2.2.4) or 500-1000ng of plasmid into 50µl of bacteria. The tubes containing the mixture were transferred to a 42°C water bath for 90seconds and then were immediately placed on ice for 5min. LB broth was then added to a final volume of 200µl and incubated at 37°C at least for 30min for the bacteria to recover. LB agar plates containing the appropriate antibiotic (carbenicillin 100µg/ml - working concentration) were pre-warmed and once the bacteria had recovered, were spread onto the plates and incubated at 37°C ON.

The resulted colonies were individually selected and grown ON at 37°C in 5ml LB broth containing antibiotics along with necessary controls to exclude the possibility of contamination. The following day, plasmids were extracted as described in section 2.2.6.

2.2.8 Plasmid extraction

Plasmid extraction was performed either for small- or large-scale culture volumes. Before any plasmid extraction approach, 500µl bacterial culture was taken and stored in -80°C for future use (mixed with 90% glycerol, 1:1). For the small-scale colony culture (5ml), the GenElute Plasmid Miniprep kit was used (Sigma-Aldrich; PLN350) as per manufacturer's instructions. For large-scale cultures (300ml), an in-house protocol was used. Bacterial suspension was aliquoted in 50ml tubes and centrifuged at 7000RPM for 10min at 4°C. The resulting pellets were resuspended in 10ml resuspension buffer (25mM Tris-HCl pH8, 10mM glucose, 10mM EDTA pH8; solution needed to be autoclaved) by a gentle mixing. Then, 20ml lysis buffer (0.2M NaOH, 1%SDS) were added and tubes are gently inverted several times to ensure solutions were well mixed and left for 5min at RT before adding 15ml neutralization buffer (3M CH_3CO_2K, 11.5% v/v glacial acetic acid). Solutions were further mixed by gentle inversion and then left on ice for 5min before centrifuged at full speed (RPM) for 15min at 4°C. The resulted supernatant was filter by placing 125mm filter paper (Fisher; FB59025) shaped into a cone onto a 50ml tube and 0.6 volumes of 100% isopropanol was added and mixed to the collected flow through before being placed for 20min at -20°C (it can also be placed at -20°C

ON). Next, the suspensions were centrifuged at 7500RPM for 15min at 4°C and the resulted pellets were washed once with 10ml 75% ethanol (at this point the pellets are combined in one tube) before being centrifuged one more time at 7500RPM for 15min at 4°C. The pellet was then resuspended in 1ml nuclease-free water with RNase mix [RNase mix: 2µl RNaseA (Thermo-Fisher Scientific; EN0531, 1µl RNase T1 (Thermo-Fisher Scientific; EN0541)] and incubated at 37°C for one hour. Afterwards, SDS and NaCl were added to the mixture at 1% and 0.5M final concentrations respectively along with 2µl Proteinase K (25mg/ml stock) for one hour at 55°C and then the samples were ready for phenol:chloroform plasmid extraction.

Based on a standard phenol:chloroform extraction protocol, one volume each of phenol (Sigma-Aldrich; P4557) and chloroform (Sigma-Aldrich; C2432) were added to the mixture and mixed vigorously before being centrifuged at maximum speed (RPM) for 3min at RT. Next, the upper aqueous layer was collected, and equal volume of chloroform was added, followed by centrifugation at maximum speed (RPM) for 3min at RT. Again, the upper aqueous layer was collected, and plasmid precipitation was achieved by adding 2.5 volumes of 100% ethanol and 1/10th volume 5M KCl followed by a maximum-speed centrifugation at RT. The resulted pellet was washed once or twice with 1ml 75% ethanol and let to air dry before resuspending in 20-40µl nuclease-free water (depends on the desired concentration).

Plasmid microinjections and embryo maintenance were performed as described in sections 2.1.1 and 2.1.2.

2.2.9 Genomic DNA extraction, and RNA extraction for cDNA synthesis

For genomic DNA extraction, ~200-300 polyps were used. Once the ASW was completely removed, the tissue was macerated and lysed by adding 200µl of DNA lysis buffer (100mM Tris HCl pH8, 50mM EDTA, 1% SDS) and by using a plastic pestle (cleaned with bleach, ethanol and diH_2O prior use). An additional 800µl of DNA lysis buffer was added and maceration was continued until there were no visible clumps. Next, 2µl of each RNaseA and RNase T1 were added and incubated at 37°C for one hour, followed by the addition of 8µl of Proteinase K (stock: 25mg/ml) and incubated for an additional 2-3 hours at 50°C. The genomic DNA was then extracted using a standard phenol:chloroform extraction protocol as described in section 2.2.8 with the replacement of KCl with 1/10th the volume of 5M NaCl.

2.3 Cellular Staining

2.3.1 Immunofluorescence (IF) staining

Polyps or larvae were first relaxed and cut as described in Section 2.1.3 prior fixation. For standard IF staining, the tissue was fixed in 4% PFA in PBS for 60min at RT or ON at 4ºC followed by three washes of 10min each with PBS with 0.3% TritonX-100 (PBSTx). For storage, the tissue was dehydrated by incubation in increasing concentrations of ethanol diluted in PBSTx and stored in -20ºC (25%, 50%, 75% and 100%; 5min each wash). Tissue was then slowly rehydrated by washing in decreasing concentrations of ethanol followed by three washes of 10min each with PBSTx. The tissue was then blocked for one hour in 3% BSA in PBSTx and primary antibodies were added ON at 4ºC (Table 2.2). The following day, tissue was washed three times 10min each with PBSTx and blocked again for 15min with 5% serum in BSA/PBSTx (goat serum unless indicated otherwise). Secondary antibodies (Table 2.3) were added based on the host of the primary antibodies in 5% serum in BSA/PBSTx for one hour in RT and then the tissue was washed three times 10min each with PBSTx. Nuclear staining was then carried out with Hoechst 33258 (use: 1 in 2000; stock: 20mg/ml; Sigma-Aldrich; B2883) for 15min at RT followed by three washes 10min each with PBSTx. Tissue was then mounted in Fluoroshield (Sigma-Aldrich; F6182) on glass microscopic slides (Fisher Scientific; 11562203).

To increase tissue permeability, after fixation the tissue could be washed in increasing concentrations of methanol followed by two washes with 100% acetone. Then, decreasing concentrations of methanol were carried out followed by the standard IF protocol described above.

Table 2.2. List of primary antibodies used.

Primary Antibody	Host Species	Source	Dilution
Anti-Piwi1	Rabbit	In house	1:2000
Anti-Piwi2	Guinea pig	In house	1:500
Anti-acetylated tubulin	Mouse	Sigma-Aldrich; T7451	1:1000
Anti-RFamide	Rabbit	Gunther Plickert	1:1000
Anti-GLWamide	Rabbit	Thomas Leitz	1:1000
Anti-Ncol1	Rabbit	Suat Ozbek	1:500
Anti-centrin2	Rabbit	Ciaran Morrison	1:500

Anti-Ncol3	Guinea pig	Suat Ozbek	1:500
Anti-GFP	Rabbit	Santa Cruz; 8334	1:1000
Anti-RFP	Rat	Chromotek; 5F8	1:1000

Table 2.3. List of secondary antibodies used.

Secondary Antibody	Host Species	Source	Dilution
Anti-rabbit AF488	Goat	Abcam; ab150077	1:500
Anti-rabbit AF594	Goat	Abcam; ab150080	1:500
Anti-rabbit AF647	Goat	Abcam; ab150079	1:500
Anti-mouse AF488	Goat	Abcam; ab150113	1:500
Anti-mouse AF594	Goat	Abcam; ab150116	1:500
Anti-mouse AF647	Goat	Abcam; ab150115	1:500
Anti-rat AF594	Goat	Abcam; ab150160	1:500
Anti-rat AF647	Goat	Abcam; ab150159	1:500
Anti-guinea pig AF594	Goat	Abcam; ab150188	1:500

Table 2.4. List of antibodies used for western blotting.

Antibody	Host Species	Source	Dilution
Goat anti-rat IgG H&L (HRP)	Goat	Abcam; ab205720	1:1000
Goat anti-rabbit IgG H&L (HRP)	Goat	Abcam; ab205718	1:1000
Goat anti-guinea pig IgG H&L (HRP)	Goat	Abcam; ab97155	1:1000

2.3.2 Nematocyte capsule staining by FITC-coupled lectin

Tissue (polyps or larvae) was prepared and cut as described in section 2.1.3 prior fixation. All the steps described below were done on the shaker and in RT unless otherwise stated. Fixation was carried out by incubating the tissue in TBS-T for 10-30min. Following, the tissue was washed three times for 5 min each with TBST-T and blocked for one hour with 2% BSA in TBS. Three more washes of 5min each were carried out with TBS, and then lectin was added in a 15µg/ml final concentration diluted in TBS-T. Lectin incubation was for one hour and samples were protected from light. Then, three more washes of 5min each with TBS were

carried out, and Hoechst (1.1000) was added for 30min. Samples were washed again for three times before mounting them in Fluoromount. Mounted samples were left overnight at 4°C to cure before imaging. Samples could be imaged only within 2-3 days after curing and could be stored in 4°C – not 20°C.

TBS (final concentrations): 20mM Tris-HCl, 100mM NaCl, 1mM $CaCl_2$, 1mM $MgCl_2$, adjust pH to 7.2 and fill up to 1000ml with dH2O.

TBS-T: add 0.5% Triton (final concentration)

2.3.3 EdU staining of cycling cells

For the EdU staining, a Click-iTEdU Alexa Fluor 488 Imaging kit was used (Invitrogen; C10337) and all the solutions were prepared according to manufacturer's instructions.

Adult polyps (intact or decapitated) were prepared as described in section 2.1.3. Prior fixation, the polyps were incubated in EdU solution for 30min or more depending on the experiment (stock concentration 10mM; 1µl EdU/1ml ASW), washed three times in ASW and incubated in $MgCl_2$ before fixation. Polyps are then fixed in 4%PFA in PBS for one hour at RT and washed once with 3% BSA in PBSTx for 30min. Next, two washes with PBSTx were carried out (1st wash: one hour; 2nd wash: 30min), followed by two washes with 3% BSA in PBSTx for 5min each. The tissue was then incubated in Click-iT cocktail for 30min (~100µl per 100 polyps; protect from light) followed by three washes of 3% BSA in PBSTx for 20min each. At this stage, polyps could be mounted for imaging or continue to IF protocol for additional staining (see section 2.3.1).

Briefly, the Click-iT cocktail was prepared by mixing 86µl 1x Click-iT reaction buffer, 4µl $CuSO_4$, 0.24µl AF488 azide, and 10µl reaction buffer additive (total volume ~100µl).

2.4 *In situ* hybridization

2.4.1 SoxB coding sequences cloning

In order to start synthesizing the probes, the whole coding sequences all three SoxB genes were cloned from gDNA or cDNA (section 2.2.9) and inserted into a pGEM-T Easy Vector System I (Promega; A1360) according to manufacturer's standard reaction protocol. Briefly, 1.5µl of the coding sequence template (~100ng/µl) was mixed with 0.5µl pGEM vector along with 0.5µl T4 DNA ligase and 2.5µl 2xrapid ligation buffer, and incubated ON at 4°C followed by normal bacterial transformation and plasmid extraction (see section 2.2.7 and 2.2.8). The plasmids were then sequenced to identify the orientation of the coding sequence within the plasmid as the pGEM vector contains both SP6 and T7 sites.

2.4.2 RNA probe synthesis (for FISH)

The coding sequences of the three SoxB genes and Piwi1 were first amplified by PCR (see section 2.2.5) from their vectors using generic SP6 and T7 primers (Appendix A) and then used as DNA templates for transcription. For the synthesis of SP6 probes, the HiScribe SP6 RNA Synthesis kit (NEB; E2070) is used and for T7 probes the HiScribe T7 High Yield RNA Synthesis kit (NEB; E2040) with a few modifications from the manufacturer's instructions (Table 2.5).

Table 2.5. Detailed description on how to make either SP6/T7 Fluorescein/Digoxigenin probes for FISH.

FOR DIGOXIGENIN PROBES	ATP	2.5 µl (5mM final conc.)
(T7 OR SP6)	GTP	2.5 µl (5mM final conc.)
	CTP	2.5 µl (5mM final conc.)
	UTP	2.5 µl (5mM final conc.)
	Digoxigenin-11-UTP (Roche; 11209256910)	3.75 µl
	DNA template	X µl (0.5 µg)
	SP6 or T7 polymerase mix	2.5 µl
	SP6 or T7 reaction buffer (10x)	2.5 µl
	RNase inhibitor (RiboLock0 (Thermo-Fisher Scientific; E00381)	0.5 µl

FOR FLUORESCEIN PROBES **(T7 OR SP6)**	Nuclease-free H_2O	X µl
	Fluorescein RNA labelling mix 10X (Roche; 11685619910)	2.5 µl
	DNA template	X µl (0.5 µg)
	SP6 or T7 polymerase mix	2.5 µl
	SP6 or T7 reaction buffer (10x)	2.5 µl
	RNase inhibitor (RiboLock0 (Thermo-Fisher Scientific; E00381)	0.5 µl
	Nuclease-free H_2O	X µl

Once the probes were made, a formaldehyde denature gel is made in order to check their quality. The 1.5% gel was prepared by dissolving 0.75g agarose in 36ml DEPC water and adding 5ml 10X MOPS and 9ml deionized formaldehyde (Sigma; F8875). The RNA samples and RiboRuler RNA ladder (Thermo Fisher Scientific; SM1821) were mixed 1:1 with 2x RNA gel loading dye (Thermo Fisher Scientific; R0641), heated for 10min at 70°C and then placed on ice for 2min. Once the gel had set, the samples/ladder were loaded and ran for 25-30min at 100V and visualized using FluorChem FC2 Imager.

2.4.3 Double FISH protocol

Tissue (embryos, larvae, feeding and sexual polyps) were cut and prepared as in section 2.1.3 prior fixation. All the reagents and buffers used from this point onwards were ice cold before use. The animals were first fixed for 90seconds in ice-cold 0.2% glutaraldehyde (stock: 25%, Sigma-Aldrich; G5882) in 4% PFA (stock: 16%, Alfa Aesar; 43368) in filtered ASW and then in 4% PFA in PBS-0.1% Tween (PTW) for one hour at 4°C followed by three quick washes with PTW. Both fixation steps were carried out in glass petri dishes and all the post-fixation steps in Eppendorf tubes. Post-fixation washes (5min each) were done in increasing concentrations of methanol in PTW (2x 25%MeOH, 2x 50%MeOH, 1x 75%MeOH, 3x 100%MeOH) and then the samples were either stored for future use or continued with the procedure. Next, the tissue was permeabilized by washes in increasing concentrations of methanol in acetone and rehydrated with washes in decreasing concentrations of methanol in PTW.

The next steps were done with reagents and buffers in RT. Following rehydration of the tissue, three PTW quick washes were done to remove any residual methanol and then the activity of PFA was quenched by two washes 5min each with glycine (2mg/ml; Fisher Scientific; BP381-1)) in PTW followed by three PTW washes. By this stage, the tissue was distributed in 24-well tissue culture plates according to the needs.

Once the tissue was allocated in the culture plate, it was pre-hybridized by adding pre-heated hybridization buffer ON (section 2.4.4), and then hybridized for two days in pre-heated hybridization buffer containing the desired probes (1ng/µl). The hybridization temperature depends on the probe with the range being 55-60°C.

Following, all the post-hybridization washes were done at hybridization temperature. First, the tissue was washed twice with a simpler version of the hybridization buffer (section 2.4.4) for 10min and 40min. Then, washes for 30min were carried out in decreasing concentrations of hybridization buffer in 2x SSC (see section000) followed by three washes of 15min each in 2x SSC.

At this point, all the washes/incubation steps were moved from hybridization temperature to RT. Quick washes in decreasing concentrations of 0.2x SSC in PTW were done followed by five quick washes in PTW. Once the post-hybridization washes were done, the endogenous peroxidase activity was quenched by incubating the tissue in 3% hydrogen peroxide (Fisher; H/1800/15) in PTW for one hour at RT protected from light followed by three washes of PTW for 10min each. The tissue was then incubated with the first antibody (anti-DIG POD, 1:1000; Roche 11207733910) in 1% blocking buffer (Roche; 11096176001) in maleic acid buffer (section 2.4.4) ON at 4°C followed by three washes of 10min each with PTW.

The developing process of the first antibody was done preferably with Rhodamine in developing buffer (section 2.4.4) with three incubations of one hour each at RT followed by an ON incubation at 4°C.

The next day, at least five PTW washes were carried out, or until the tissue has no residual Rhodamine or Fluorescein, and then the tissue was either prepared for mounting or a second antibody incubation. If the tissue was prepared with a single probe, it was then stained with the nuclear marker Hoechst (1:2000) in PTW for 15min and washed and mounted in 100mM Tris-pH8 in 50% TDE (Sigma; 166782).

In the case of a double FISH, after the ON incubation with the developing buffer, the tissue was washed thoroughly with PTW and then washed once for 10min with 0.1M glycine pH2

followed by three quick PTW washes. The tissue was then shortly blocked with 1% blocking buffer in maleic acid buffer and incubated with the second antibody (anti-Fluorescein POD, 1:1000, Roche; 11426346910) in 1% blocking buffer in maleic acid buffer ON at 4ºC followed by three washes of 10min each with PTW.

The developing, post-developing washes, nuclear staining and mounting were done the same way as described above but instead of Rhodamine, Fluorescein was used. After the post-developing washes but before TDE washes and mounting, the tissue could be quickly washed with increasing concentrations of methanol in PBS and then with decreasing concentrations of the same solutions to remove background staining.

2.4.4 Buffers and solutions (for FISH)

All the solutions and buffers were made with DEPC water.

DEPC water: 500µl DEPC (Sigma; D5758) in 1L MiliQ water. Mixed well and left ON at 37ºC. Autoclaved the next day.

10X PBS in DEPC H_2O: 80g NaCl, 2g KCl, 14.4g Na_2HPO_4, 2.4g KH_2PO_4 (per 1000ml)

20X SSC in DEPC H_2O: 175.3g NaCl, 88.2g $Na_3C_6H_5O_7$ (per 1000ml)

Hybridization buffer (per 40ml): 20ml formamide (Sigma-Aldrich; F9037), 10ml 20x SSC pH4, 100µl heparin (20mg/ml; Sigma-Aldrich; H3393), 100µl Tween20 (Sigma-Aldrich; P1379), 2ml 20% SDS (Sigma-Aldrich; L3771), 100µl salmon sperm DNA (Sigma-Aldrich; D1626), 40mg blocking buffer powder, 1% dextran sulfate (Alfa Aesar; J70796), fill to 40ml with DEPC water and heat to help dissolve.

"Simpler" hybridization buffer (per 40ml): 20ml formamide, 10ml 20x SSC pH7.5, 100µl Tween20, 2ml 20% SDS, 100µl heparin (20mg/ml), fill to 40ml with DEPC water.

1X Maleic acid buffer (per 500ml): 6.91g Maleic acid (Sigma-Aldrich; M0375), 4.38g NaCl (Sigma-Aldrich; S7653) and adjust the pH to 7.5 by adding NaOH pellets (Fisher; S/4920/53).

Rhodamine/Fluorescein: Prepared as described in Wolenski *et al.*, Nat Protoc, 2013

Developing buffer: 2% dextran sulfate in PTW, 0.001% H_2O_2, 1:100 Rhodamine or Fluorescein, 1:200 Iodophenol (100mg/ml in 100% ethanol). Always add fresh H_2O_2, Rhodamine/Fluorescein and Iodophenol.

2.4.5 DNA probe synthesis (for SABER FISH)

Before starting to make the probes, all the reagents and tubes were placed on metal tube holders on ice to keep them ice cold.

Next, the "oligo pool" was made by mixing the required amount of oligos (concentration: 10µM) to have a final volume of 10µl. For example, if 15 oligos were used per probe, then 0.67µl from each oligo was used to have a total volume of 10µl. After making the oligo pool, in a separate PCR tube 10µl of the desired hairpin was added and left on ice until needed.

The master mix was then prepared as follow and placed in the tube with the exact order as written here:

1. 10µl - 10X ThermoPol buffer (or 10X PBS)
2. 44µl - nuclease-free H_2O
3. 10µl - 100mM $MgSO_4$
4. 5µl - dNTP mix (A, T, C only; 6mM each)
5. 10µl - 1µM CleanG
6. 1µl - Bst LF polymerase

The above master mix (80µl) was added to the PCR tube already containing the hairpin (90µl total). The tubes were then placed in a PCR machine and the following program was used:

1. Heat cycler to 37°C
2. Pause the program and insert the tubes containing the master mix + hairpin
3. Incubate for 15min at 37°C
4. Pause the program, add the oligo pool and mix well
5. Incubate for 4 hours at 37°C
6. Heat to 80°C for 20min
7. Cool down to 4°C

Once the PCR reaction was done, the Monarch PCR & DNA clean-up kit (NEB #T1030S) was used to elute the probes according to manufacturer's instructions. Nanodrop was then used to measure the single-stranded DNA amount.

2.4.6 SABER FISH protocol

Tissue was fix and dehydrated the same way like in the normal fluorescence *in situ* hybridisation described in section 2.4.3. Samples were then bleached by incubating in 1%

H_2O_2 diluted in 100% MeOH (ice cold) for 45 min (RT / on the rocker), followed by 2 quick washes with ice-cold 100% MeOH. Then, tissues were permeabilised by quick washing in decreasing and then increasing concentrations of methanol diluted in acetone (1x 75% MeOH, 1x 50% MeOH, 2x 25% MeOH, 1x 50% MeOH, 1x 75% MeOH, 1x 100% MeOH), followed by rehydration with quick washes in decreasing concentrations of methanol in PTW (1x 75% MeOH, 1x 50% MeOH, 1x 25% MeOH).

The next steps are done with reagents and buffers in RT. Following rehydration of the tissue, three PTW quick washes are done to remove any residual methanol and then the activity of PFA is quenched by two washes 5min each with glycine (2mg/ml; Fisher Scientific; BP381-1)) in PTW followed by three PTW washes. By this stage, the tissue is distributed in 24-well tissue culture plates according to the needs.

Samples were then washed once for 5 min in Triethanolamine pH8 (TEA), followed by another wash in TEA pH8 with the addition of 6µl of acetic anhydrite. Acetic anhydrite would form a drop-like appearance in the well and so the samples were left on the rocker until the drop was dissolved. Another wash with TEA followed but this time 12µl of acidic anhydrite were added and placed on the rocker until drop was dissolved. A few washes with PTW followed.

Samples were then placed in Whyb buffer (pre-warmed at 43°C) and incubated at 43°C for 10 min. Whyb buffer was then replaced with Hyb1 buffer (pre-warmed at 43°C) and placed in a 43°C incubator overnight (pre-hybridisation). The next day, probes were pre-heated to 60°C in Hybe buffer and once Hyb1 buffer was removed, probes in Hybe buffer were added. Probes were added at a concentration of 1µg/120µl (e.g. 96µl hybe buffer, 5µl of 200ng/µl of probe 1, 5µl of 200ng/µl of probe 2, and 14µl diH_2O). Since Hyb1 buffer was very viscous, in order to remove it without losing any samples, it was quickly diluted with Whyb. Tissue was then incubated with the probes for two days at 43°C.

All the following steps were done at hybe temperature and all the reagents were pre-warmed (43°C). Probes were removed and replaced with Whyb buffer for 10 min. Probes could be re-used up to three times. Then, two washes with Whyb buffer for 30 min each were done, followed by a 10 min wash with 50% Whyb buffer in 2x SSCTw. Two more washes with 2X SSCTw were followed for 10 min each.

The steps followed were performed at 37°C. 2x SSCTw was replaced with PTW (two quick washes), and samples were then transferred in a 37°C incubator. Once the samples were warmed up to 37°C, Hyb2/fluor solution was added and samples were incubated for one hour

at 37°C. Hyb2/fluor solution was also pre-warmed at 37°C before it was added to the samples (e.g. 96µl Hyb2 buffer, 2.4µl fluor oligo 1, 2.4µl fluor oligo 2, and 19.2µl diH_2O).

After thay, Hyb2/fluor solution was replaced with pre-warmed Whyb2 for a 10 min incubation at 37°C followed by two washes of 5 min each with PTW. Nuclear staining was then performed in RT by diluting Hoechst in PTW (1:2000) and incubating the samples for 45-60 min at RT. Samples were then quickly washed twice with PTW and mounted in 97% TDE. Samples were imaged within 4 days.

2.4.7 Buffers and solutions (for SABER FISH)

All solutions were made using diH_2O instead of DEPC water.

Whyb (wash hyb buffer): 2XSSC pH7, 1% Tween20, 40% formamide, fill up with diH_2O.

Hyb1 (pre-hybridisation): 2XSSC pH7, 1% Tween20, 40% formamide, 10% Dextran sulfate, fill up with diH_2O.

Hyde buffer: 20ml formamide, 10ml 20x SSC pH4, 100µl heparin (20mg/ml, 100µl Tween20, 2ml 20% SDS, 100µl salmon sperm DNA, 40mg blocking buffer powder, 1% dextran sulfate, fill to 40ml with diH_2O and heat to help dissolve.

Hyb2 (for fluorescence detection): 1X PBS, 0.2% Tween20, 10% Dextran sulfate, fill up with diH_2O.

Whyb2: 1X PBS, 0.1% Tween20, 30% formamide, fill up with diH_2O.

2X SSCTw: 2X SSC pH7, 0.1% Tween20

2.5 Gain and loss of function approaches

2.5.1 Short-hairpin RNA interference

For short-hairpin RNA interference experiments, primers were designed to clone unique sites of the three SoxB genes (Appendix A). Stock primers (100mM) containing a T7 site were directly used and incubated at 98°C for 2min and then left in RT for 10min to anneal; 2µl of each primer were used and mixed with nuclease-free water to a final reaction volume of 20µl. Following, T7 transcription was carried out by using the total reaction volume from the previous step (20µl) as a DNA template along with 3.5µl of each NTP (ATP, GTP, UTP, CTP;

100mM stock concentration), 4µl of 10x reaction buffer and 3µl of T7 RNA polymerase mix (HiScribe T7 High Yield RNA Synthesis kit, NEB; E2040). The mixture was then incubated ON at 37°C. The next day, the products were DNase treated for one hour at 37°C with 40µl of DNase solution (5µl DNaseI in 35µl RDD buffer; Qiagen RNAse-free DNase set; 79254) and RNA was isolated by using Quick-RNA MiniPrep kit (Zymo Research; R1054) following manufacturer's instructions. The eluted RNA was quantified using NanoDrop and the quality was checked by running a formaldehyde denature gel (section 2.4.2). Embryos were injected at a concentration of 250 ng/µl for all three SoxB genes, and for Piwi1/Piwi2.

2.5.2 Overexpression constructs

Plasmid construct for SoxB1 ectopic expression was designed as illustrated in Fig. 2.2.

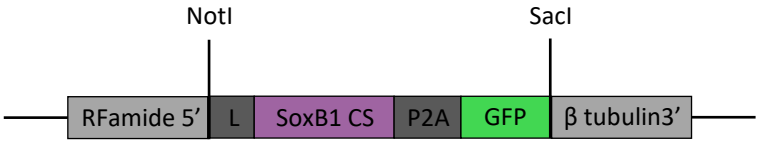

Figure 2.2. Construct design for over-expressing *SoxB1* in RFamide context.

Primers with overhang restriction sites and a linker on the forward primer only were designed for the coding sequence to be amplified from the plasmid generated in section 2.4.1. Following, this fragment was inserted by restriction digest (see section 2.2.6) to an already digested Piwi1::AP2::P2A::Piwi1 plasmid (AP2 was digested out) and the Linker::SoxB1::P2A::GFP cassette was digested out from the plasmid in order to be ligated into RFamide plasmid.

Once the insertion was confirmed by both sequencing and PCR, the plasmid was transformed into bacteria, followed by bacterial culture and plasmid extraction as described in sections 2.2.7 and 2.2.8.

2.6 *In vivo* imaging

Polyps from transgenic colonies were isolated and decapitated (see section 2.1.3). Next, they were transferred carefully in 35mm imaging dishes with a glass bottom (Ibidi; D 263) and 0.5% low-melt agarose in filtered ASW was placed drop by drop on individual polyps in order

to secure them as closer to the bottom of the dish as possible. Once the polyps were settled, low-melt agarose was poured in the dish in order to cover the whole bottom and once it was polymerized, an Andor spinning disc confocal microscope was used to generate time-lapse movies. Data were then analysed using ImageJ/Fiji software (ImageJ 1.52i version).

2.7 Flow cytometric techniques

2.7.1 Tissue dissociation

Adult polyps were cut from their colonies as described in section 2.1.3 and placed in 0.5% pronase (Sigma-Aldrich; 10165921001) in filtered ASW (20 polyps/200µl) for 2-3 hours with constant rocking in RT. Every 30 min a gentle mixing was given to accelerate the process. Once the tissue was fully dissociated, the reaction was stopped by adding BSA at a final concentration of 0.1%. Following, the cell suspension was passed through a 100µm filter to remove any residual clumps. By this point, cell suspensions were transferred to FACS tubes (Sarstedt; 55.1578) (Fig. 2.3).

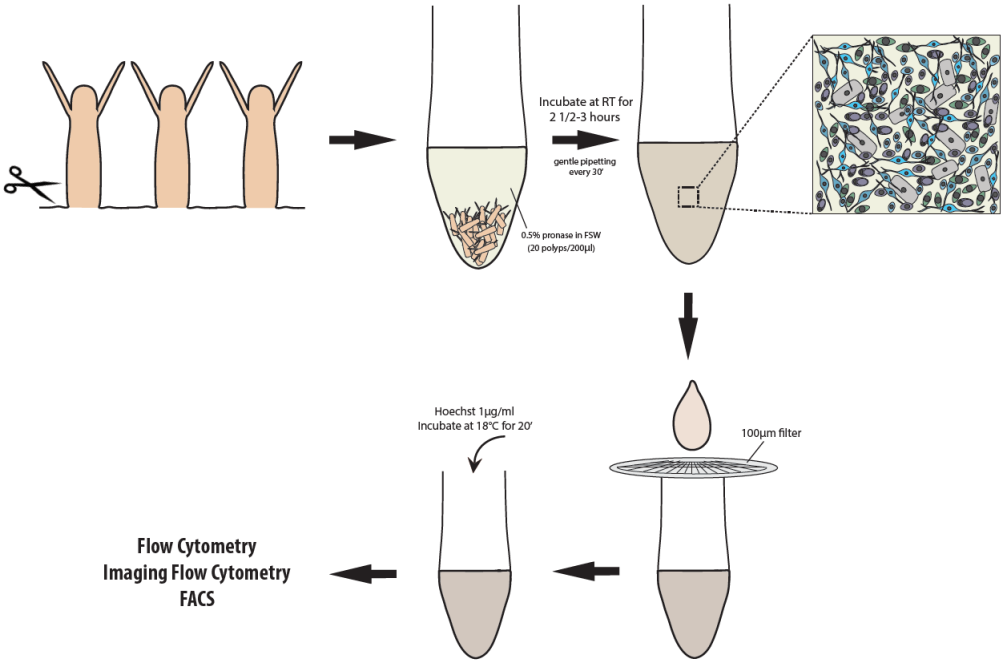

Figure 2.3. Schematic representation of tissue dissociation procedure for flow cytometric analysis. For details see section 2.7.1

2.7.2 Flow Cytometry

After tissue dissociation, cells were stained with 7.5µl of 1mg/ml Hoechst33342 per 200µl cell suspension (37.5µg/ml; Sigma-Aldrich 14533) for 20 min at 18ºC and analysed using BD FACSCanto II (Becton-Dickinson Biosciences). The gating of distinct cell populations was performed using the BD FACSDiva™ software (Becton-Dickinson Biosciences) based on the transgene (GFP) and Hoechst expression levels of the cells. Wild type cells were always used as a control and to set the gates. The resulted data were analysed using FlowJo V10 software (FlowJo). For the measurement of GFP and Hoechst fluorescence levels, the blue (488nm) and violet (405nm) excitation lasers were used with 530/30nm and 450/50nm optical filters respectively.

2.7.3 Imaging Flow Cytometry

To determine the morphological nature of the cell populations identified by flow cytometry, the ImageStream^x Mark II imaging flow cytometer (Amnis) was utilized. Cells were prepared as described in sections 2.7.1 and 2.7.2. The gating was performed using the INSIRE™ software and data were analysed using the IDEAS™ software (Amnis).

2.7.4 Fluorescence-activated cell sorting and RNA extraction

A hundred polyps from each reporter line (x3 clones) were dissociated as described in section 2.7.1 and stained with a nuclear marker as in section 2.7.2. The cells were gated based on their GFP and Hoechst fluorescent intensity using the BD FACSDiva software and sorted on a BD FACSAria II flow cytometer (Becton-Dickinson Biosciences) using a 100 µm nozzle size. Cells were sorted directly into 5ml tubes containing 600 µl Trizol for subsequent RNA extraction using the Direct-zol™ RNA MiniPrep kit (Zymo Research R2050) based on manufacturer's inctructions. Extra cells were sorted directly into sea water for purity check. To avoid applying more stress to the cells, the sheath fluid of the instrument was replaced by filtered sea water.

2.7.5 Cell cycle analysis

For cell cycle analysis, cells were prepared as described in section 2.7.1 and nuclear staining was performed as stated in section 2.7.2. The only thing that changed was the way the data were analysed. Detailed analysis can be found in section 5.5.

2.8 Protein detection by Western blotting

2.8.1 Protein extraction

Prior to protein extraction, polyps were starved for two days. For a good yield of protein, 3-5mg of tissue were homogenized by adding 10% w/v of RIPA buffer (150mM NaCl, 0.1% Triton X-100, 0.5% sodium deoxycholate, 0.1% SDS, 50mM Tris HCl pH8). EDTA-free protease inhibitor cocktail (Roche; 11873580001) at a final concentration of 1X was added fresh every time. Once the tissue was fully homogenized with a pestle, the samples were left on ice for 30min and then centrifuged at 1000g for 10min at 4°C. The protein concentration was then measured by using the Pierce BCA Protein Assay kit (Thermo Fisher Scientific; 23227) according to manufacturer's instructions. The protein extract was then transferred to a new tube and either stored at -80°C or used straight away.

Sample preparation for gel loading was achieved by boiling them for 5min at 95°C in 2X PG loading buffer (100mM Tris HCl pH6.4, 4% SDS, 0.01%bromophenol blue, 20% glycerol).

2.8.2 Gel preparation and protein transfer

Both SDS gels – separating and stacking – were made as outline below (Tables 2.6, 2.7, 2.8):

Separating gel (12% or 15% depending on the protein size):

Table 2.6. Detailed recipe for 12% separating gel.

12% gel	**5ml**	**10ml**	**15ml**	**20ml**	**25ml**	**30ml**
dH_2O	1.7ml	3.3ml	5ml	6.6ml	8.3ml	9.9ml
30% acrylamide (Fisher; BP1410-01)	2ml	4ml	6ml	8ml	10ml	12ml
1.5M Tris (pH 8.8)	1.3ml	2.5ml	3.8ml	5ml	6.3ml	7.5ml
10% SDS	50ul	100ul	150ul	200ul	250ul	300ul
10% APS (Sigma Aldrich; A3678)	50ul	100ul	150ul	200ul	250ul	300ul
TEMED (Roth; 2367.1)	2ul	4ul	6ul	8ul	10ul	12ul

Table 2.7. Detailed recipe for 15% separating gel.

15% gel	5ml	10ml	15ml	20ml	25ml	30ml
diH_2O	1.2ml	2.3ml	3.5ml	4.6ml	5.7ml	6.9ml
30% acrylamide	2.5ml	5ml	7.5ml	10ml	12.5ml	5ml
1.5M Tris (pH 8.8)	1.3ml	2.5ml	3.8ml	5ml	6.3ml	7.5ml
10% SDS	50ul	100ul	150ul	200ul	250ul	300ul
10% APS	50ul	100ul	150ul	200ul	250ul	300ul
TEMED	2ul	4ul	6ul	8ul	10ul	12ul

Stacking gel:

Table 2.8. Detailed recipe for stacking gel.

	1ml	2ml	3ml	4ml	5ml	6ml	8ml	10ml
diH_2O	680ul	1.4ml	2.1ml	2.7ml	3.4ml	4.1ml	5.5ml	6.8ml
30% acrylamide	170ul	330ul	500ul	670ul	830ul	1ml	1.3ml	1.7ml
1M Tris (pH 6.8)	130ul	250ul	380ul	500ul	630ul	750ul	1ml	1.25ml
10% SDS	10ul	20ul	30ul	40ul	50ul	60ul	80ul	100ul
10% APS	10ul	20ul	30ul	40ul	50ul	60ul	80ul	100ul
TEMED	1ul	2ul	3ul	4ul	5ul	6ul	8ul	10ul

When making the gels, TEMED was added last and APS was added before that to avoid rapid polymerization of the gel. After pouring the separating gel, 500µl of 100% isopropanol was added to the top of the gel to ensure the gel was set straight. Once the gel was polymerized, isopropanol was removed, and the stacking gel was carefully poured along with the comb. After the gels were set, they were inserted into the electrophoresis tank system, and 1x running buffer (25mM Tris base, 190mM Glycine, 0.1% SDS in diH_2O) was poured until the system was fully covered. Once the samples along with the ladder (PageRuler Prestained Protein Ladder, Thermo Fisher Scientific; 26619) were prepared as described in section 2.9.1 and loaded into the gel, they were run for ~2hours at 100V (or until the protein ladder dye reached the bottom of the gel).

At this point, the gels were removed from the tank system and the proteins run on the gel could be visualized to make sure they are present by Coomassie staining (section 2.8.3).

Following, each gel was 'sandwiched' between pre-soaked sponges and filter paper. The sponges were soaked in pre-chilled 1x transfer buffer composed of 25mM Tris, 190mM Glycine, 20% Methanol – in diH_2O; 10X buffer was stored without Methanol. Also, the nitrocellulose transfer membrane (Thermo Fisher Scientific; 88018) was placed directly on top of the gel in a negative to positive direction in order for the proteins to be transferred to the membrane and not run out from the other site. The 'sandwich' was then placed and secured into a casket which in turn it was placed into the tank system covered with 1x transfer buffer, placed in 4ºC (cold room) and run ON at 20V.

The next day, the efficiency of the protein transfer was checked by washing the membrane with Ponceau S solution (Sigma Aldrich; P7170) for a few minutes or until the protein bands start appearing. The membrane was then washed a few times with PTW (1x PBS, 0.1% Tween 20) or until the solution is colourless.

2.8.3 Coomassie staining

For protein detection by Coomassie staining, the protein samples and the gel running procedures were as described in section 2.9.1 and 2.9.2. Once the proteins were run, the gels were boiled in Coomassie staining buffer (500ml buffer: 50% Methanol, 10% Acetic acid, 0.5g Brilliant Blue R – Sigma Aldrich; B7920, 0.5g Brilliant Blue G – Sigma Aldrich; B0770 – in diH_2O) and left to rock at RT for 10min. Next, the Coomassie staining buffer was removed, replaced by de-stain buffer (30% Methanol, 10% Acetic acid – in diH_2O) and boiled again. The de-stain buffer was frequently changed until protein bands were visible and easily distinguishable. The gel could then be used to transfer the proteins onto transfer membrane and continued to antibody staining.

2.8.4 Antibody staining

Prior to antibody staining, the gels and protein extracts were prepared and run as described in the above sections. After a few washes with PTW, the membrane was blocked for one hour with 3% BSA in PTW, and then incubated with primary antibody (section 2.3.1) ON at 4ºC. The following day, the membrane was washed a few times with PTW (at least 5min each wash) and the HRP (secondary) antibody (section 2.3.1) was added diluted in 3% BSA in PTW and

incubated for one hour at RT. The membrane was then washed again a few times with PTW, and protein bands were visualized using the Pierce ECL Western Blotting Substrate Solution (Thermo Fisher Scientific; 32106) as per manufacturer's instructions. Briefly, 1:1 dilution was placed directly onto the membrane, incubated for one minute (protected from light) and then immediately after, imaged using a pre-cooled CCD camera.

2.9 SoxB1 antibody production

2.9.1 Protein expression, induction and extraction

Primers were designed to amplify a fragment of SoxB1 coding sequence – containing a 6x HisTag sequence in the N terminal region – which did not include the HMG box or other conserved sites between the three SoxB genes (Appendix A). The cloned fragment was then inserted into a pET-3a expression vector by restriction digest (see section 2.2.6), transformed into chemically competent *E. coli* bacteria as described in section 2.2.7 and plasmid was extracted as described in section 2.2.8. Following, plasmid extraction was carried out (see section 2.2.8), transformed again into Rosetta DE3 pLysS bacteria and plated onto carbenicillin-containing LB agar plates and incubated ON at 37°C.

The resulted colonies were selected the next day and added to 20ml of LB broth containing both carbenicillin (final concentration 100µg/ml; stock: 100mg/ml) and chloramphenicol (final concentration 34µg/ml; stock: 34mg/ml in ethanol). The bacterial cultures were incubated ON at 37°C and the following day added to 1L of LB broth containing both antibiotics. The culture was incubated at 37°C and closely monitored until OD reached 0.5-0.6 (3-4hours). At this point, 1ml of media was taken, centrifuged for at full speed for 10min at RT and the pellet was stored at -20°C for Western blot analysis.

In order to initiate protein induction, Isopropyl β-D-1-thiogalactopyranoside (IPTG) was added at a final concentration of 0.4mM (stock: 1M). To avoid/reduce degradation product accumulation, the culture was incubated at 25°C instead of 37°C. Every hour for four hours, 1ml aliquots were taken, centrifuged at full speed for 10min at RT, and pellets were stored at -20°C for Western blot analysis. The remaining culture was spun down in 500ml tubes for 20min at 30000g (Avanti J20 XPI centrifuge; JLA 10.5 roter) and the resulted pellets were stored stored at -20°C for Western blot analysis.

To confirm the protein expression level, the aliquots collected at the above steps (uninduced and during induction) were spun again for 1min at 11000g to remove any residual supernatant. The resulted pellets were lysed by resuspending in 200µl 1X protein gel buffer and heated to 95°C for 5min. Samples were then loaded and run on SDS PAGE gel and protein was visualized by Coomassie staining (section 2.8.3).

Once induction was confirmed, the remaining pellets (resulted from the 50ml aliquots) were lysed by resuspending them in 30ml of fresh pre-chilled native extraction buffer (0.1M Tris HCl pH8, 0.5M NaCl, 10% glycerol, 1% NP-40, 1mM DTT, 0.1mM PMSF). Following, the pellet

solution was sonicated in order to achieve a lump-free solution using the following settings: time: 1'; amplitude: 40%; pulse on: 5''; pulse off: 10''. This process was repeated until a lump-free solution is achieved.

2.9.2 Soluble Vs Insoluble protein expression

To determine whether the protein was soluble or insoluble, 1ml aliquot was taken from the sonicated product and centrifuged at RT for 10min at full speed. The supernatant was transferred to a separate tube and the pellet was resuspended in 1ml of pre-chilled native extraction buffer. Both supernatant and pellet solutions were then tested for protein presence by running them on SDS PAGE gel and visualized by Coomassie staining (section 2.8.3). The remainder of the sonicated product was aliquoted in 50ml tubes (Thermo Scientific Nalgene; 3119-0050) centrifuged at RT for 20min at 30000g (Avanti J20 XPI centrifuge; JA-17 rotor) and both supernatant and pellet were stored in -20°C until protein solubility was identified.

Since the protein of interested was found in the pellet, an insoluble protein purification approach was taken. The stored pellet was resuspended and washed twice in 30ml of wash buffer (0.1mM DTT, 50mM Tris pH7.5, 100mM NaCl – in diH_2O) and spun down for 15min at 30000g. The supernatant was then discarded and 1ml of DMSO was added without mixing. The tube was placed on a rocker at RT for 30-60min until the pellet was fully dissolved. For further solubilization, 5ml of Buffer A (final concentrations: 50mM Tris HCl pH7.5; 50mM NaCl; 20mM imidazole – in diH_2O) were added to the pellet solution and left on rocker for an additional one hour. The solution was then centrifuged at 30000g for 15min. The supernatant was kept and further diluted by adding 30-35ml of Buffer A. To finally purify the protein, the supernatant solution was injected to a column chromatographer using HisTrap HP nickel column (Ettan Liquid Chromatograph; GE). The purity of the protein was then confirmed by running the samples on SDS PAGE gel and visualized by Coomassie staining (section 2.8.3).

2.9.3 Antibody production

The final purified protein extracts were shipped to Eurogentec in Belgium for immunization into host animals (2X rats). The total amount of protein sent was 1.2mg (0.768mg/ml) and two rats were immunized for a period of 28 days in which four injections with the antigen took place. Pre-immune, medium and final bleed serums were shipped back to us for use.

Chapter 3: Characterisation of the nervous system

3.1: Introduction & Aims

3.2: Nervous system establishment during embryogenesis

3.3: Nervous system characterisation in adult stages

3.4: Summary

3.1 Introduction & Aims

Nervous system development is a fine-tuned process involving many transcription factors and other key regulators. Several studies provided evidences of the different genes involved during this process in cnidarians (see section 1.7) but a more in-depth characterisation of the nervous system is lacking from the literature.

Neurogenesis begins when ectodermal cells (also endodermal cells in cnidarians) acquire the neurogenic potential. Following, neural progenitors or precursors arise within the particular domain (neurogenic ectoderm or endoderm) and pattern themselves stochastically or invariant depending on the animal. Afterwards, neural progenitor cells will either directly differentiate to neurons or give rise to proliferating neural progenitors which in turn can asymmetrically self-renew. Finally, neural progenitors will either remain integrated within the neuroepithelium or internalise by delamination, ingression, or invagination (Hartenstein and Stollewerk, 2015).

Many genetic modules of the early neurogenesis which guide cells through proliferative phases toward post-mitotic cells are highly conserved throughout the animal kingdom. For instance, the SoxB family of transcriptional regulators provide neurogenic potential and at the same time inhibit neuronal differentiation by maintaining neural progenitors in an undifferentiated state (Sasai, 2001). Basic helix-loop-helix (bHLH) transcription factors, known as proneural genes, have also been found to regulate neurogenesis in various species across the animal kingdom such as *Drosophila* and various vertebrates (Quan and Hassan, 2005), and the sea anemone *Nematostella vectensis* (Richards and Rentzsch, 2015).

In order to start understanding how neurogenesis is established, I characterised the composition of *Hydractinia*'s neurodevelopment at three embryonic stages; pre-planula larvae (24 HPF), early planula larvae (48 HPF), late planula (72 HPF), as well as at the adult stages including feeding and male/female sexual polyps. The main aim of this chapter was to determine the timing of the emergence of various cell populations along the neural lineage.

I used established markers for this characterisation including two neuropeptide markers (GLWamide and RFamide), a pan-neural/cilia marker (acetylated tubulin), two nematoblast markers (Ncol1 and Ncol3), a stem cell marker (Piwi1), and an S-phase marker (EdU).

With this characterisation, I aim to shed light into how the nervous system is established in *Hydractinia* and how a fully functional neuronal network during adulthood is presented.

3.2 Nervous system establishment during embryogenesis

Firstly, I used neuronal lineage markers that are expressed in differentiated neurons. As seen in Fig. 3.3, the neuropeptide GLWamide was expressed in a small subset of cells at 24 HPF and by 48 HPF a fine network of sensory neurons was established primarily in the aboral pole of the planula and to a less extend also in the oral side. By 78 HPF, a stage at which the nervous system of the larvae has been fully established, the GLWamide^{+} neurons were concentrated on the aboral end of the larva; an area where these neurons are highly needed for metamorphosis induction as discussed in the introduction chapter (Schmich *et al*., 1998; Leitz, 1998).

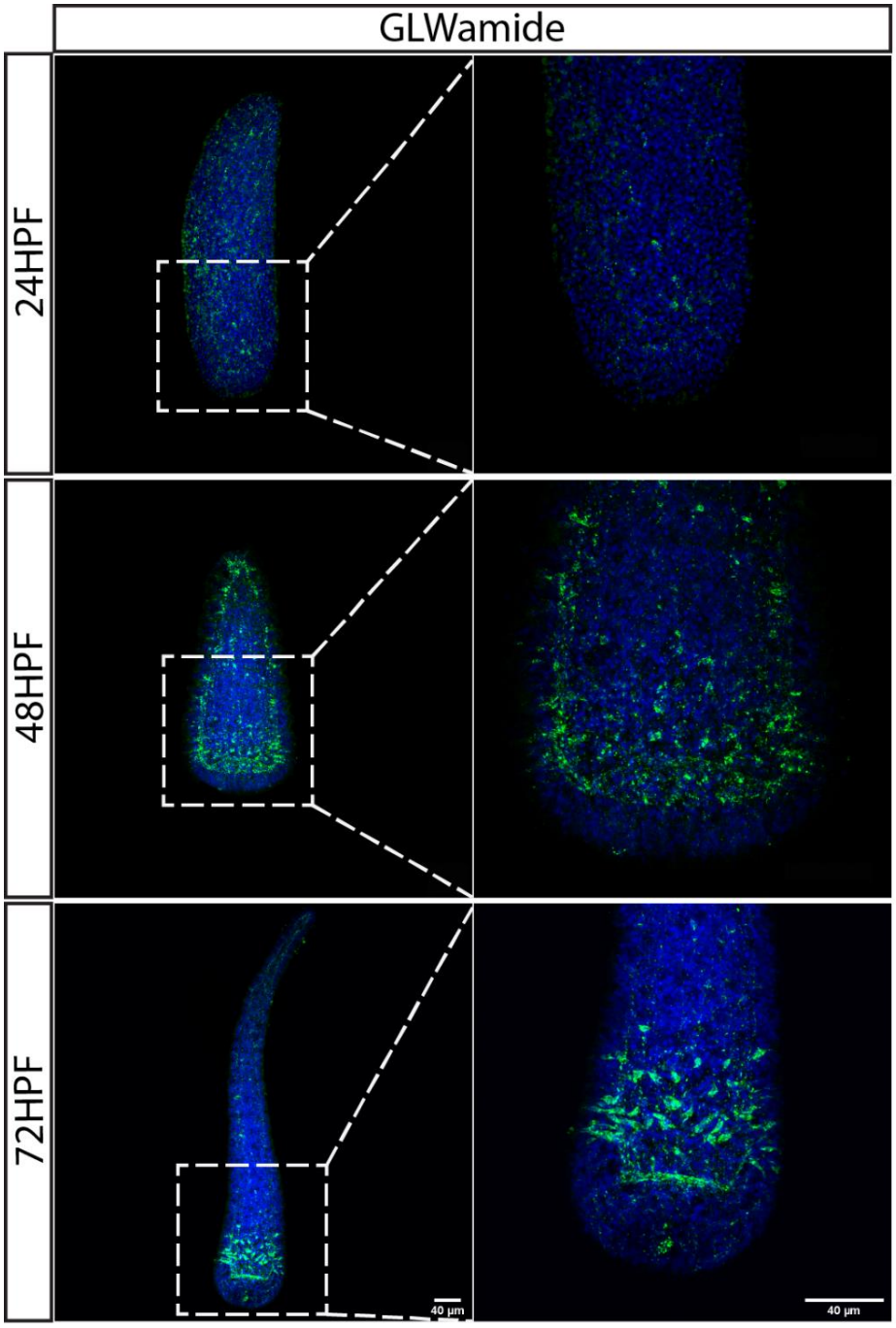

Figure 3.1. Visualisation of GLWamide$^+$ neurons during larval development in *Hydractinia* by IF. Images are z-stack projections. Green: GLWamide; Blue: Hoechst. Scale bar: 40µm.

Next, a second neuronal lineage marker was used; the neuropeptide RFamide. As seen in Fig. 3.2, RFamide$^+$ neurons were not seen at the early planula stage (24 HPF), but later in development (48 HPF onwards). These neurons were also located in the aboral side of the larva as they also have a role in metamorphosis (Katsukura *et al*., 2003).

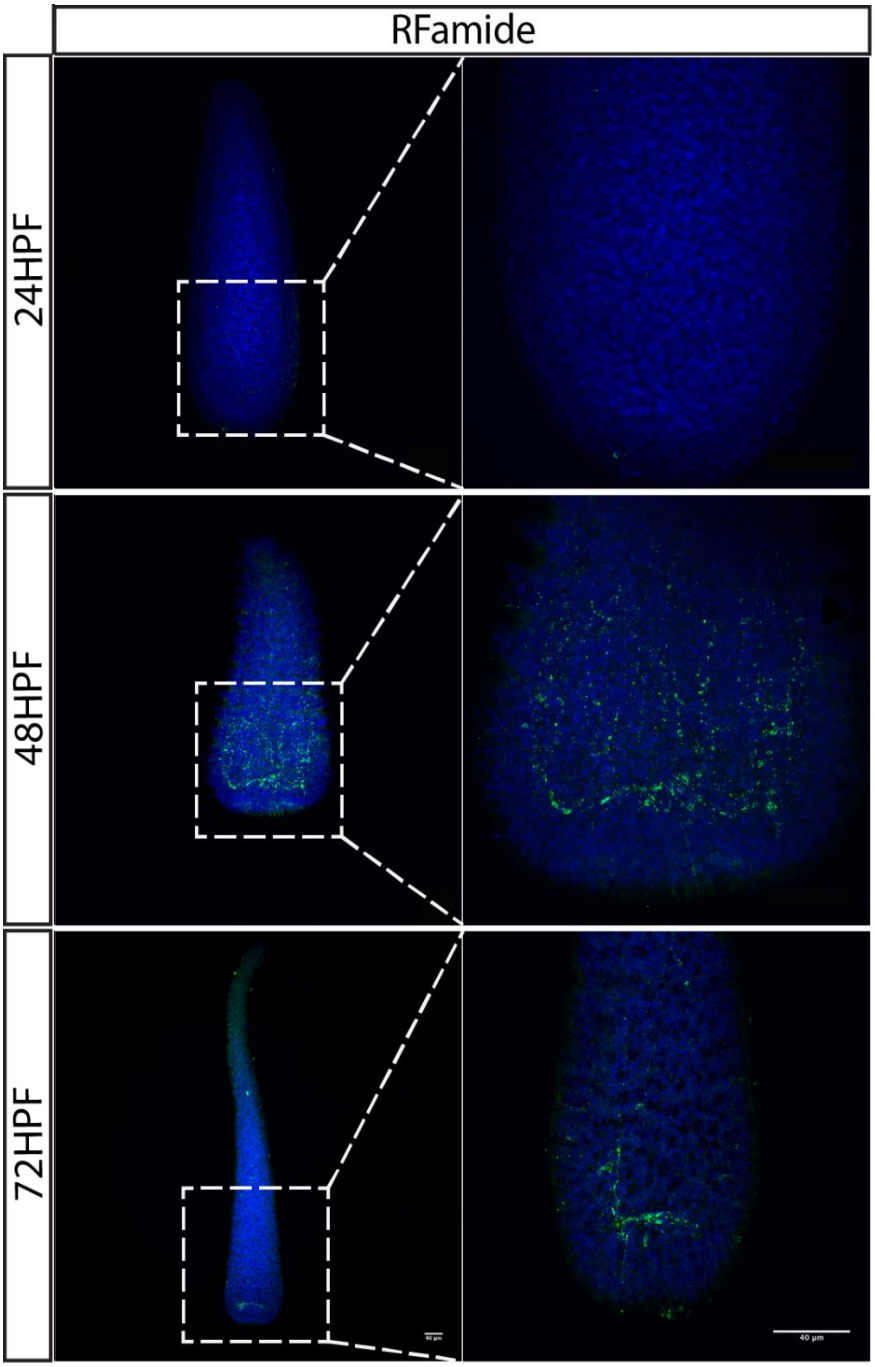

Figure 3.2. Visualisation of RFamide$^+$ neurons during larval development in *Hydractinia* by IF. Images are z-stack projections. Green: RFamide; Blue: Hoechst. Scale bar: 40µm.

I then used an anti-acetylated tubulin antibody to stain cilia and neurons during larval development (Fig. 3.3). At the early stages of development, cilia predominantly express this marker and at the later stages a network of both cilia and neuronal-like cells is formed. Among cnidarians, anti-acetylated alpha tubulin antibody is used as a pan-neural marker including staining of cilia and cnidocytes, as shown in previous studies (Dupre and Yuste, 2017; Quiroga Artigas *et al*., 2018; Plachetzki *et al*., 2012).

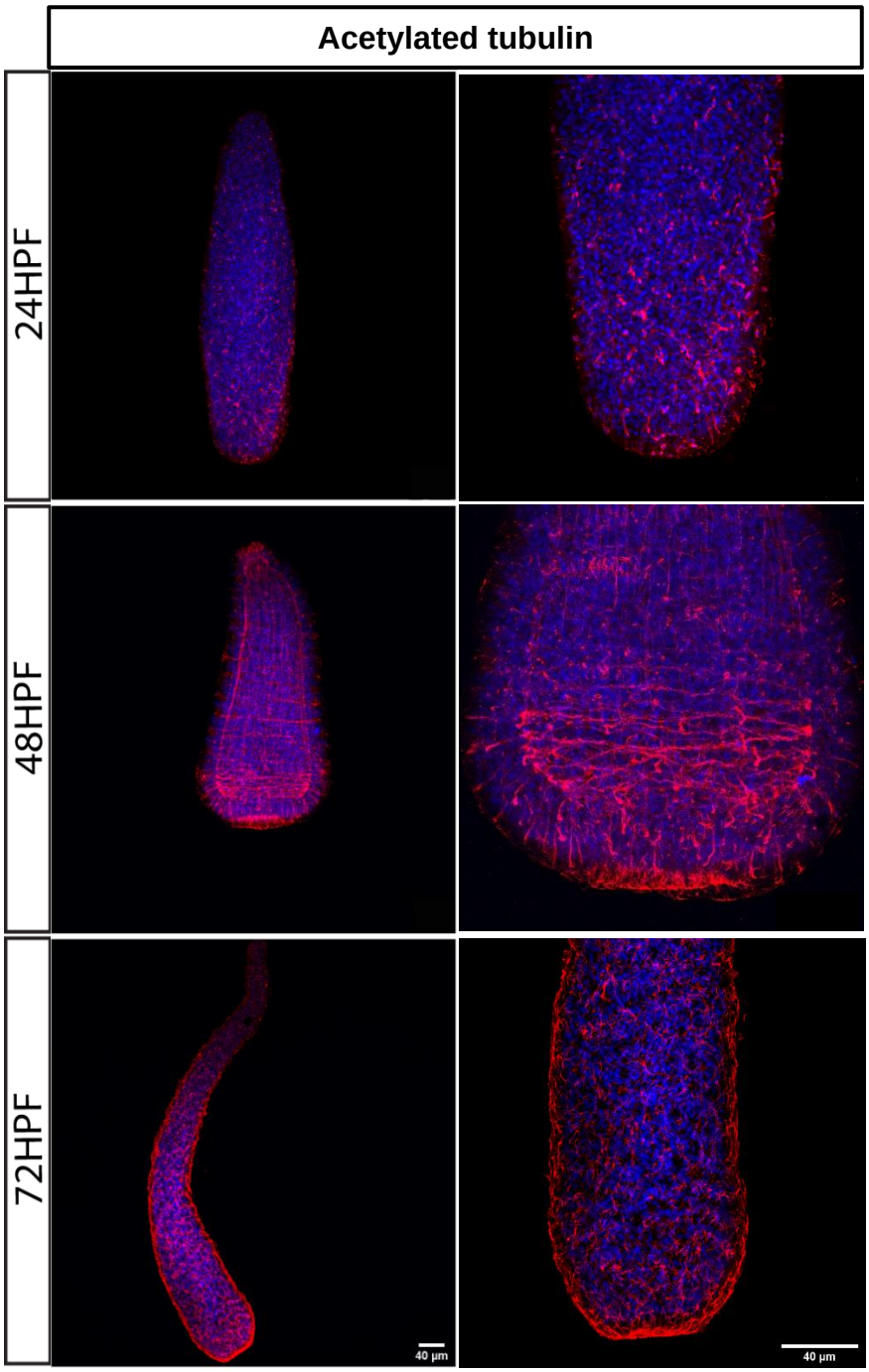

Figure 3.3. Visualisation of acetylated tubulin^{+} cilia and putative neurons during larval development in *Hydractinia* using IF. Images are z-stack projections. Red: acetylated tubulin; Blue: Hoechst. Scale bar: 40µm.

In addition, nematoblast (Ncol3) and stem cell (Piwi1) markers were used in order to determine the distribution of these cells during development. As seen in Fig. 3.4, both nematoblasts and stem cells are distributed throughout the gastrodermal layer of the early planula and as the larva develops further, they are more concentrated in the oral part of the animal.

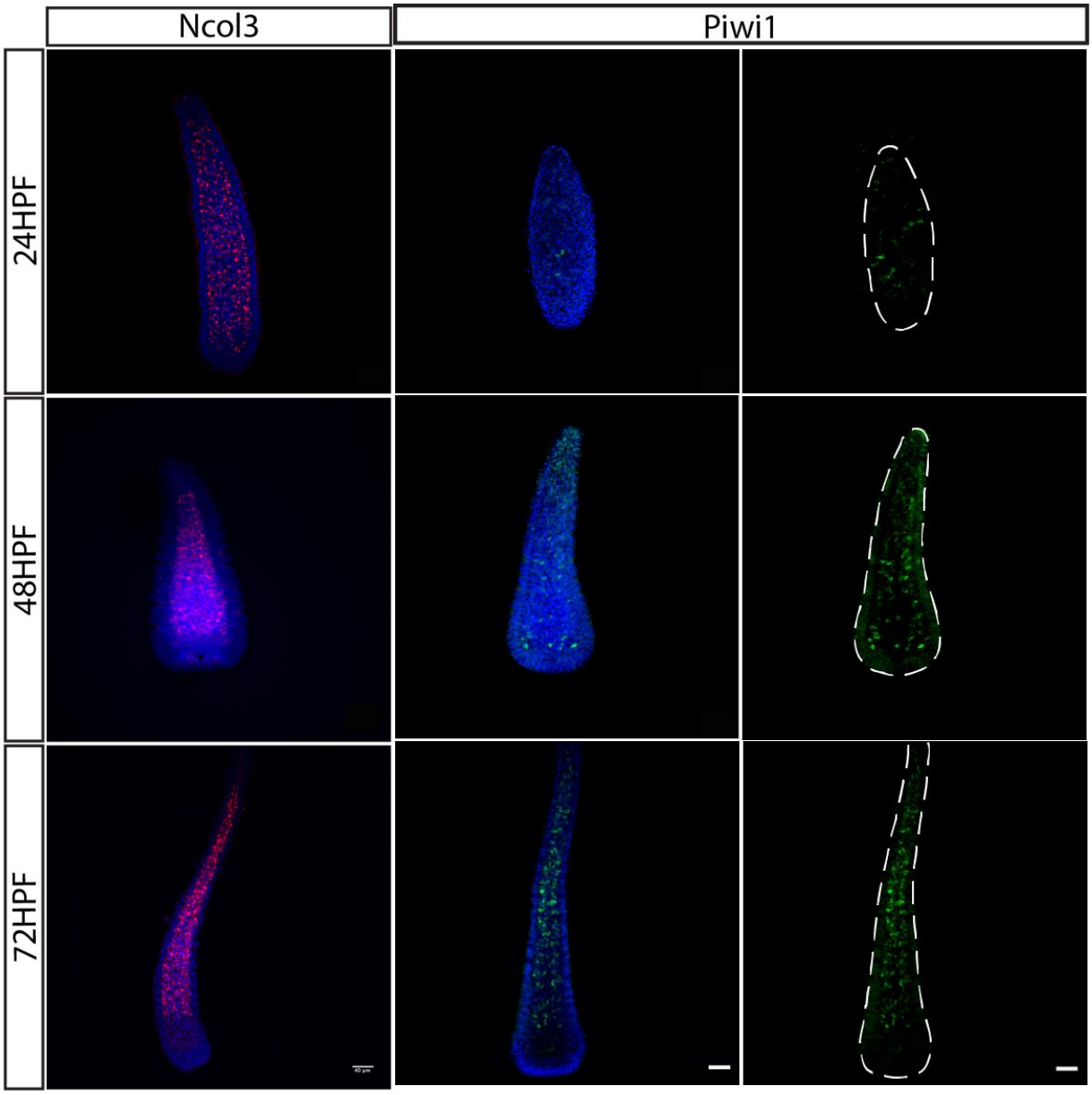

Figure 3.4. Distribution of nematoblasts (Ncol3^{+}) and stem cells (Piwi1^{+}) during larval development in *Hydractinia*, studied by IF. Images are z-stack projections. Red: Ncol3; Green: Piwi1; Blue: Hoechst. Scale bar: 40µm.

In order to check the proliferation status of the various developmental stages, EdU incubation assays were performed. As it can be seen in Fig. 3.5, during the pre-planula stage, proliferative cells are found both epidermal and gastrodermal and as the larva develops, proliferative cells become restricted to the gastrodermis, consistent with the location of i-cells and progeny (Gahan *et al*., 2016).

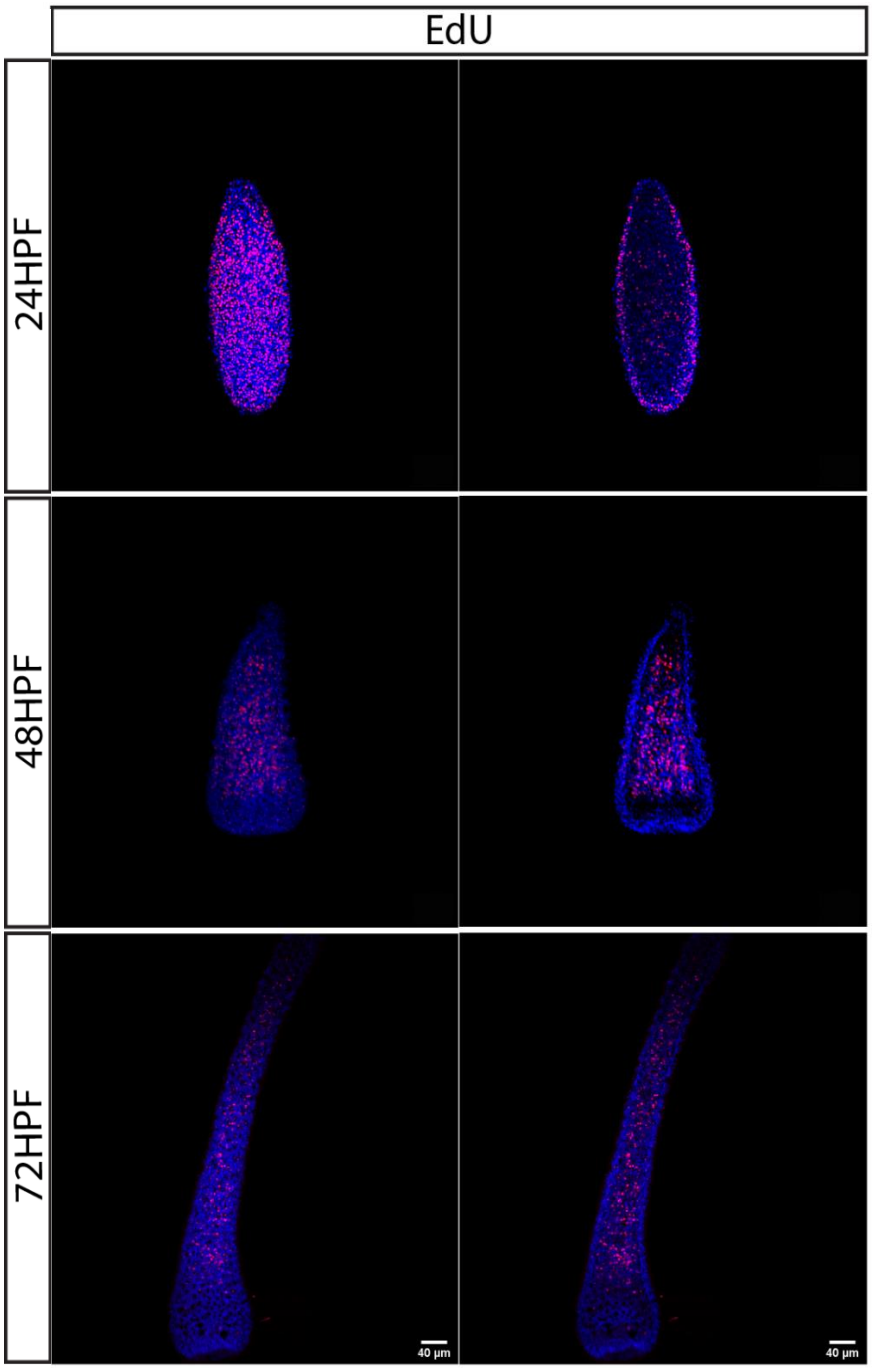

Figure 3.5. Visualisation of proliferative cells (EdU^+) during larval development in *Hydractinia*. On the left column the epidermis of the larva can be seen and on the right column the gastrodermis is shown. Images are z-stack projections. Red: EdU; Blue: Hoechst. Scale bar: 40µm.

The final part of the embryonic and larval nervous system characterisation was the analysis of nematocyst distribution. As seen in Fig. 3.6, at 24 HPF, nematocysts are only present in small numbers. As the larva develops nematocysts are easily distinguishable on the epidermis of the animal with a much higher presence on the oral side of the larva than on the aboral side.

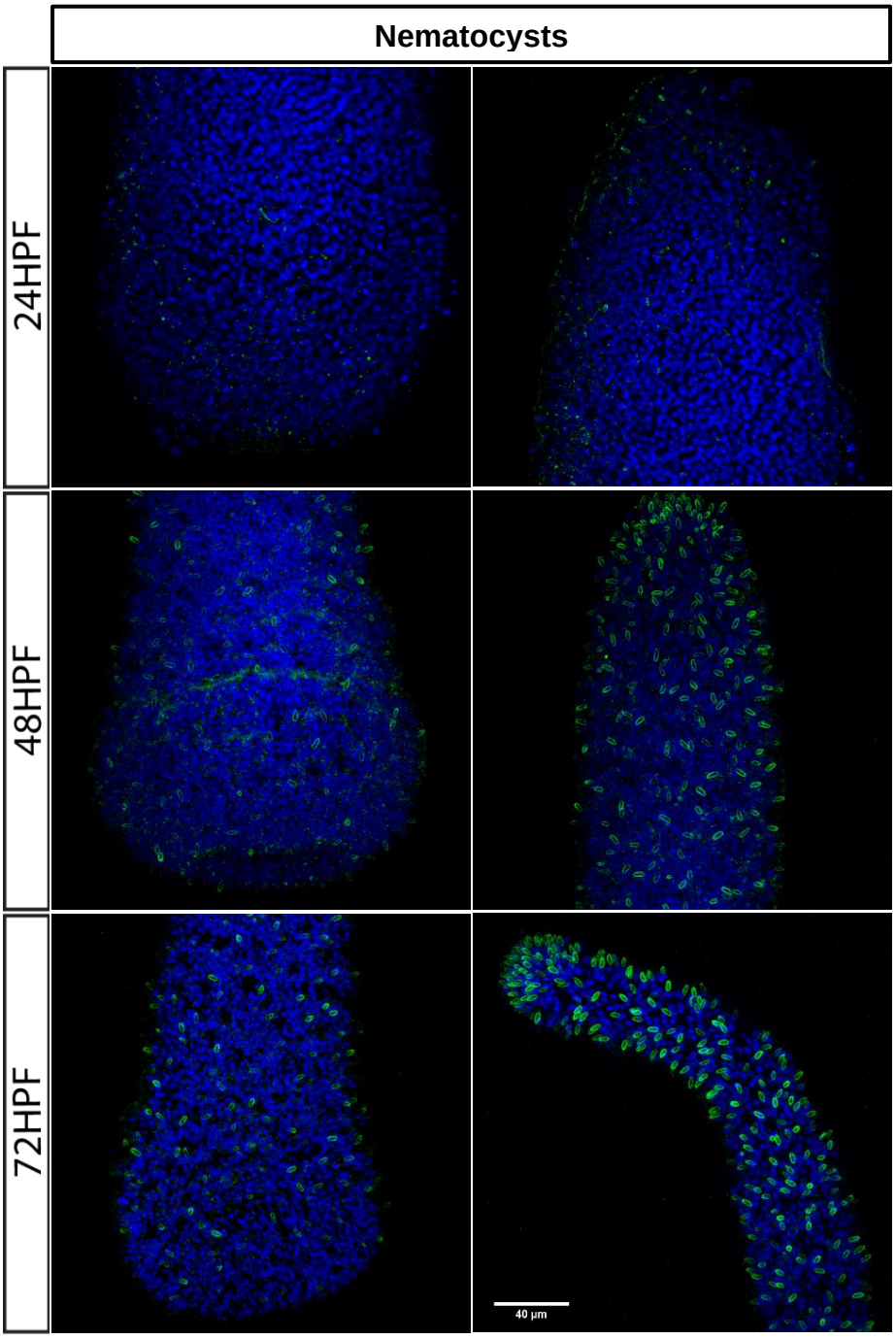

Figure 3.6. Visualisation of nematocysts during larval development in *Hydractinia*. On the left column the aboral side of the larva can be seen and on the right column the oral side is shown. Images are z-stack projections. Green: lectin-GFP (nematocysts); Blue: Hoechst. Scale bar: 40µm.

3.3 The nervous system of adult polyps

The same approach as in the above section was used to characterise the nervous system in the adult stages of *Hydractinia*. I used antibodies against two neuropeptides, GLWamide and RFamide, to locate the differentiated neurons expressing these neuronal lineage markers.

As seen in Fig. 3.7, these two neuropeptides have distinct expression patterns. GLWamide^{+} neurons are mostly expressed in the body column of the feeding polyp with a small subset seen in the head region. In contrast, the RFamide^{+} neurons are primarily located in the head region and in the tentacles, with some ganglionic neurons running along the body column of the polyp.

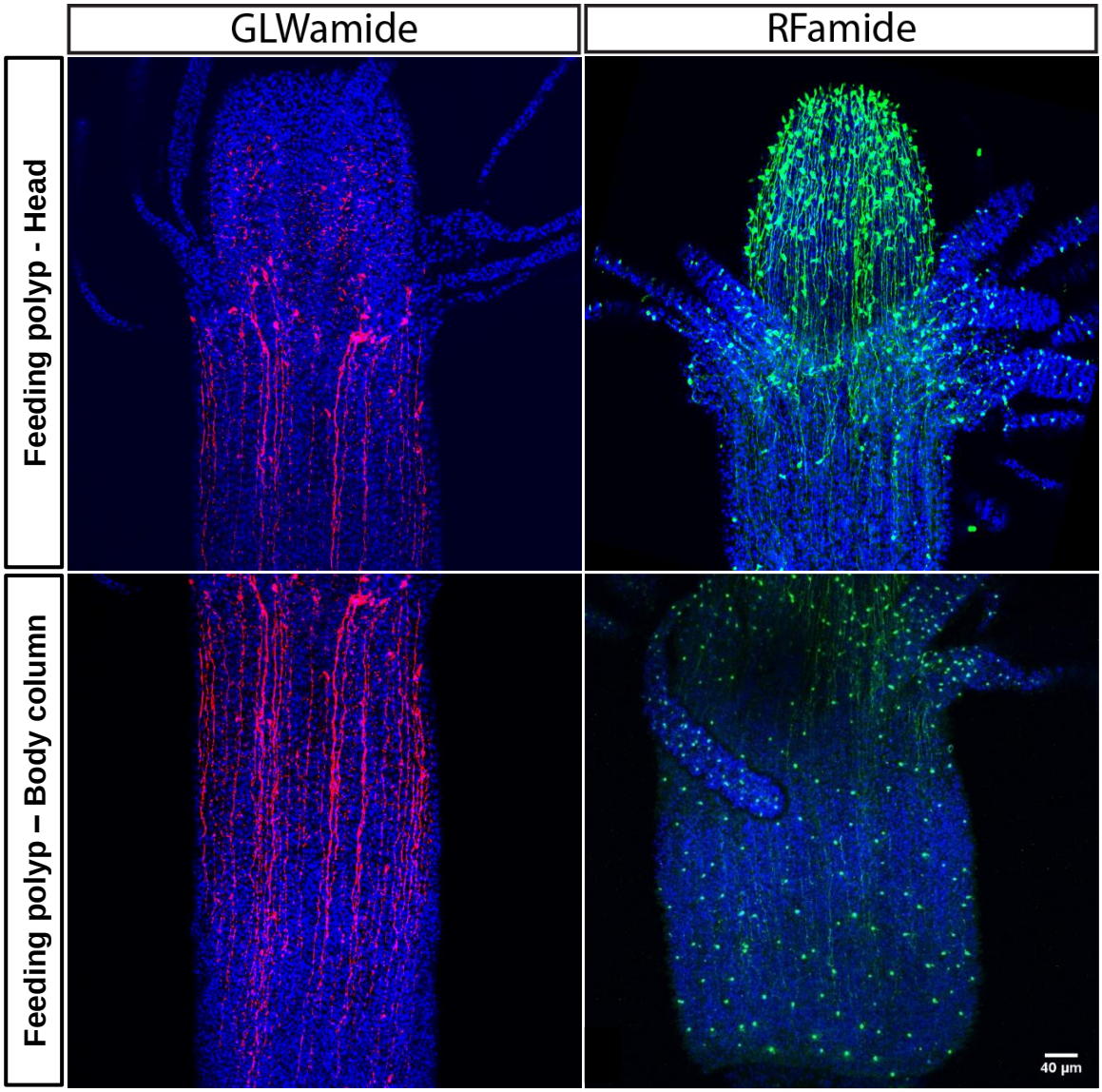

Figure 3.7. Distribution of GLWamide^{+} and RFamide^{+} neurons in the head and body regions of feeding polyps of *Hydractinia*. Images are z-stack projections. Red: GLWamide; Green: RFamide; Blue: Hoechst. Scale bar: 40µm.

In the sexual polyps, these neuropeptides also exhibit distinct expression patterns. The GLWamide-expressing cells are mostly located in the sporosacs of both male and female sexual polyps, whereas the RFamide-expressing cells are found in the body column of these types of polyps (Fig. 3.8).

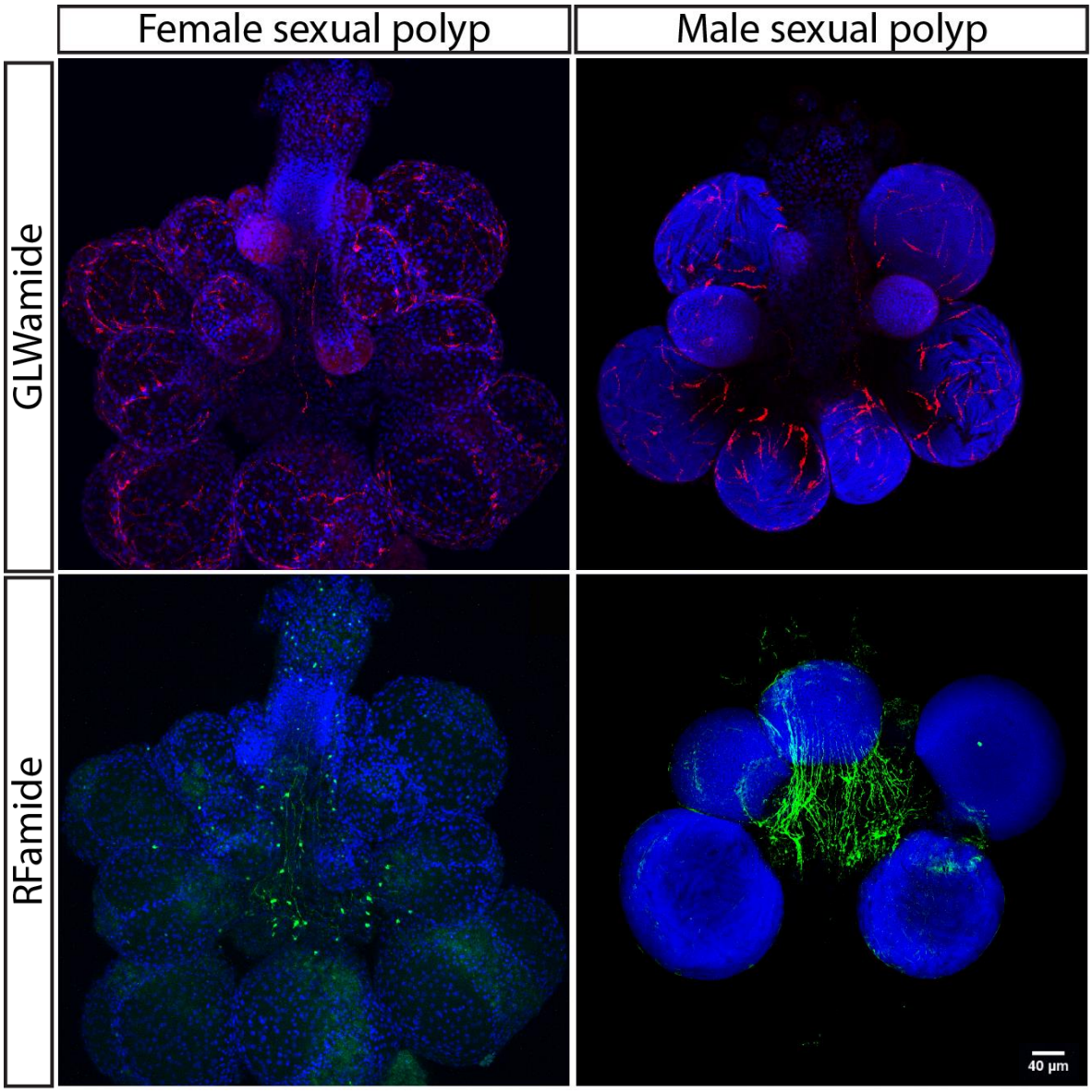

Figure 3.8. Distribution of GLWamide$^+$ and RFamide$^+$ neurons in sexual polyps (male and female) of *Hydractinia*. Images are z-stack projections. Red: GLWamide; Green: RFamide; Blue: Hoechst. Scale bar: 40µm.

Next, I checked where acetylated tubulin was located in feeding and sexual polyps. As shown in Fig. 3.9, acetylated tubulin was predominantly found in ciliated cells and cnidocytes (based on cell morphology) surrounding the tentacles of the polyps.

In the female sexual polyp, acetylated tubulin$^+$ cells were found in the space separating individual oocytes within a sporosac. On the other hand, in the male sexual polyp, acetylated tubulin$^+$ cells were found surrounding each sporosacs. In the mature sporosacs, these cells resembled muscle cells based on their morphology. In both types of sexual polyps, acetylated tubulin$^+$ cells were also found in the head region.

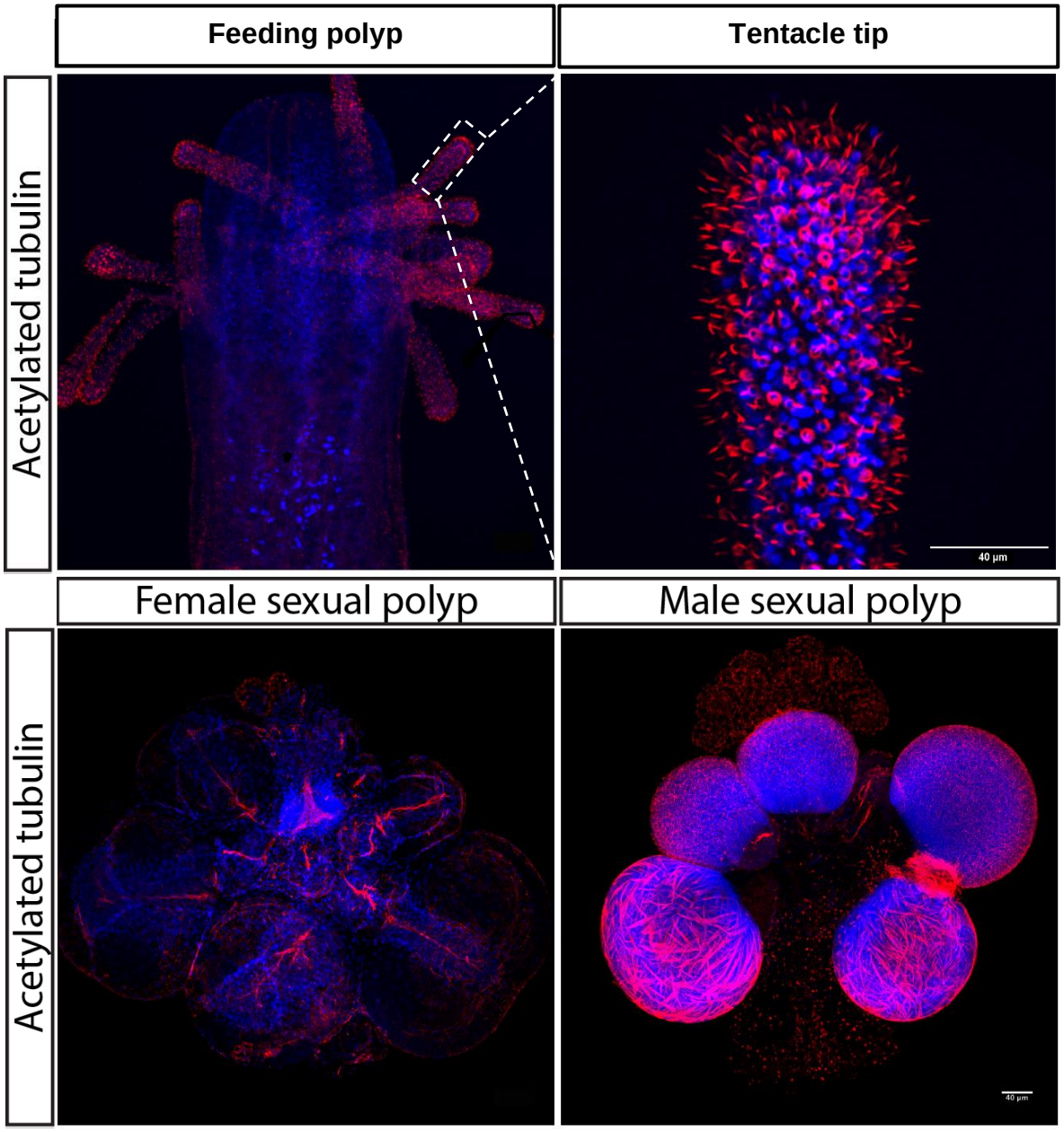

Figure 3.9. Distribution of cells positive for acetylated tubulin in feeding and sexual polyps (male and female). Images are z-stack projections. Red: acetylated tubulin; Blue: Hoechst. Scale bar: 40µm.

Cells expressing the two nematoblast markers, Ncol1 and Ncol3 were located in the body column of the feeding polyp (Fig. 3.10). The two nematoblast markers were largely co-expressed. As shown before by other groups, Ncol1 and Ncol3 minicollagens are expressed in early stage developing cnidocytes (Zenkert *et al*., 2011; Babonis and Martindale, 2017). No expression is observed in the oral part of the animal, i.e. above the tentacles.

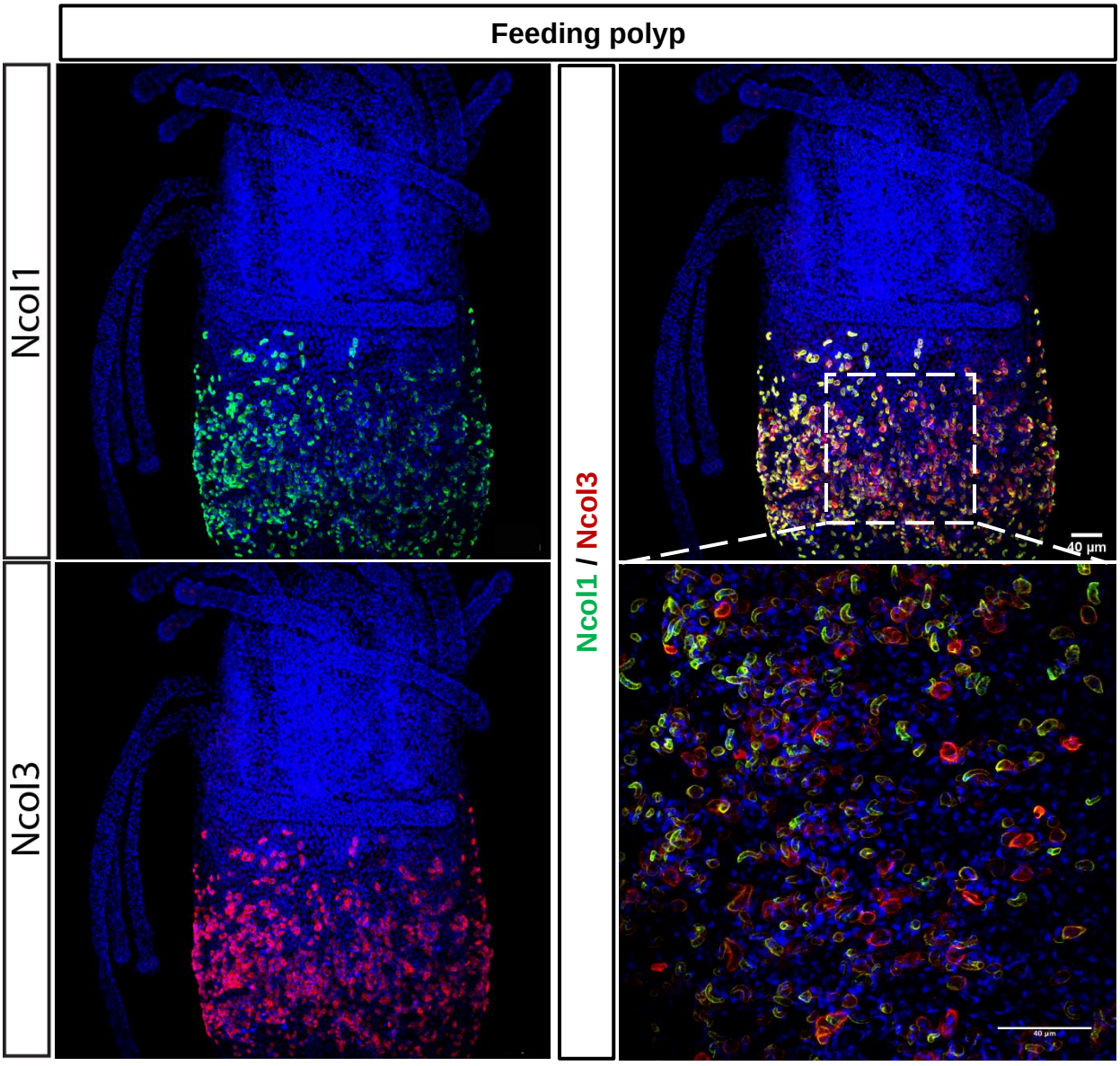

Figure 3.10. Distribution of cells positive for the nematoblast markers Nocl1 and Ncol3 in feeding polyp of *Hydractinia*. On the left column the expression of each marker is shown alone, and on the right column the co-expression is presented in low and high magnification. Images are z-stack projections. Green: Ncol1; Red: Ncol3; Blue: Hoechst. Scale bar: 40µm.

The two nematoblast lineage markers are also highly co-expressed in the male sexual polyps of *Hydractinia*, namely in the body column of the animal as seen in Fig. 3.11.

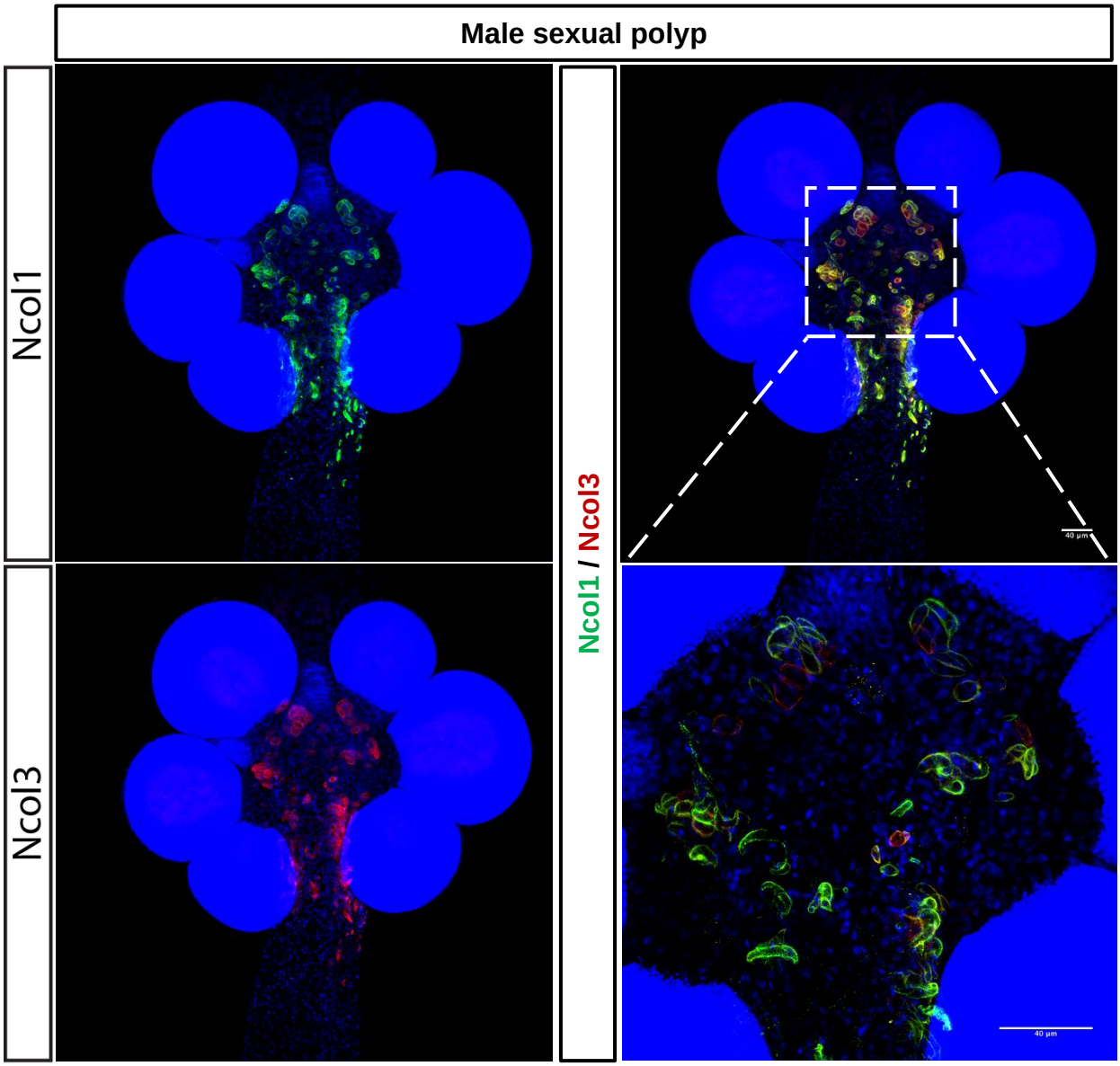

Figure 3.11. Distribution of cells positive for the nematoblast markers Nocl1 and Ncol3 in the male sexual polyp of *Hydractinia*. On the left column the expression of each marker is shown and on the right column the co-expression of them is presented in low and high magnification. Images are z-stack projections. Green: Ncol1; Red: Ncol3; Blue: Hoechst. Scale bar: 40µm.

3.4 Summary

In this chapter I aimed to characterise how the nervous system is composed in *Hydractinia* during larval development as well as in the adult stages (feeding and sexual polyps). By using known neuronal markers as well as a stem cell marker, I was able to show the structure and distribution of neuronal populations.

During the early stages of neurogenesis (24 HPF / pre-planula larva), proliferative cells are spread throughout the epidermis and gastrodermis, but in later stages of development this process is strictly confined to the gastrodermis. Stem cells (Piwi1$^+$ cells) and nematoblasts (Ncol3$^+$ cells) are located since the early stages of development in the gastrodermis. No i-cells or nematoblasts were detected in the epidermis.

Distinct populations of neurons expressing the neuropeptides GLWamide and RFamide are established at different timeframes from each other. GLWamide$^+$ neurons appear at an earlier stage than the RFamide$^+$ neurons during development. Also, the appearance of nematocysts is not highly noticed during the early stages of development, but at later stages the numbers are increased with many of them concentrated at the oral side of the larva.

At the adult stages, the cells with proliferative potential like nematoblasts are in the epidermis of the polyp in a confined area in the body column. A similar pattern is observed in the sexual polyps as well. The RFamide$^+$ neurons are concentrated in the head region of the adult polyp forming a neuronal network. Some of these neurons are also found in the tentacles as well as along the body column of the animal. In sexual polyps, these neurons are mostly found in the body column. As seen in feeding polyps, the location of the GLWamide$^+$ neurons is distinct from the RFamide$^+$ neurons; however, neurons expressing the GLWamide neuropeptide are mostly found in the body column of feeding polyps but in sexual polyps they are predominantly found in the tissue surrounding the sporosacs. This suggests division of the polyp anatomy into distinct neuronal territories.

Another marker used for the characterisation of the nervous system was acetylated tubulin which also marks cilia. During larval development, acetylated tubulin$^+$ cells are found in the epidermal tissue but in the adult stages it is restricted to the epidermis. Its expression pattern in sexual polyps is of great interest which will be discussed in Chapter 6.

Summarising these findings, the nervous system of *Hydractinia* is unusual in animals in that it originates in the endodermal layer. Additional markers are highly needed to fully characterise hydrozoan nervous systems and their development.

Chapter 4: SoxB transcription factors and their roles in development and regeneration

4.1: Introduction and Aims

Transcriptional regulators are essential for guiding cells to a specific identity. SoxB transcription factors are central in neurodevelopment. Their presence or absence determines whether a neural precursor cell will self-renew or differentiate into a specialized cell. They maintain the neuroectoderm in a proliferative state as they provide neurogenic potential but at the same time inhibit neural differentiation (Sasai, 2001; Elkouris *et al*., 2011). The expression of SoxB factors is under the control of various signaling pathways, notably the BMP and the Wnt pathways (Mizuseki *et al*., 1998; Niehrs, 2010). In mammals, 20 Sox proteins have been identified and classified into groups (SoxA-SoxH) based on the degree of amino acid identity within the HMG (high mobility group)-box (Reiprich and Wegner, 2015). In Cnidarians, specifically in Anthozoa and Hydrozoa, an almost complete set of homologous genes that have critical roles in bilaterian neurodevelopment (neurogenesis, neuronal specification and network formation) has been described. Among them are the proneural basic helix loop helix (bHLH) factors, SoxB genes, zinc-finger protein genes, and neuron specific RNA binding proteins (RBPs) (Watanabe *et al*., 2009).

In *Hydractinia*, three SoxB genes are present, namely *SoxB1*, *SoxB2* and *SoxB3* (Flici *et al*., 2017). As was previously shown, *SoxB2* is predominantly expressed in proliferative neural progenitor cells, and *SoxB3* in differentiated neurons and nematocytes.

The main aim of this chapter was primarily to understand how SoxB genes in *Hydractinia* regulate embryonic neurogenesis and their contribution, if any, to the re-establishment of adult nervous system upon injury. Specifically, I aimed to characterize the third SoxB transcription factor – SoxB1 – as no studies to date described its expression pattern and role. In addition, Flici *et al*. (2017) showed a partial overlap in terms of expression and function of SoxB2 and SoxB3, and one of my goals was to find whether SoxB1's expression overlaps with SoxB2 or SoxB3 in the neural lineage. For this, I wanted to characterise the spatial expression of all three SoxB genes by *in situ* hybridization. My main hypothesis was that SoxB genes are expressed sequentially along the neuronal lineage.

Another aim was to generate transgenic reporter lines for these genes in order to assess their roles during nervous system regeneration *in vivo*. Also, in order to confirm the hypothesis that the SoxB genes are expressed sequentially along the neural lineage, I aimed to generate double transgenic reporter lines, namely SoxB1/SoxB2 and SoxB2/SoxB3, and visualize the transition from one to the other by *in vivo* single-cell tracing during regeneration, a context where extensive neurogenesis occurs.

I also wanted to understand the roles of the SoxB genes in development. To evaluate the knockdown effects of these genes, I used various antibody-based markers to stain 3 days post fertilisation (DPF) larvae. I chose this specific timepoint as by this stage of larval development, the animals should be metamorphosis competent and exhibit a fully developed and functional nervous system. Short hairpin RNA-mediated gene knockdowns have been demonstrated by our group and other groups to be highly efficient compared to other methods such as morpholino and RNAi (Dubuc *et al*., 2020; He *et al*., 2018).

4.2: Spatial expression of SoxB genes in *Hydractinia*

The expression pattern of the three SoxB genes present in *Hydractinia* was determined by *in-situ* hybridization. *SoxB1* was expressed in both male and female sexual polyps. Particularly, *SoxB1* was always found in cells expressing *Piwi1*, which includes i-cells as well as germ cells. In more detail, in the male sexual polyp, *SoxB1* was found in the germinal zone in which stem cells commit to become germ cells (Dubuc *et al*., 2020), as well as in i-cells (Fig. 4.1). In the female sexual polyp, the same trend was present as different stages of developing oocytes expressed *SoxB1* and *Piwi1* (Fig. 4.2). In both polyp types, *Piwi1* and *SoxB1* were always co-expressed suggesting that the latter could be used as an i-cell and germ cell, similar to *Piwi1/Piwi2*.

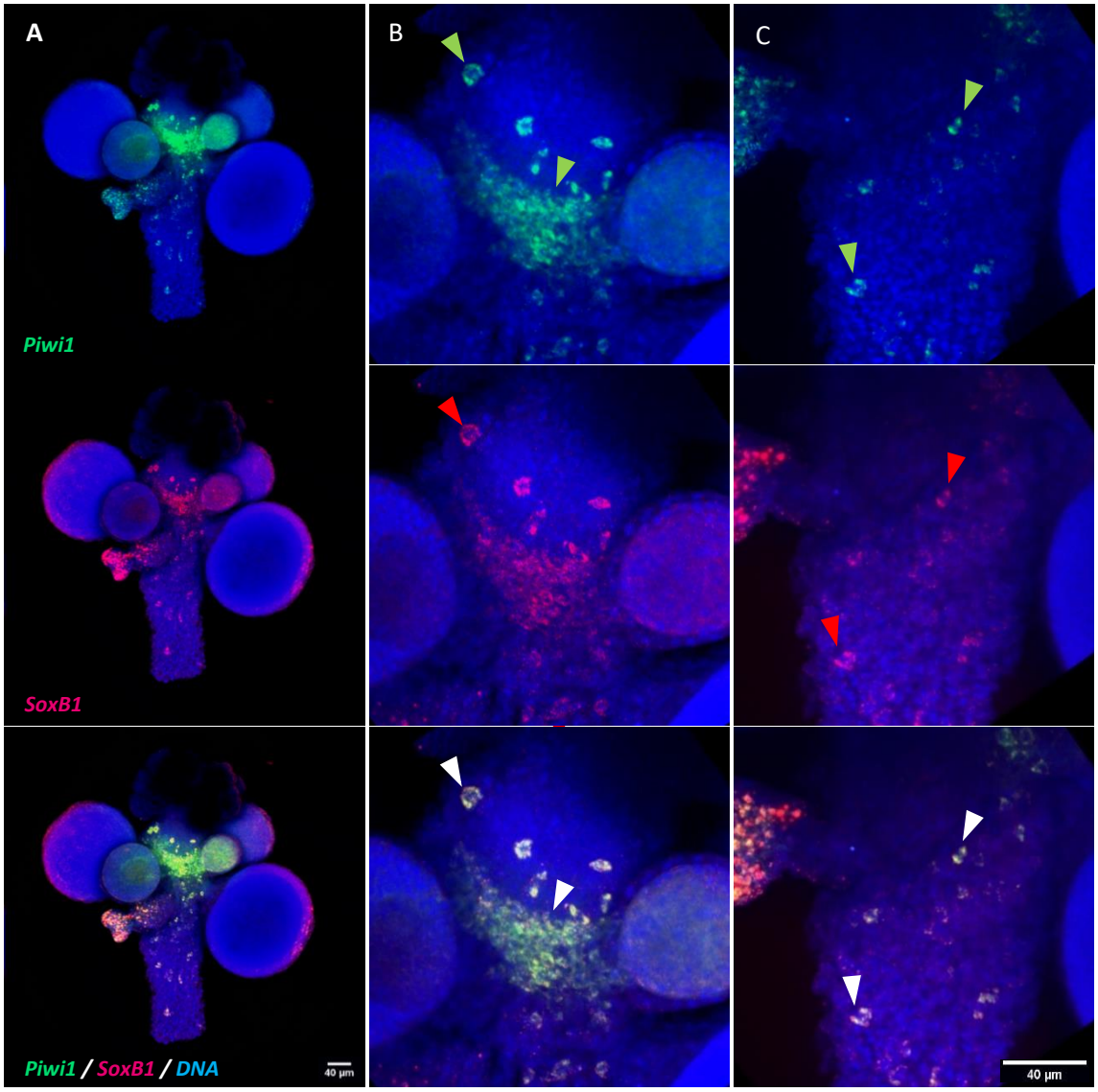

Figure 4.1. Double fluorescence *in-situ* hybridization of *SoxB1* and *Piwi1* in the male sexual polyp of *Hydractinia*. A lower magnification of the sexual polyp shows a very similar expression pattern for both genes (A), and a closer look confirms the full co-expression of those genes in the same cells. These cells include germ cells (B) and i-cells (C). Green arrows: *Piwi1*$^{+}$ cells, red arrows: *SoxB1*$^{+}$ cells, white arrows *Piwi1*$^{+}$/*SoxB1*$^{+}$ cells. Low magnification images are z-stack projections and the higher magnification images are single optical slices. Green: *Piwi1*; Red: *SoxB1*; Blue: Hoechst. Scale bar: 40µm.

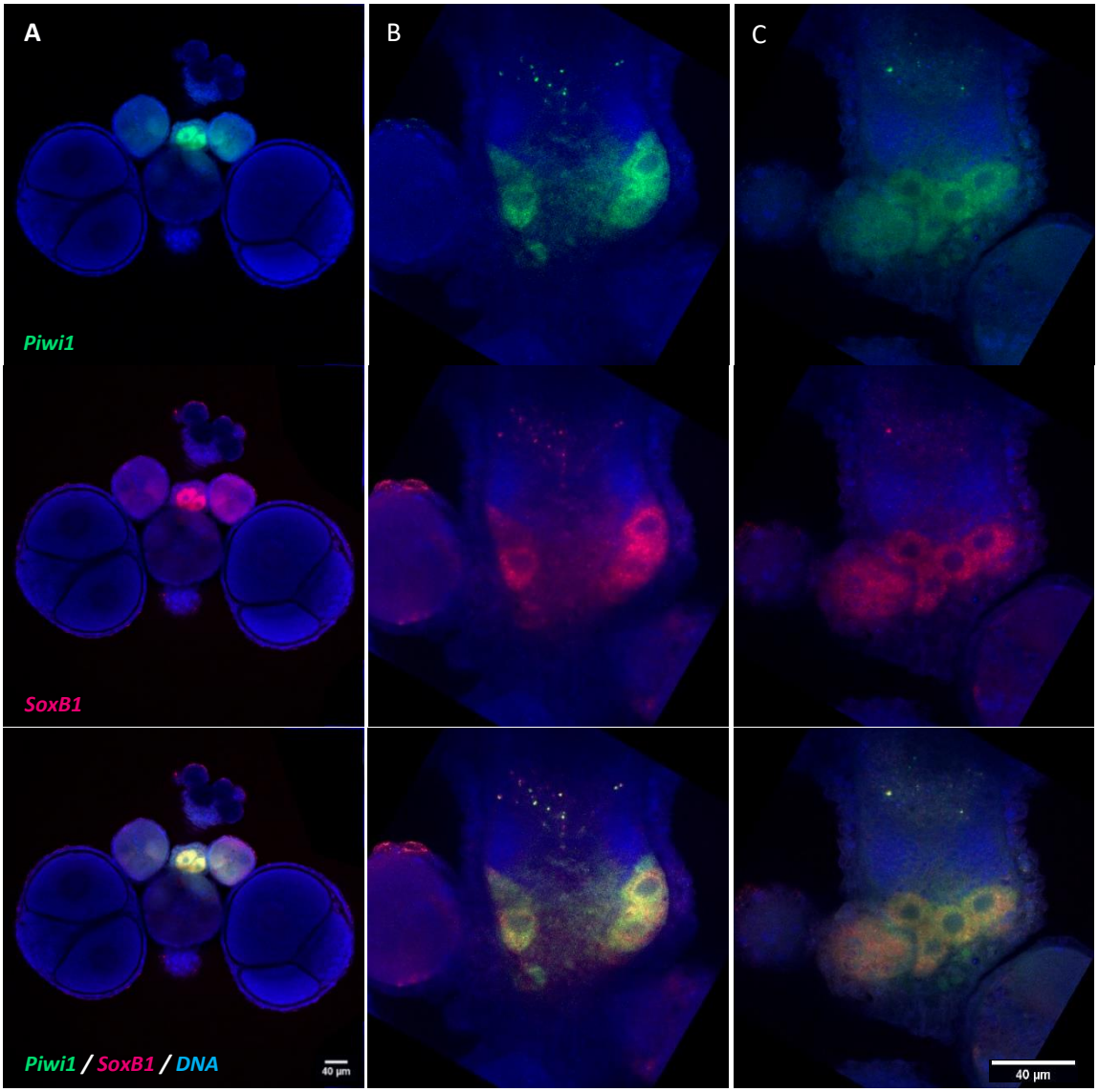

Figure 4.2. Double fluorescence *in-situ* hybridization of *SoxB1* and *Piwi1* in the female sexual polyp of *Hydractinia*. A lower magnification of the sexual polyp shows co-expression of these genes (A), and a closer look confirms the full co-expression in developing oocytes. Different focal planes show developing oocytes at different stages (B and C). Images are single optical slices. Green: *Piwi1*; Red: *SoxB1*; Blue: Hoechst. Scale bar: 40µm.

I also checked the expression of *SoxB1* in feeding polyps to see if its expression pattern overlaps with *Piwi1*, like in the sexual polyps, by single-molecule fluorescence *in situ* hybridization. Indeed, as shown in Fig. 4.3, *SoxB1* was expressed in the lower body of the animal where most i-cells reside and was fully co-expressed with *Piwi1*. As shown in the same figure, *SoxB1*$^{+}$ cells are only found in the proliferative zone of the animal and nearly absent outside of this area. In hypostome, the most oral part of the animal, *SoxB1* was not present at all.

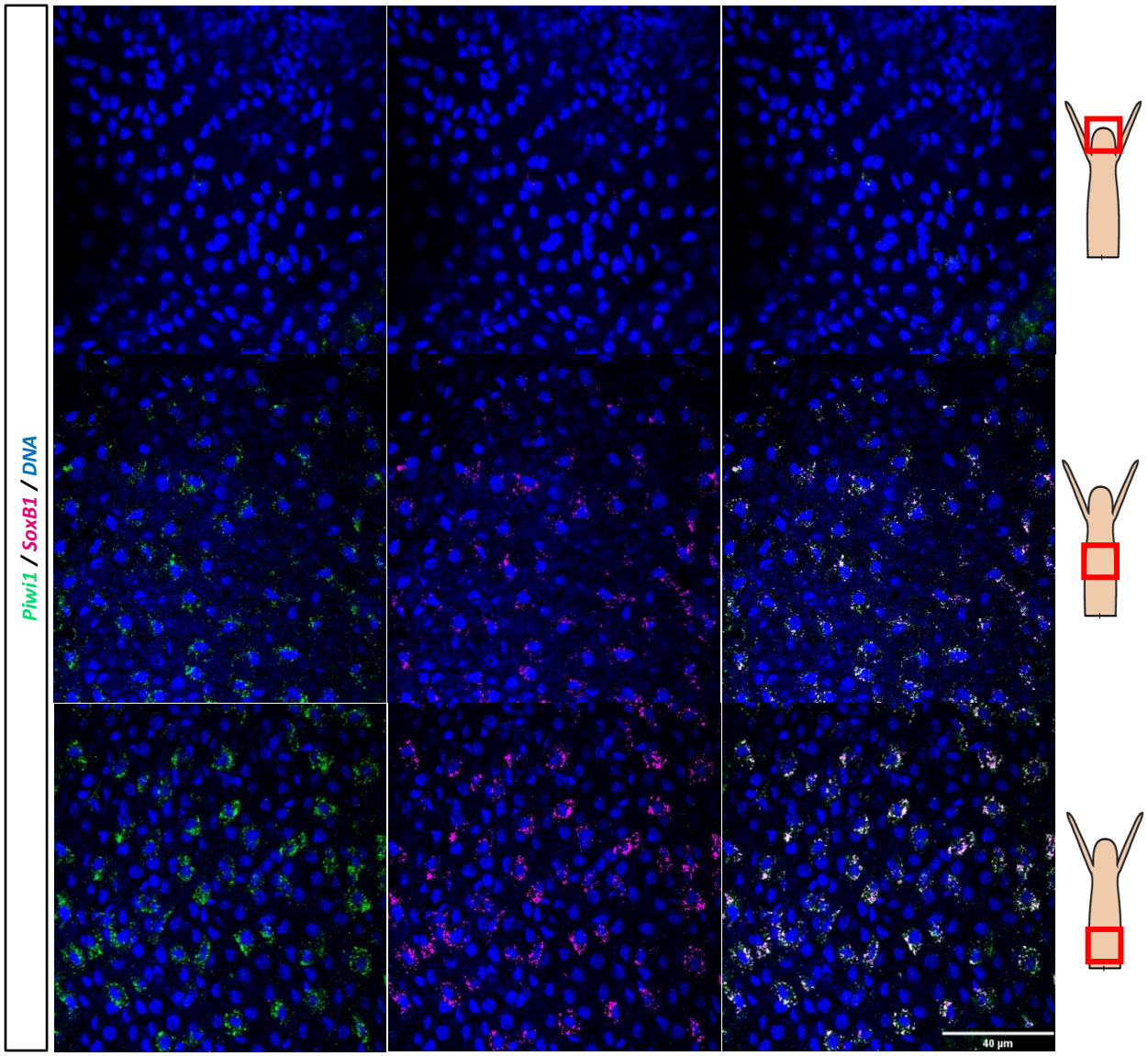

Figure 4.3. Single-molecule fluorescence *in-situ* hybridization of *SoxB1* and *Piwi1* in the feeding polyp of *Hydractinia*. *SoxB1* is always co-expressed with *Piwi1* and a strong expression is observed in the proliferative band of the animal, which is located at the lower body. Expression is also observed, though at much lower levels, in the rest of the body column but not in the head region. Images are single optical slices. Green: *Piwi1*; Red: *SoxB1*; Blue: Hoechst. Scale bar: 40µm.

Next, I performed single-molecule fluorescence *in-situ* hybridization to examine the expression patterns of *SoxB1* and *SoxB2* in feeding polyps. *SoxB1* and *SoxB2* partially overlapped, suggesting a sequential expression of those genes. Another possibly scenario is the existence of a separated cell population expressing both genes, resulting to three distinct populations: $SoxB1^{+}/SoxB2^{-}$, $SoxB1^{+}/SoxB2^{+}$, $SoxB1^{-}/SoxB2^{+}$. In more detail, as seen in Fig. 4.4, in the lower part of the body column, only *SoxB1* was expressed while *SoxB2* was not. *SoxB2* started being expressed higher in the body column and at this stage was co-expressed with *SoxB1*. Further up in the body column, the expression of *SoxB1* was gradually diminished whereas that of *SoxB2* was gradually enhanced in a reverse correlation.

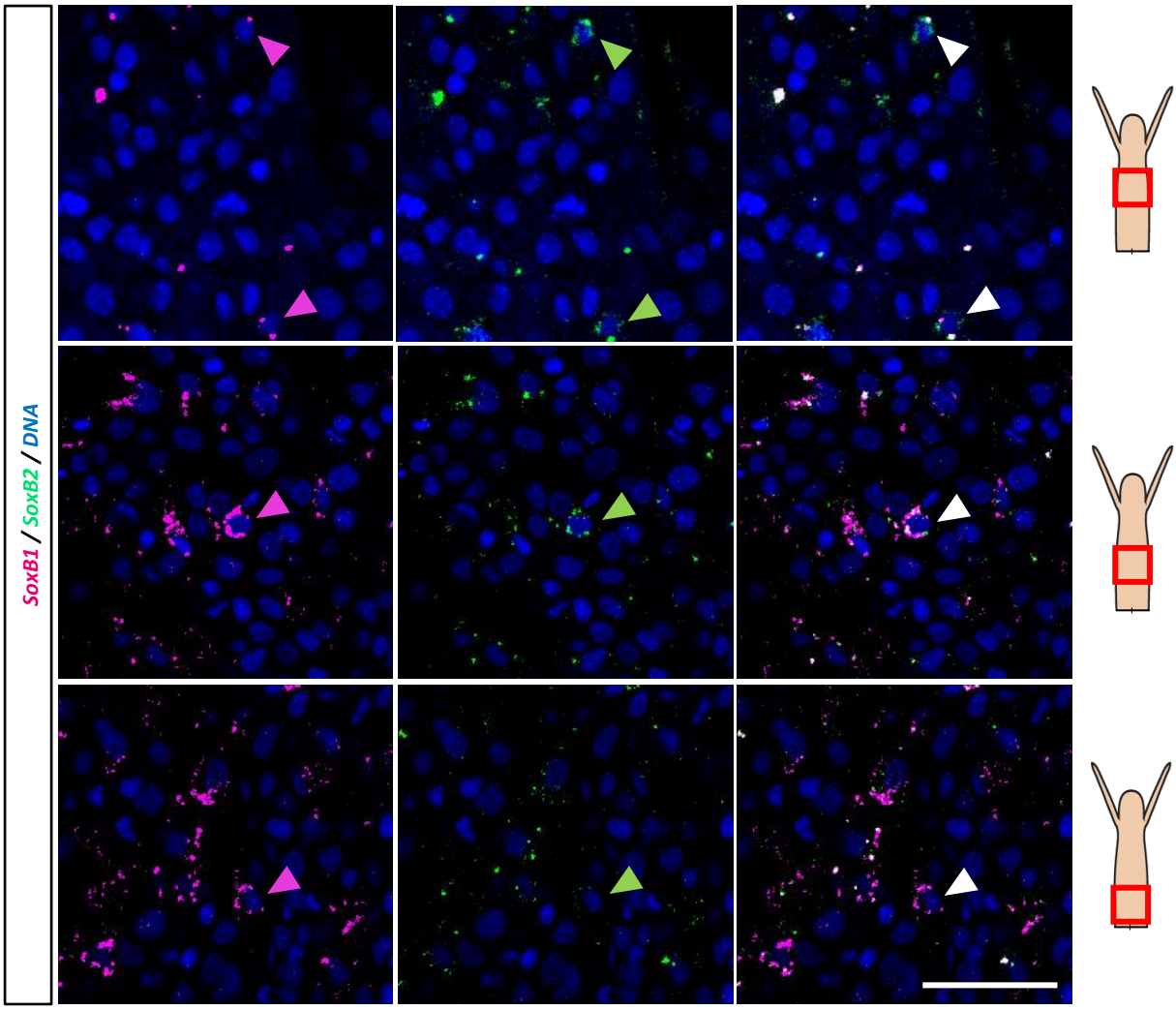

Figure 4.4. Single molecule fluorescence *in-situ* hybridization of *SoxB1* and *SoxB2* in the feeding polyp of *Hydractinia*. *SoxB1* is widely expressed in the lower part of the body, an area in which *SoxB2* is scarcely expressed. More orally, *SoxB2* is widely co-expressed with *SoxB1*. Further orally, *SoxB1* is gradually reduced whereas *SoxB2* is enhanced in a reverse correlation (pink arrows show $SoxB1^{+}$ cells, green arrows show $SoxB2^{+}$ cells and white arrows show $SoxB1^{+}$ / $SoxB2^{+}$ cells). Images are single optical slices. Red: *SoxB1*; Green: *SoxB2*; Blue: Hoechst. Scale bar: 40 μm.

A similar phenomenon was observed when I performed single-molecule fluorescence *in-situ* hybridization to examine the expression patterns of *SoxB2* and *SoxB3* in feeding polyps, as seen in Fig. 4.5. *SoxB2* and *SoxB3* partially overlapped in the body column of the animal suggesting that these two genes are also sequentially expressed during neurogenesis. Another possibly scenario is the existence of a separated cell population expressing both genes, resulting to three distinct populations: SoxB2^{+}/SoxB3^{-}, SoxB2^{+}/SoxB3^{+}, SoxB2^{-}/SoxB3^{+}. Higher expression of *SoxB2* was observed in the body column, whereas *SoxB3* was highly expressed in the upper part of the animal, close to the base of the tentacles. In the upper part of the body column *SoxB2* was gradually diminished while *SoxB3* expression was enhanced in a reverse correlation.

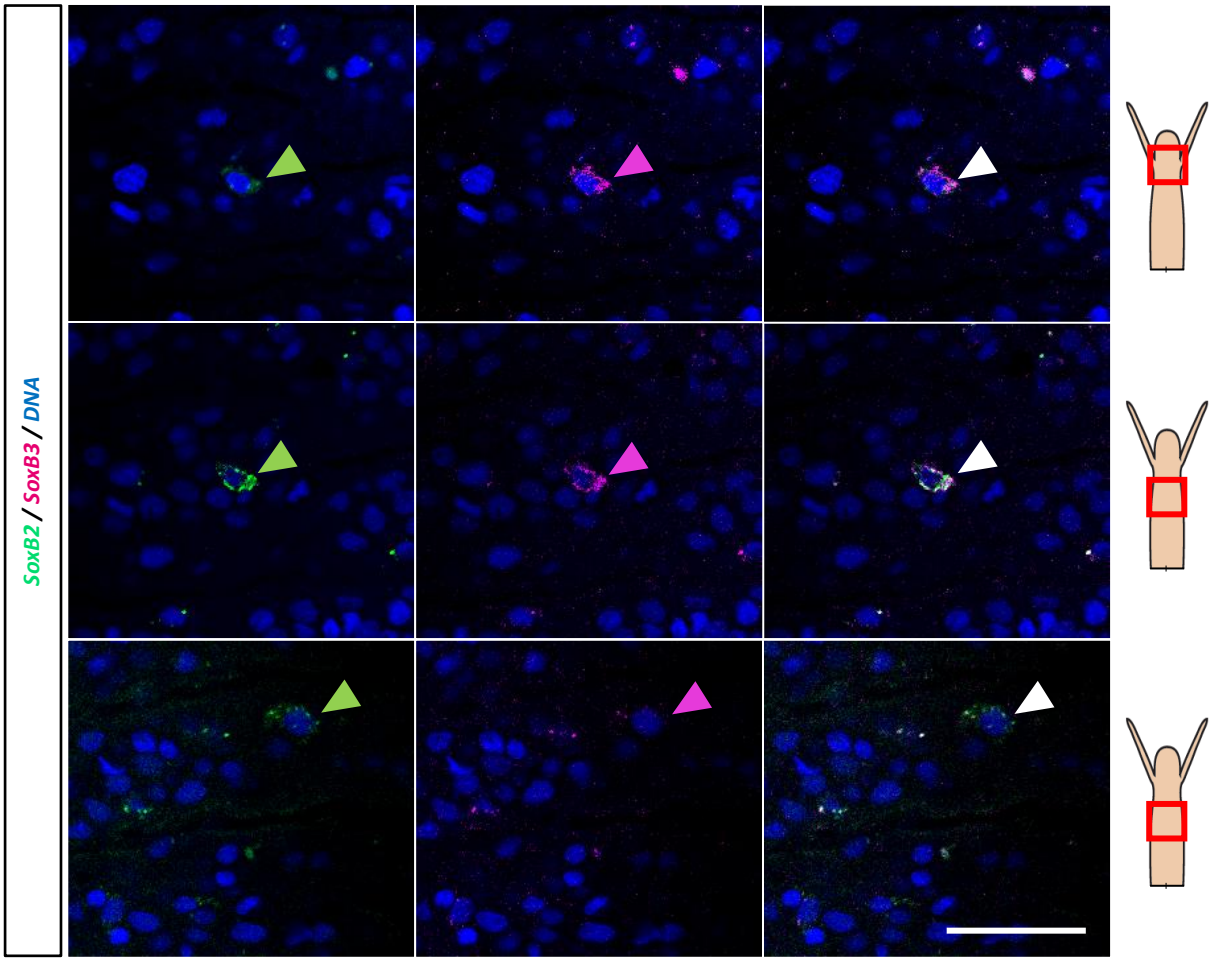

Figure 4.5. Single-molecule fluorescence *in-situ* hybridization of *SoxB2* and *SoxB3* in a feeding polyp of *Hydractinia*. *SoxB2* is expressed in mid body column, an area in which *SoxB3* is low. Towards the oral end, *SoxB3* gradually starts been co-expressed with *SoxB2*. Further orally, *SoxB2* is gradually downregulated whereas *SoxB3* is enhanced in a reverse correlation. Green arrows show SoxB2^{+} cells, pink arrows show SoxB3^{+} cells, and white arrows show SoxB2^{+} / SoxB3^{+} cells. Images are single optical slices. Green: *SoxB2*; Red: *SoxB3*; Blue: Hoechst. Scale bar: 80µm.

4.3: Generation of SoxB1 and SoxB2 transgenic reporter lines

To monitor *in vivo* the dynamics of SoxB1^{+} cells during larval development, I generated a reporter line expressing tdTomato under the genomic control elements of *SoxB1,* (see Section 2.2.2). By time-lapse imaging, I was able to visualise how these cells behave over a period of 48 hours as shown in Fig. 4.5. Every hour, a stack of confocal images was taken by spinning disc microscopy, starting at 24 hours post fertilisation (HPF) until 72 HPF – a point at which larvae are fully developed and ready for metamorphosis induction. As shown below, *SoxB1*-tdTomato^{+} cells were rare during the first hours of imaging but as the larva developed, these cells became numerous in the gastrodermal tissue of the larva. These results are consistent with the known location of i-cells, residing in this tissue layer in *Hydractinia* embryos and larvae. The relatively low numbers of *SoxB1*-tdTomato^{+} cells during the early stages of development does not necessarily indicate low numbers of i-cells, as the maturation time of the fluorescent protein tdTomato may contribute a delay.

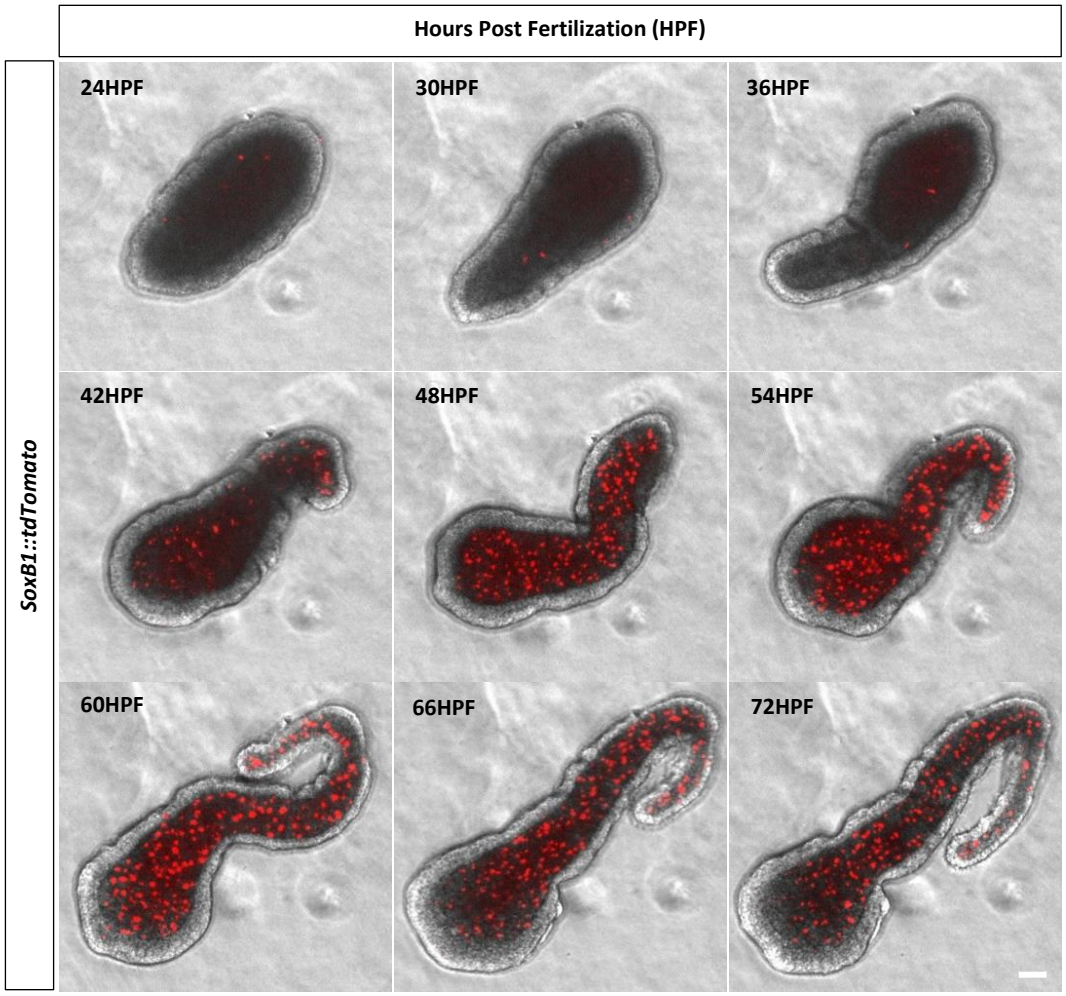

Figure 4.5. *In vivo* tracking of SoxB1-tdTomato^{+} cells during larval development over the course of 48 hours – from 24 HPF to 72 HPF. Images are z-stack projections of a few slices. Red: tdTomato. Scale bar: 40µm.

I used feeding polyps from *SoxB1::tdTomato* colonies to check their proliferation status by an S-phase marker (EdU) and a stem cell marker (Piwi1). I concluded that *SoxB1*-tdTomato^{+} cells are cycling stem cells as they were positive for both markers and were located in the proliferative zone of the body column of the feeding polyp. No tdTomato fluorescence was observed in the head region (Fig. 4.6).

Both male and female SoxB1 colonies were generated. As seen in Fig. 4.7, *SoxB1*-tdTomato^{+} cells are present in the young sporosacs and body column of the male sexual polyp. In the female sexual polyp, the oocytes are *SoxB1*-tdTomato^{+} and due to the long half-life of the fluorescence protein, the different stages of oocyte maturation are observed as a function of fluorescence brightness. These results are consistent with the *SoxB1/Piwi1 in situ* hybridisation experiments as shown in Fig. 4.3, confirming the faithfulness of this reporter line and the role of SoxB1 as i-cell/germ cell marker.

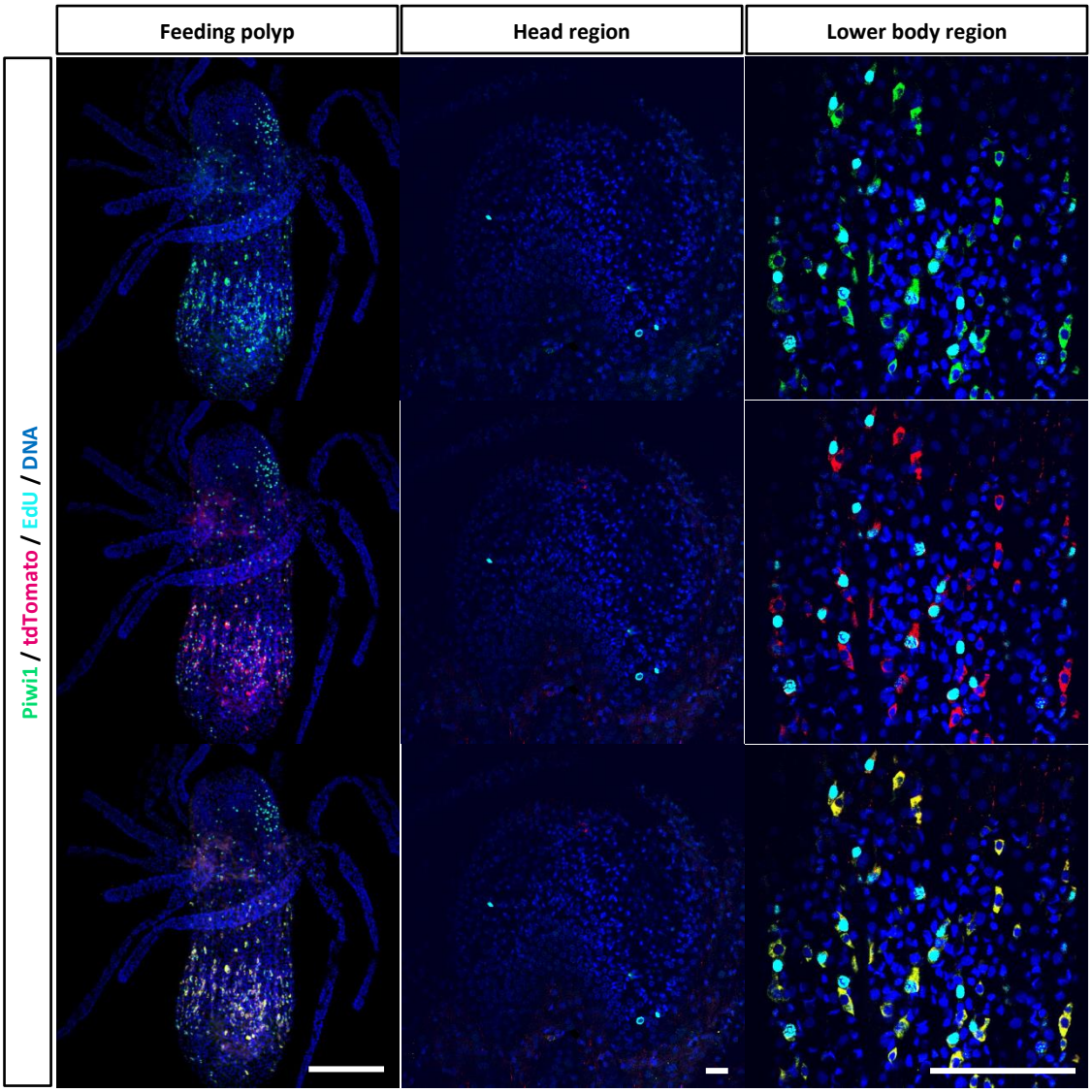

Figure 4.6. *SoxB1* transgenic reporter feeding polyps. Polyps were stained with anti-RFP to detect the fluorescent protein of the transgene (red), with anti-Piwi1 antibody for stem cells (green), and with S-phase marker EdU (cyan). *SoxB1*-tdTomato transgene is expressed in i-cells (Piwi1^{+} cells) and they are also cycling cells. No staining was observed in the head region as expected and most of the staining was seen in the proliferative area in the body column. Low magnification images (feeding polyp) are z-stack projections and the higher magnification images (head region & lower body region) are single optical slices. Green: Piwi1; Red: tdTomato; Cyan: EdU; Blue: Hoechst. Scale bar: 40µm.

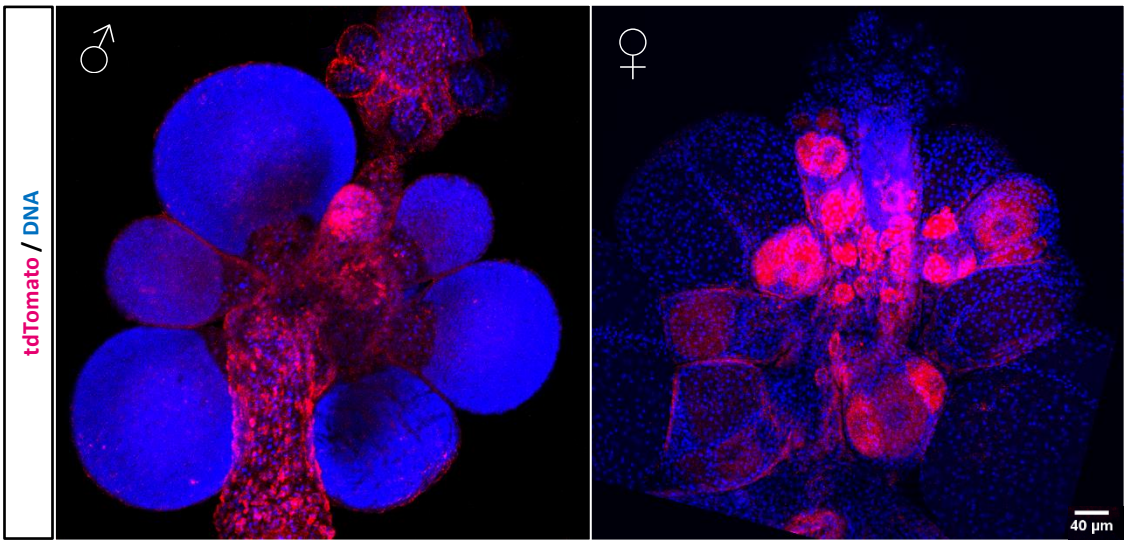

Figure 4.7. SoxB1 transgenic reporter male and female sexual polyps. *SoxB1*-tdTomato is expressed in i-cells and young sporosacs in the male, and in oocytes in the female, as observed by IF. Images are z-stack projections. Red: tdTomato; Blue: Hoechst. Scale bar: 40µm.

I also generated a reporter line expressing GFP under the genomic control elements of *SoxB2*. *SoxB2*-GFP^{+} cells were expressed throughout the epidermis at the larval stage in elongated, neuronal-like cells in the aboral pole (Fig. 4.8A). Moreover, in the primary polyp, neuronal-like cells were highly concentrated in the head region (Fig. 4.8B, B', B'') and inter-connected neurons were found in the stolons (Fig. 4.8C). Throughout the body of the adult polyp neuronal- and nematoblast-like *SoxB2*-GFP^{+} cells were observed (Fig. 4.8D).

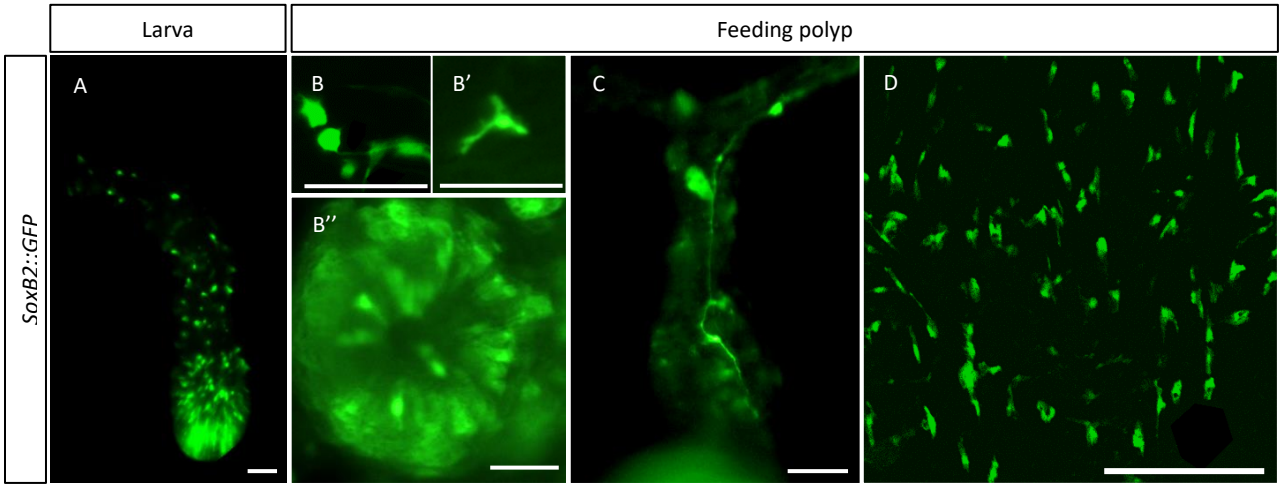

Figure 4.8. Live imaging of *SoxB2* transgenic reporter animals. (A) *SoxB2*-GFP is expressed in the epidermal layer in the larval stage mostly in the aboral pole. (B) In neuronal-like cells in the head region (B-B''). (C) Long interconnected neurons were found in the stolons of the primary polyp. (D) Neuronal- and nematoblast-like cells were observed in the body column of the adults. Red: GFP; Blue: Hoechst. Scale bars: 40 µm.

After establishing stable *SoxB1* and *SoxB2* transgenic reporter animals, I generated double transgenic animals by crossing *SoxB1* and *SoxB2* colonies in order to use them for single cell tracing studies as will be shown in the following section. By characterizing the double transgenic animals by IF, I observed a similar pattern consistent with the double *in situ* hybridisation results (see Fig. 4.4). As shown in Fig. 4.9, cells expressing both transgenes were observed at various levels as well as cells expressing either fluorescence protein.

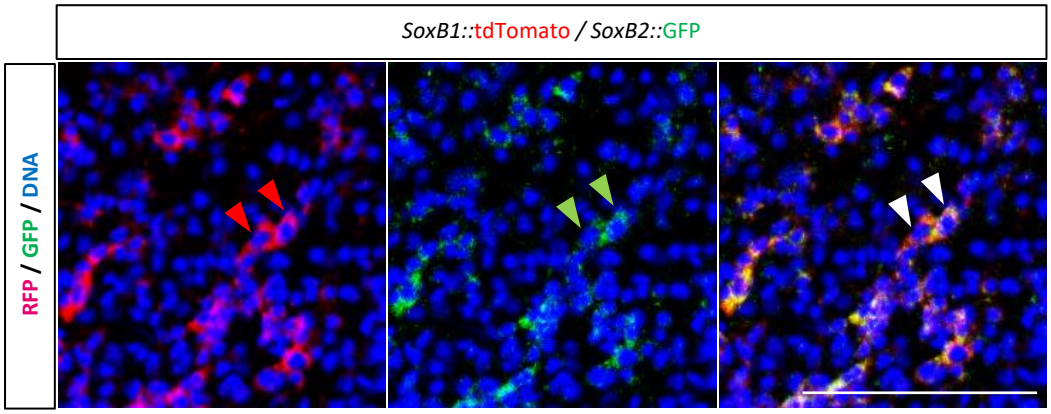

Figure 4.9. Characterisation of SoxB1 / SoxB2 double transgenic reporter animal by IF. Cells expressing both transgenes at various levels were found as shown by the examples pointed by the arrows, consistent with the *in-situ* hybridisation findings (red arrows show SoxB1$^+$ cells, green arrows show SoxB2$^+$ cells, and white arrows show SoxB1$^+$ / SoxB2$^+$ cells). Images are single optical slices. Red: tdTomato; Green: GFP; Blue: Hoechst. Scale bar: 40µm.

4.4: Tracing of single cells during nervous system regeneration

Hydractinia head regeneration requires proliferation and blastema formation. During this regeneration process, *Hydractinia* can replace not only cell types that are required for basic head structure such as epithelial cells, but also neurons and nematocytes. To date, the contribution of post-mitotic neurons, as well as neural progenitors in nervous system re-establishment has not been documented. In this section, I aimed to understand how these cell types contribute to head regeneration.

Previous members of the lab (Dr J. Gahan & S. Quillinan) generated a transgenic reporter line expressing GFP under the genomic control elements of the neuropeptide RFamide precursor. I utilised this animal and I generated second generation transgenic animals in order to understand whether this type of neurons contribute to nervous system regeneration upon injury/decapitation. Head regeneration in *Hydractinia* takes two to three days to be completed and by generating time-lapse movies, I was able to trace individual neurons and determine their fate and contribution to head regeneration.

I first identified individual neurons based on their morphology and location in the body column and followed them during first 20 HPD. As shown in Fig. 4.10, neurons located both in the lower and the higher parts of the body column do not contribute to head regeneration as they remain static and non-proliferative over the course of 20 hours. (Figs. 4.11, 4.12).

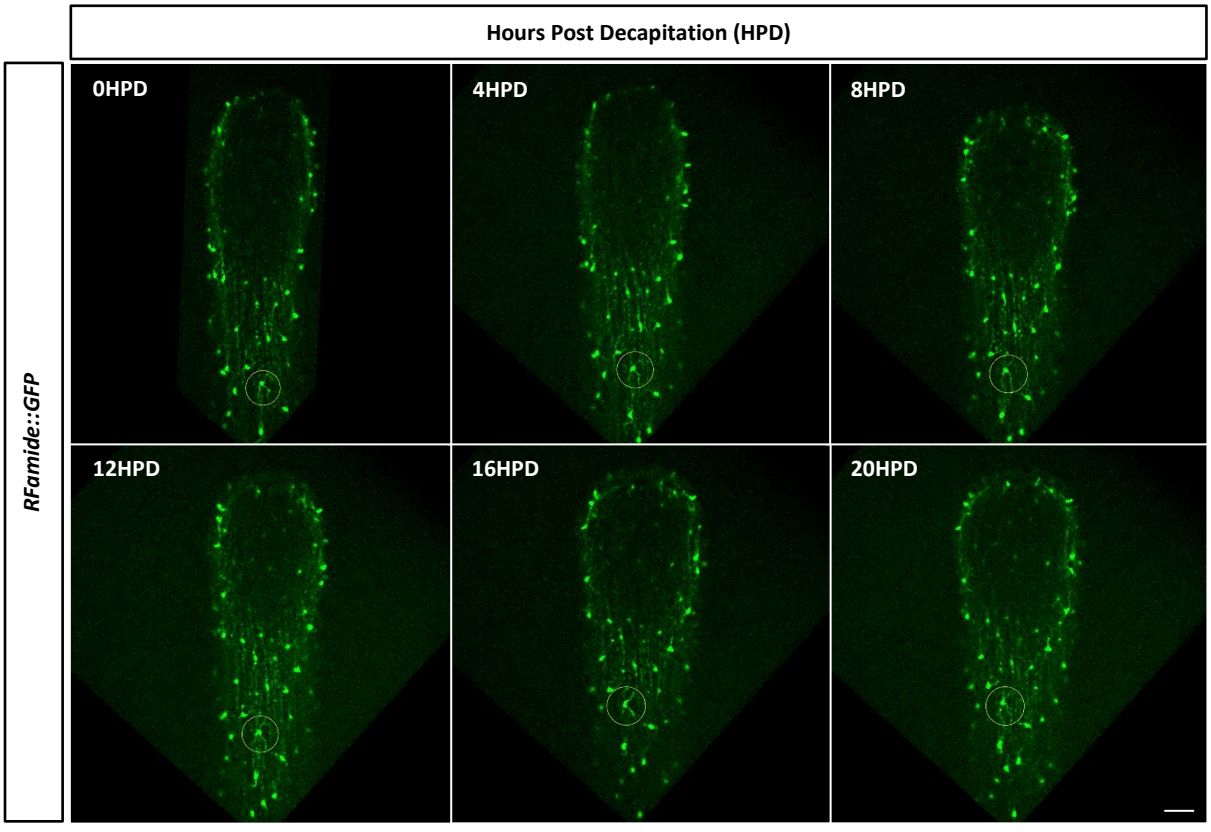

Figure 4.10. In vivo tracing of RFamide-GFP$^+$ neurons during regeneration located in the lower part of the body column. After following an individual neuron (circled), no migration was observed indicating no role during this process. Images are single optical slices. Green: GFP. Scale bar: 40µm

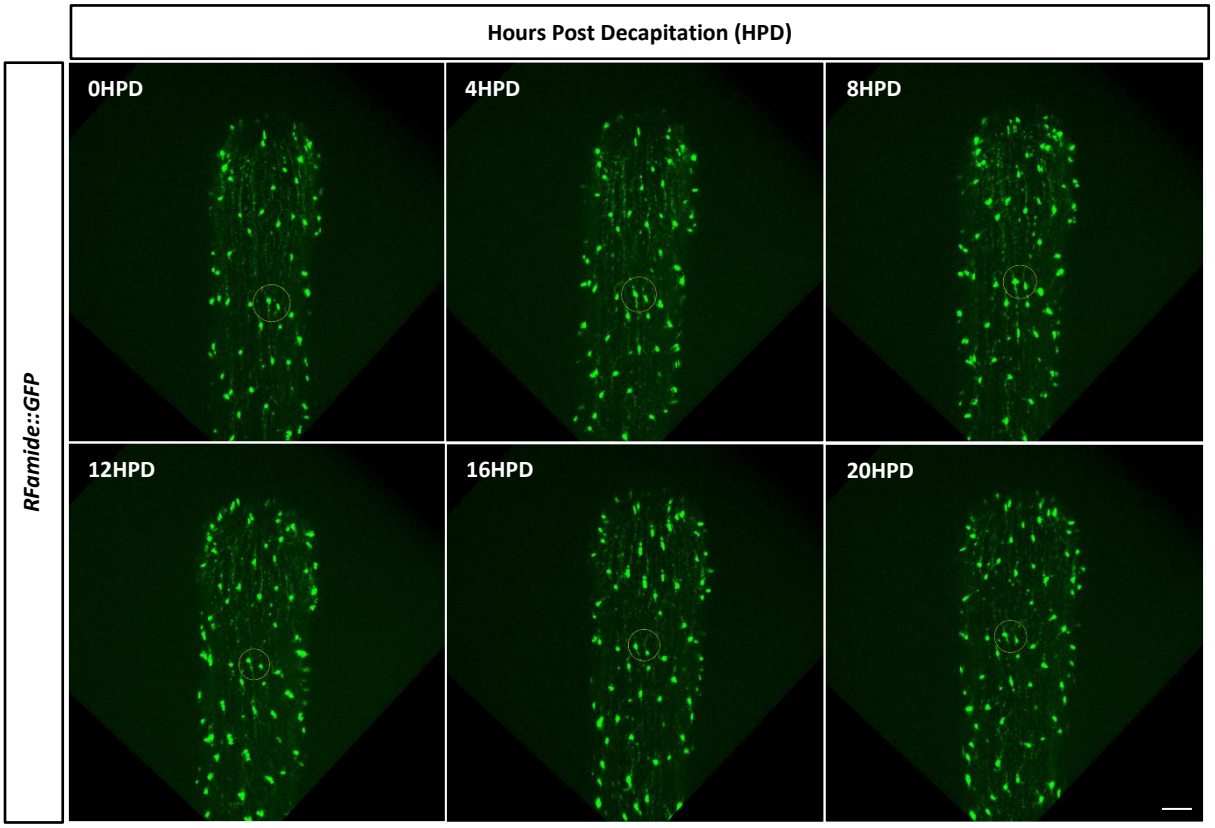

Figure 4.11. *In vivo* tracing of RFamide-GFP$^+$ neurons during regeneration located in the upper part of the body column. After following an individual neuron (circled), no migration was observed indicating no role during this process. Images are single optical slices. Green: GFP. Scale bar: 40 µm.

Since there was no visible migration or any signs of contribution of the *RFamide*-GFP$^+$ neurons to regeneration during the first 20 hours of head regeneration, I made time-lapse movies from 24 HPD – 72 HPD, a timeframe at which the nervous system and the head are fully re-established. I followed individual neurons, as seen in Fig. 4.12, and the same behaviour was observed. *RFamide*-GFP$^+$ neurons did not migrate to the injury side to contribute to blastema formation and/or nervous system regeneration, nor did they proliferate. Instead, they stayed at the original position and at the same time a new network of RFamide$^+$ neurons appeared as the head was regenerated, suggesting that *de novo* neurogenesis was the main source of neurons to the regenerating new head.

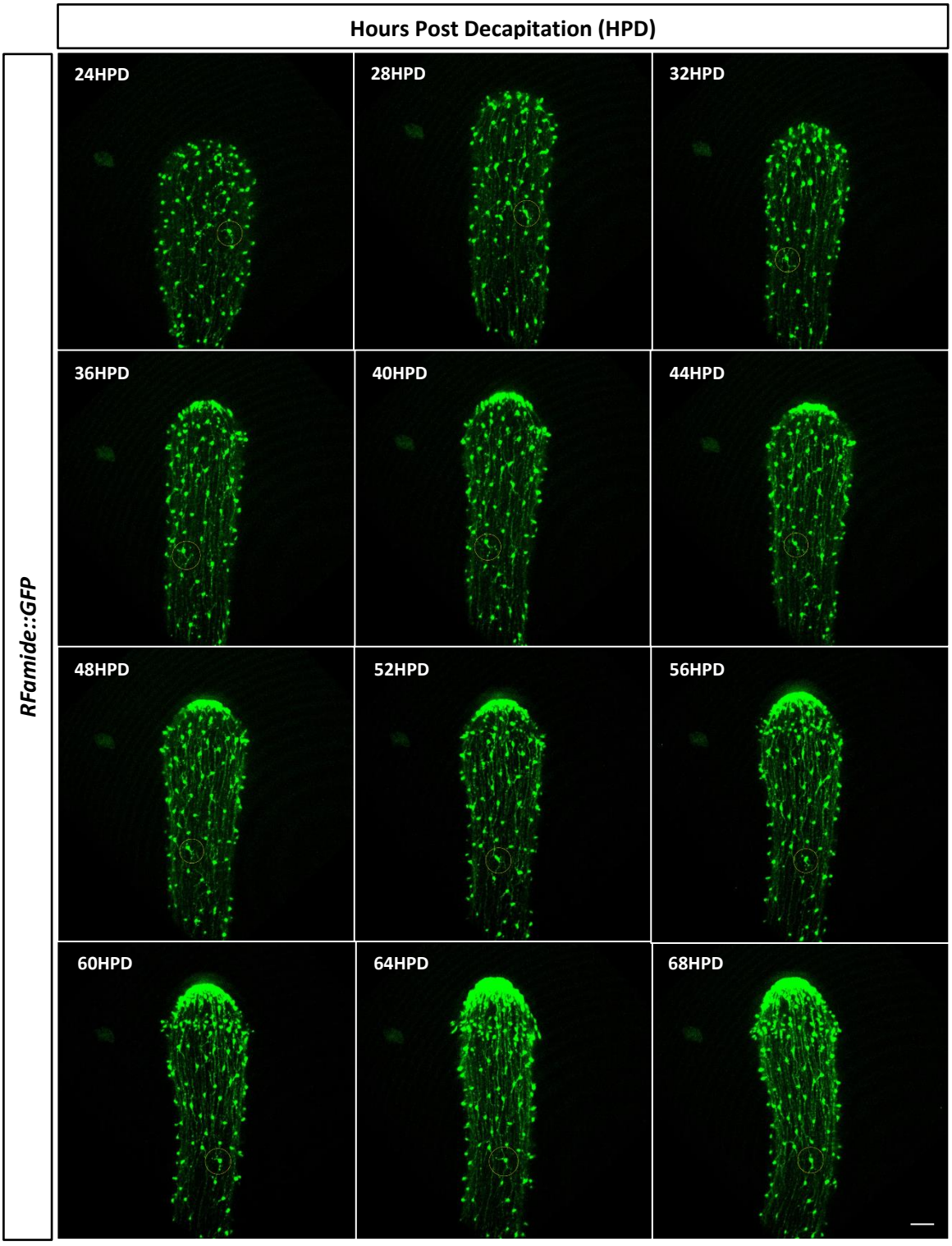

Figure 4.12. *In vivo* tracing of *RFamide*-GFP^{+} neurons during head regeneration from 24 HPD until 72 HPD. An individual neuron (circled) is shown in the time series. No significant migration was observed. Images are z-stack projections of a few slices. Green: GFP. Scale bar: 40 µm.

To test the hypothesis of *de novo* neurogenesis during head regeneration, I decapitated animals, performed a pulse EdU incorporation (30 minutes) to detect cells that undergo proliferation, and fixed the decapitated animals at 12 HPD, 24 HPD, 36 HPD and 48 HPD. I stained the samples with anti-Piwi2 antibody to label i-cells.

As seen in Fig. 4.13, in the intact head, only a few cells are proliferative and stem cells are not present. Instead, there is a fine network of RFamide neurons covering the whole area. During blastema formation (first 24 HPD), there is a huge increase in proliferation as indicated by the presence of EdU^+ and $Piwi2^+$ cells (most of them are $EdU^+/Piwi2^+$ cells). A few $RFamide^+$ cells are also present at these stages, but most probably are remnants of the nervous system. At the next time point I checked (36 HPD), new tissue was present above the blastema zone which was most likely the newly formed head. In this newly formed area, RFamide neurons were present and the absence of proliferation and stem cell markers (no co-expression) suggests *de novo* neurogenesis. By 48 HPD, tentacle buds were formed and more $RFamide^+$ neurons were present in this area.

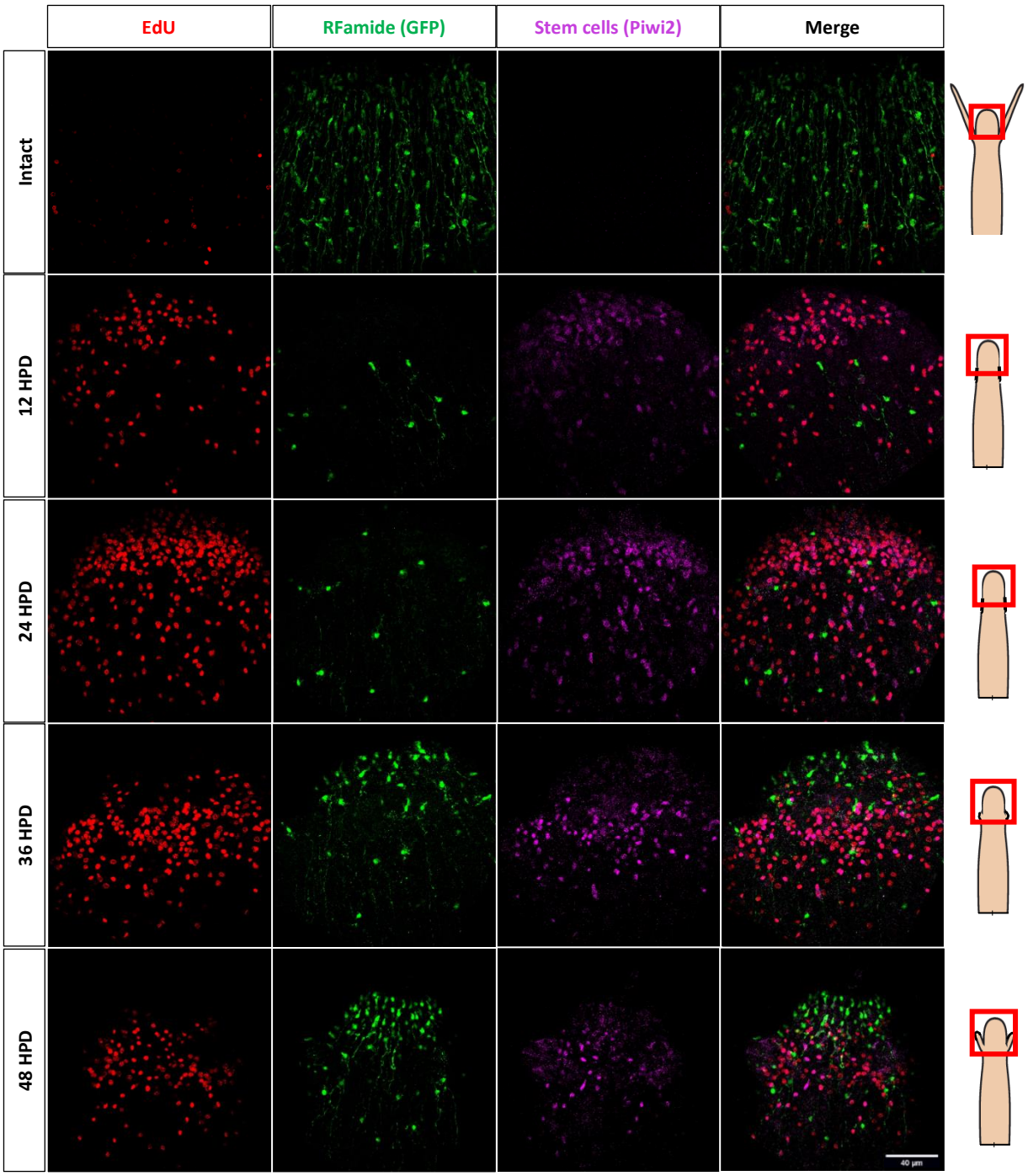

Figure 4.13. *De novo* neurogenesis during head regeneration. Time-course experiment in which the proliferation status (EdU), stem cell distribution (Piwi2), and neuronal contribution (RFamide) in nervous system re-establishment was documented (up to 48 HPD). Images are z-stack projections of a few slices. Red: EdU; Green: GFP; Purple: Piwi2. Scale bar: 40 µm.

Once the G1 *SoxB2::GFP* transgenic reporter line was established, I was able to observe how *SoxB2*-GFP$^+$ cells behave during head regeneration by *in vivo* tracing.

As seen in Fig. 4.14, SoxB2-GFP$^+$ cells increase in numbers during the early stages of regeneration. Late on, the increase in cell numbers was mostly concentrated in the injury side in order to re-establish the missing head region. The increasing number of GFP$^+$ cells was unlikely to be primarily due to mitosis, given the short time elapsing. *Hydractinia* i-cells and progeny have a cell cycle duration of approximately 24 hours (McMahon, 2018). A scenario in which i-cells differentiate to neural progenitors and start expressing *SoxB2* is more plausible.

Figs. 4.15, 4.16, and 4.17 show a follow up of individual cells from the lower part of the body, from a position closer to the injury side, and from the blastema area, respectively. In the absence of a nuclear marker, and due to the low resolution of the images, it is difficult to draw a final conclusion on the dynamics of *SoxB2*$^+$ cell behaviour in these cases. The data are consistent with both proliferation of existing *SoxB2*$^+$ cells and with a scenario of i-cells become committed to the neural lineage and start expressing *SoxB2*.

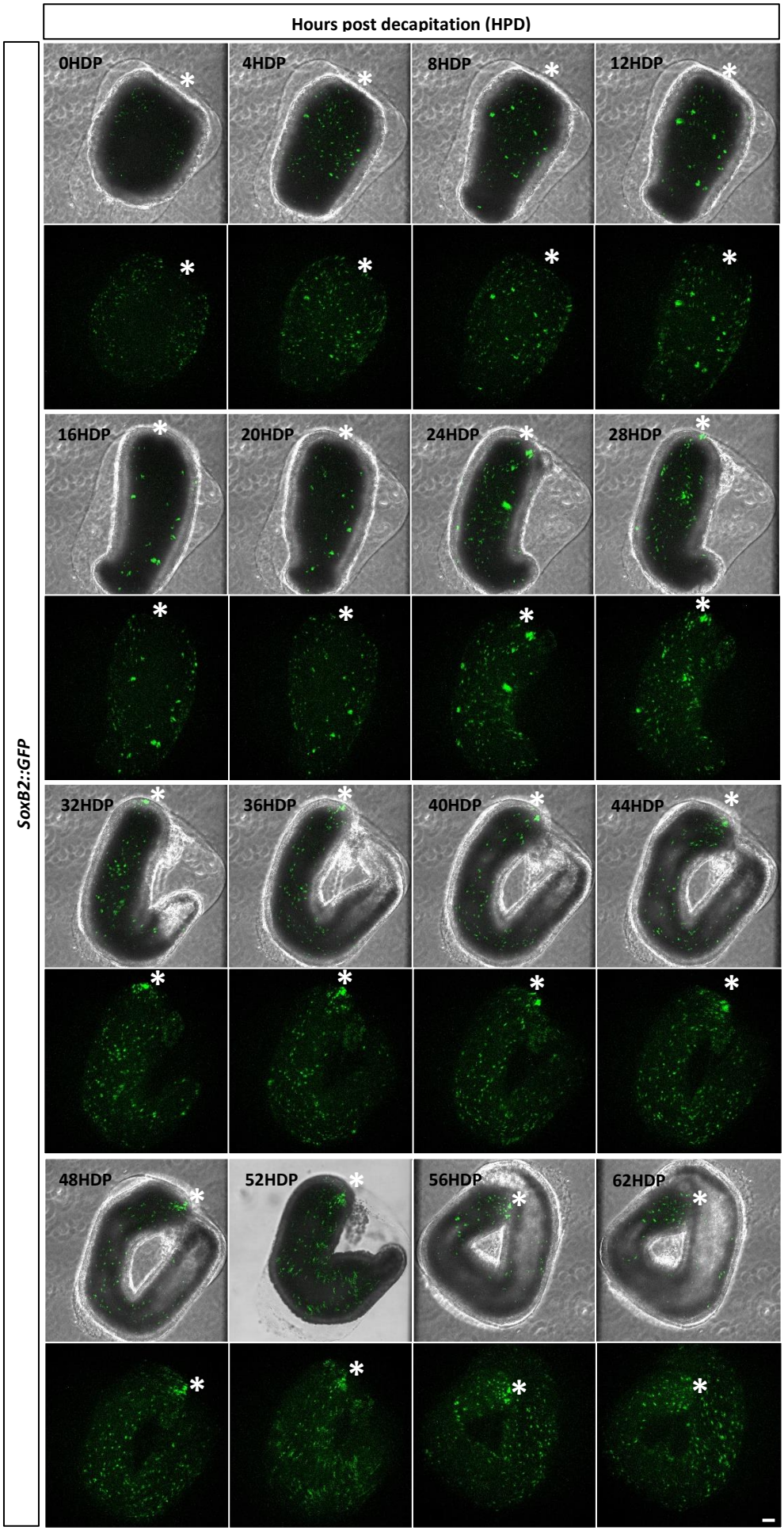
Hours post decapitation (HPD)
SoxB2::GFP
0HDP
4HDP
8HDP
12HDP
16HDP
20HDP
24HDP
28HDP
32HDP
36HDP
40HDP
44HDP
48HDP
52HDP
56HDP
62HDP

Figure 4.14. *In vivo* tracing of *SoxB2*-GFP^{+} neurons during head regeneration – from 0 HPD until 72 HPD. Asterisk denotes oral side. Images are z-stack projections. Green: GFP. Scale bar: 40 µm.

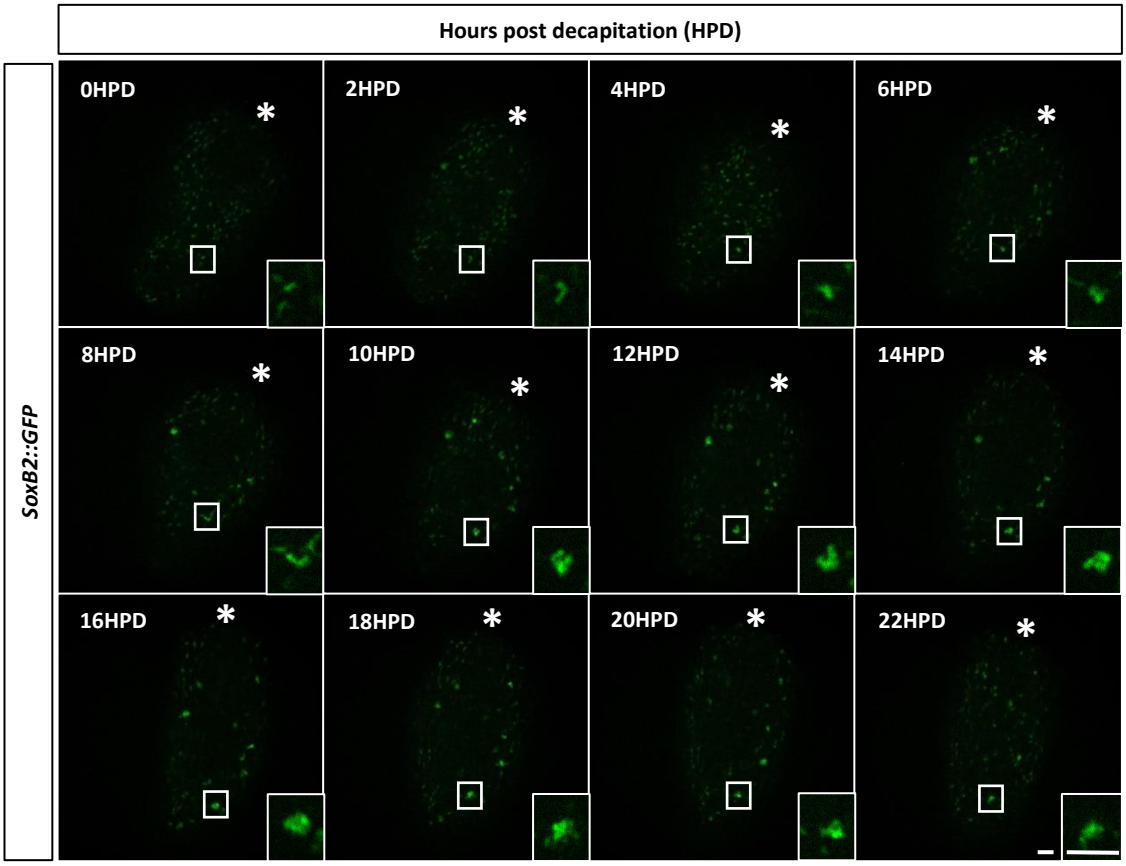

Figure 4.15. *In vivo* tracing of individual SoxB2-GFP^{+} cell during head regeneration. Asterisk denotes oral side. Images are single optical slices. Green: GFP. Scale bar: 40 µm.

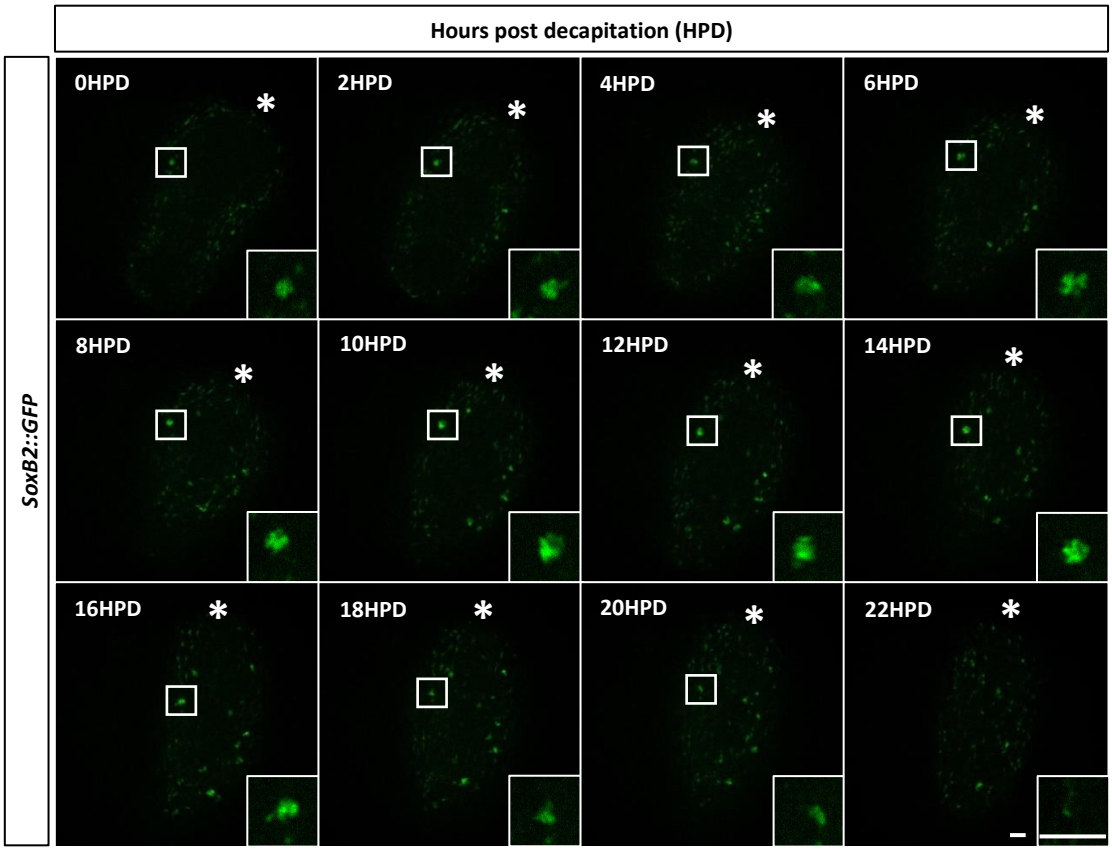

Figure 4.16. *In vivo* tracing of individual SoxB2-GFP⁺ cell during head regeneration. Asterisk denotes oral side. Images are single optical slices. Green: GFP. Scale bar: 40 µm.

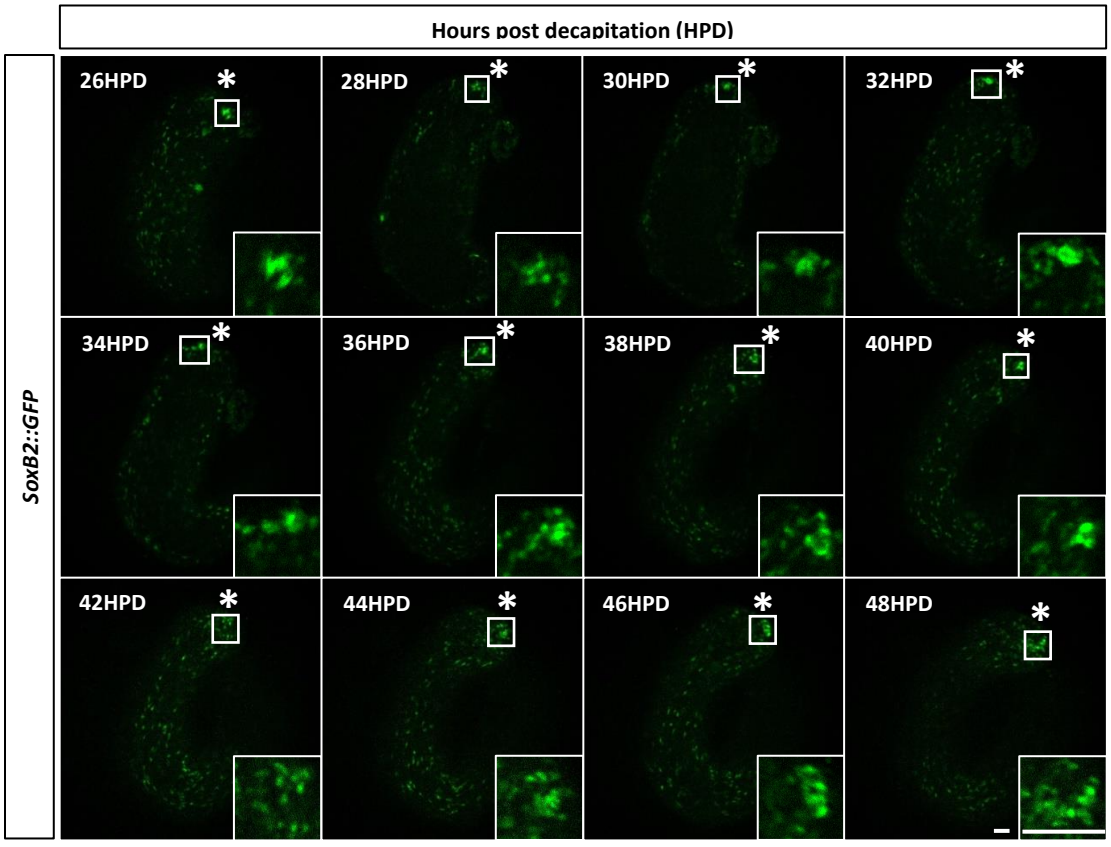

Figure 4.17. *In vivo* tracing of individual SoxB2-GFP⁺ cell during head regeneration. Asterisk denotes oral side. Images are single optical slices. Green: GFP. Scale bar: 40 µm.

Based on the in-situ hybridisation results, there was a strong indication that *SoxB1* and *SoxB2* are sequentially expressed in the neural lineage as it was previously shown that *SoxB2* is expressed in neural progenitor cells (Flici *et al.*, 2017). In order to provide more evidences to support this notion, I generated a double transgenic reporter line by crossing *SoxB1::tdTomato* and *SoxB2::GFP* reporter animals. By single cell tracing, I was able to show that SoxB1^{+} cells transitioned to SoxB2^{+} cells in a regeneration context over a short time period of only few hours (Fig. 4.18, 4.19, 4.20, 4.21) as they commit to the neural lineage. Since the half-life of both tdTomato and GFP fluorescence proteins is long, the transition from SoxB1 to SoxB2 was clearly visible. These findings confirm the sequential expression of these transcription factors in the neural lineage.

My initial goal was to also show the transition from SoxB2 to SoxB3 by the same method, but I was not successful in making the third reporter line (SoxB3).

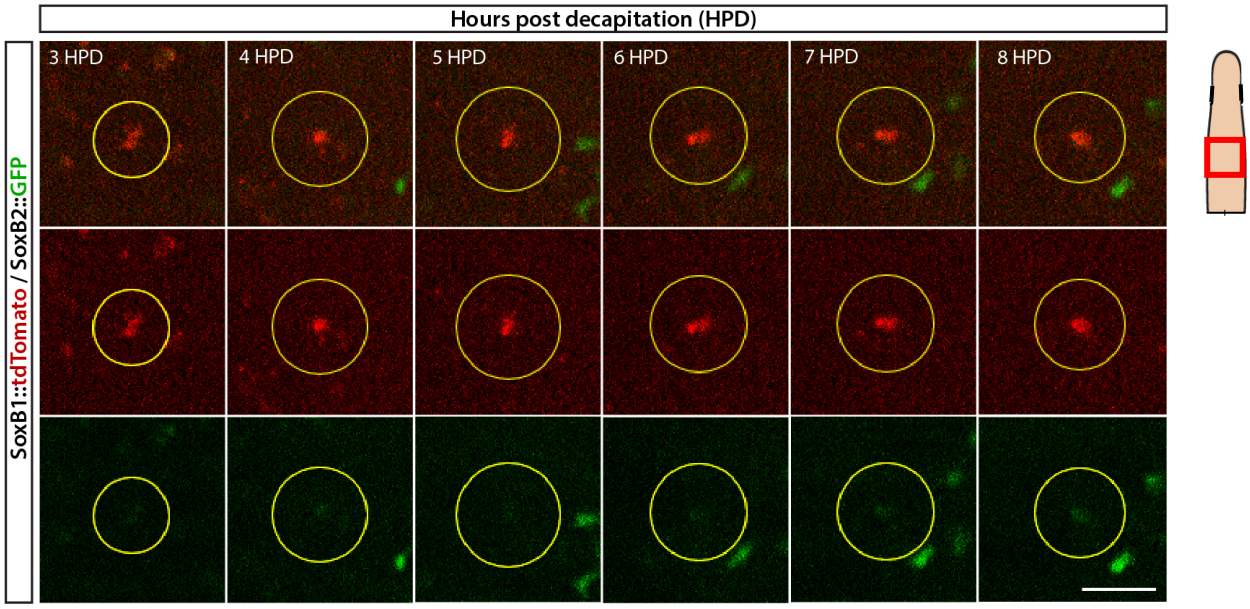

Figure 4.18. In vivo tracing of individual *SoxB1*-tdTomato^{+} cell transitioning to *SoxB2*-GFP^{+} cell during head regeneration. A single *SoxB1*-tdTomato^{+} cell over the course of few hours becomes double positive as the same cell starts expressing *SoxB2*-GFP as the cell commits to the neural lineage. Images are single optical slices. Red: tdTomato; Green: GFP. Scale bar: 40 µm.

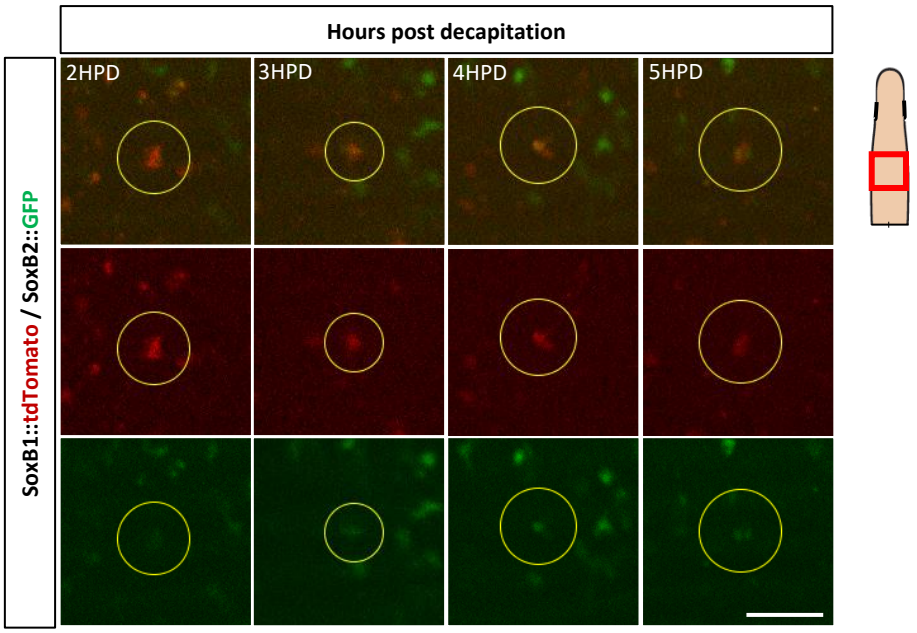

Figure 4.19. In vivo tracing of individual *SoxB1*-tdTomato⁺ cell transitioning to *SoxB2*-GFP⁺ cell during head regeneration. A single *SoxB1*-tdTomato⁺ cell over the course of few hours becomes double positive as the same cell starts expressing *SoxB2*-GFP as the cell commits to the neural lineage. Images are single optical slices. Red: tdTomato; Green: GFP. Scale bar: 40 µm.

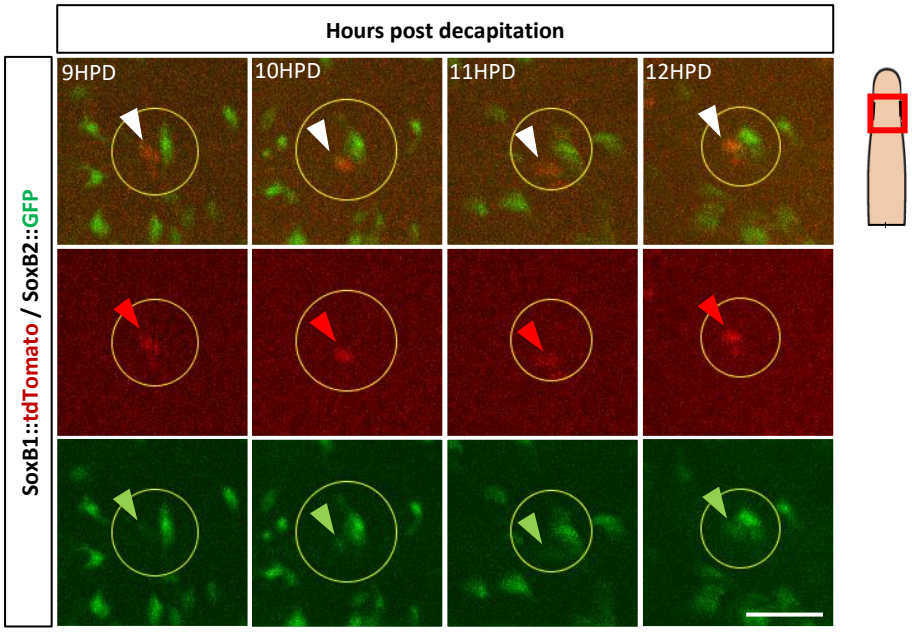

Figure 4.20. In vivo tracing of individual *SoxB1*-tdTomato⁺ cell transitioning to *SoxB2*-GFP⁺ cell during head regeneration. A single *SoxB1*-tdTomato⁺ cell over the course of few hours becomes double positive as the same cell starts expressing *SoxB2*-GFP as the cell commits to the neural lineage. Images are single optical slices. Red: tdTomato; Green: GFP. Scale bar: 40 µm.

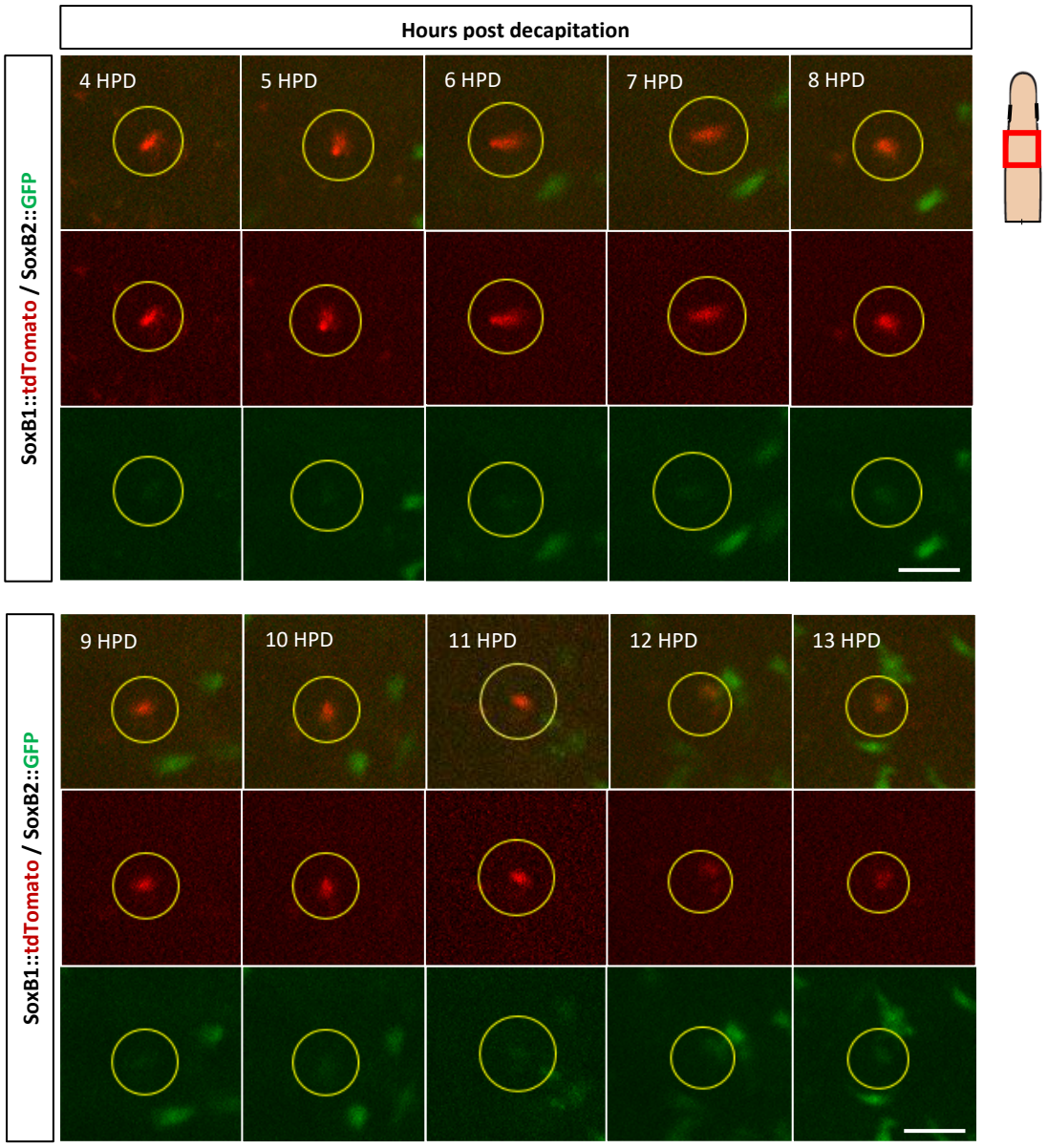

Figure 4.21. *In vivo* tracing of individual *SoxB1*-tdTomato⁺ cell transitioning to *SoxB2*-GFP⁺ cell during head regeneration. A single *SoxB1*-tdTomato⁺ cell over the course of few hours becomes double positive as the same cell starts expressing *SoxB2*-GFP as the cell commits to the neural lineage. Images are single optical slices. Red: tdTomato; Green: GFP. Scale bar: 40 µm.

4.5: Knockdown studies of SoxB genes during development

In order to decipher the roles of *SoxB1*, *SoxB2* and *SoxB3* during embryogenic and larval development, I knocked down these genes via shRNA-mediated gene silencing. shRNA was injected into one-cell stage embryos and at 3 days post fertilisation (HPF), larvae were fix and stained using various antibodies of known markers. This time point was chosen as by this stage the nervous system is fully developed in untreated larvae that are capable of metamorphosis following induction.

I first checked the effect of the knock downs on nematoblasts and i-cells using anti-Ncol1 and anti-Piwi1 antibodies respectively. As shown in Fig. 4.22, when *SoxB1* was downregulated, a decrease in nematoblast population was observed but surprisingly, the opposite effect was observed by *SoxB2* downregulation. This suggests a suppressive role of SoxB2 on the differentiation of nematoblasts during nematogenesis. When *SoxB3* was downregulated, no obvious effect on nematogenesis was observed.

I-cells were affected only when *SoxB1* was downregulated, as expected. As shown in Fig. 4.1, 4.2, 4.3, *SoxB1* was co-expressed with *Piwi1* and its downregulation reduced i-cell numbers. Downregulation of either *SoxB2* or *SoxB3* did not affect i-cell numbers; the former is expressed in neural progenitor cells and the latter in differentiated neuronal cells (Flici *et al*., 2017). Therefore, their downregulation was not expected to directly affect i-cells.

Three additional phenotypes were observed in shSoxB1-injecetd animals. first, knockdown larvae were markedly smaller (Fig. 4.26); second, they had reduced locomotion (data not shown); finally, their metamorphosis competence was severely compromised (Fig. 4.25).

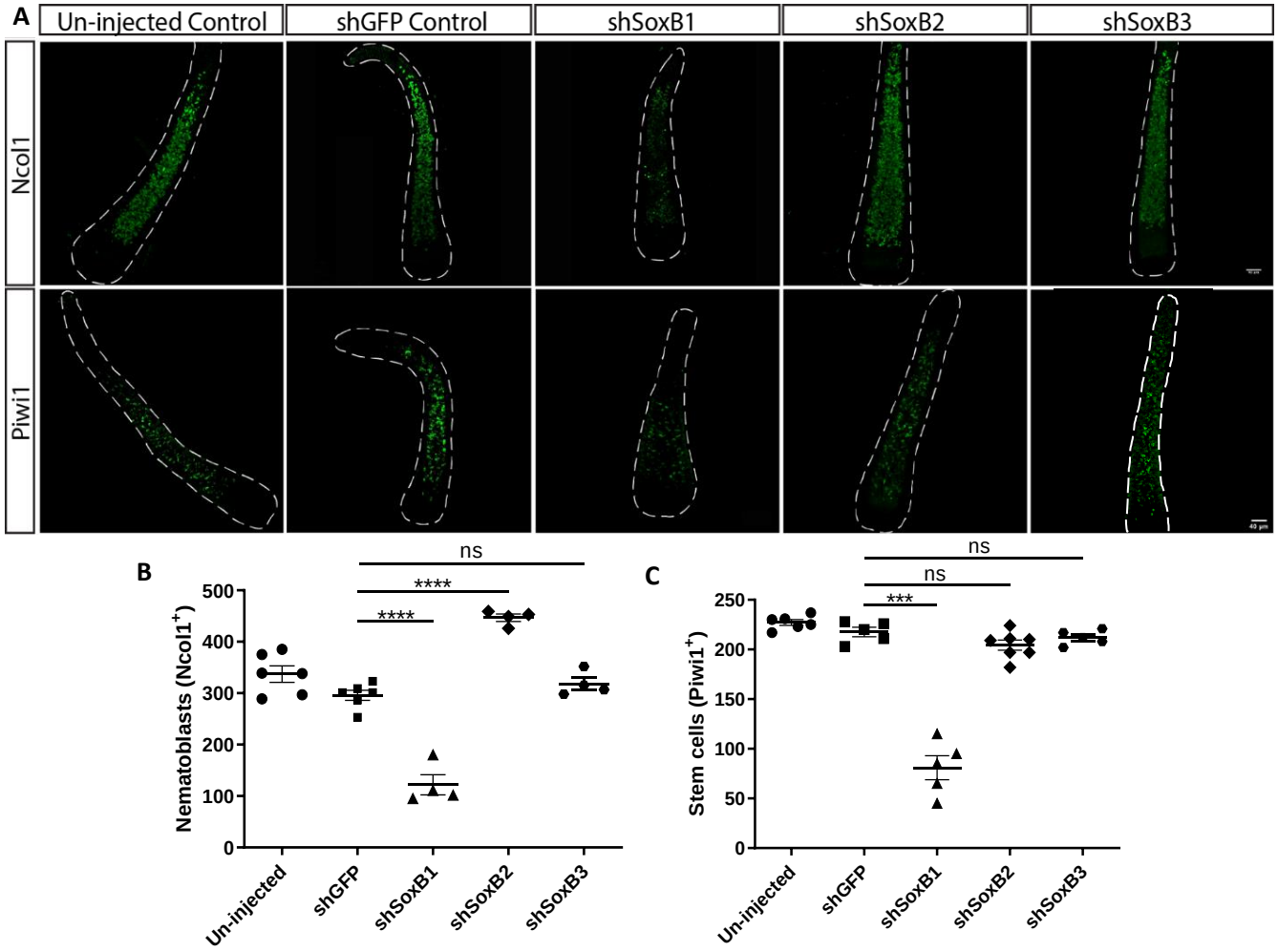

Figure 4.22. (A) Downregulation of *SoxB1*, *SoxB2* and *SoxB3* via shRNA-mediated gene silencing. I-cells (Piwi1^{+}) and nematoblasts (Ncol1^{+}) are significantly reduced when *SoxB1* was downregulated, whereas knock down of *SoxB2* and *SoxB3* did not affect these populations. Nematoblasts were increased upon downregulation of *SoxB2*, suggesting a suppressive role of at least a subpopulation of these cells in nematogenesis. *SoxB3* downregulation did not affect any of these populations. Images are z-stack maximum projections. Scale bar: 40 µm. Statistical analysis on the effect of *SoxB1*, *SoxB2* and *SoxB3* downregulation in nematoblasts (B) and stem cells (C). All the statistical analysis was done in GraphPad Prism 8.0.2 using Unpaired t-test (***P≤0.001, ****P≤0.0001).

In order to test if cell proliferation was affected, I performed a pulse EdU incorporation (30 minutes) to detect S-phase cells in 3 days-old larvae injected with either shSoxB1, shSoxB2, or shSoxB3. Cycling cells of both control animals (uninjected and shGFP-injected) were located gastrodermally, as expected (see also Fig. 3.5). Unexpectedly, proliferative cells were found in both the epidermal and the gastrodermal layers of larvae injected with shSoxB1, but these cells were not i-cells as they did not express Piwi1 (Fig. 4.23). Most probably the cells found in the epidermis would eventually go through apoptosis. Proliferative cells (EdU^{+}) in larvae injected with either shSoxB2 or SoxB3, were slightly reduced (Fig. 4.23). Since *SoxB2*

is expressed in neural progenitors, the reduction in proliferative cells by shSoxB2 was expected. From in situ hybridisation experiments (Fig. 4.5), a subpopulation of cells expressing both *SoIxB2* and *SoxB3* was observed, and the reduction of proliferative cells in shSoxB3 animals could explain this observation.

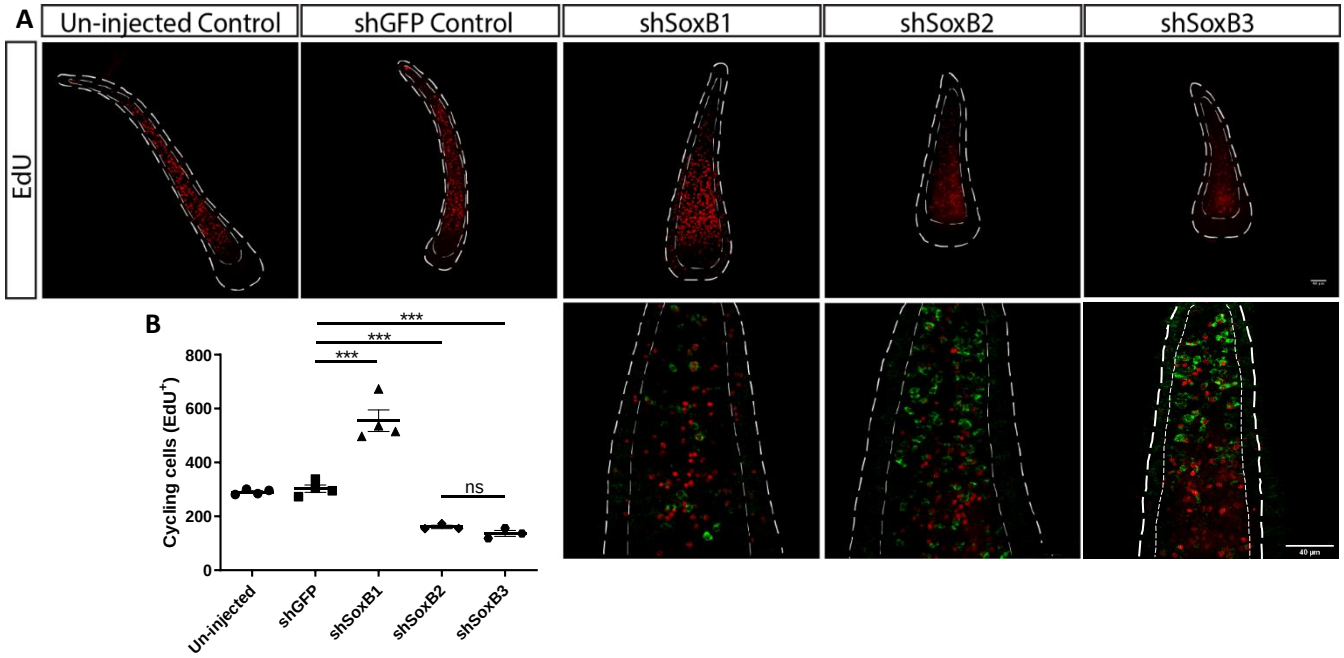

Figure 4.23. Downregulation of *SoxB1*, *SoxB2* and *SoxB3* via shRNA-mediated gene silencing affected proliferation. Proliferative cells (EdU^+) were found in the epidermal layer of shSoxB1 larvae, and a reduction was observed in both shSoxB2 and shSoxB3 larvae. (second row) In a higher magnification (second row) EdU^+ cells found in the epidermis of shSoxB1 larvae are not i-cells as they don't express Piwi1. shSoxB2 and shSoxB3-injected larvae did not exhibit the same phenotype; all proliferative cells resided in the gastrodermis in these larvae. Images are z-stack maximum projections. Red: EdU; Green: Piwi1. Scale bar: 40 µm. Statistical analysis on the effect of *SoxB1*, *SoxB2* and *SoxB3* downregulation in cycling cells (B). All the statistical analysis was done in GraphPad Prism 8.0.2 using Unpaired t-test (***$P \leq 0.001$).

Given the defective locomotion of *SoxB1* knockdown larvae, I investigated whether ciliogenesis was affected when any of the SoxB genes was downregulated. As shown in Fig. 4.24, cilliogenesis was extremely defective in shSoxB1 larvae. These animals showed an abnormal cilia layer covering the epidermis of the larvae (Fig 4.24 – surface view) which could explain the swimming deficiencies of these animals; also, their inner neuronal network was highly disorganized/absent. shSoxB2-injected larvae exhibited a much milder cilia phenotype and the gastrodermal neuronal network was not visibly affected. shSoxB3 larvae exhibited normal cilia and nervous system phenotype epidermal.

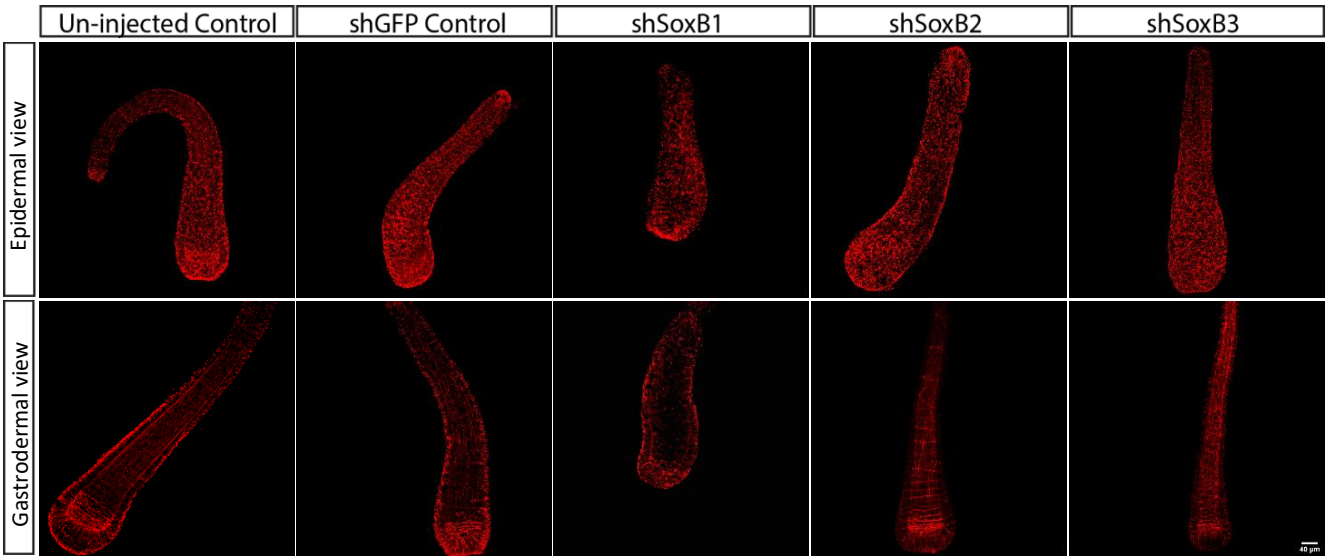

Figure 4.24. Effect of downregulation of *SoxB1*, *SoxB2* and *SoxB3* via shRNA-mediated gene silencing on cliogenesis. Downregulation of *SoxB1* highly affected ciliogenesis as cilia on the surface of the larvae seemed highly disorganized. The gastrodermal neuronal network was nearly absent. *SoxB2* knock down slightly affected cilia on the surface of the larva, but no effect was observed in the gastrodermal nervous system. Downregulation of *SoxB3* had no visible effect on cilia or gastrodermal neurons. These observations were based on IF using anti-acetylated tubulin antibody. Images are z-stack maximum projections. Red: acetylated tubulin. Scale bar: 40 µm.

Since SoxB genes are key players in neurogenesis, I stained shSoxB1, shSoxB2 or shSoxB3 – injected larvae with antibodies against two neuropeptides, GLWamide and RFamide, to see if the downregulation of SoxB genes had any effect on neurons (Fig. 4.25). *SoxB1* downregulation affected the generation of GLWamide$^+$ as well as RFamide$^+$ neurons. The lack of GLWamide$^+$ neurons explains the incompetence of these animals to metamorphose, consistent with the thought role of these neuropeptides in metamorphosis (Plickert *et al.,* 2003). On the other hand, downregulation of *SoxB2* affected only RFamide$^+$ neurons while the GLWamide$^+$ ones were still present and appeared normal. These animals could metamorphose, as expected. The selective effect of *SoxB2* downregulation on different neuronal subtypes is consistent with the prioritisation in GLWamide$^+$ neurogenesis as they are essential for metamorphosis induction. Another possible explanation was that GLWamide$^+$ neurons were generated before RFamide$^+$ neurons. *SoxB3* knockdown has not visibly affected any neuronal population.

Validation of the knockdowns was done by injecting shRNA for each SoxB gene individually and then performed single-molecule *in situ* hybridisation as shown in Fig. 4.27.

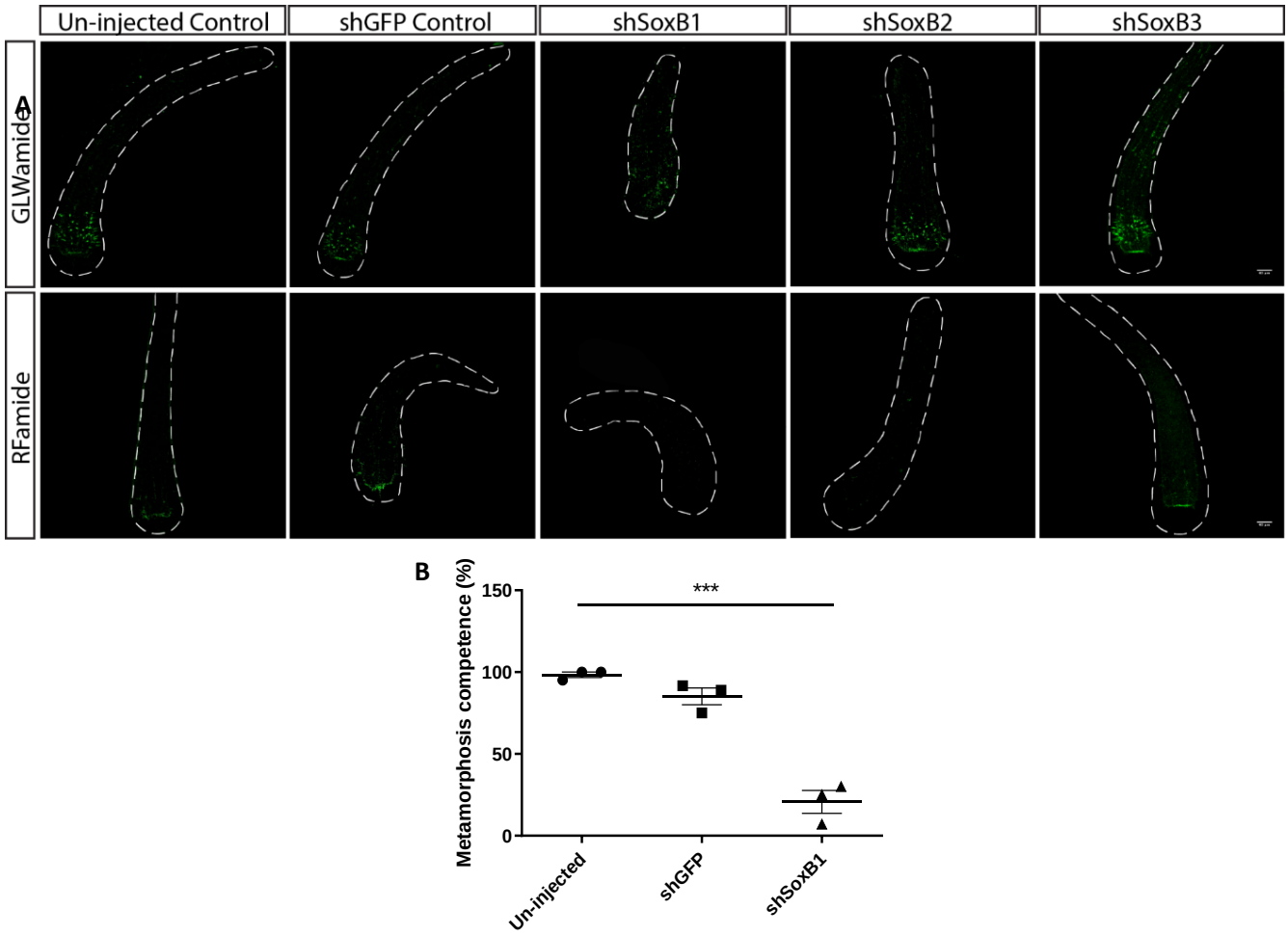

Figure 4.25. Downregulation of *SoxB1*, *SoxB2* and *SoxB3* via shRNA-mediated gene silencing and their effect on GLWamide$^+$ and RFamide$^+$ neurons (A). Downregulation of *SoxB1* diminished both differentiated neuronal cell populations, whereas downregulation of *SoxB2* affected only RFamide$^+$ neurons. Neither neuronal cell population was affected by *SoxB3* knockdown. Images are z-stack maximum projections. Scale bar: 40 µm. Statistical analysis on the effect of *SoxB1* downregulation in metamorphosis competence (B). All the statistical analysis was done in GraphPad Prism 8.0.2 using Unpaired t-test (***$P \leq 0.001$).

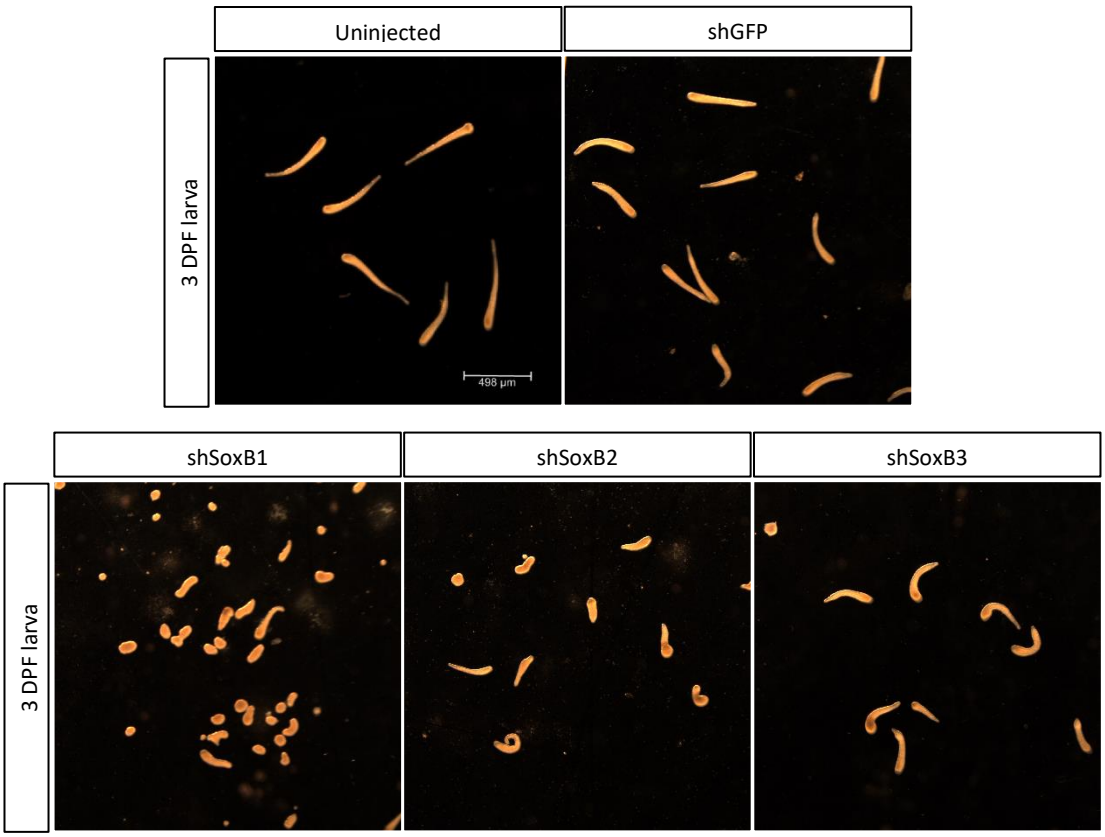

Figure 4.26. Morphology of control, shGFP-injected, shSoxB1-injected, shSoxB2-injected, and SoxB3-injected larvae. Scale bar: 498µm.

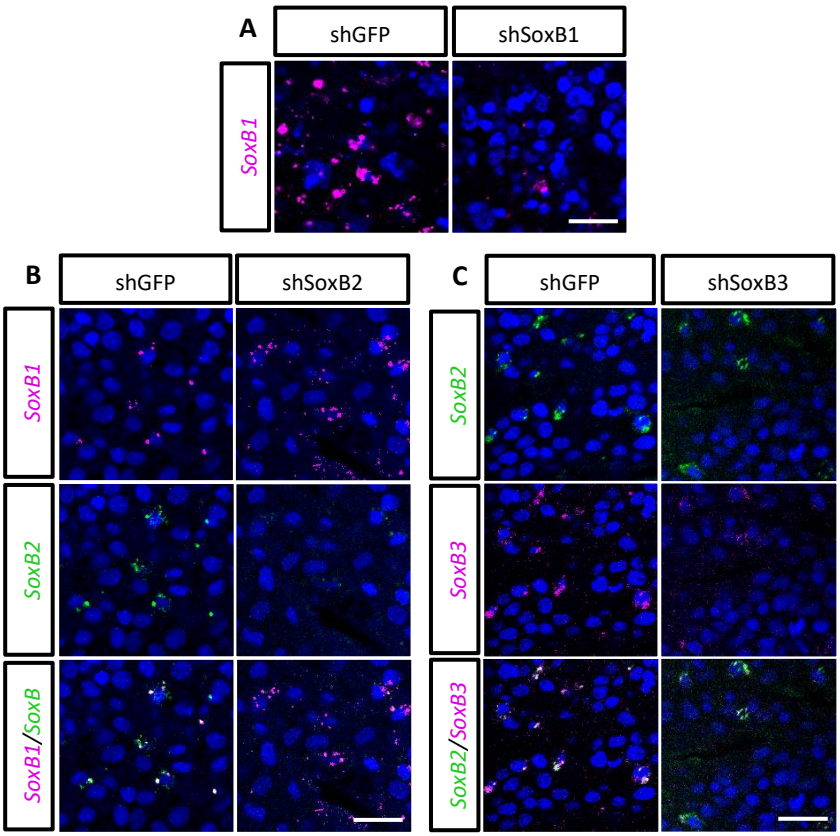

Figure 4.27. Validation of shSoxB1, shSoxB2 and SoxB3 knockdowns by single molecule fluorescence *in-situ* hybridization on 3DPF larvae. (A) Larvae injected with shSoxB1 showed lower expression levels of *SoxB1* compared to the control animals. (B) Larvae injected with shSoxB2 showed lower expression levels of *SoxB2* compared to the control animals and *SoxB1* levels remained unaffected. (C) Larvae injected with shSoxB3 showed lower expression levels of *SoxB3* compared to the control animals and *SoxB2* levels remained unaffected. Images are single optical slices. Scale bar: 40 µm.

4.6: Ectopic expression of *SoxB1*

Forced expression of pluripotency genes in differentiated somatic cells can reprogram them back to an undifferentiated state in mammals and in *Hydractinia* (Takahashi and Yamanaka, 2006; Millane *et al*., 2011). Given that *SoxB1* is homologous with mammalian *Sox2* and expressed exclusively in i-cells, I decided to investigate whether its expression in a differentiated cell type could destabilise the fate of these cells. For this, I forced-expressed *SoxB1* in a neuronal context by inserting its coding sequence in the *RFamide*::GFP reporter line plasmid. After generating the plasmid, I injected it in single-cell embryos and after metamorphosis, I fixed and stained primary polyps bearing this transgene. These animals expressed SoxB1-GFP in a subset of the neurons, cells that do not express *SoxB1* normally.

As shown in Fig. 4.28, these animals were able to metamorphose normally and there was not an obvious defect in the morphology of the polyps. Forced expression of *SoxB1* in neurons was most likely lethal as the remnants of GFP^+ cells seem to be in the vacuoles of phagocytic cells. These polyps were also counter-stained with the nematoblast marker Ncol1 to see if this neuronal context over-expression may had forced these neurons to change their fate into a more primitive one. This, however, was not the case as no GFP^+/$Ncol1^+$ cells were observed.

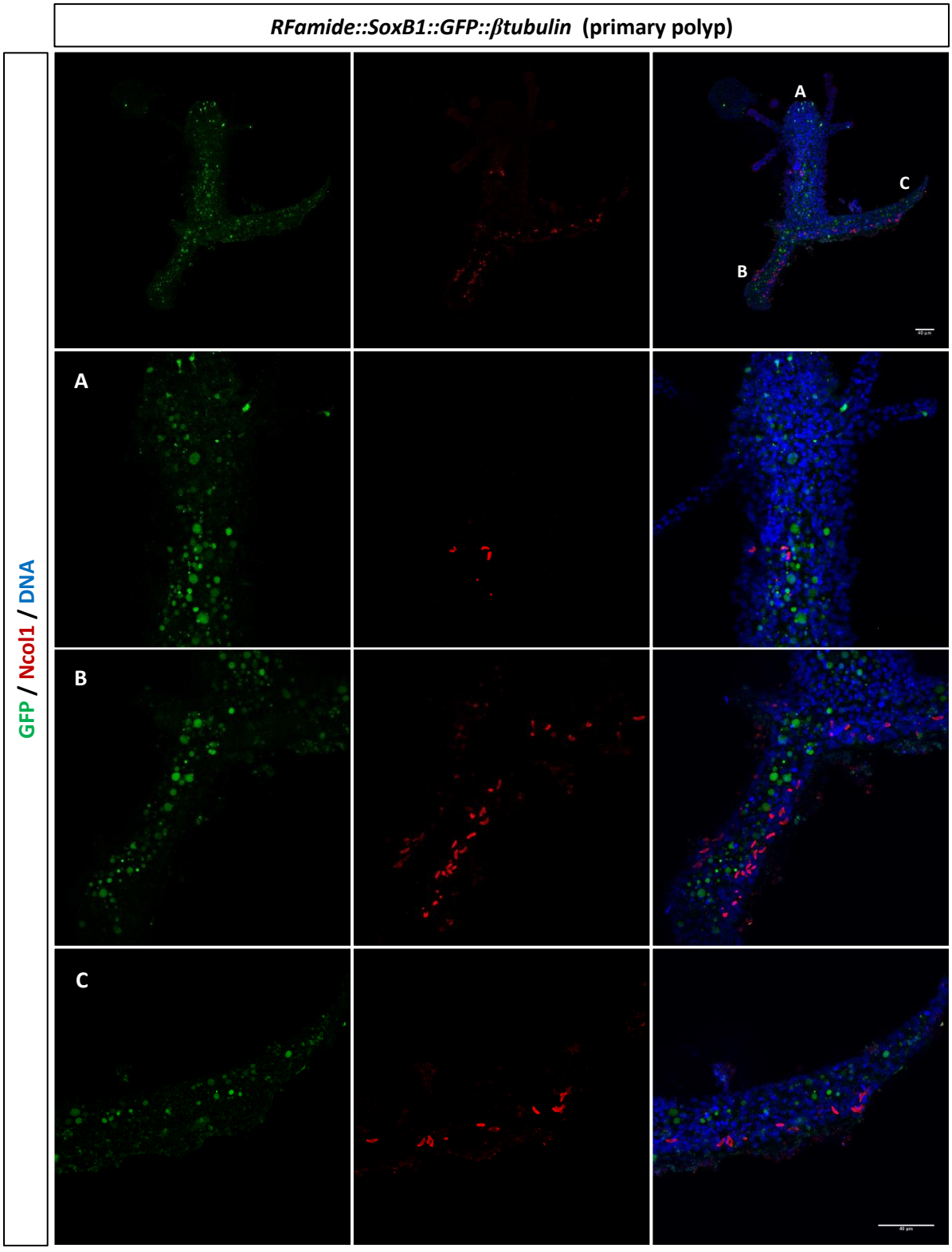

Figure 4.28. Forced expression of SoxB1-GFP in a neuronal context was lethal. Remnants of GFP could be seen in the vacuoles of phagocytic cells. (A) Polyp head and body. (B) Part of stolonal tissue. (C) Part of stolonal tissue. GFP was identified by direct fluorescence; Ncol1 by IF. Images are z-stack maximum projections. Green: GFP; Red: Ncol1; Blue: Hoechst. Scale bar: 40 µm.

4.7: Summary

In this chapter I first aimed to show the spatial expression of the three SoxB genes present in *Hydractinia*. By double fluorescence *in situ* hybridization I showed that *SoxB1* is expressed in i-cells and male and female germ cells, as it was always co-expressed with *Piwi1* – a classical i-cell/germ cell marker. Thus, *SoxB1* can be used instead of *Piwi1/Piwi2* to identify these cells.

I found that *SoxB1* was partially co-expressed with *SoxB2*, and *SoxB2* partially co-expressed with *SoxB3*. These results suggest a sequential expression of the three transcription factors in the pathway leading from uncommitted i-cells to neural progenitors and then to neurons.

I successfully generated *SoxB1* and *SoxB2* transgenic reporter lines in order to monitor *in vivo* their dynamic expression during regeneration. *SoxB2*$^{+}$ neural progenitors seemed to proliferate and/or be induced upon injury, but the detailed behaviour was difficult to assess in the absence of a nuclear marker and the low resolution of *in vivo* imaged cells. *SoxB1/SoxB2* double transgenic reporter animals and *in vivo* single-cell tracing enabled me to confirm the sequential expression of these two genes along the neural lineage.

I was also interested to see the contribution of differentiated neurons during nervous system regeneration. By utilizing the *RFamide*::GFP transgenic reporter line and following individual neurons *in vivo* in a regeneration context, I observed that differentiated neurons do not contribute to neuronal regeneration; instead, *de novo* neurogenesis is the primary mechanism contributing neurons to the new head.

Unfortunately, I was not able to generate a *SoxB3* transgenic reporter line in order to evaluate the contribution of SoxB2^{+} cells to other neural cell types.

By downregulating SoxB genes during development, I was able to reveal their roles during nervous system establishment during development. *SoxB1* knockdown affected all cell types examined as this gene is expressed in i-cells (section 4.2). These animals had compromised ciliogenesis, could not swim normally and their size was much smaller than control animals. this is consistent with a lower number if i-cells that are thought to contribute to all cell types in *Hydractinia*. Downregulation of *SoxB2* affected only specific populations of neurons, suggesting a preferential generation of cell types based on their need for larval metamorphosis. Another possible explanation for the reduction of RFamide^{+} neurons and not the GLWamide^{+} ones was that during neuronal development, the latter are established before the former ones. *SoxB3* knockdown resulted in no visible phenotype. This could either

be explained by a functional redundancy between SoxB2 and SoxB3, or that the defects were not visible by IF. Additional markers along the neuronal lineage would allow a better characterisation of the roles of these genes.

Finally, ectopic expression of *SoxB1* in a neuronal context (RFamide^{+} neurons), resulted in death of these cells. Remnants of GFP was observed in the vacuoles of phagocytic cells. Transgenic primary polyps were also stained with a nematoblast marker (Ncol1), as the initial hypothesis was that over expression of *SoxB1* would result in forcing the neurons to change their fate to a more primitive one along the neuronal lineage; this was not the case.

Chapter 5: Analysis of *Hydractinia* cell types by flow cytometry and RNA sequencing

5.1 Introduction & Aims

Since its invention in the 1950s (Coulter, 1953), flow cytometry has been widely employed in order to obtain fluorescence characteristics of single cells and microorganisms. Combined with the ability to group cells based on their size and granularity as well as other characteristics (Wilkerson, 2012), it has become one of the most used techniques initially in immunology and later in many other disciplines. This popular laser-based technology relies predominantly on one principle: the measurement of light scattering and fluorescence emission. The light scattering is related to the morphological properties of the cell whereas the fluorescence emission is proportional to the amount of fluorescent probe/marker found to the cell (Adan *et al*., 2017).

Not long after the development of this technology, Fulwyler applied this principle to physically sort cells and fluorescence-activated cell sorting (FACS) has emerged (Fulwyler, 1965), changing the field and providing limitless opportunities for new discoveries.

In the past decade, due to further technological advances and increased need for high-throughput and multiparametric analysis, imaging flow cytometry (IFC) was developed (Barteneva *et al*., 2012). While retaining the main features of conventional flow cytometry (light scattering and fluorescence emission), IFC also utilizes optical imaging functionality at informative spatial resolution which relies on high-speed cameras that use time delay and integration (TDI) technique providing higher sensitivity when imaging moving cells (Han *et al*., 2016).

Although flow cytometric analysis has been available to studies on bilaterian and some non-bilaterian animal models for many years, *Hydractinia* researchers were lacking this essential technique from their toolbox. The main aim of this chapter was to find a way to reveal the transcriptional profile along the neuronal lineage by utilising dissociated cells from transgenic reporter animals. For that, I wanted to find a reliable and reproducible technique to achieve that. In this chapter, I describe the establishment of flow cytometry, IFC and FACS, the identification and characterization of various cell types from transgenic reporter animals, as well as cell cycle analysis of various cell types that has never been done before in *Hydractinia*.

5.2 Characterization of dissociated cells from transgenic reporter animals by FC

In order to start characterizing *Hydractinia* cells, a gating strategy during both data acquisition and analysis was first established. As shown in Fig. 5.1, cell suspensions are first run without any nuclear staining and all events are gated out. This allows to discriminate between cells and debris as the latter will not have any nuclear signal. The same gate is then applied for cells stained with the nuclear marker such that debris stays out of the gate. Next, a second discrimination between single cells and cluster of cells must be made. Since the cell suspension is a highly heterogeneous mixture, most cells are considered as "single" (variety of cell sizes) and only the ones that fall clearly outside of this population are gated out (based on density plot). In the next step, the selected "singlets" are gated based on the fluorescence profile. In order to properly set the gates during both data acquisition and analysis, cells from wild-type animals are first used to discriminate between fluorescent and non-fluorescent populations. Once the non-fluorescence gate is set, the same gating strategy is followed for analysing transgenic reporter animals. The GFP^+ (or other fluorescent proteins) cells are then distinguishable from the GFP^- ones.

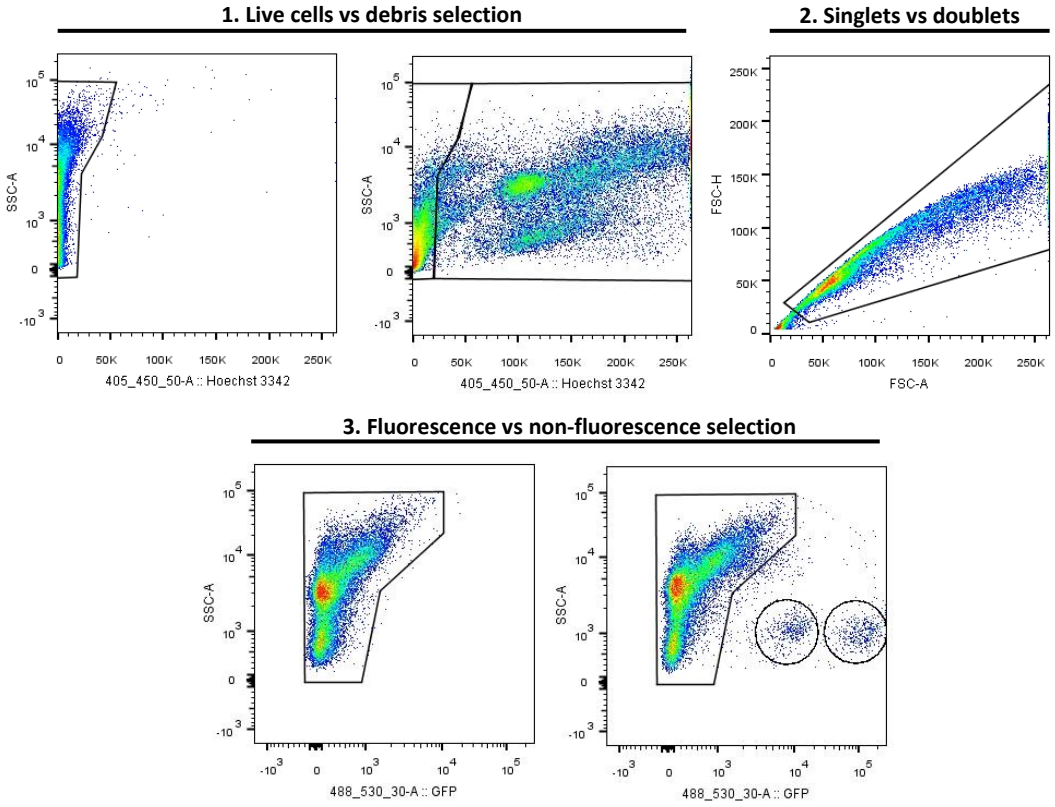

Figure 5.1. Gating strategy for analysing dissociated cells from transgenic reporter animals by flow cytometry. Cells are first gated based on their Hoechst profile, then based on singlets vs doublets discrimination and finally based on their fluorescence profile (GFP^- vs GFP^+). As an example, the *RFamide::GFP* line is shown.

The above gating strategy was implemented in order to characterize various transgenic reporter lines currently available in the lab.

For the purposes of this chapter I used the following transgenic reporter animals:

- *Piwi1::*GFP transgenic reporter line: stem cells
- *SoxB2::*GFP transgenic reporter line: neural progenitors
- *RFamide::*GFP transgenic reporter line: differentiated neurons
- *Actin::*GFP: transgenic reporter line: epithelial cells
- *AP2::*GFP: transgenic reporter line: germ cells
- *Piwi1::*GFP */ β-tubulin::*mScarlet double transgenic reporter line: *Piwi1* – stem cells, *β-tubulin* – ubiquitous expression
- *Eef1α* CRISPR/Cas9-mediated knock-in reporter line (GFP) – ubiquitous expression

Flow cytometric profiling of the transgenic reporter lines resulted in some expected patterns but even more interesting it was able to detect cellular subpopulations within some lines (Fig. 5.2).

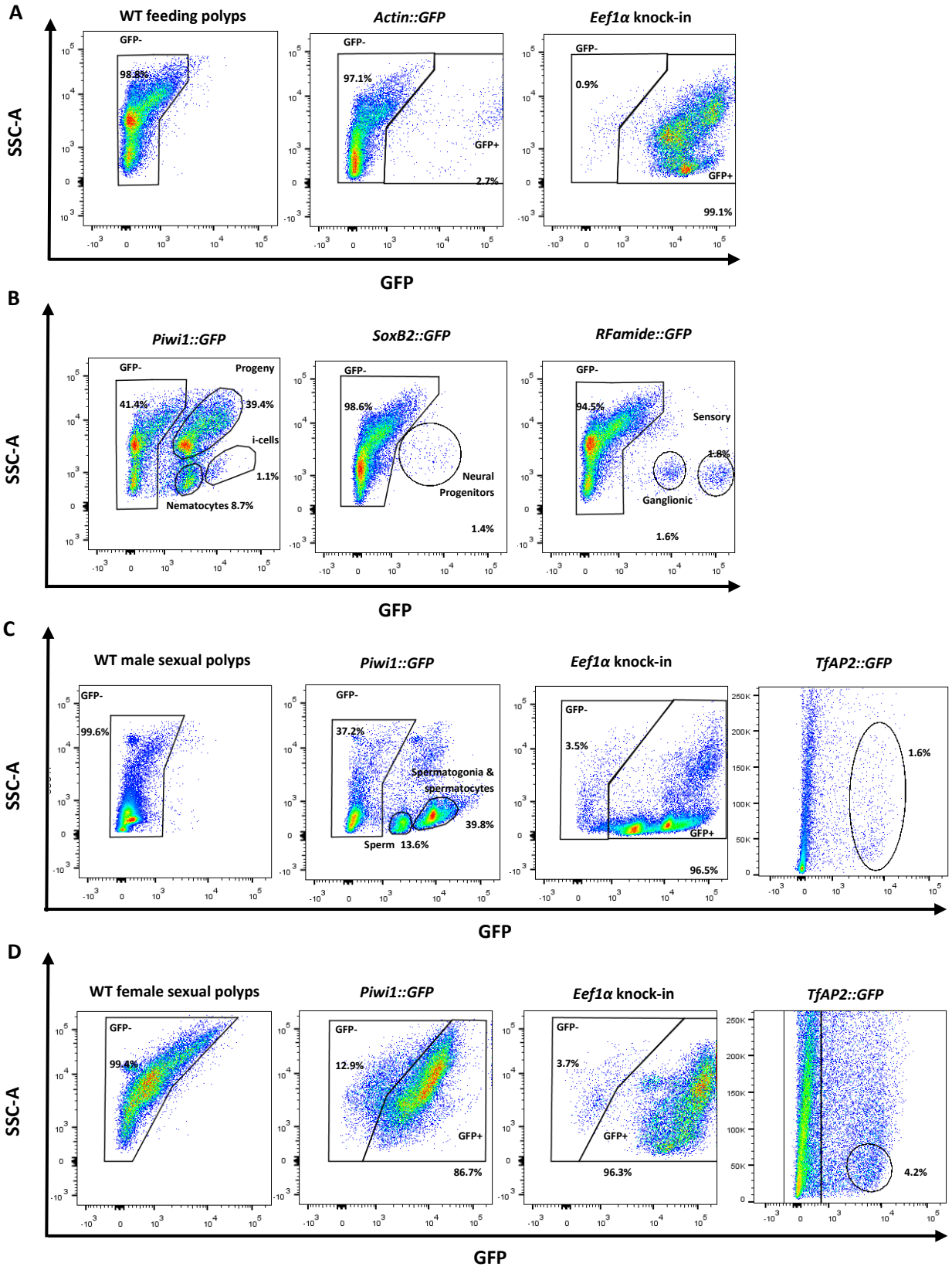

Figure 5.2. Flow cytometric profiles of transgenic reporter lines. Characterization includes feeding polyps (A, B), male (C) and female (D) sexual polyps. The nature of the reporter line and the polyp type is indicated in each plot.

As shown in Fig. 5.2A, the fluorescence profile of the *Eef1a* knock-in line it was as expected, and virtually all the cells are GFP$^+$. Less than 1% of the dissociated tissue falls into the non-fluorescence gate be this can be due to some residual debris and/or the presence of fragmented cells. Next, the epithelial reporter line *actin::GFP* gives a nice cluster of high GFP$^+$ cells and some cells scattered around. Based on previous studies (Künzel *et al*., 2010), *actin::GFP* transgenic reporter animals express the transgene predominantly in epithelial cells. Since all the experiments described in this chapter were done with dissociated cells from polyps and did not include any stolonal tissue, the amount of actin-GFP$^+$ cells found by flow cytometry was in line with the observations in intact polyps.

The profile of *Piwi1*::GFP line (Fig. 5.2B) was one of the most interesting ones, given that the GFP transgene is expressed in this animal only in i-cells from which all lineages derive. Therefore, it was to expect that all, or nearly all cells would have some levels of fluorescence. Overall, the distribution of cells based on their GFP expression resolved into three major subpopulations in the feeding polyps. A rare, high GFP$^+$ population was identified along with a wide population of cells showing lower levels of GFP and a smaller population of cells with the lowest levels of GFP. As it will be discussed in the next section (see section 5.4), these populations are characterized as i-cells, progeny, and nematocytes, respectively.

The profile of GFP-expressing cells under the genomic control elements of *SoxB2* was relatively simple as only one cluster of cells was identified with various levels of GFP expression. Surprisingly, when the *RFamide::GFP* reporter line was examined, two distinct subpopulations were identified. Based on the level of GFP fluorescence, the highest GFP$^+$ population was named “sensory” (sensory neurons). This was based on observations from the intact polyp where I observed the brightest neurons were located in the very oral part of the head (hypostome). The second population was named “ganglionic” (ganglionic neurons) again based on the location of these neurons in the polyp. These neurons are the ones running along the body column with very long neurite projections.

Next, since I now had a reliable method to identify distinct populations based on their fluorescence intensity using flow cytometry, I examined cells from both male and female sexual polyps. As shown in Fig. 5.2C-D, the profile of cell clustering from wild-type male and female sexual polyps is markedly different from each other and from wild-type feeding polyps due to the fact that different cell types are presented in these two types of cells including the presence of gametes – sperm cells and oocytes at different stages of development. As can been appreciated from the flow profile of the *Piwi1::GFP* male sexual

cells (Fig. 5.2C), the cells are clustered based on their GFP fluorescence in two subpopulations. As it will be explained in section 5.3, these populations were mature spermatocytes and spermatogonia. In the male sexual polyps of the Eef1a reporter line, the majority of the cells were GFP^+ as expected. In the female sexual polyps (Fig. 5.2D), no distinct populations were identified in the wild-type animals nor in the *Piwi1::GFP* and Eef1a reporter lines. In the two reporter lines, no distinct population were identified due to the fact that i-cells give rise to all the cell types including the gametes and hence the majority of the cells would be GFP^+. Also, the flow cytometric profiles from male and female sexual polyps of *TfAP2*::GFP transgenic reporter animal (Fig. 5.2C) were identified and further characterised by IFC as shown later on in Fig. 5.10.

As will be discussed in the next section (section 5.3), the populations identified by IF were further characterised by IFC based both on the fluorescence intensity levels and the area of the cells. In addition, the morphology of the populations examined, revealed their identity, for example, nematocytes have a distinct morphology – the nematocyst. Another example was the neuronal nature of some subpopulations by the presence of neurites. The sperm cells were also identified based on the characteristic tale these cells have. Further observations and evidences of the nature of distinct subpopulations within a transgenic reporter animal can be found in the next section.

5.3 Identification of distinct cell populations by Imaging Flow Cytometry

In order to further characterize the nature of the populations identified in the previous section by conventional flow cytometry, imaging flow cytometry (IFC) was implemented. In brief, IFC functions as a conventional flow cytometer with the addition of taking a bright field/ fluorescence image of every event. By using IFC, there is the advantage of having a bright field and/or fluorescence image of each cell analysed by the system. This advantage provides the ground of identifying and characterising unknown cell populations in a very short timeframe. Since the two approaches – flow cytometry and imaging flow cytometry – implement different cytometers and software, a slightly different gating strategy had to be established. As shown in Fig. 5.3, the cells in focus are first selected based on the normalized frequency of the bright field, and then single cells are selected based on the aspect ratio. Since the cell suspension is highly heterogeneous, all the cells were selected to avoid excluding cells of highly irregular shape, such as neurons. In a homogeneous cell population, the cells would normally shift towards Aspect Ratio=1 as this function measures the roundness of a cell.

In the following step, cells labelled with the nuclear marker Hoechst33342 were selected to exclude any cell debris and these cells were then plotted based on their fluorescence intensity. With IFC, I was able to examine reporter lines expressing both GFP and mScarlet fluorescence proteins in different cellular contexts.

.

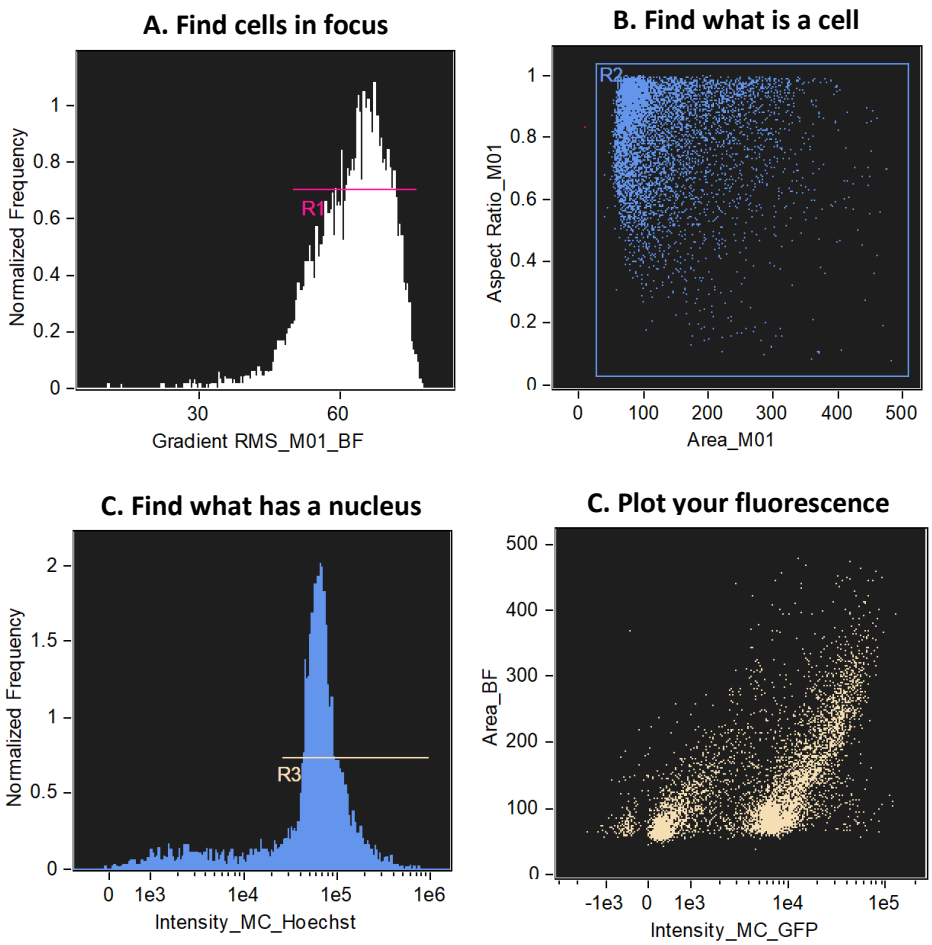

Figure 5.3. Workflow on how data analysis from imaging flow cytometry is performed. First, cells in focus are selected, followed by a selection based on the area of the cells. Since this was a heterogeneous population, all cells were selected. Then, cells that incorporated the nuclear dye Hoechst are selected and finally plotted based on the fluorescence expression levels.

I characterized the three distinct populations of the *Piwi1::GFP* feeding polyps, identified in the previous section, the two populations from the *Piwi::GFP* male sexual polyps, the two populations of the *RFamide::GFP* feeding polyps. Finally, I included the double transgenic reporter line *Piwi1::GFP ßtubulin::mScarlet* (Fig. 5.4).

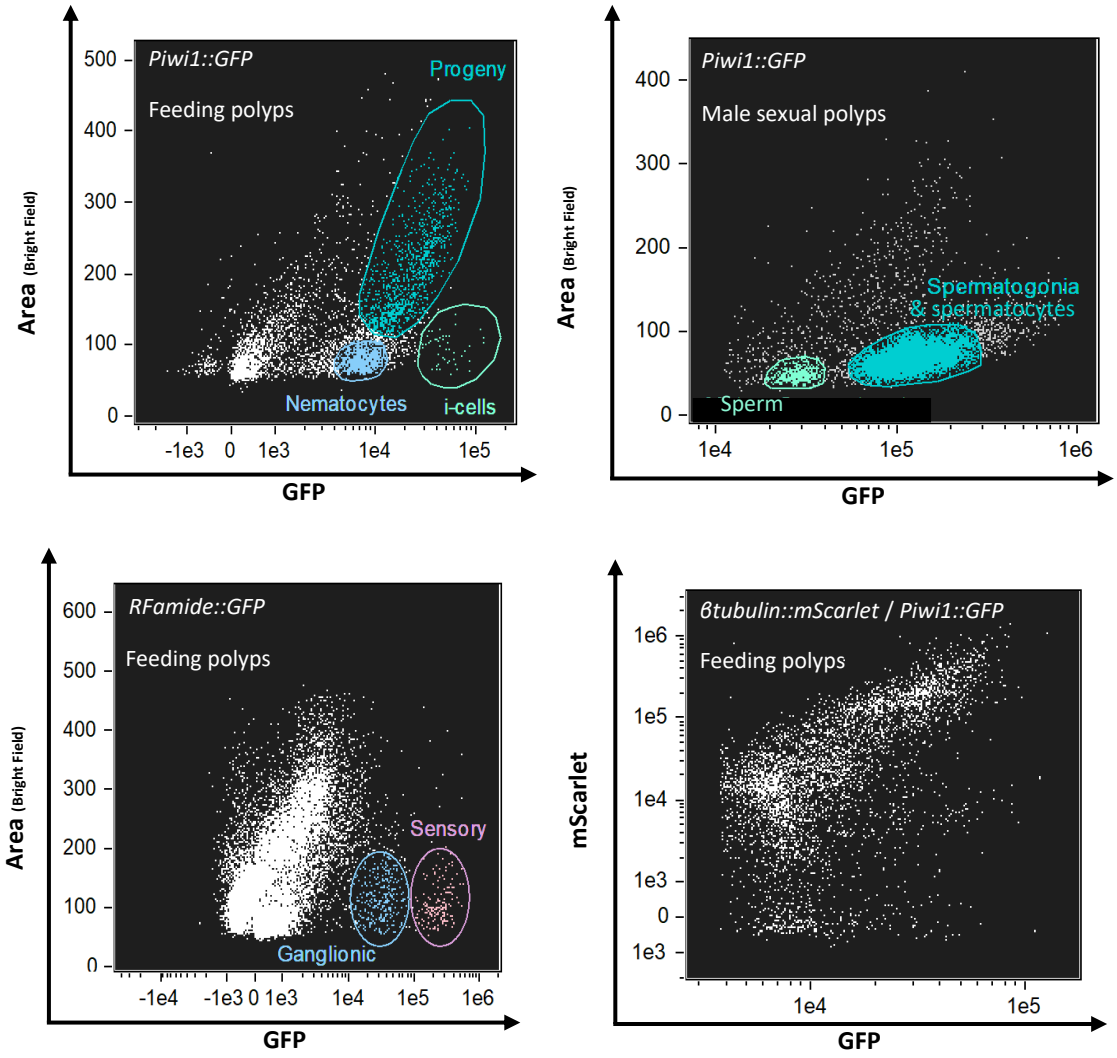

Figure 5.4. Clustering profiles of cells from transgenic reporter lines by IFC. Overall, similar patterns were observed in both FC and IFC. The nature of the reporter line and the polyp type is indicated in each plot.

Having a morphological view of the distinct populations I was able to assign each population of the Piwi1 line to a stage along the stem cell lineage (Fig. 5.5). The rare population found expressing high levels of GFP appeared to be a homogeneous population consistent of cells relatively small with a large nucleus compared to the cytoplasm – a classical property of stem cells. In addition, using the Side Scatter parameter (SSC) which indicates the complexity of a cell, these cells appeared not complex at all suggesting their undifferentiated state. Following, the next cluster of cells (always based on their GFP-expression levels), included cells at different stages of the i-cells' progeny. In this population, enlarged cells can be found as well as cells undergoing proliferation (two nuclei). In addition, these cells are relatively complex based on their SSC profile suggesting cells committed to proliferation and

differentiation. The third and last population characterized with IFC from this line was determined to be a cluster of nematocytes solely based on their unique morphology bearing a capsule.

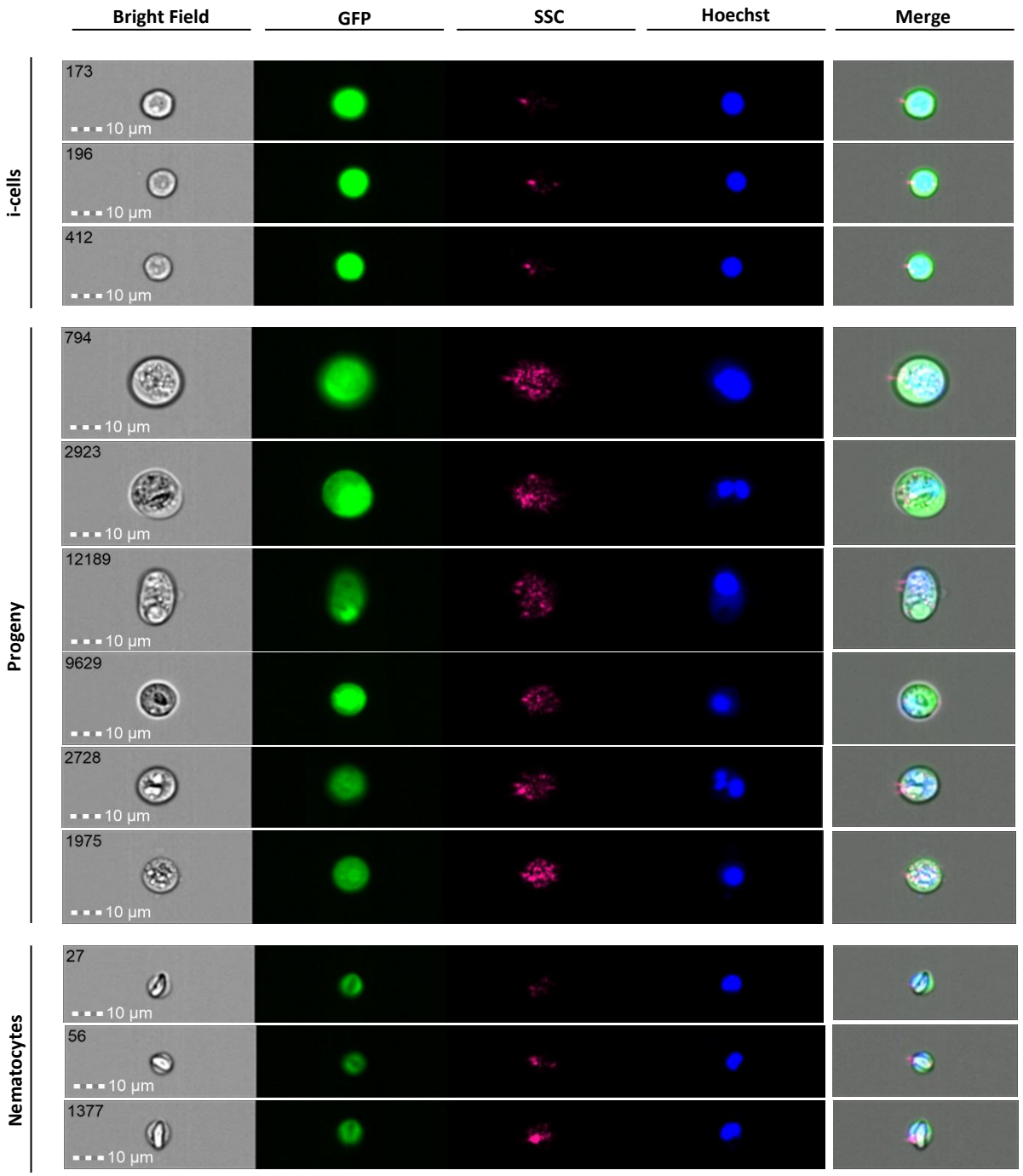

Figure 5.5. Flow cytometric imaging of the i-cells, committed and differentiated progeny, and nematocytes from the feeding polyps of a *Piwi1::GFP* reporter animals (images were taken at 40X).

Next, male sexual polyps were further characterized by IFC (Fig.6). The spermatogonia population is a heterogeneous mixture containing cells representing the various stages of spermiogenesis, and cells undergoing mitosis could also been seen. As a cell undergoes meiosis, its size reduces accordingly and ultimately it will reach the final stage of a sperm cell. The second population is composed of sperm cells, an observation based on the visibility of the sperm tail.

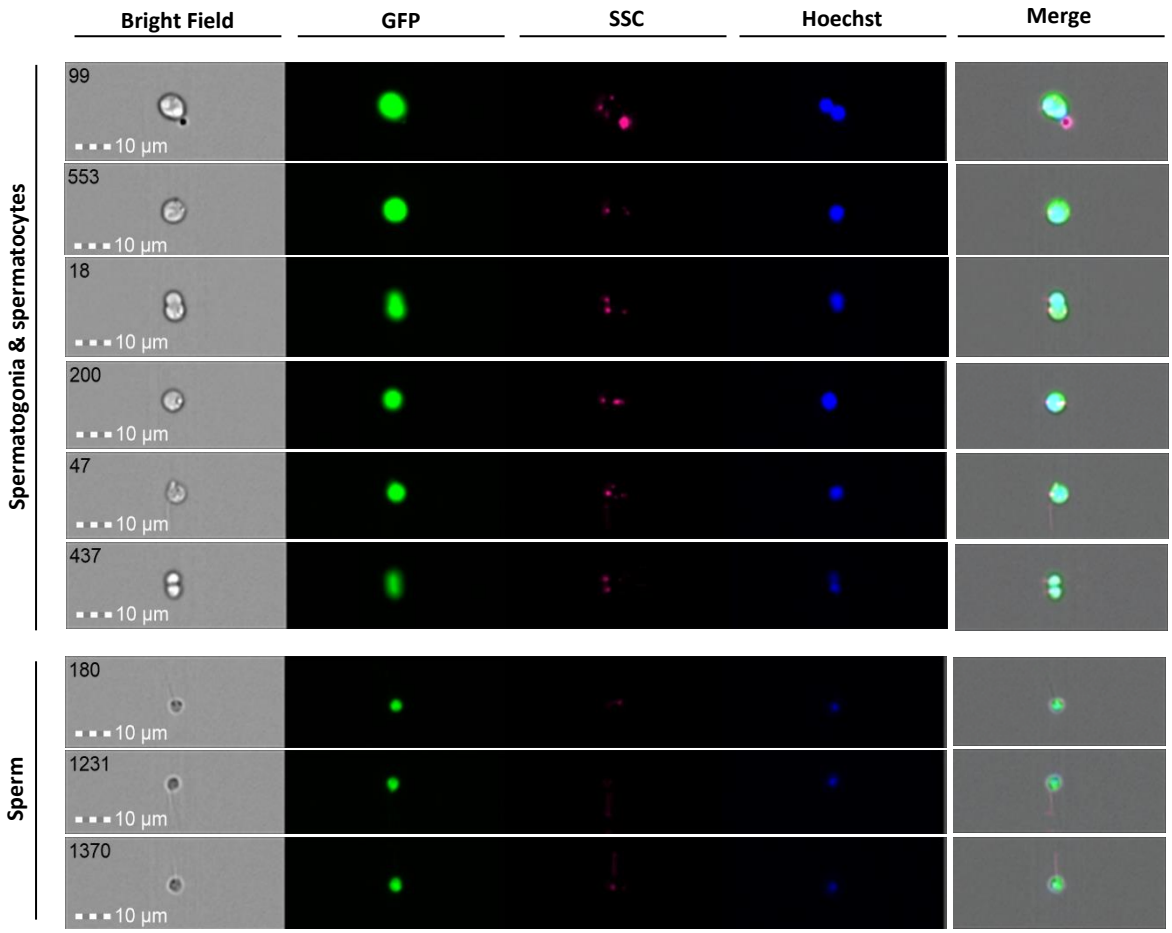

Figure 5.6. Flow cytometric imaging of cells at different stages of spermiogenesis and mature sperm cells from the male sexual polyps of *Piwi1::GFP* reporter line (images were taken at 40X).

As mentioned above, the flow cytometric profile of the *RFamide::GFP* line revealed two distinct populations. Following IFC analysis, there were no clear differences regarding the morphology of the two groups but there was a clear distinction in terms of fluorescence intensity (Fig.7).

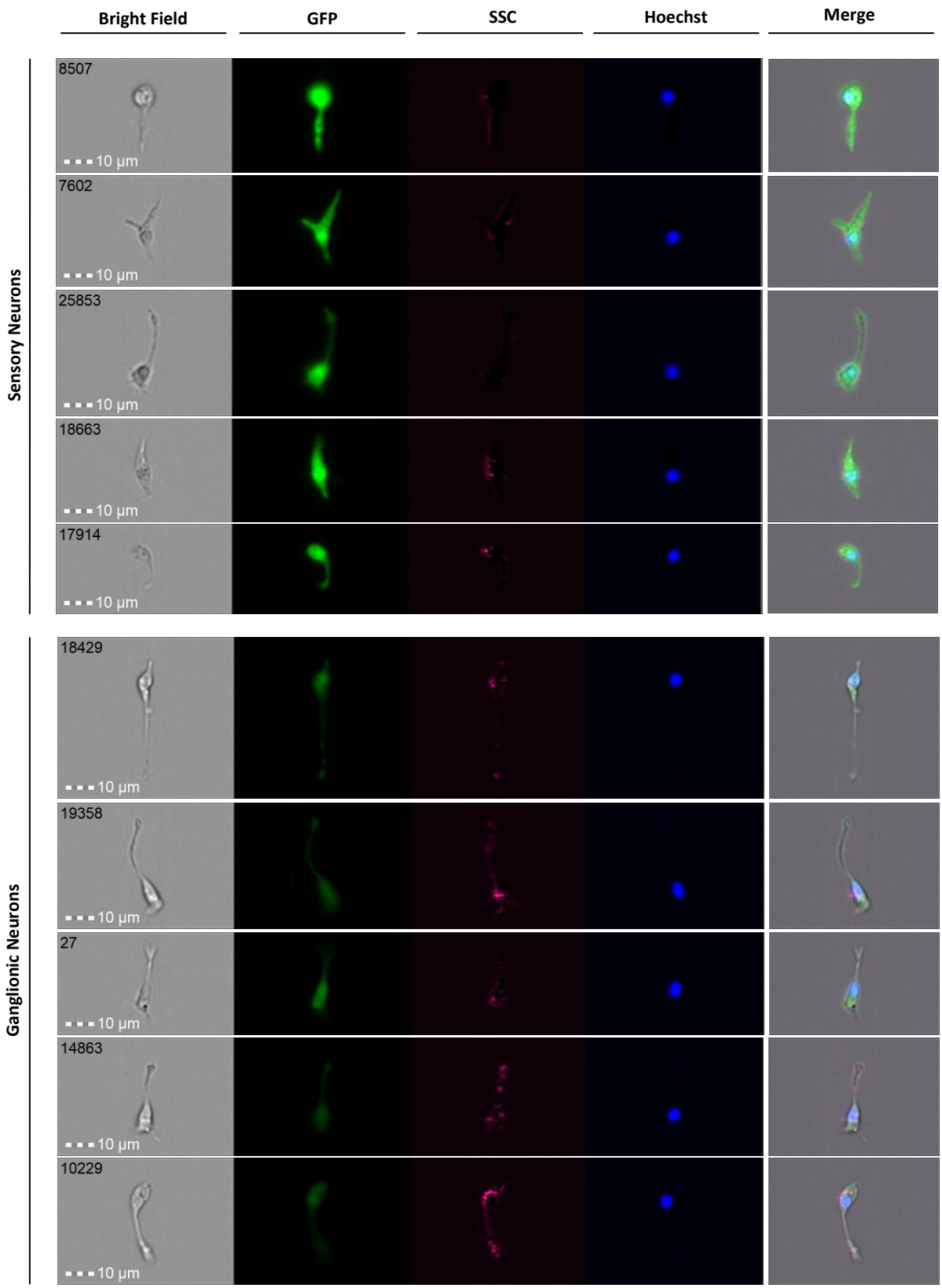

Figure 5.7: Flow cytometric imaging of neuronal cells (sensory and ganglionic) expressing different levels of GFP from the feeding polyps of *RFamide::GFP* reporter line (images were taken at 40X).

Unlike the conventional flow cytometry, I could explore more reporter lines expressing red fluorescence proteins, like mScarlet, by IFC due to laser availability. I analysed a double transgenic animal expressing GFP under the genomic control elements of *Piwi1* and mScarlet driven by *β–tubulin* control elements.

Most of the cells were fluorescent at both channels and the flow profiles showed similar patterns to the respective single reporter animals (Fig. 8A, B). Surprisingly, the i-cells did not express the red fluorescent protein (Fig. 8C); the entire i-cell population was missing from the profile of *β–tubulin::mScarlet* plot.

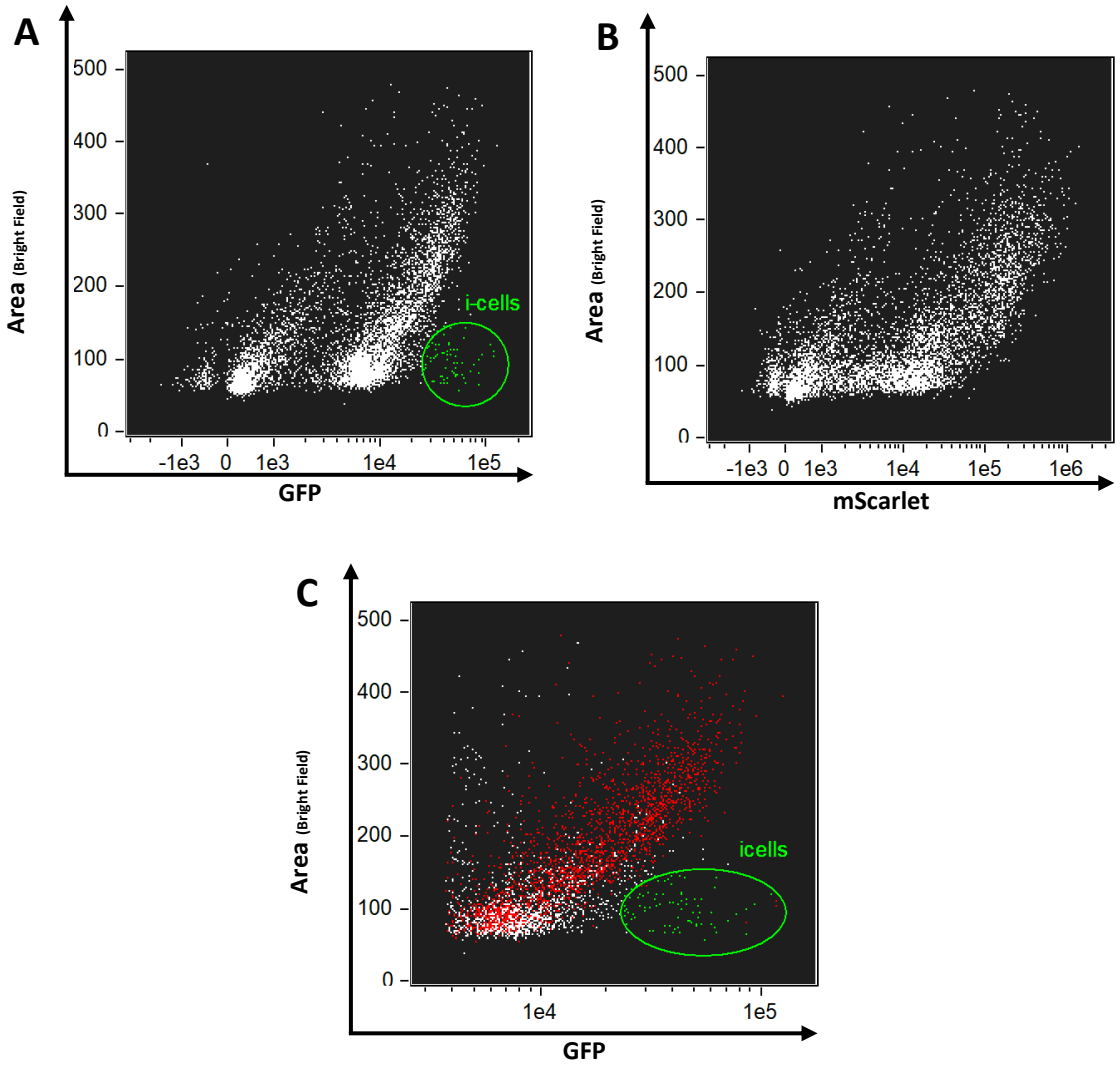

Figure 5.8: Flow cytometric profile (IFC) of *Piwi1::GFP* and *β-tubulin::mScarlet* double transgenic reporter animal. A similar pattern is shown to single reporter animals in terms of fluorescence intensity (A, B). The i-cell population do not express any mScarlet fluorescence protein (C; white: Piwi1, red: βtubulin, green: i-cells).

In order to confirm the findings, three different colonies were analysed, and all the cells were examined. In Fig. 5.9, a selection is shown of representative cells from each population.

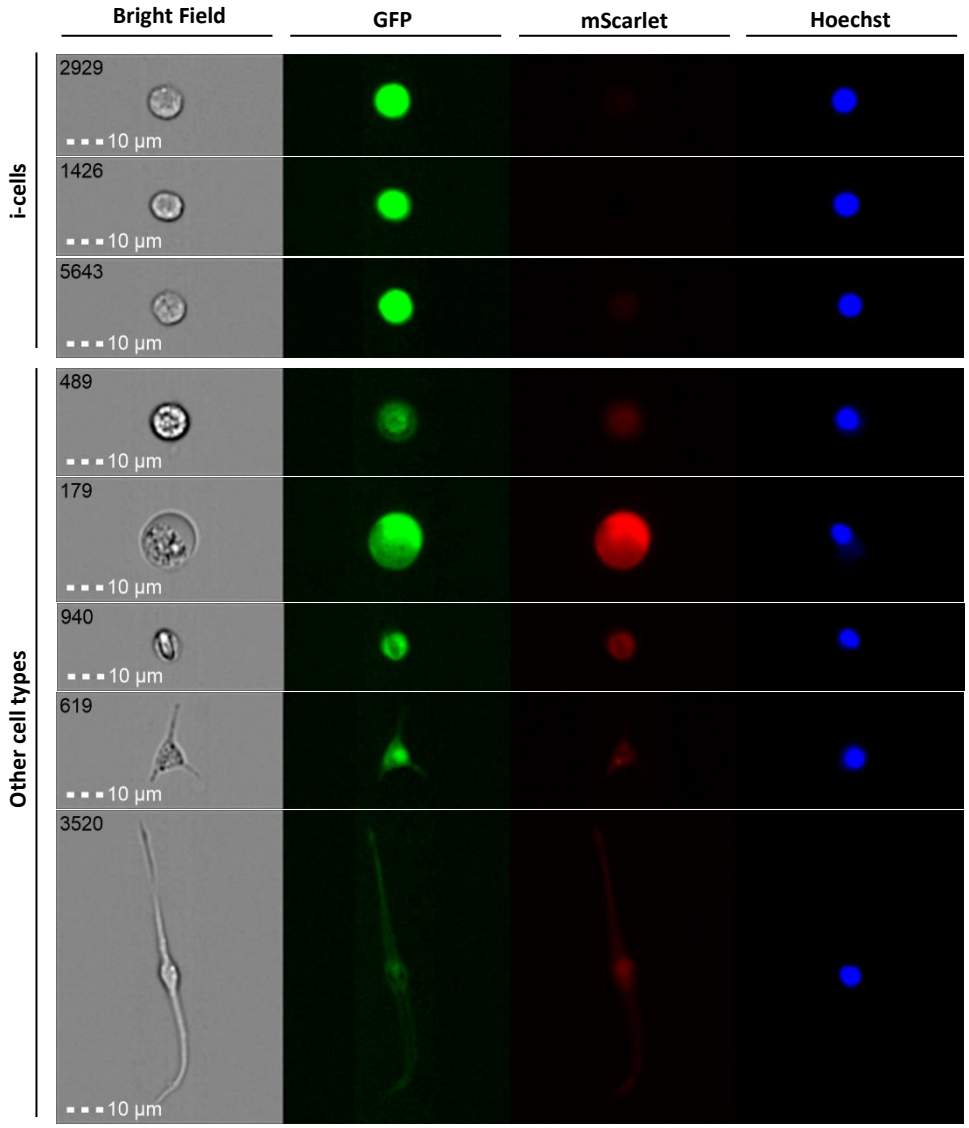

Figure 5.9: Imaging flow cytometric documentation of the i-cells expressing only GFP, and different types of progeny and differentiated cells, expressing both GFP and mScarlet fluorescence proteins from the feeding polyps of a *Piwi1::GFP/ βtubulin::mScarlet* double reporter animal (images were taken at 40X).

In addition, I analysed the transgenic reporter line *TfAP2*::GFP by IFC (Dubuc *et al.*, 2020). As shown in Fig.5.10, strong GFP expression is found in relatively small cells and as these cells commit, their progeny would still express the fluorescence protein due to its long half-life. In addition, no significant GFP expression is found in other cells types such as neurons and nematocytes, suggesting that the TfAP2^{+} cells did not give rise to somatic cells.

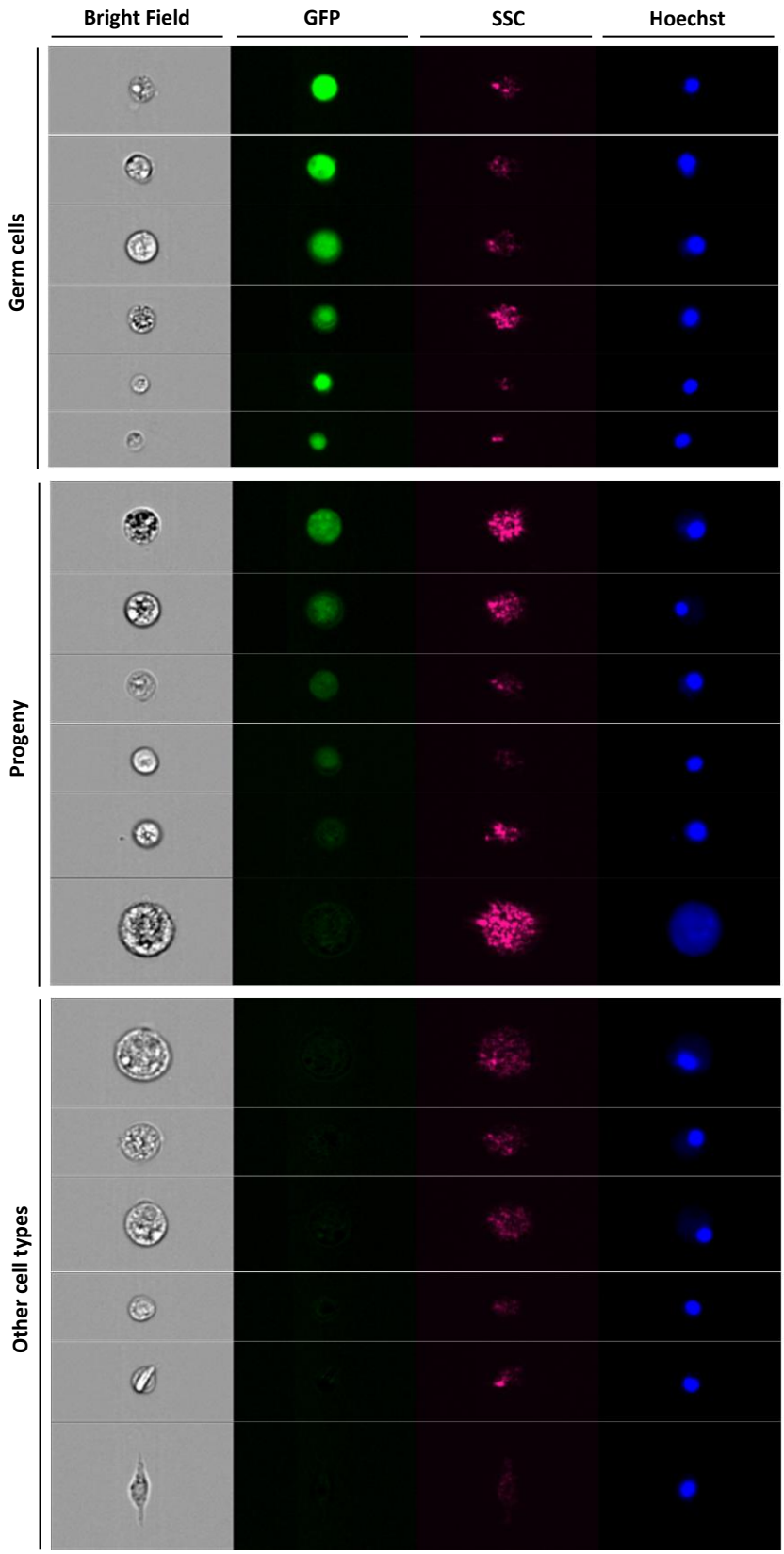

Figure 5.10: Imaging flow cytometric documentation of the germ cells expressing GFP, progeny still expressing GFP due to its long half-life, and other cell types not expressing GFP from dissociated female sexual polyps of a Tf*AP2::GFP* reporter animal (images were taken at 40X.

5.4 Transcriptional profiling of the neuronal lineage by FACS and RNA sequencing

After establishing flow cytometric protocols for *Hydractinia* and identifying unique populations by utilizing transgenic reporter animals, I sorted some populations of high interest along the neuronal lineage in order to identify novel markers for each by RNA sequencing. This part of my project was done in collaboration with Dr Paul Gonzalez and Dr Andy Baxevanis from the National Human Genome Research Institute (NHGRI), National institutes of Health (NIH), USA.

Three reporter lines were selected for the RNA sequencing: i-cells (*Piwi1::GFP*), neural progenitors (*SoxB2::GFP*), ganglionic and sensory neurons (*RFamide::GFP*). In addition, the GFP^- population from each reporter line was also sorted as a control (Fig. 5.11).

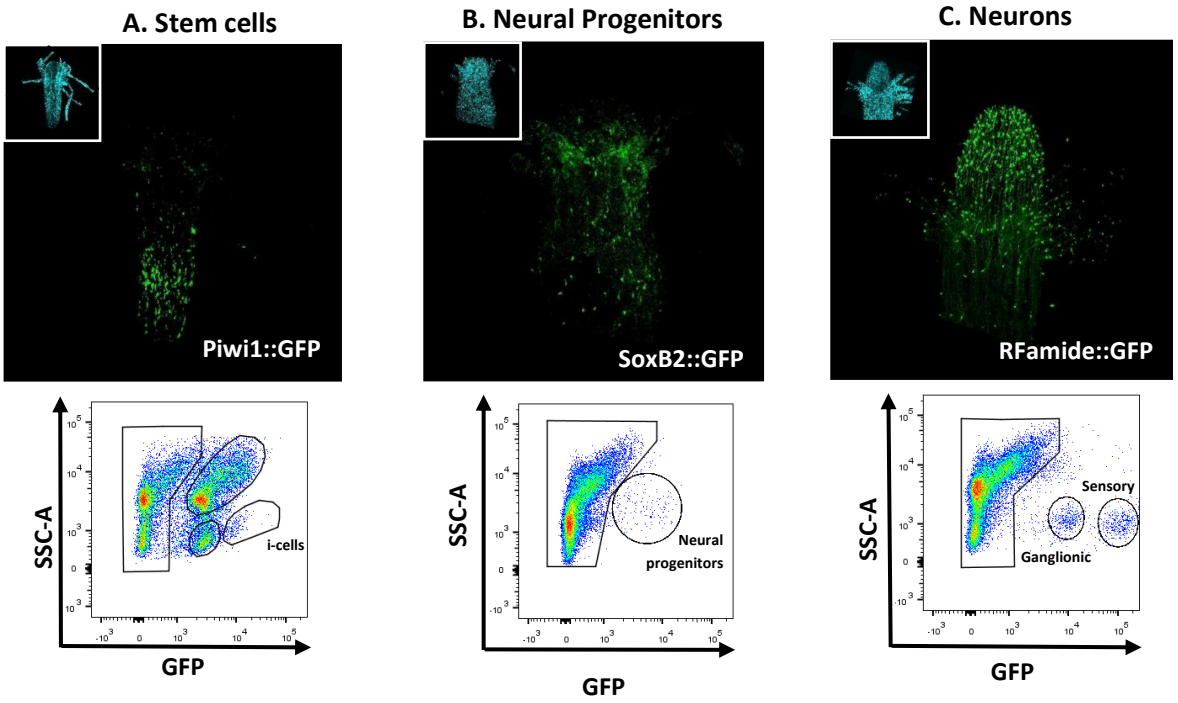

Figure 5.11. Reporter animals whose cells used for RNA-seq. (A) *Piwi1::GFP*. (B) *SoxB2::GFP*. (C) *RFamide::GFP*. Distribution of GFP^+ cells, representing the expression pattern of the corresponding genes shown both in whole-animals and flow profiling patterns.

In order to check the purity of the sorted populations, sorted cells were re-run through the cytometer. As shown in Fig. 5.12, ~80-100% of re-run cells ended up within the same gate, indicating high purity of the sorted cells and confirming the efficiency of my protocols.

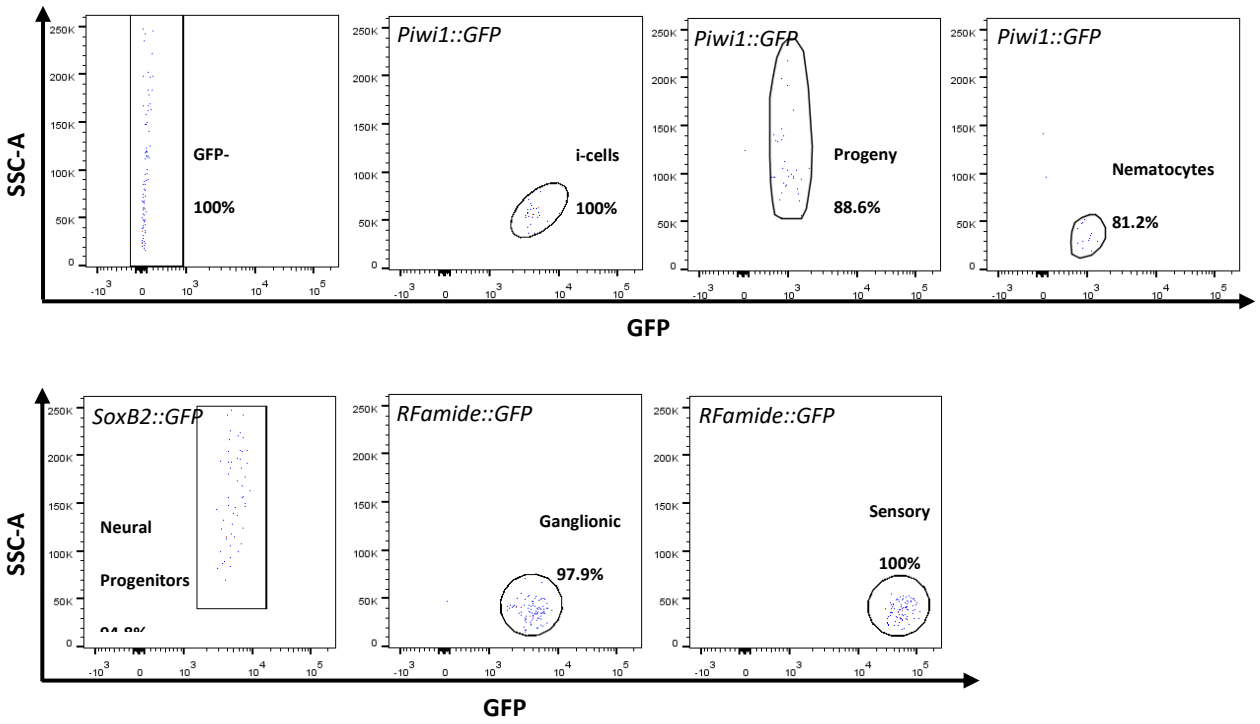

Figure 5.12. Purity check plots of the sorted populations to assess sorting efficiency. All the sorted populations fell into the same gates before and after sorting, indicating high purity.

In addition, the aforementioned populations within each reporter line were analysed based on their cell size (FSC) and granularity (SSC). The three populations from the Piwi1 reporter line were clustered in unique areas adding another layer of validation supporting the differences between those cells. As is can be appreciated from Fig. 5.13A, i-cells have a small size and relatively low complexity. Nematocytes are slightly smaller than i-cells. On the other hand, the progeny population includes cells varying greatly in cell size and complexity, reflecting their heterogeneous nature. The SoxB2 line displayed cells with a wide range of size and complexity for the same reason (Fig. 5.13B). The two populations resulted from the RFamide line had the same properties in terms of cell size and complexity despite the marked difference in the intensity levels of GFP fluorescence (Fig. 5.13C), consistent with their similar morphological features (Fig. 5.7).

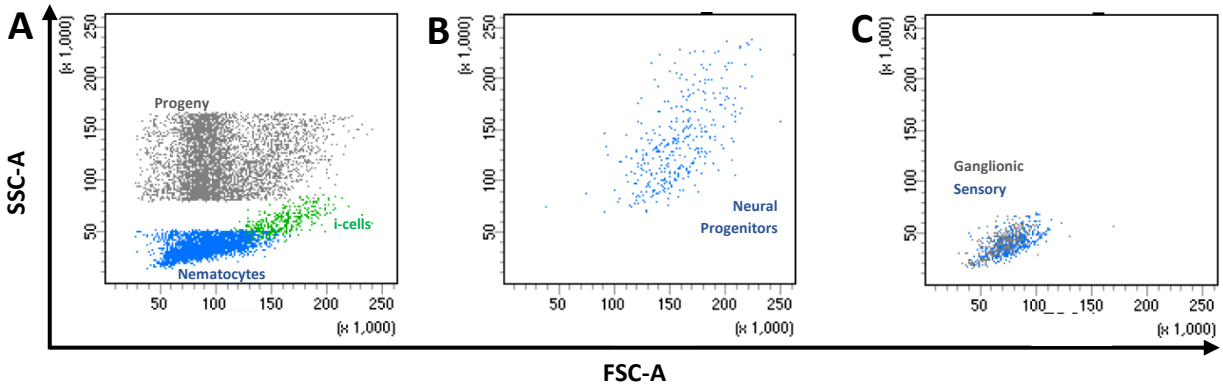

Figure 5.13. Flow cytometric analysis of the different sorted populations based on cell size and complexity. (A) i-cells and nematocytes. (B) Neural progenitors. (C) RFamide^{+} sensory and ganglionic neurons.

Unfortunately, the nematocyte and progeny populations were not sequenced due to low amount and/or quality of RNA.

Nevertheless, the transcriptional profile of the i-cells (*Piwi1::GFP*), neural progenitors (*SoxB2::GFP*), and the ganglionic and sensory neuronal (*RFamide::GFP*) populations was uncovered by differential expression analysis.

Differential expression (DE) analysis was performed on the various combinations of cell populations as shown in table 5.1.

Piwi1 i-cells	**Vs**	Control (GFP^{-})
SoxB2 NPs	**Vs**	Control (GFP^{-})
Sensory neurons	**Vs**	Control (GFP^{-})
Ganglionic neurons	**Vs**	Control (GFP^{-})
Piwi1 i-cells	**Vs**	SoxB2 NPs
SoxB2 NPs	**Vs**	Piwi1 i-cells
Sensory neurons	**Vs**	Ganglionic neurons
Ganglionic neurons	**Vs**	Sensory neurons
SoxB2 NPs	**Vs**	Sensory neurons
Sensory neurons	**Vs**	SoxB2 NPs
SoxB2 NPs	**Vs**	Ganglionic neurons
Ganglionic neurons	**Vs**	SoxB2 NPs

Table 5.1: Combinations of different cell populations that differential expression analysis was based on.

Based on DE analysis between i-cells and control cells (GFP^-), i-cells expressed mostly pluripotency genes such as *Vasa*, *Nanos*, *Smad4* and *Prdm13*. When *SoxB2*-GFP^+ cells were compared to control cells, some very interesting genes were observed. For example, the ETS transcription factor *ERG* was differentially expressed and members of the ETS family of TFs are key regulators of embryonic development, cell proliferation and differentiation (based on NCBI Gene). *BTBD1* which is involved in neurogenesis was also expressed in these cells as well as *LASP1* which is has roles in pattern specification.

The DE analysis of the two populations of $RFamide^+$ neurons revealed some very interesting findings. Both populations expressed the RFamide precursor gene but when the sensory neurons compared to ganglionic, the former expressed higher levels of the RFamide precursor. In addition, this population of neurons expressed the *Gsx* parahox gene *Cnox-2*, as well as *neural tubulin α, Astacin2*, and *EYA2*. On the other hand, when ganglionic neurons were compared to sensory neurons, the former expressed higher levels of *Ash*, *CRIM1* (venom toxin), and various minicollagen genes (e.g. minicollagen 1, minicollagen 8 precursor). Surprisingly, based on the DE analysis, both neuronal populations expressed genes involved in embryonic development such as *Brachyury* (sensory neurons), in spermatogenesis - *Boule*, and cnidarian egg lectin (ganglionic neurons). These interesting results will be further discussed in Chapter 6.

In addition, when the transcriptome of $SoxB2^+$ cells was compared to either sensory or ganglionic neurons, roughly the same results were obtained. In both comparisons, $SoxB2^+$ cells seem to express genes such as TF *ERG*, *LAPS1*, *PaxC* and TF *GATA*. All these genes could be used as potential markers for neural progenitors in the future, but further studies are needed.

The full gene list can be found in Appendix C.

5.5 Cell cycle profiling of distinct cell types

The cell cycle profile of a given population can be informative to understanding the biology of these cells. I used quantification of DNA content by FC to analyse the cell cycle of each of the populations that were characterised previously. After unsuccessfully trying various ways to fix and permeabilize the cells in order to use DNA-binding dyes applicable in other systems, such as mammalian cells, I was able to optimize a protocol for working with live cells. Cell cycle analysis opens a new window of opportunities to our model system, one that was not feasible before.

The first step towards that goal was to find a way to analyse the data. The gating strategy applied is a similar one used for mammalian cell systems and it is shown in Fig. 5.14.

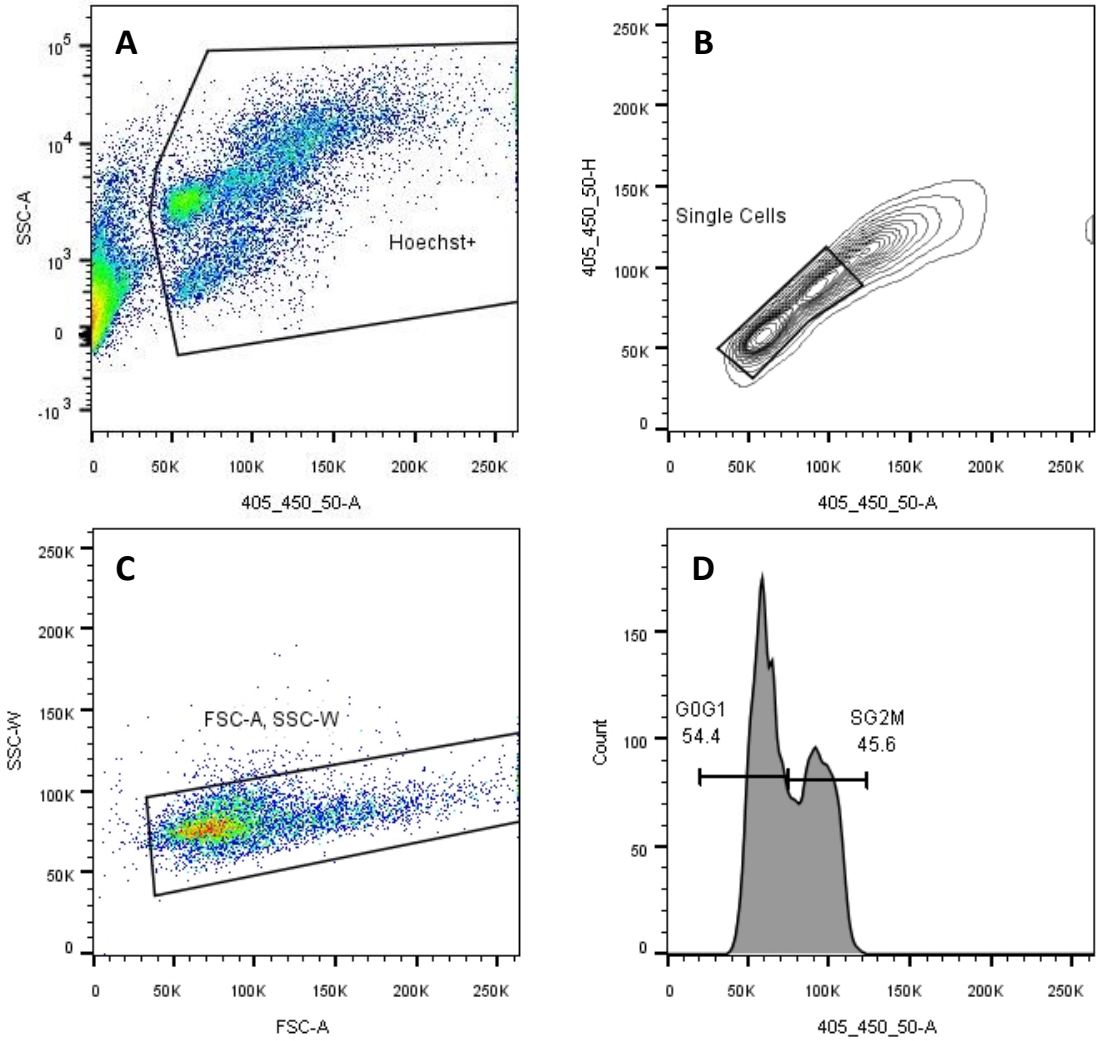

Figure 5.14. Workflow on how data analysis for cell cycle profiling is performed. (A). Cells are first gated based on their Hoechst profile, then (B) based on two different parameters of Hoechst (Height: H and Area: A), followed by (C) "clean-up" gating and finally (D) a histogram is plotted based on DNA content. As an example, unsorted cells from a wild type animal are shown with the presence of the characteristic two peaks. Numbers on the plots indicate the order for analysis.

As indicated in the above figure, the resulted histogram is composed by the 2N and 4N characteristic peaks representing cells in the G_0/G_1 and G_2/M phases, respectively. There is no clear S phase which is normally represented as a plateau between the two phases and one explanation for that is that the genome size of *Hydractinia* is significantly smaller from mammals and, hence, cells spend much less time in this phase. For that reason, the G_2/M phase is named S/G_2/M.

Once the parameters for both data acquisition and analysis were established, populations of interest from various reporter lines were analysed. As shown in Fig. 5.15, the three populations characterized in the previous sections from the *Piwi1::GFP* reporter line exhibited each distinct cell cycle profiles. The cells considered to be the rare i-cell pool, are all in the S/G_2/M phase (Fig. 5.15A) whereas the nematoblast/nematocyte population was mostly presented in the G_0/G_1 with some of the cells probably undergoing proliferation and hence the small "shoulder" (Fig. 5.15C). On the other hand, the heterogeneous population of progenitors includes cells in both phases (Fig. 5.15B).

Based on the selected images presented by IFC (Fig. 5.5), i-cells appeared to be in G_0/G_1 as the nucleus was relatively small or not being enlarged. On the other hand, cell cycle profiling of this population (Fig. 5.15A), showed that all the cells were found in the S/G_2/M phase. This observation can be explained in three ways. First, the images showed in Fig. 5.5 were a selection of this population, whereas cell cycle analysis was performed on all gated cells. Second, the IFC images are based on a camera detector and hence is not necessarily equivalent to the cell cycle analysis for which a conventional flow cytometer was used. Third and last, some cells were probably in S phase based on the small shoulder found in the cell cycle analysis. Since there is no definitive way to identify this S phase based on this way of performing cell cycle analysis in *Hydractinia* for the moment, all cells are considered being in the S/G_2/M phase.

In addition, the two distinct populations identified and characterized by IFC from the male sexual polyps of the same reporter line were also examined. The spermatogonia & spermatocyte population contains cells in both cell cycle phases as it is composed by cells are different and stages in the cell cycle (Fig. 5.15D), whereas the mature sperm cells do not fall into any of these two cell cycle phases and instead their DNA content is significantly less as their haploid (Fig. 5.15E).

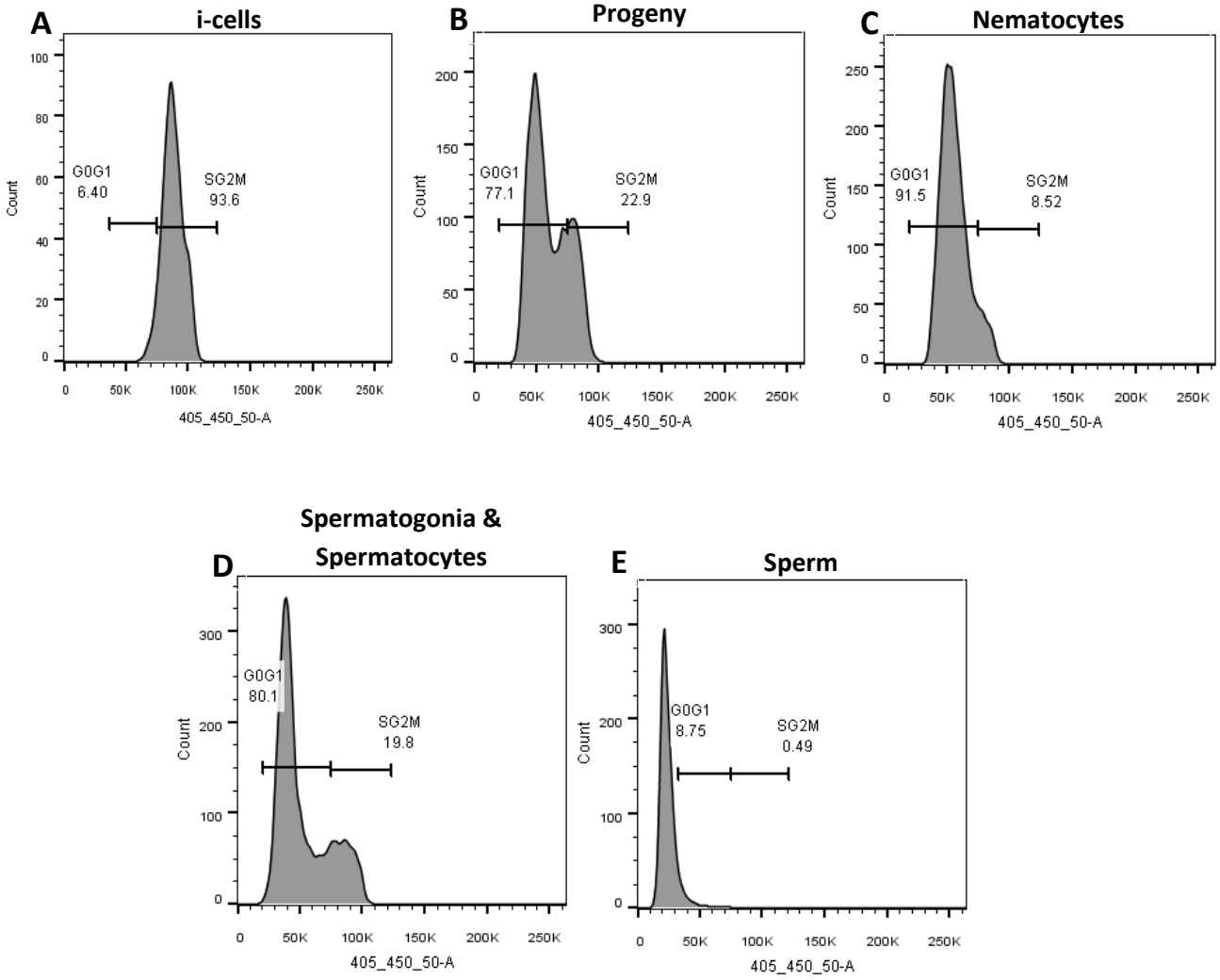

Figure 5.15. Cell cycle profile of cell subpopulations identified in the *Piwi1::GFP* reporter line. A-C are from feeding polyps, D & E from male sexual polyps. (A) i-cells are found in S/G_2/M phase. (B) Heterogeneous progeny can be found in all phases of the cell cycle. (C) Nematoblasts and nematocytes are mostly in the G_0/G_1 phase. (D) Spermatogonia and spermatocytes are found in all phases of the cell cycle. (E) Sperm have half the amount of DNA.

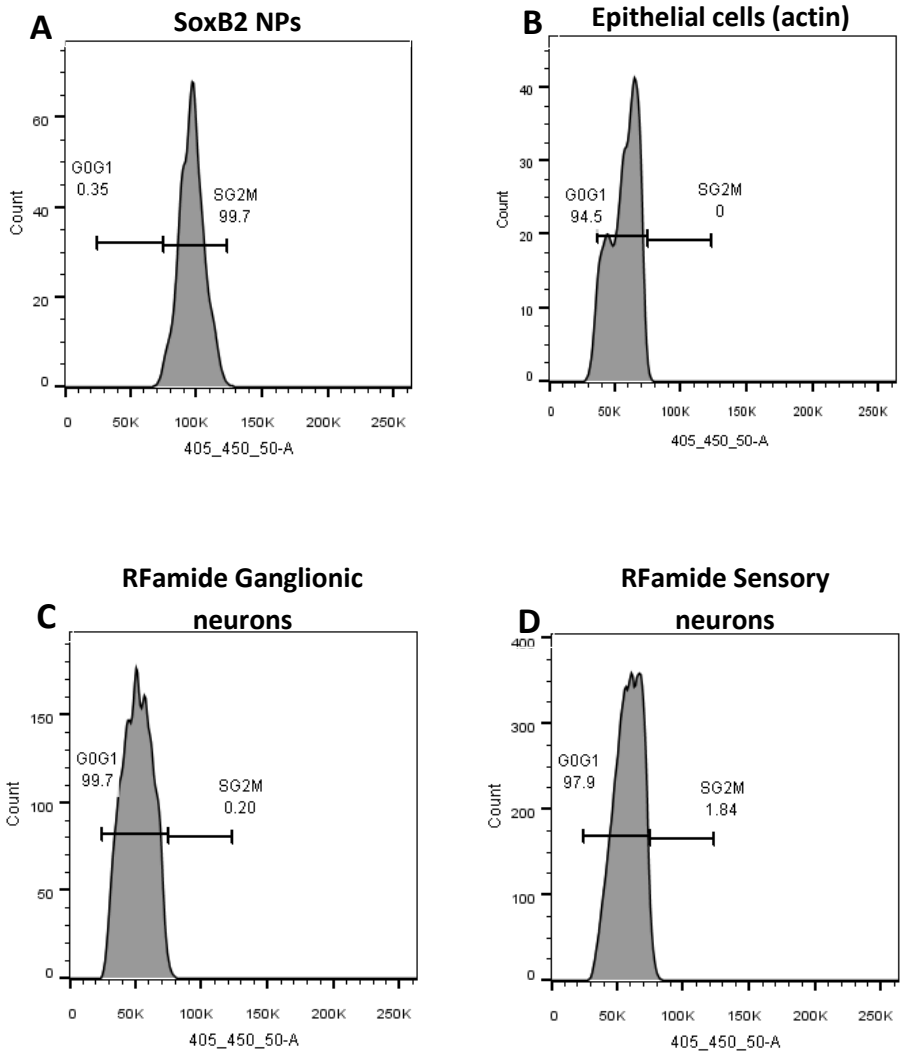

Figure 5.16. Cell cycle profiles of GFP$^+$ cells form the *SoxB2::GFP* (A), *actin::GFP* (B), and the *RFamide::GFP* transgenic reporter animals (C, D). (A) Neural progenitors are found in in S/G_2/M phase. (B) Epithelial cells are in G_0/G_1 phase. (C, D) Ganglionic and sensory neurons are found in G_0/G_1 phase.

GFP$^+$ cells from the *SoxB2::GFP* reporter line were in the S/G_2/M phase, similar to i-cells and consistent with their role as neural progenitors (Fig. 5.16A). In contrast, both subpopulations found in the *RFamide::GFP* reporter line were found in the G_0/G_1 phase (Fig. 5.16C-D), in line with these cells being terminally differentiated. Surprisingly, the epithelial cells from the *actin::GFP* reporter animal were mostly found in the G_0/G_1 phase, unlike epithelial cells in *Hydra* (Fig. 5.16B). However, due to the lack of identifying a clear S phase, some of the actin-GFP$^+$ cells may already be in that phase.

5.6 Summary

In this chapter I aimed to characterise distinct cell populations from various transgenic reporter animals using flow cytometry. For this, I establish flow cytometric techniques in *Hydractinia* – a powerful toolbox not available until today in this animal model. By first optimizing conventional flow cytometry, then imaging flow cytometry, and finally cell cycle analysis, I was able to identify novel subpopulations of *Hydractinia* cells. For example, by characterizing the *Piwi1::GFP* reporter line, I have identified a rare, putative stem cell population, based on high *Piwi1* promoter-driven GFP expression profile in combination with forward and side scatter characteristic, and cell cycle profile, all typical of stem cells in other animals. Cells representing different stages in spermatogenesis were identified similarly. Another example showing the importance of this technology was the division of the RFamide^{+} neurons into two subpopulations – consistent with observations on whole animals. Finally, I was able to isolate cells after their characterization and perform RNA sequencing. This enables us to show the transcriptional profile along the neuronal lineage – a crucial step to start understanding how neurogenesis is controlled in this animal.

Collectively, the establishment of flow cytometry provides new opportunities for the community of researchers using Hydractinia as a model system. It will enable addressing fundamental questions lineage commitment and identifying novel cell populations and their transcriptional network that control their fate.

Chapter 6: Discussion

6.1: Nervous system composition during development and adulthood

6.2: Versatile roles of SoxB genes during development and regeneration

6.2.1: *SoxB1* is an i-cell/germ cell marker

6.2.2: SoxB genes regulate embryonic neurogenesis

6.2.3: Lineage tracing during nervous system regeneration reveals *de novo* neurogenesis of post-mitotic neurons and sequential expression of *SoxB1* and *SoxB2*

6.3: Establishment of flow cytometric techniques in *Hydractinia*

6.3.1: Identification of distinct cell populations by FC, IFC and cell cycle analyses

6.3.2: Transcriptional profiling of the neural lineage

6.4: Concluding remarks

6.1: Nervous system composition during development and adulthood

Members of the early-branching metazoan phylum of Cnidaria are well-recognized as a sister group to bilaterians making them an ideal candidate to study the evolution of eumetazoan nervous system (Hejnol *et al.*, 2009). Their nervous system is relatively simple, organized as a nerve net instead of a more centralized system like in bilaterians, and it is primarily composed by sensory and ganglionic neurons and a third highly specialized neuronal type called nematocytes (Galliot *et al*, 2009). Nonetheless, a diffuse nerve net is not a very accurate characterization as the distribution of neurons is not homogenous. Based on previous studies, *Hydra* exhibits distinct patterns of nerve cell densities throughout the adult polyp with most of them been in the head region (Grimmelikhuijen *et al*., 1989; Koizumi *et al.*, 1990). Also, in the hydrozoan medusa *Polyorchis penicillatus*, the same observations were reported. Neurons expressing the neuropeptide RFamide were highly concentrated in the manubrium and tentacle buds (Grimmelikhuijzen and Spencer, 1984).

A great amount of work was done in more classical cnidarian models such as *Hydra* and *Nematostella* regarding the in-depth characterization of nervous system composition during both embryogenesis and adult stages, but *Hydractinia* was lacking this information. For this reason, I decided to fully characterize the structure of its nervous system both in developmental stages and in adult polyps (feeding and sexual) by using current established markers: RFamide and GLWamide neuropeptide markers, the pan-neural/cilia marker acetylated tubulin, Ncol1 and Ncol3 nematoblast markers, the Piwi1 stem cell marker, and an S-phase marker (EdU).

Consistent with previous studies showing the endodermal origin of neurogenesis in *Hydractinia* (Kanska and Frank, 2013; Bradshaw *et al*., 2015; Flici *et al*., 2017), I observed that proliferative cells such as Ncol3$^+$ nematoblasts and Piwi1$^+$ stem cells are located in the gastrodermis throughout larval development (Fig. 3.4). Also, *SoxB2*$^+$ NPCs are found primarily in the gastrodermis of the animal, unlike in *Nematostella*. In this anthozoan, neurogenesis commences in both gastrodermal and epidermal layers (Nakanishi *et al*., 2012). In *Hydractinia*, I found proliferative cells of unknown nature in both epidermis and gastrodermis at the early stages of embryogenesis (24 HPF – Fig. 3.5).

GLWamide$^+$ neurons, but not RFamide$^+$ ones, were observed throughout development in the epidermis. RFamide$^+$ neurons appeared in later stages of development, between 24 HPF and 48 HPF. This is in contrast with studies done in *Podocoryne* larva, as RFamide$^+$ neurons first detected at 24 HPF in the mid-body region showing no axial polarity (Groger and Schmid,

2001). In *Hydractinia*, these neurons are highly concentrated in the aboral end of planulae and they appear slightly later in development. In contrast, GLWamide$^+$ neurons are initially present throughout the body at the early stages of development (24 HPF) but later are highly concentrated in the aboral end of the larva (Fig. 3.1). They were always found in the epidermis forming aboral clusters, unlike *Nematostella* in which they are found in the endodermal layer forming oral clusters (Watanabe *et al*., 2014). This subset of neurons is essential for metamorphosis induction and any disruption will lead to failure (Schmich *et al*., 1998; Leitz, 1998). RFamide$^+$ neurons are also involved in metamorphosis mediation by acting antagonistically to GLWamides and inhibit metamorphosis (Katsukura *et al.,* 2003, 2004). Nematocysts were also detected in the epidermis of the developing larva with a much higher presence on the oral than on aboral side (Fig. 3.6). These observations suggest that these types of neurons and nematocysts exhibit axial polarity during development and establishment of the larval nervous system.

In the feeding polyps of *Hydractinia*, all cell types examined were present in the epidermal layer. As expected, cells with proliferative potential such as i-cells and early nematoblasts (Fig. 3.10) were present in the body column of the polyp and not in the oral part, consistent with previous studies (Bradshaw *et al*., 2015). RFamide$^+$ and GLWamide$^+$ neuronal populations were found in distinct regions from each other. Most of RFamide$^+$ neurons were present in the oral part of the animal, whereas GLWamide$^+$ neurons were found predominantly in the body column. This suggests division of the polyp anatomy into distinct neuronal territories. Based on the morphology of these cells. RFamide$^+$ neurons are a heterogeneous population containing sensory and ganglionic cells and this was confirmed by the flow cytometric profile of *RFamide::GFP* transgenic reporter animals (Fig. 5.2). Their transcriptional profile was different from each other as well (section 5.4).

Unsurprisingly, these neuronal populations also show distinct distribution patterns in the sexual polyps (Fig. 3.8, 3.9). The presence of GLWamide$^+$, RFamide$^+$ and acetylated tubulin$^+$ neurons in sporosacs of both male and female polyps may reflect an ancient role in the medusa stage, which has been lost in *Hydractinia* ancestor. In addition, acetylated tubulin$^+$ cells, especially in male sporosacs, resemble muscle cells based on their morphology, which is also consistent with an ancestral role of these structures, probably used for swimming by the medusa (Weber, 1989).

Collectively, these findings showcase a much more complex nervous system in *Hydractinia* than previously thought, and I propose a model of embryonic (Fig. 6.1) and adult (Fig. 6.2)

nervous system composition. This model could be improved by additional markers to fully characterize the composition of hydrozoan nervous systems and their development.

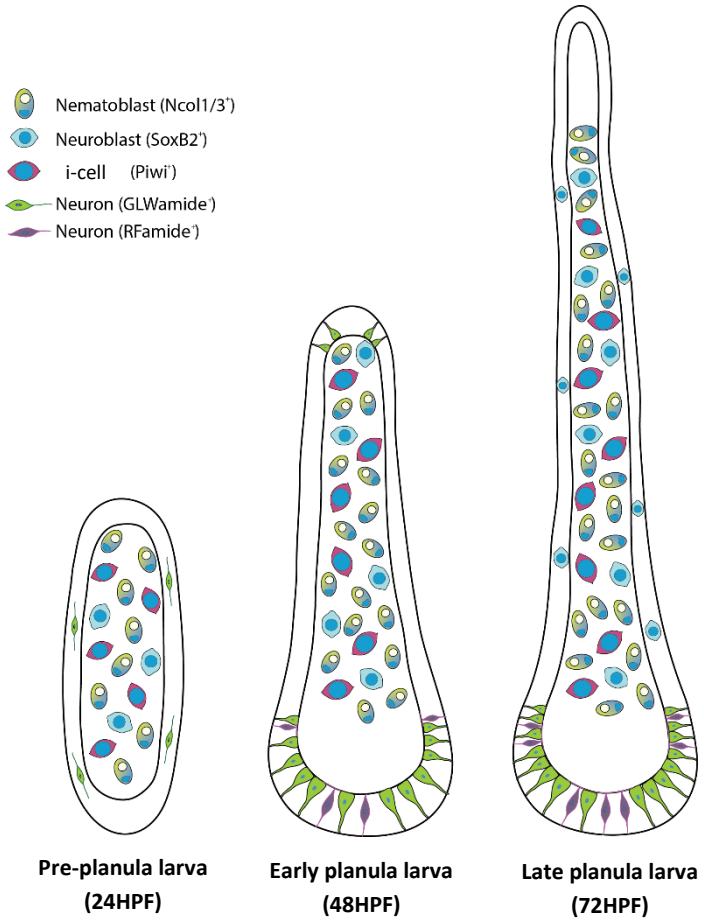

Figure 6.1. Proposed model regarding the composition of the nervous system during development in *Hydractinia*.

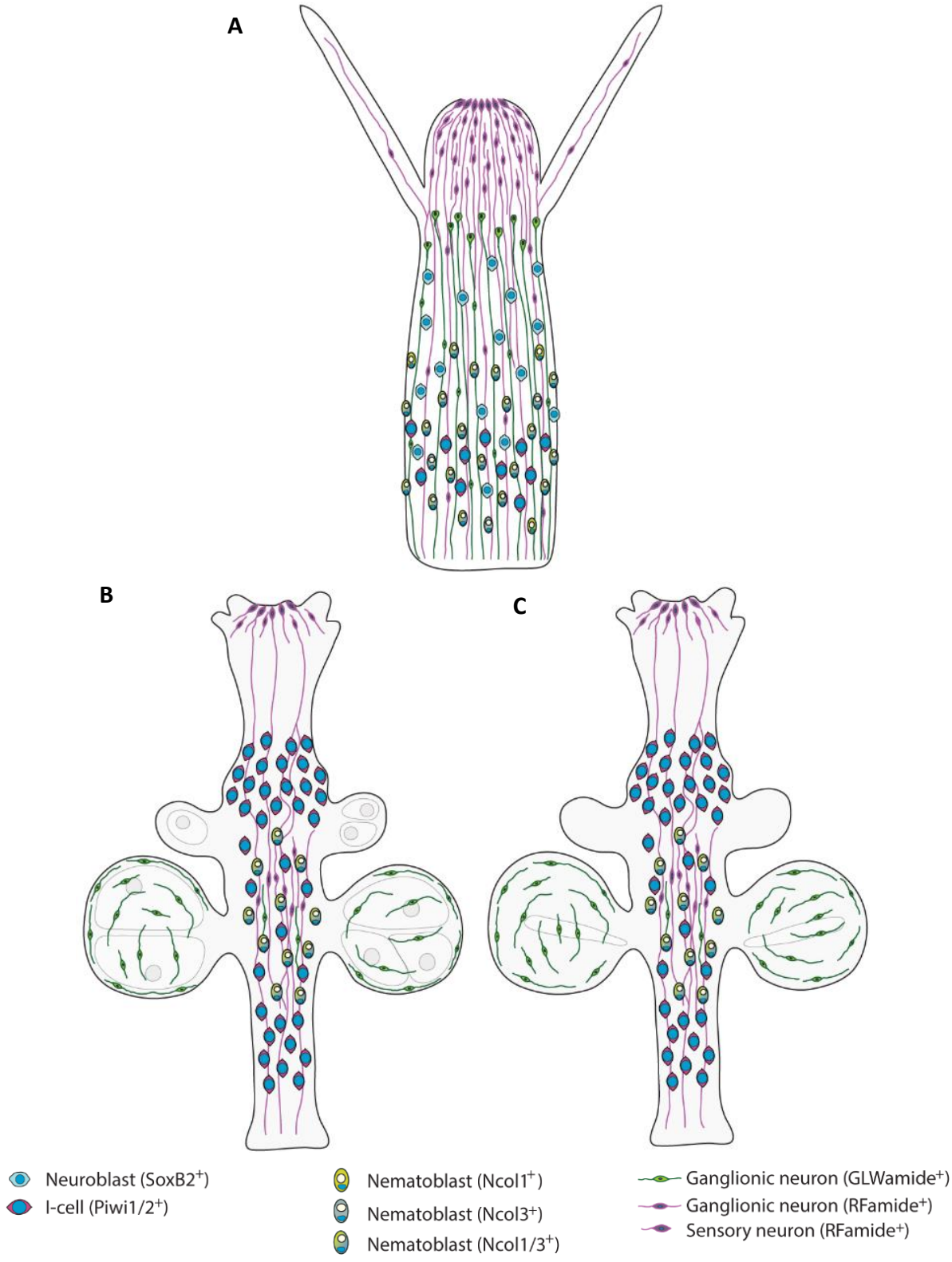

Figure 6.2. Proposed model regarding the composition of the nervous system in adult polyps in *Hydractinia* including (A) feeding, (B) female sexual, and (C) male sexual polyps.

6.2: Versatile roles of SoxB genes during development and regeneration

Hydractinia has three SoxB genes, namely *SoxB1*, *SoxB2* and *SoxB3*, and a previous study showed that SoxB2 and SoxB3 positively regulate neurogenesis (Flici *et al.,* 2017). *SoxB2* is primarily expressed in neuroblasts and nematoblasts, whereas *SoxB3* is found in post-mitotic cells committed to become neurons and nematoblasts (Flici *et al*, 2017). Despite the extensive work done on these two SoxB genes, little is known about the origin of the cells expressing them and, on the expression, and function of *SoxB1* in the neural lineage.

6.2.1: *SoxB1* is an i-cell/germ cell marker

Since *SoxB2* was found to be expressed in NPCs and *SoxB3* in post-mitotic neurons and nematocytes, I hypothesized that *SoxB1* acts upstream of these two genes and expressed in self-renewing cells, possibly with a broader developmental potential, like mammalian *Sox2* which is expressed in embryonic stem cells and in neural stem cells (Sarkar and Hochedlinger, 2013).

By *in situ* hybridization approaches, I showed that *Hydractinia SoxB1* gene is indeed expressed in i-cells (Fig. 4.3) and in male (Fig. 4.1) and female germ cells (Fig. 4.2), always co-expressed with *Piwi1* – an established i-cell/germ cell marker. Notably, *SoxB1* is found in the germinal zone in which stem cells commit to become germ cells (DuBuc *et al*., 2020) in female and male sexual polyps and also in developing oocytes. In feeding polyps, *SoxB1*$^{+}$ cells were only found in the proliferative zone of the animal, co-expressing with *Piwi1*.

By generating *SoxB1::tdTomato* transgenic reporter animals, I was able to show the gastrodermal origin of *SoxB1*$^{+}$ cells which is consistent with the location of i-cells. Next, by shRNA-mediated gene silencing, I disrupted *SoxB1* function and, as expected, all cell types examined were affected including i-cells (section 4.2) and their progeny, confirming the hypothesis. Lastly, when *SoxB1* was ectopically expressed in neurons it resulted in death of these cells, contrary to my initial hypothesis that this forced expression would result in their reprogramming to a more primitive state, like in mammals (Takahashi and Yamanaka, 2006). Differentiated cells can be reprogrammed to an embryonic-like state by defined factors. Takahashi and Yamanaka (2006) showed that by force-expressing only few defined factors in differentiated cells, pluripotent stem cells can be directly induced. These core transcription factors include Oct3/4, Sox2, c-Myc, and Klf4 are also essential for maintaining pluripotency in ES cells. Based on these findings, my initial hypothesis was that by ectopically expressing

SoxB1 in differentiated cells, I would observe the conversion of neurons to cells in a more primitive state, as observed in mammals. Unfortunately, that was not the case suggesting that maybe more core transcription factors are needed at the same time in order to induce pluripotency.

Based on these findings, I showed for the first time in cnidarians that a SoxB gene can be used as a stem and germ cell marker. Therefore, I suggest that *SoxB1* is functionally equivalent to mammalian *Sox2*.

6.2.2: SoxB genes regulate embryonic neurogenesis

In order to understand how and if *SoxB1*, *SoxB2* and *SoxB3* affect embryogenesis and neurogenesis/nematogenesis in *Hydractinia*, I knocked down these genes via shRNA-mediated gene silencing by injecting once-cell stage embryos. This was developed in our lab recently (DuBuc *et al*., 2020).

SoxB1 knockdown affected all cell types examined as expected from an i-cells marker (Fig. 4.21, 4.22, 4.23, 4.24). Since GLWamide$^+$ neurons were affected as well, shSoxB1-injected larvae were not able to metamorphose. In addition, these larvae were markedly smaller, and exhibited reduced locomotion probably due to defective ciliogenesis. Indeed, acetylated tubulin staining showed irregular ciliation pattern. A recent study in planarians (Ross *et al*., 2018), showed that a SoxB1 homologue, *soxB1*-2, marks ectodermal-lineage progenitors and is required for the differentiation of ciliated epidermal and sensory neuronal cells. *soxB1*-2 inhibition led to abnormal sensory neuron regeneration which caused seizure-like movements and phenotypes associated with loss of sensory modalities. This suggests a conserved role of *SoxB1* between planarians and cnidarians based on the similar phenotypes I observed upon inhibition of *SoxB1* in *Hydractinia*.

Knockdown of *SoxB2* affected RFamide$^+$ neurons but surprisingly, GLWamide$^+$ neurons were not affected. A previous study (Flici *et al*., 2017) suggested that *SoxB2*$^+$ cells give rise to all neural cell types. The lack of GLWamide phenotype in embryogenesis suggests a preferential generation of cell types (in this case, GLWamide$^+$ neuronal cell types) based on their need for larval metamorphosis. A similar phenomenon has been reported in *Nematostella* in which individual neuronal subtypes displayed differential regenerative potential under starvation (Havrilak *et al*., 2019). Surprisingly, *SoxB2* knockdown resulted in increased numbers of nematoblasts (Fig. 4.21). A possible explanation of this finding is that high levels of SoxB2

suppress nematogenesis. This is not the case in adults (Flici *et al*., 2017), perhaps because the dynamics of NPCs' proliferation and differentiation is distinct in embryos. According to this scenario, embryonic NPCs are more biased by default towards neuronal differentiation (which indeed appear earlier than nematocytes), a process promoted by SoxB2 in embryonic but not adult NPCs. Proliferation was also affected by shSoxB2 injection, which is in line with previous findings indicating that *SoxB2*$^{+}$ cells are proliferative NPCs (Flici *et al*., 2017). These results were partly in contrast with studies done in *Nematostella*, where downregulation of *NvSoxB(2)* resulted in reduced nematoblasts, but RFamide^{+} neurons were absent like in *Hydractinia* (Richards and Rentzsch, 2014). This suggests a partially conserved role of NvSoxB(2)$^{+}$ and SoxB2^{+} in NPCs between *Hydractinia* and *Nematostella*. Upon downregulation of *SoxB3*, no visible phenotype was observed, suggesting functional redundancy between *SoxB2* and *SoxB3*, or that defects in neurons and nematocytes are not visible by IF.

These data suggest that, first, cnidarian embryonic and adult neurogenesis are distinct; second, that neurogenesis and nematogenesis include several intermediate stage cells that have not been characterised yet. To identify these stages, further studies are needed. For example, generation of transgenic reporter lines for various genes along the neural lineage would allow *in vivo* examination of the dynamics and contributions of distinct genes to this process.

6.2.3: Lineage tracing during nervous system regeneration reveals *de novo* neurogenesis of post-mitotic neurons and sequential expression of *SoxB1* and *SoxB2*

Regeneration is the process by which any lost body part is restored identically or largely similar to its original size, structure, and function through various mechanisms (Bely and Nyberg, 2009). The very first studies documenting extensive regeneration potential were performed using the freshwater cnidarian *Hydra* (Lenhoff and Lenhoff, 1986). Since then, *Hydra* (Galliot, 2012) as well as many other cnidarian models uncover the exact molecular mechanisms govern the process of regeneration, including *Nematostella* (Dubuc *et al.*, 2014; Bossert *et al*., 2013; Passamaneck and Martindale, 2012) and *Hydractinia* (Brashaw *et al*., 2015; Gahan *et al*., 2016; Flici *et al*., 2017).

Like planarians, which are one of the most well-studied animals due to their extraordinary regenerative capacities (Reddien and Sanchez Alvarado, 2004), *Hydractinia*'s response to

injury is characterised by stem cells (neoblasts in planarians, i-cells in *Hydractinia*) migration to the injury side in order to form a blastema and regenerate the missing body part (Bradshaw *et al*., 2015).

However, the role of other cell types during a regenerative response has not been studied in *Hydractinia*. For that, I examined the contribution of differentiated RFamide$^+$ neurons and SoxB2$^+$ NPCs and their progeny to head regeneration.

My findings show that differentiated neurons, in this case RFamide$^+$ neurons, do not contribute to nervous system regeneration as they remain static and non-proliferative over the course of 72 HPD (Fig. 4.10, 4.11, 4.12), a time frame during which the regenerative process had been completed. This observation shows that *de novo* neurogenesis is the main mechanism contributing neurons to the regenerating new head. Indeed, during regeneration (0-48 HPD), I did not observe any RFamide$^+$ neurons expressing proliferation and stem cell markers confirming the *de novo* neurogenesis scenario (Fig. 4.13).

Interestingly, even though *Hydra* and *Hydractinia* exhibit similar nerve nets composed of both sensory and ganglionic RFamide$^+$ neurons, the contribution of this type of neurons to head regeneration differs at least in one aspect: as I showed by single-cell tracing, RFamide$^+$ neurons do not migrate and the source of new neurons in the regenerating head is through *de novo* neurogenesis. However, in *Hydra*, it has been shown that neurons constantly change their axial location due to the constant displacement of epithelial tissue, in which they are embedded, towards the extremities where they are eventually sloughed off (Campbell 1967, 1973, 1974). Indeed, it was shown by Yaross *et al* (1986) that a subset of neurons of the net is displaced toward and sloughed off at the ends of the tentacles at the same rate as the epithelial cells of these structures. In addition, Koizumi and Bode (1986), showed that neurons expressing FMRFamide-like immunoreactivity (FLI) can switch from FLI$^-$ to FLI$^+$ and vice versa in response to changes in their axial position. *Hydractinia* epithelial tissue dynamic is different; these cells do not move; instead they are replaced individually by migratory i-cells (Flici, unpublished data). These findings suggest the employment of different mechanisms by distinct neuronal populations among cnidarians in order to maintain and regenerate the nervous system. It will also be very interesting to identify the contribution of other neuronal cell types to head regeneration. For example, it was also shown in *Hydra* that upon depletion of i-cells, ganglionic neurons of the body column converted into epidermal sensory cells of the hypostome (Koizumi *et al.,* 1988). Based on the characterisation of the nervous system (see section 3.3), we now know that GLWamide$^+$ neurons are predominantly

located in the body column of *Hydractinia*, unlike RFamide$^+$ neurons. Based on their morphology, they are ganglionic cells, and hence, a reporter transgenic line of this neuropeptide can be generated and the contribution of this type of neurons can be studied by single-cell tracing and compared to *Hydra*.

I was also interested to examine how *SoxB2*-GFP$^+$ cells behave during head regeneration by *in vivo* tracing. Based in the findings, *SoxB2*$^+$ neural progenitors seemed to proliferate and/or be induced upon injury, but the detailed behaviour was difficult to be assessed in the absence of a nuclear marker and the low resolution of *in vivo* imaged cells (Fig. 4.14, 4.15, 4.16, 4.17). The rapid increase of *SoxB2*-GFP$^+$ cells was unlikely to be due to mitosis given the short time elapsing, as *Hydractinia* i-cells and progeny have a cell cycle duration of approximately 24 hours (McMahon, 2018). A plausible scenario is that i-cells differentiate to NPCs and start expressing *SoxB2*. It has been shown in *Nematostella* (Richards and Rentzsch, 2014) that *NvSoxB(2)* is expressed in NPCs and during embryogenesis *NvSoxB(2)*$^+$ cells are found in uneven clusters indicating asynchronous cell division, possibly indicating differential self-renewal and/or acquisition of distinct fates by sibling cells within the neuronal/nematocyte lineages. This may be the case in *Hydractinia* as well, as clusters of *SoxB2*-GFP$^+$ cells were found upon decapitation suggesting the *de novo* appearance of these cells through proliferation and/or differentiation to become neurons or nematocytes to re-establish the missing nervous system.

Studies in frogs, lizards, salamanders, and fish also suggest activation of neural stem/progenitor cells upon brain injury by increased proliferation and neurogenesis and hence the origin of regenerated neurons (Endo *et al*., 2007; Font *et al*., 2001; Kaslin *et al*., 2008; Kirsche and Kirsche, 1961; Parish *et al*., 2007; Tanaka and Ferretti, 2009; Zupanc and Clint, 2003). In addition, it has been shown in zebrafish that adult brain efficiently regenerates and restores tissue architecture upon injury by increased proliferation of NPCs, upregulation of neuronal-fate determining gene transcription which in turn give rise to neuroblasts that migrate to the injury side where they differentiate into mature neurons (Kroehne *et al*., 2011). This suggests a conserved mechanism across animalia as a similar mechanism was observed in *Hydractinia* during head regeneration.

Based on double fluorescence in situ hybridization findings, *SoxB1* was partially co-expressed with *SoxB2*, and *SoxB2* with *SoxB3,* suggesting their sequential expression along the neural lineage. By generating *SoxB1/SoxB2* double transgenic reporter animals and performing *in vivo* single-cell tracing I was able to confirm the sequential expression of these two genes

along the neural lineage (Fig. 4.18, 4.19, 4.20). Unfortunately, I was not able to generate *SoxB3* transgenic reporter animals and I could not confirm its sequential expression with *SoxB2*. However, their partial expression overlap, also seen in previous study (Flici *et al.*,2017), together with the remnant GFP fluorescence in neurons and nematoblasts in the transgenic *SoxB2* reporter animal (Fig. 4.8) due to long GFP half-life, support this notion.

My work represents a proof-of-concept for single-cells analysis *in vivo* in *Hydractinia*. Studying how cells make decisions in a whole animal context is quite unprecedented to my knowledge and shows the power of *Hydractinia* to serve as model for cell fate commitment acquisition also in other cell lineages.

6.3: Establishment of flow cytometric techniques in *Hydractinia*

Flow cytometric analysis has been available for studies in bilaterian and some non-bilaterian model systems for many years, but the *Hydractinia* research community was lacking this essential technique form its toolbox. However, as described in Chapter 5, I have successfully established flow cytometric techniques such as conventional flow cytometry (FC), imaging flow cytometry (IFC), fluorescence-activated cell sorting (FACS) and FC-based cell cycle analysis for this animal model. This not only contributed novel data on Hydractinia cells already (DuBuc *et al*., 2020; this study) but will also enable researchers using *Hydractinia* as an animal model to address other fundamental questions on cell biology.

6.3.1: Identification of distinct cell populations by FC, IFC and cell cycle analyses

After establishing flow cytometric techniques, I analysed various reporter transgenic reporter animals and identified novel subpopulations of *Hydractinia* cells. By characterising the *Piwi1::GFP* reporter line, I have identified a rare, putative stem cell population. This was based on a number of characteristics: first, these cells had high *Piwi1* promoter-driven GFP fluorescence; second, they had forward and side scatter characteristic, and morphological properties consistent with typical stem cells in other animals; third, their cell cycle, lacking a pronounced G_1 phase, resembles that of mammalian embryonic stem cells (Savatier *et al*., 2002; Hindley and Philpott, 2013); finally, this population silenced *β-tubulin::mScarlet* transgene, in line with stem cells' behaviour to suppress foreign genetic elements to maintain high genomic stability. These novel findings will contribute further to the advancement on the current knowledge regarding stem cell biology in *Hydractinia*. Another

example showing the importance of this technology was the division of RFamide$^+$ neurons into two subpopulations – consistent with *in vivo* observations in *Hydra* (Koizumi and Bode 1986).

In addition, most epithelial cells in *Hydractinia* are not proliferative as they were found in the G_0/G_1 phase of the cell cycle. This is in contrast with studies done in *Hydra*. *Hydra* has three distinct stem cell populations: epidermal and gastrodermal epithelial stem cells, and i-cells (Galliot and Schmid, 2002) and they are mostly found at the G_2 phase (Buzgariu *et al*., 2014). This finding highlights again the importance of the establishment of flow cytometric techniques in *Hydractinia* – a tool that will contribute to the advancement of this animal model.

6.3.2: Transcriptional profiling of the neural lineage

Based on the differential analysis performed on isolated cell populations, potential markers along the neuronal lineage have been identified which will enable us to start understanding how neurogenesis is controlled in *Hydractinia*.

Interesting candidate genes were identified in *SoxB2*$^+$ NPCs. For example, the ETS transcription factor *ERG* which was found in this analysis, and has roles in embryonic development, cell proliferation and differentiation, and its overexpression has been observed in prostate tumours (Clark and Cooper, 2009). In addition, *BTBD1*, a member of BTB-ZF transcription factors family was identified. Members of this family have been initially characterized in detail due to their roles in myelocytic leukaemia (Siggs and Beutler, 2012). A recent study in *Drosophila* showed that TtK69 (BTB-ZF transcription factor ortholog of the human promyelocytic leukemia) plays a central role in shaping neural cell lineages by regulating progenitor cell cycle exit and cell-fate commitment (Simon *et al.,* 2019). PaxC was also upregulated in the transcriptome of *SoxB2*$^+$ NPCs. Pax genes are a family of conserved transcription factors and interestingly, it has been shown in *Nematostella* that *PaxA*, not *PaxC*, plays a critical role in cnidocyte development (Babonis and Martindale, 2017). It will be of great interest to further investigate if Pax genes' functions are conserved among cnidarians.

The transcriptome of RFamide$^+$ neurons reveals very interesting candidate genes as well. First, sensory neurons expressed higher levels of the RFamide precursor gene. One possibility is that sensory neurons are generated prior to ganglionic cells, or since sensory neurons are located in the hypostome are replaced much more frequently than ganglionic ones, and

that's why higher amounts of remnant precursor gene is observed. Also, these sensory neurons express the *Gsx* parahox gene *Cnox-2*. *Cnox-2* most likely supports neurogenesis in *Hydra*, *Clytia* and *Acropora* (Galliot *et al*., 2009). It has been previously shown in *Hydractinia*, that *Cnox-2* expression is associated with key aspects of axial patterning (Cartwrigh *et al*., 2006), and in *Podocoryna* it has been suggested that this gene is involved in the establishment of anterior-posterior axis during development (Masuda-Nakagawa *et al*., 2000). In any case, it will be very interesting to see how this gene is involved in neurogenesis and whether its role is conserved throughout cnidarian species. RFamide$^+$ ganglionic neurons expressed high levels of *Ash* which is involved in the development of a subset of *Nematostella* nervous system (Layden *et al*., 2012), and in *Hydra* it is expressed in developing nematocytes and sensory neurons (Hayakawa *et al*., 2004). Furthermore, they express *CRIM-1* which has been suggested to be involved in central nervous system development in vertebrates (Kolle *et al.,* 2000). It has been shown that this gene mediates organogenesis via its interaction with growth factors such as BMPs, TGFβs, and VEGFs (Iyer *et al.,* 2016). All these findings, a much broader implication of these neuronal types in the formation of the nervous system in *Hydractinia* that previously thought.

A striking finding was the expression of genes involved in embryonic developmental processes in both subpopulations of RFamide$^+$ neurons. Ganglionic neurons express *Boule* and *Cnidarian egg lectin* (*Cel*), which are involved in spermatogenesis (Sekine *et al*., 2015) and oogenesis (Mali *et al*., 2011), respectively. While *Boule* has not been studied in *Hydractinia*, *in situ* hybridization analyses of *Cel* showed this gene to be expressed exclusively in oocytes. Hence, the detection of these genes in neurons could be due to contamination. An additional peculiarity was the T-box transcription factor *Brachyury* that was expressed in sensory neurons. This gene is expressed in the head region in other cnidarians and its upregulation in my sorted cells might reflect their axial position rather than their cellular identity as sensory neurons. Transcriptomic analysis of sensory neurons from aboral regions could clarify this point.

6.4: Concluding remarks

SoxB transcription factors are key regulators of stem and progenitor cell fate with a central role in neurogenesis. Since neurogenesis in *Hydractinia*, unlike most animals, is of endodermal origin, its establishment and regulation are of great interest. Based on the data collected for this present PhD thesis, I propose the following model regarding SoxB neuronal lineage establishment (Fig. 6.3). In this proposed model, *SoxB1* is expressed in stem and germ cells along with *Piwi1*, and then there is a transient phase in which *SoxB1* is downregulated and at the same time *SoxB2* is upregulated as i-cells commit to the neuronal lineage. Then, *SoxB2*$^{+}$ neural progenitors along with *SoxB3* regulate neurogenesis by various modes, such as suppression of nematogenesis from a subset of this population, and positive regulation of distinct neuronal populations. In addition, I propose a preferential generation of neuronal populations based on their contribution to the survival of the animal.

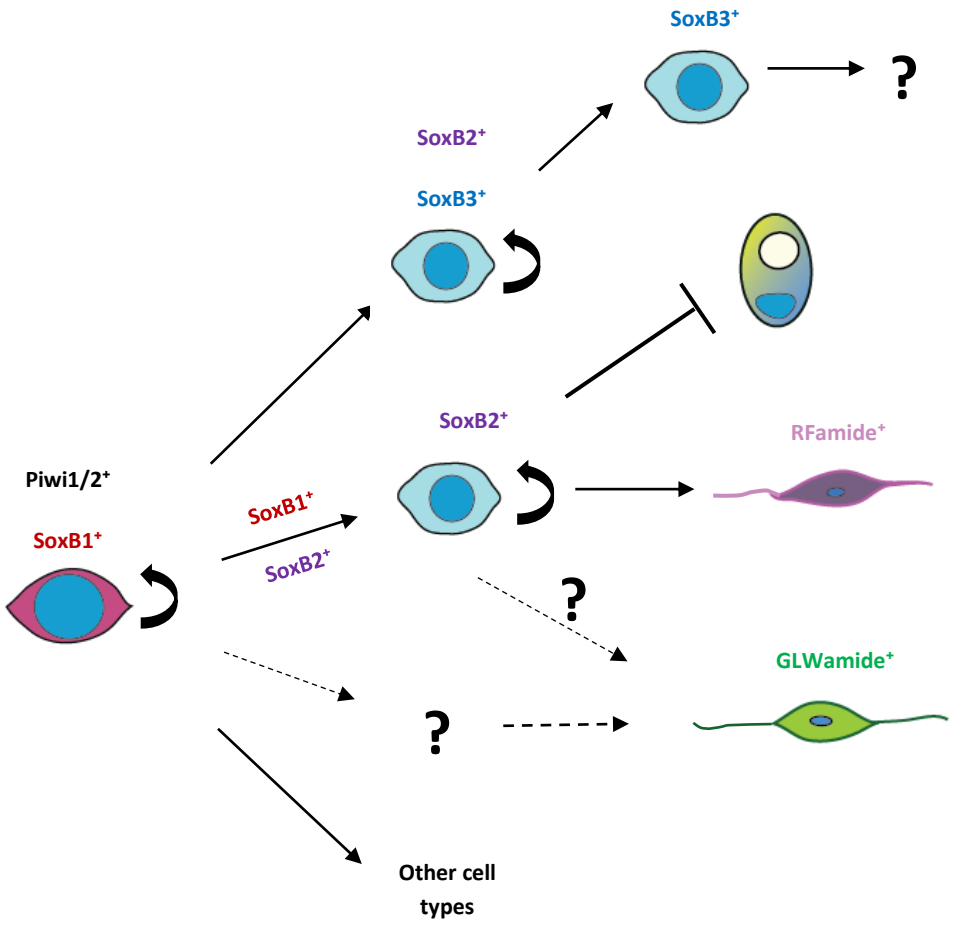

Figure 6.3. Proposed model regarding the versatile roles of SoxB transcription factors during embryonic neurogenesis.

Moreover, neural progenitors and post-mitotic neurons contribute to neuronal regeneration upon decapitation in different ways which opens a new window of opportunities to investigate in greater detail how this process is facilitated.

In combination with potentially novel candidates along the neuronal lineage based on the transcriptome of SoxB2^{+} NPCs and post-mitotic RFamide^{+} neurons, we have the opportunity to start understanding how neurogenesis is controlled in this fascinating animal and enable us to address fundamental questions regarding lineage commitment.

Chapter 7: References

Adan, A., Alizada, G., Kiraz, Y., Baran, Y., Nalbant, A. (2017). Flow Cytometry: basic principles and applications. *Crit Rev Biotechnol*, 37(2): 163-176.

Adler, C.E. and Sanchez Alvarado, A. (2015). Types or States? Cellular dynamics and regenerative potential. *Trends Cell Biol*, 25(11): 687-696.

Anderson, P.A., Thompson, L.F., Moneypenny, C.G. (2004). Evidence for a common pattern of peptidergic innervations of cnidocytes. *Biol. Bull*, 207: 141–146.

Angelozzi, A., and Lefebvre, V. (2019). SOXopathies: Growing Family of Developmental Disorders Due to SOX Mutations. *Trends in Genet*, 35 (9): 658-671.

Babonis, L.S., Martindale, M.Q. (2017). PaxA, but not PaxC, is required for cnidocyte development in the sea anemone *Nematostella vectensis*. *EvoDevo*, 8:14.

Ball, E.E., Hayward, D.C., Reece-Hoyes, J.S., Hislop, N.R., Samuel, G., Saint, R., Harrison, P.L., Miller, D.J. (2002). Coral development: from classical embryology to molecular control. *Int. J. Dev. Biol*, 46, 671-678.

Barteneva, N.S., Fasler-Kan, E., Vorobjev, I.A. (2012). Imaging Flow Cytometry: Coping with Heterogeneity in Biological Systems, *J. Histochem. Cytochem*, 60, 723–733.

Bayraktar, O.A., Boone, J.Q., Drummond, M.L., Doe, C.Q. (2010). Drosophila type II neuroblast lineages keep Prospero levels low to generate large clones that contribute to the adult brain central complex. *Neural Dev,* 5, 26.

Bely, A.E. and Nyberg, K.G. (2010). Evolution of animal regeneration: re-emergence of a field. *Trends Ecol Evol*, 25(3): 161-170.

Bely A.E. and Wray G.A. (2001) Evolution of regeneration and fission in annelids: insights from engrailed- and orthodenticle-class gene expression. *Development*, 128: 2781-2791.

Berkovitz, G.D., Fechner, P.Y., Marcantonio, S.M., Bland, G., Stetten, G., Goodfellow, P.N., Smith, K.D., Migeon, C.J. (1992). The role of the sex-determining region of the Y chromosome (SRY) in the etiology of 46, XX true hermaphroditism. *Hum. Genet,* 88: 411-416.

Berta, P., Hawkins, J.R., Sinclair, A.H., Taylor, A., Griffiths, B.L., Goodfellow, P.N., Fellous, M. (1990). Genetic evidence equating SRY and the testis-determining factor. *Nature,* 348: 448-450.

Bertrand, N., Castro, D.S., Guillemot, F. (2002). Proneural genes and the specification of neural cell types. *Nat. Rev. Neurosci*. 3, 517-530.

Bode, H.R. (1996). The interstitial cell lineage of hydra: a stem cell system that arose early in evolution. *J Cell Sci,* 109 (pt6): 1155-1164.

Bode, H.R. (2009). Axial patterning in *Hydra*. *Cold Spring Harbour* perspectives in biology 1: a000463.

Bode, H.R., Heimfeld, S., Chow, M.A., Huang, L.W. (1987). Gland cells arise by differentiation from interstitial cells in Hydra attenuate. *Dev Biol*, 122:577-585.

Bosch, T.C., Anton-Erxleben, F., Hemmrich, G., Khalturin, K. (2010). The Hydra polyp: nothing but an active stem cell community. *Dev Growth Differ*, 52 (1): 15-25.

Bosch, T.C. and David, C.N. (1987). Stem cells of *Hydra magnipapillata* can differentiate into somatic cells and germ line cells. *Dev Biol*, 121: 182-191.

Bossert, P.E., Dunn, M.P., Thomsen, G.H. (2013). A staging system for the regeneration of a polyp from the aboral physa of the anthozoan cnidarian *Nematostella vectensis*. *Dev Dyn*, 242: 1320-1331.

Bowles, J., Schepers, G., and Koopman, P. (2000). Phylogeny of the SOX family of developmental transcription factors based on sequence and structural indicators. *Dev. Biol*, 227: 239–255.

Bowman, S. K., Rolland, V., Betschinger, J., Kinsey, K. A., Emery, G. and Knoblich, J. A. (2008). The tumour suppressors Brat and Numb regulate transit-amplifying neuroblast lineages in *Drosophila*. *Dev. Cell,* 14: 535-546.

Boyer, L., Plath, K., Zeitlinger, J., Brambrink, T., Medeiros, L., Lee, T., Levine, S., Wernig, M., Tajonar, A., Ray, M., Bell, G.W., Otte, A.P., Vidal, M., Gifford, D.K., Young, R.A., Jaenisch, R. (2006). Polycomb complexes repress developmental regulators in murine embryonic stem cells. *Nature*, 441:349–402.

Bradshaw, B., Thompson, K., Frank, U. (2015). Distinct mechanisms underlie oral vs aboral regeneration in the cnidarian *Hydractinia echinata, eLife*, 4: e05506.

Bridge, D., Cunningham, C.W., Desalle, R., Buss, L.W. (1995). Class level relationships in the phylum Cnidaria: molecular and morphological evidence. *Mol Biol Evol*, 12: 679-689.

Brockes, J.P. and Kumar, A. (2008). Comparative aspects of animal regeneration. *Annu Rev Cell Dev Biol,* 24: 525-549.

Buescher, M., Hing, F.S., Chia, W. (2002). Formation of neuroblasts in the embryonic central nervous system of *Drosophila melanogaster* is controlled by *SoxNeuro*. *Development,* 129: 4193–4203.

Buzgariu, W., Crescenzi, M., Galliot, B. (2014). Robust G2 pausing of adult stem cells in *Hydra*. *Differentiation*, 87: 83-99.

Bylund, M., Andersson, E., Novitch, B., Muhr, J. (2003). Vertebrate neurogenesis is counteracted by *Sox1-3* activity. *Nat Neurosci*, 6:1162–1170.

Calegari, F., Haubensak, W., Haffner, C., Huttner, W.B. (2005). Selective lengthening of the cell cycle in the neurogenic subpopulation of neural progenitor cells during mouse brain development. *J Neurosci*, 25: 6533-6538.

Call, M.K., Grogg, M.W., Tsonis, P.A. (2005). Eye on regeneration. The Anatomical Record Part B: *The New Anatomist* 287B: 42-48.

Campbell, R.D. (1967). Tissue dynamics of steady state growth in *Hydra littoralis*. II. Patterns of tissue movement. *J Morphol,* 121: 19-28.

Campbell, R.D. (1973). Vital marking of single cells in developing tissues: India ink injection to trace tissue movements in *Hydra*. *J Cell Sci*, 13: 651-661.

Campbell, R.D. (1974). Cell movements in *Hydra*. *Amer Zool,* 14:523-535.

Carstensen, K., Rinehart, K.L., McFarlane, I.D., Grimmelikhuijzen, C.J.P. (1992). Isolation of Leu-Pro-Pro-Gly-Pro-Leu-Pro-Arg-Pro-NH2 (Antho-RPamide), an N-terminally protected, biologically active neuropeptide from sea anemones. *Peptides,* 13: 851–857.

Cartwright, P., Halgedahl S.L., Hendricks J.R., Jarrard, R.D., Marques, A.C., Collins, A.G., Lleberman, B.S. (2007). Exceptionally preserved jellyfishes from the Middle Cambrian. *PLoS One*, 2: e1121.

Cartwright, P., Schierwater, B., Buss, L.W. (2006). Expression of a *Gsx* parahox gene, *Cnox-2*, in colony ontogeny in *Hydractinia* (Cnidaria: Hydrozoa). *J Exp Zool B Mol Dev Evol*, 306 (5):460-469.

Cavallaro, M., Mariani, J., Lancini, C., Latorre, E., Caccia, R., Gullo, F., Valotta, M., DeBiasi, S., Spinardi, L., Ronchi, A., Wanke, E., Brunelli, S., Favaro, R., Ottolenghi, S., Nicolis, S.K. (2008). Impaired generation of mature neurons by neural stem cells from hypomorphic *Sox2* mutants. *Development*, 135:541–598.

Chen, X., Xu, H., Yuan, P., Fang, F., Huss, M., Vega, V., Wong, E., Orlov, Y., Zhang, W., Jiang, J., Loh, Y.H., Yeo, H.C., Yeo, Z.X., Narang, V., Govindarajan, K.R., Leong, B., Shahab, A., Ruan, Y., Bourque, G., Sung, W.K., Clarke, N.D., Wei, C.L., Ng, H.H. (2008). Integration of external signalling pathways with the core transcriptional network in embryonic stem cells. *Cell*, 133:1106–1123.

Chera, S., Ghila, L., Dobretz, K., Wenger, Y., Bauer, C., Buzgariu, W., Martinou, J.C., Galliot, B. (2009). Apoptotic cells provide an unexpected source of Wnt3 signalling to drive *Hydra* head regeneration. *Dev Cell*, 17: 279-289.

Clark, J.P. and Cooper, C.S. (2009). ETS gene fusions in prostate cancer. *Nat Rev Urol*, 6: 429-439.

Collins, A.G. (2002). Phylogeny of Medusozoa and the evolution of cnidarian life cycles. *J Evol Biol*, 15, 418-432.

Coulter, W.H. (1953). US Patent 2, 656, 508.

Daly, M., Brugler, M.R., Cartwright, P., Collins, A.G., Dawson, M.N., Fautin, D.G., France, S.C., Mcfadden, C.S., Opresko, D.M., Rodriguez, E., Romano, S.L., Stake, J.L. (2007). The phylum Cnidaria: A review of phylogenetic patterns and diversity 300 years after Linnaeus. *Zootaxa*. Magnolia Press, 1668: 127–182.

David, C.N. (2012). Interstitial stem cells in Hydra: multipotency and decision-making. *Int J Dev Biol*, 56 (6-8): 489-497.

David, C.N. and Murphy, S (1977). Characterisation of interstitial stem cells in hydra by cloning. *Dev Biol*, 58(2): 372-383.

David, C.N., Oezbek, S., Adamczyk, P., David, C.N., Ozbek, S., Adamczyk, P., Meier, S., Pauly, B., Chapman, J., Hwang, J.S., Gojobori, T., Holstein, T.W. (2008) Evolution of complex structures: minicollagens shape the cnidarian nematocyst. *Trends Genet,* 24: 431–438.

Dubuc, T.Q., Ryan, J.F., Martindale, M.Q. (2019) “Dorsal-Ventral” genes are part of an ancient axial patterning system: evidence from *Trichoplax adhaerens* (Placozoa), *Mol Biol Evol*, 36 (5):966-973.

Dubuc, T.Q., Schnitzler, C.E., Chrysostomou, E., McMahon, E.T., Febrimarsa, Gahan, J.M., Buggie, T., Gornic, S.G., Hanley, S., Barreira, S.N., Gonzalez, P., Baxevanis, A.D., Frank, U. (2020). Transcription factor AP2 controls cnidarian germ cell induction. *Science*, 367 (6479): 757-762.

Dubuc, T.Q., Traylor-Knowles, N., Martindale, M.Q. (2014). Initiating a regenerative response; cellular and molecular features of wound healing in the cnidarian *Nematostella vectensis. BMC Biology*, 12:24.

Duffy, D.J., Plickert, G., Künzel, T., Tilmann, W., Frank, U. (2010). Wnt signaling promotes oral but suppresses aboral structures in *Hydractinia* metamorphosis and regeneration. *Development*, 137: 3057-3066.

Dunn, C.W., Hejnol, A., Matus, D.Q., Pang, K., Browne, W.E., Smith, S.A., Seaver, E., Rouse, G.W., Obst, M., Edgecombe, G.D., Sørensen, M.V., Haddock, S.H.D., Schmidt-Rhaesa, A., Okusu, A., Kristensen, R.M., Wheeler, W.C., Martindale, M.Q., Giribet, G. (2008). Broad phylogenomic sampling improves resolution of the animal tree of life. *Nature*, 452: 745-749.

Dupre, C. and Yuste, R. (2017). Non-overlapping neural networks in *Hydra vulgaris*. *Curr Biol*, 27 (8): 1085-1097.

Elkouris, M., Balaskas, N., Poulou, M., Politis, P.K., Panayiotou, E., Malas, S., Thomaidou, D., Remboutsika, E. (2011) *Sox1* maintains the undifferentiated state of cortical neural progenitor cells via the suppression of Prox1-mediated cell cycle exit and neurogenesis. *Stem Cells*, 29: 89–98.

Endo, T., Yoshino, J., Kado, K., Tochinai, S. (2007). Brain regeneration in anuran amphibians. *Dev Growth Differ*, 49, 121–129.

Ferrero, E., Fischer, B., Russell, S. (2014). *SoxNeuro* orchestrates central nervous system specification and differentiation in *Drosophila* and is only partially redundant with *Dichaete*. *Genome Biol*. 15(5): R74.

Flici, H., Schnitzler, C.E., Millane, R.C., Govinden, G., Houlihan, A., Boomkamp, S.D., Shen, S., Baxevanis, A.D., Frank, U. (2017) An evolutionarily conserved SoxB-Hdac2 crosstalk regulates neurogenesis in a Cnidarian. *Cell Rep*, 18: 1395-1409.

Font, E., Desfilis, E., Perez-Canellas, M.M., Garcia-Verdugo, J.M. (2001). Neurogenesis and neuronal regeneration in the adult reptilian brain. *Brain Behav Evol*, 58, 276–295.

Fortunato, S., Adamski, M., Bergum, B., Guder, C., Jordal, S., Leininger, S., Zwafink, C., Rapp, H.T., Adamska, M. (2012). Genome-wide analysis of the sox family in the calcareous sponge *Sycon ciliatum*: multiple genes with unique expression patterns. *Evol Dev*, 3: 14.

Francois, M., Koopman, P., Beltrame, M. (2010). SoxF genes: key players in the development of the cardio-vascular system. *Int J Biochem Cell Biol*, 42: 445-448.

Frank, U., Leitz, T., Müller, W.A. (2001). The hydroid *Hydractinia*: a versatile, informative cnidarians representative. *BioEssays*, 23: 963-971.

Frank, U., Plickert, G., Müller, W.A. (2009). Cnidarian interstitial cells: the dawn of stem cell research. *Stem Cells in Marine Organisms, Springer*, pp: 33-59.

Fritzenwanker, J.H. and Technau,U. (2002). Induction of gametogenesis in the basal cnidarian *Nematostella vectensis* (Anthozoa). *Dev Genes Evol*, 212: 99- 103.

Fulwyler, M.J. (1965). Electronic separation of biological cells by volume. *Science*, 150: 910-911.

Fujisawa, T., and Hayakawa, E. (2012). Peptide signaling in *Hydra Int J Dev Biol*, 56: 543–550.

Furuyama, K., Kawaguchi, Y., Akiyama, H., Horiguchi, M., Kodama, S., Kuhara, T., Hosokawa, S., Elbahrawy, A., Soeda, T., Koizumi, M., Masui, T., Kawaguchi, M., Takaori, K., Doi, R., Nishi, E., Kakinoki, R., Deng, J.M., Behringer, R.R., Nakamura, T., Uemoto, S. (2011). Continuous cell supply from a Sox9-expressing progenitor zone in adult liver, exocrine pancreas and intestine. *Nat genet*, 43: 34–75.

Gahan, J.M., Bradshaw, B., Flici, H., Frank, U. (2016). The interstitial stem cells in Hydractinia and their role in regeneration. *Curr Opin Genet Dev*, 40: 65-73.

Gahan, J.M., Schnitzler, C.E., Dubuc, T.Q., Doonan, L.B., Kanska, J., Gornik, S.G., Barreira, S., Thompson, K., Schiffer, P., Baxevanis, A.D., Frank, U. (2017) Functional studies on the role of Notch signalling in *Hydractinia* development. *Dev Biol*, 428(1): 224-231.

Galliot, B. (2012). *Hydra*, a fruitful model system for 270 years. *Int J Dev Biol*, 56: 411-423.

Galliot, B. and Quiquand, M. (2011). A two-step process in the emergence of neurogenesis. *Eur J Neurosci*, 34, 847-862.

Galliot, B., Quiquand, M., Ghila, L., de Rosa, R., Miljkovic-Licina, M., Chera, S. (2009). Origins of neurogenesis, a cnidarian view. *Dev Biol,* 332:2-24.

Galliot, B., and Schmid, V. (2002). Cnidarians as a model system for understanding evolution and regeneration. *Int J Dev Biol,* 46: 39-48.

Genikhovich, G. and Technau, U. (2009). The starlet sea anemone *Nematostella vectensis*: an anthozoan model organism for studies in comparative genomics and functional evolutionary developmental biology. *Cold Spring Harb. Protoc*, pdb emo129.

Gierer, A., Berking, S., Bode, H., David, C.N., Flick, K., Hansmann, G., Schaller, H., Trenkner, E. (1972). Regeneration of *Hydra* from cell reaggregates. *Nat New Biol,* 239: 98-101.

Gimelli, S., Caridi, G., Beri, S., McCracken, K., Bocciardi, R., Zordan, P., Dagnino, M., Fiorio, P., Murer, L., Benetti, E., Zuffardi, O., Giorda, R., Wells, J.M., Gimelli, G., Ghiggeri, G.M. (2010). Mutations in SOX17 are associated with congenital anomalies of the kidney and the urinary tract. *Hum Mutat,* 31: 1352-1359.

Glauber, K.M., Dana, C.E., Steele, R.E. (2010) Hydra. Curr Biol, 20:964–965.

Graham, V., Khudyakov, J., Ellis, P., Pevny, L. (2003). SOX2 functions to maintain neural progenitor identity. *Neuron*, 39: 749–814.

Grimm, D., Bauer, J., Wise, P., Krüger, M., Simonsen, U., Wehland, M., Infanger, M., Corydon, T.J. (2019). The role of SOX family members in solid tumours and metastasis. *Semin Cancer Biol*, doi: 10.1016/j.semcancer.2019.03.004.

Grimmelikhuijzen, C.J. (1985) Antisera to the sequence Arg- Phe-amide visualize neuronal centralization in hydroid polyps. *Cell Tissue Res*, 241: 171–182.

Grimmelikhuijzen, C.J., Graff, D., Koizumi, O., Westfall, J.A., McFarlane, I.D. (1989). Neurons and their peptide transmitters in Coelenterates N.A. Series (Ed.), Serie A: Life Sciences, 188, Plenum Press, New York, pp. 95-109.

Grimmelikhuijzen, C.J., Graff, D., Koizumi, O., Westfall, J.A., McFarlane, I.D. (1991) Neuropeptides in coelenterates: a review. Hydrobiologia, 216/217: 555–563.

Grimmelikhuijzen C.J., Spencer A.N. (1984) FMRFamide immunoreactivity in the nervous system of the medusa *Polyorchis penicillatus*. *J Comp Neurol*, 230: 361-371.

Groger, H. and Schmid, V. (2001). Larval development in Cnidaria: a connection to Bilateria? *Genesis*, 29: 110-114.

Gubbay, J., Collignon, J., Koopman, P., Capel, B., Economou, A., Munsterberg, A., Vivian, N., Goodfellow, P., Lovell-Badge, R. (1990). A gene mapping to the sex-determining region of the mouse Y chromosome is a member of a novel family of embryonically expressed genes. *Nature*, 346: 245–295.

Guedelhoefer, O.C.T. and Sanchez Alvarado, A. (2012). Amputation induces stem cell mobilization to sites of injury during planarian regeneration. *Development,* 139: 3510-3520.

Han, Y., G, Y., Zhang, A.C., Lo, Y.H. (2016). Review: imaging technologies for flow cytometry. *Lab Chip*, 16(24): 4639-4647.

Harley, V.R., Clarkson, M.J., Argentaro, A. (2003). The molecular action and regulation of the testis-determining factors, SRY (sex-determining region on the Y chromosome) and SOX9 [SRY-related high-mobility group (HMG) box 9]. *Endocr Rev*, 24 (4): 466-487.

Hartenstein, V. (2006) The neuroendocrine system of invertebrates: a developmental and evolutionary perspective. *J Endocrinol*, 190: 555–570.

Hartenstein, V., Stollewerk, A. (2015) The evolution of early neurogenesis. *Dev Cell*, 32: 390-407.

Havrilak, J.A., Al-Shaer, L., Akinci, N., Amiel, A., Rottinger, E., Layden, M.J. (2019). Dynamics and variability in regenerative potential of neuronal subtypes in the *Nematostella* nerve net. BioRxiv, doi: 10.1101/685917.

Hayakawa, E., Fujisawa, C., Fujisawa, T. (2004). Involvement of *Hydra* achaete-scute gene CnASH in the differentiation pathway of sensory neurons in the tentacles. *Dev Genes Evol*, 214: 486–492.

He, S., del Viso, F., Chen C.Y., Ikmi, A., Kroesen, A.E., Gibson, M.C. (2018). An axial Hox code controls tissue segmentation and body patterning in *Nematostella vectensis*. *Science*, 361 (6409): 1377-1380.

Hejnol, A., Obst, M., Stamatakis, A., Ott, M., Rouse, G.W., Edgecombe, G.D., Martinez, P., Baguñà, J., Bailly, X., Jondelius, U., Wiens, M., Müller, W.E., Seaver, E., Wheeler, W.C., Martindale, M.Q., Giribet, G., Dunn, C.W. (2009) Assessing the root of bilaterian animals with scalable phylogenomic methods. *Proc Biol Sci*, 276 (1677): 4261-4270.

Hemmrich, G., Khalturin, K., Boehm, A.M., Puchert, M., Anton-Erxleben, F., Wittlieb, J., Klostermeier, U.C., Rosenstiel, P., Oberg, H.H., Domazet-Loso, T., Sugimoto, T., Niwa, H., Bosch, T.C. (2012). Molecular signatures of the three stem cell lineages in Hydra and the emergence of stem cell function at the base of multicellularity. *Mol Biol Evol*, 29(11): 3267-3280.

Hindley, C. and Philpott, A. (2013). The cell cycle and pluripotency. *Biochem J*, 451 (pt2): 135-143.

Holstein, T. (1981). The morphogenesis of nematocytes in *Hydra* and *Forskalia*: an ultrastructural study. *J Ultrastruct Res*, 75: 276-290.

Holstein, T. W., Hobmayer, E., Technau, U. (2003). Cnidarians: an evolutionarily conserved model system for regeneration? Developmental dynamics: an official publication of the American Association of Anatomists, 226: 257-267.

Hyman, L.H. (1940). The Invertebrates: Protozoa through Ctenophora. McGraw-Hil Book Company. Inc New York.

Irrthum, A., Devriendt, K., Chitayat, D., Matthijs, G., Glade, C., Steijlen, P.M., Fryns, J.P., Van Steensel, M.A.M., Vikkula, M. (2003). Mutations in the transcription factor gene SOX18 underlie recessive and dominant forms of hypotrichosis-lymphedema-telangiectasia. *Am J Hum Genet,* 72: 1470-1478.

Iyer, S., Pennisi, D.J., Piper, M. (2016). *Crim1-*, a regulator of developmental organogenesis. *Histol Histopathol*, 31 (10): 1049-1057.

Jager, M., Quéinnec, E., Chiori, R., Le Guyader, H., Manuel, M. (2008). Insights into the early evolution of SOX genes from expression analyses in a ctenophore. *J Exp Zool*, 310B: 650-667.

Jager, M., Quéinnec, E., Houliston, E., Manuel, M. (2006). Expansion of the SOX gene family predated the emergence of the Bilateria. *Mol Phylogenet Evol*, 39: 468-477.

Jager, M., Quéinnec, E., Le Guyader, H., Manuel, M. (2011) Multiple Sox genes are expressed in stem cells or in differentiating neuro-sensory cells in the hydrozoan *Clytia hemisphaerica*. *Evol Dev*, 2: 12.

Jopling, C., Boue, S., Belmonte, J.C.I. (2011). Dedifferentiation, transdifferentiation and reprogramming: three routes to regeneration. *Nat Rev Mol Cell Biol,* 12: 79- 89.

Chapman, J.A., Kirkness, E.F., Simakov, O., Hampson, S.E., Mitros, T., Weinmaier, T., Rattei, T., Balasubramanian, P.G., Borman, J., Busam, D., Disbennett, K., Pfannkoch, C., Sumin, N., Sutton, G.G., Viswanathan, L.D., Walenz, B., Goodstein, D.M., Hellsten, U., Kawashima, T., Prochnik, S.E., Putnam, N.H., Shu, S., Blumberg, B., Dana, C.E., Gee, L., Kibler, D.F., Law, L., Lindgens, D., Martinez, D.E., Peng, J., Wigge, P.A., Bertulat, B., Guder, C., Nakamura, Y., Ozbek, S., Watanabe, H., Khalturin, K., Hemmrich, G., Franke, A., Augustin, R., Fraune, S., Hayakawa, E., Hayakawa, S., Hirose, M., Hwang, J.S., Ikeo, K., Nishimiya-Fujisawa, C., Ogura, A., Takahashi, T., Steinmetz, P.R., Zhang, X., Aufschnaiter, R., Eder, M.K., Gorny, A.K., Salvenmoser, W., Heimberg, A.M., Wheeler, B.M., Peterson, K.J., Böttger, A., Tischler, P., Wolf, A., Gojobori, T., Remington, K.A., Strausberg, R.L., Venter, J.C., Technau, U., Hobmayer, B., Bosch, T.C., Holstein, T.W., Fujisawa, T., Bode, H.R., David, C.N., Rokhsar, D.S., Steele, R.E. (2010). The dynamic genome of *Hydra*. *Nature*, 464: 592-596.

Juliano, C.E., Lin, H., Steele, R.E. (2014) Generation of transgenic *Hydra* by embryo microinjection. *J Vis Exp*, 91:51888.

Kamachi, Y., Kondoh, H. (2013). Sox proteins: regulators of cell fate specification and differentiation. *Development*, 140: 4129-4144.

Kanska, J. and Frank, U. (2013). New roles for Nanos in neural cell fate determination revealed by studies in a cnidarian. *J Cell Sci*, 126: 3192-3203.

Kaslin, J., Ganz, J., Brand, M. (2008). Proliferation, neurogenesis and regeneration in the non-mammalian vertebrate brain. *Philos Trans R Soc Lond B Biol Sci,* 363, 101–122.

Kass-Simon, G., and Pierobon, P. (2007). Cnidarian chemical neurotransmission, an updated overview. *Comp Biochem Physiol A Mol Integr Physiol,* 146: 9–25.

Katsukura, Y., Ando, H., David, C.N., Grimmelikhuijzen, C.J.P., Sugiyama, T. (2004). Control of planula migration by LWamide and RFamide neuropeptides in *Hydractinia echinata*. *J Exp Biol*, 207: 1803-1810.

Katsukura, Y., David, C.N., Grimmelikhuijzen, C.J., Sugiyama, T. (2003). Inhibition of metamorphosis by RFamide neuropeptides in planula larvae of *Hydractinia echinata*. *Dev Genes Evol*, 213(12): 579-586.

Kelava, I., Rentzsch, F., Technau, U. (2015). Evolution of eumetazoan nervous systems: insights from cnidarians. *Philos Trans R Soc Lond B Biol Sci,* 370(1684), pii: 20150065.

Kelberman, D., Dattani, M.T. (2007). Genetics of septo-optic dysplasia. *Pituitary*, 10: 393-407.

Khalturin, K., Anton-Erxleben, F., Milde, S., Plo¨ tz, C., Wittlieb, J., Hemmrich, G., Bosch, T.C. (2007) Transgenic stem cells in *Hydra* reveal an early evolutionary origin for key elements controlling self-renewal and differentiation. *Dev Biol*, 309: 32–44.

Kim, I., Saunders, T., Morrison, S. (2007). Sox17 dependence distinguishes the transcriptional regulation of fetal from adult hematopoietic stem cells. *Cell,* 130: 470–553.

Kim, J., Chu, J., Shen, X., Wang, J., Orkin, S. (2008). An extended transcriptional network for pluripotency of embryonic stem cells. *Cell*, 132: 1049–1110.

King, N., Westbrook, M.J., Young, S.L., Kuo, A., Abedin, M., Chapman, J., Fairclough, S., Hellsten, U., Isogai, Y., Letunic, I., Marr, M., Pincus, D., Putnam, N., Rokas, A., Wright, K.J., Zuzow, R., Dirks, W., Good, M., Goodstein, D., Lemons, D., Li, W., Lyons, J.B., Morris, A., Nichols, S., Richter, D.J., Salamov, A., Sequencing, J.G., Bork, P., Lim, W.A., Manning, G., Miller, W.T., McGinnis, W., Shapiro, H., Tjian, R., Grigoriev, I.V., Rokhsar, D. (2008). The genome of the choanoflagellate *Monosiga brevicollis* and the origin of metazoans. *Nature*, 451(7180): 783-788.

Kinnamon, J.C. and Westfall, J.A. (1982) Types of neurons and synaptic connections at hypostome-tentacle junctions in *Hydra*. *J Morphol*, 173: 119–128.

Kirsche, W. and Kirsche, K. (1961). [Experimental studies on the problem of regeneration and function of the tectum opticum of *Carassium carassium* L.]. Z. *Mikrosk. Anat. Forsch*, 67: 140–182.

Koizumi, O. and Bode, H.R. (1986). Plasticity in the nervous system of adult *Hydra*: I. The position-dependent expression of FMRFamide-like immunoreactivity. *Dev Biol,* 116 (2): 407-421.

Koizumi, O., Heimfeld, S., Bode, H.R. (1988). Plasticity in the nervous system of adult *Hydra*: II. Conversion of ganglion cells of the body column into epidermal sensory cells of the hypostome. *Dev Biol*, 129 (2): 358-371.

Koizumi, O., Itazawa, M., Mizumoto, H., Minobe, S., Javois, L.C., Grimmelikhuijzen, C.J., Bode, H.R. (1992). Nerve ring of the hypostome in *Hydra*. I. Its structure, development, and maintenance. *J Comp Neurol,* 326: 7–21.

Koizumi, O., Mizumoto, H., Sugiyama, T., Bode, H.R. (1990). Nerve net formation in the primitive nervous system of *Hydra*—an overview. *Neurosci Res Suppl*, 13: S165-170.

Koizumi, O., Sato, N., Goto, C. (2004) Chemical anatomy of *Hydra* nervous system using antibodies against hydra neuropeptides: a review. *Hydrobiologia,* 530/531: 41–47.

Kolle, G., Georgas, K., Holmes, G.P., Little, M.H., Yamada, T. (2000). *CRIM1*, a novel gene encoding a cysteine-rich repeat protein, is developmentally regulated and implicated in vertebrate CNS development and organogenesis. *Mech Dev*, 90 (2): 181-193.

Kopp, J.L., Ormsbee, B.D., Desler, M., Rizzino, A. (2008). Small increases in the level of Sox2 trigger the differentiation of mouse embryonic stem cells. Stem Cells, 26(4): 903-911.

Kortschak, R.D., Samuel, G., Saint, R., Miller, D.J. (2004). EST analysis of the cnidarians *Acropora millepora* reveals extensive gene loss and rapid sequence divergence in the model invertebrates*. Curr. Biol*, 13: 2190-2195.

Kowalczyk, T., Pontious, A., Englund, C., Daza, R.A., Bedogni, F., Hodge, R., Attardo, A., Bell, C., Huttner, W.B., Hevner, R.F. (2009) Intermediate neuronal progenitors (basal progenitors) produce pyramidal-projection neurons for all layers of cerebral cortex. *Cereb Cortex*, 19: 2439–2450.

Kraus, Y., Flici H., Hensel, K., Plickert, G., Leitz, T., Frank, U. (2014). The embryonic development of the cnidarian *Hydractinia echinata*. *Evol Dev*, 16 (6): 323-338.

Kroehne, V., Freudenreich, D., Hans, S., Kaslin, J., Brand, M. (2011). Regeneration of the adult zebrafish brain from neurogenic radial glia-type progenitors. *Development*, 138: 4831-4841.

Künzel, T., Heiermann, R., Frank, U., Müller, W.A., Tilmann, W., Bause, M., Nonn, A., Helling, M., Schwarz, R.S., Plickert, G. (2010). Migration and differentiation potential of stem cells in the cnidarian *Hydractinia* analyzed in GFP-transgenic animals and chimeras. *Dev Biol*, 348: 120-129.

Lengfeld, T., Watanabe, H., Simakov, O., Lindgens, D., Gee, L., Law, L., Schmidt, H.A., Ozbek, S., Bode, H., Holstein, T.W. (2009). Multiple Wnts are involved in *Hydra* organizer formation and regeneration. *Dev Biol*, 330 (1): 186-199.

Lange A.W., Haitchi, H.M., LeCras, T.D., Sridharan, A., Xu, Y., Wert, S.E., James, J., Udell, N., Thurner, P.J., Whitsetta, J.A. (2014). Sox17 is required for normal pulmonary vascular morphogenesis. *Dev Biol,* 387: 109-120.

Larroux, C., Fahey, B., Liubicich, D., Hinman, V.F., Gauthier, M., Gongora, M., Green, K., Wörheide, G., Leys, S.P., Degnan, B.M. (2006). Developmental expression of transcription factor genes in a demosponge: insights into the origin of metazoan multicellularity. *Evol Dev,* 8: 150-173.

Layden, M.J., Boekhout, M., Martindale, M.Q. (2012). *Nematostella vectensis* achaete-scute homolog NvashA regulates embryonic ectodermal neurogenesis and represents an ancient component of the metazoan neural specification pathway. *Development*, 139:1013–1022.

Leitz, T. (1998). Metamorphosin A and related peptides: a novel family of neuropeptides with morphogenic activity. *Ann NY Acad Sci,*839: 105-110.

Lenhoff, S. G. and Lenhoff, H. M. (1986). *Hydra* and the Birth of Experimental Biology, 1744: Abraham Trembley's Memoirs Concerning the Natural History of a Type of Freshwater Polyp with Arms Shaped Like Horns (Boxwood Press, Pacific Grove, 1986).

Levine, A.J. and Brivanlou, A.H. (2007) Proposal of a model of mammalian neural induction. *Dev Biol*, 308: 247–256.

Lilly, A.J., Lacaud, G., Kouskoff, V. (2017). SOXF transcription factors in cardiovascular development. *Semin Cell Dev Biol,* 63: 50-57.

Lloyd, P.E., Kupfermann, I., Weiss, K.R. (1987). Sequence of small cardioactive peptide A: A second member of a class of neuropeptides in *Aplysia. Peptides*, 8: 179–183.

Magie, C.R., Pang, K., Martindale, M.Q. (2005). Genomic inventory and expression of Sox and Fox genes in the cnidarian *Nematostella vectensis*. *Dev Genes Evol,* 215: 618-630.

Mali, B., Millane, C., Plickert, G., Frohme, M., Frank, U. (2011). A polymorphic, thrombospondin domain-containing lectin is an oocyte marker in *Hydractinia*: implications for germ cell specification and sex determination. *Int j Dev Biol*, 55: 103-108.

Mansukhani, A., Ambrosetti, D., Holmes, G., Cornivelli, L., Basilico, C. (2005). *Sox2* induction by FGF and FGFR2 activating mutations inhibits Wnt signaling and osteoblast differentiation. *J Cell Biol*, 168:1065–1141.

Manuel, M. (2009). Early evolution of symmetry and polarity in metazoan body plans. *C R Biol*, 332: 184– 209.

Marlow, H. and Arendt, D. (2014). Evolution: ctenophore genomes and the origin of neurons. *Curr Biol*, 24: R757-R761.

Marlow, H.Q., Srivastava, M., Matus, D.Q., Rokhsar, D., Martindale, M.Q. (2009). Anatomy and development of the nervous system of *Nematostella vectensis*, an anthozoan cnidarian. *Dev Neurobiol*, 69(4): 235–254.

Martin, V.J. (1988). Development of nerve cells in hydrozoan planulae: I. Differentiation of ganglionic cells. *Biol Bull,* 174: 319-329.

Masuda-Nakagawa, L.M., Gröer, H., Aerne, B.L., Schmid, V. (2000). The HOX-like gene Cnox2-Pc is expressed at the anterior region in all life cycle stages of the jellyfish *Podocoryne carnea*. *Dev Genes Evol*, 210 (3): 151-156.

Masui, S., Nakatake, Y., Toyooka, Y., Shimosato, D., Yagi, R., Takahashi, K., Okochi, H., Okuda, A., Matoba, R., Sharov, A., Ko, M.S., Niwa, H. (2007). Pluripotency governed by Sox2 via regulation of Oct3/4 expression in mouse embryonic stem cells. *Nat Cell Biol*, 9:625–660.

Matsushima, D., Heavner, W., Pevny, L. (2011). Combinatorial regulation of optic cup progenitor cell fate by SOX2 and PAX6. *Development,* 138:443–497.

McMahon Emma (2018). Characterization of Piwi^{+} stem cells in *Hydractinia*. PhD thesis, NUIG, http://hdl.handle.net/10379/7174.

Millane, R.C., Kanska, J., Duffy, D.J., Seoighe, C., Cunningham, S., Plickert, G., Frank, U. (2011). Induced stem cell neoplasia in a cnidarian by ectopic expression of a POU domain transcription factor. *Development*, 138: 2429-2439.

Miller, M. A., Technau, U., Smith, K. M., Steele, R. E. (2000). Oocyte development in *Hydra* involves selection from competent precursor cells. *Dev Biol*, 224: 326-338.

Mizuseki, K., Kishi, M., Shiota, K., Nakanishi, S., Sasai, Y. (1998) SoxD: an essential mediator of induction of anterior neural tissues in Xenopus embryos. *Neuron*, 21: 77–85.

Morgan, T.H. (1901). Regeneration. The Macmillan Company, New York.

Moroz, L.L., Kocot, K.M., Citarella, M.R., Dosung, S., Norekian, T.P., Povolotskaya, I.S., Grigorenko, A.P., Dailey, C., Berezikov, E., Buckley, K.M., Ptitsyn, A., Reshetov, D., Mukherjee, K., Moroz, T.P., Bobkova, Y., Yu, F., Kapitonov, V.V., Jurka, J., Bobkov, Y.V., Swore, J.J., Girardo, D.O., Fodor, A., Gusev, F., Sanford, R., Bruders, R., Kittler, E., Mills, C.E., Rast, J.P., Derelle, R., Solovyev, V.V., Kondrashov, F.A., Swalla, B.J., Sweedler, J.V., Rogaev, E.I., Halanych, K.M., Kohn, A.B. (2014). The ctenophore genome and the evolutionary origins of neural systems. *Nature*, 510: 109-114.

Morris, H.R., Panico, M., Karplus, A., Lloyd, P.E., Piniker, B. (1982). Identification by FAB-MS of the structure of a new cardioactive peptide from *Aplysia. Nature*, 300: 643–645.

Müller, W.A. (1969) Auslösung der Metamorphose durch Bakterien bei den Larven von *Hydractinia echinata. Zool Jb Anat,* 86: 84–95.

Müller, W.A. (1973). Induction of metamorphosis by bacteria and ions in the planulae of *Hydractinia echinata*; an approach to the mode of action. *PublSeto Mar Biol Lab 20 Proc Second Int Symp Cnidaria,* 195-208.

Müller, W.A., Teo, R., Frank, U. (2004). Totipotent migratory stem cells in a hydroid. *Dev Biol*, 275: 215-24.

Müller, W.A., Wieker, F., Eiben, R. (1976). Larval adhesion, releasing stimuli and metamorphosis. In: Mackie GO eds; Coelenterate Ecology and Behavior,Plenum Press New York, London, 339-346.

Nakanishi, N., Renfer, E., Technau, U., Rentzsch, F. (2012). Nervous systems of the sea anemone *Nematostella vectensis* are generated by ectoderm and endoderm and shaped by distinct mechanisms. *Development*, 139: 347-357.

Niakan, K., Ji, H., Maehr, R., Vokes, S., Rodolfa, K., Sherwood, R., Yamaki, M., Dimos, J., Chen, A., Melton, D., McMahon, A.P., Eggan, K. (2010). Sox17 promotes differentiation in mouse embryonic stem cells by directly regulating extraembryonic gene expression and indirectly antagonizing self-renewal. *Genes & Development*, 24: 312-338.

Nicotra, M.L., Powell, A.E., Rosengarten, R.D., Moreno, M., Grimwood, J., Lakkis, F.G., Dellaporta, S.L., Buss, L.W. (2009). A hypervariable invertebrate allodterminant. *Curr Biol,* 19: 583–589.

Niehrs, C. (2010) On growth and form: a Cartesian coordinate system of Wnt and BMP signaling specifies bilaterian body axes. *Development*, 137: 845–857.

Nillni, E.A., Luo, L.G., Jackson, I.M., McMillan, P. (1996). Identification of the thyrotropin-releasing hormone precursor, its processing products, and its coexpression with convertase 1 in primary cultures of hypothalamic neurons: Anatomic distribution of PC1 and PC2. *Endocrinology,* 137: 5651–5661.

Nishimiya-Fujisawa, C. and Kobayashi, S. (2012). Germline stem cells and sex determination in *Hydra*. *Int J Dev Biol,* 56: 499–508.

Noctor, S.C., Martı´nez-Cerdeno, V., Ivic, L., Kriegstein, A.R. (2004) Cortical neurons arise in symmetric and asymmetric division zones and migrate through specific phases. *Nat Neurosci*, 7: 136–144.

Okubo, T., Pevny, L., Hogan, B. (2006). Sox2 is required for development of taste bud sensory cells. *Genes & Development*, 20:2654–2663.

Orkin, S., and Hochedlinger, K. (2011). Chromatin connections to pluripotency and cellular reprogramming. *Cell,* 145: 835–885.

Parish, C.L., Beljajeva, A., Arenas, E., Simon, A. (2007). Midbrain dopaminergic neurogenesis and behavioural recovery in a salamander lesion-induced regeneration model. *Development,* 134, 2881–2887.

Passamaneck, Y.J. and Martindale, M.Q. (2012). Cell proliferation is necessary for the regeneration of oral structures in the anthozoan cnidarian *Nematostella vectensis*. *BMC Dev Biol,* 12: 34.

Pennisi, D., Gardner, J., Chambers, D., Hosking, B., Peters, J., Muscat, G., Abbott, C., Koopman, P. (2000). Mutations in Sox18 underlie cardiovascular and hair follicle defects in ragged mice. *Nat Genet,* 24: 434-437.

Pevny, L. and Nicolis, S. (2010). Sox2 roles in neural stem cells. *Int J Biochem Cell Biol*, 42: 421–424.

Pick, K., Philippe, H., Schreiber, F., Erpenbeck, D., Jackson, D., Wrede, P., Wiens, M., Alié, A., Morgenstern, B., Manuel, M. (2010). Improved phylogenomic taxon sampling noticeably affects nonbilaterian relationships. *Mol Biol Evol*, 27: 1983-1987.

Plachetzki, D.C., Fong, C.R., Oakley, T.H. (2012). Cnidocyte discharge is regulated by light and opsin-mediated phototransduction. *BMC Biol*, 10: 17.

Plickert, G., Frank, U., Müller, W.A. (2012) *Hydractinia*, a pioneering model for stem cell biology nd reprogramming somatic cells in pluripotency. *Int J Dev Biol*, 56: 519-534.

Plickert, G., Schetter, E., Verhey-Van-Wijk, N., Schlossherr, J., Steinbuchel, M., Gajewski, M. (2003). The role of α-amidated neuropeptides in hydroid development – Lwamides and metamorphosis in *Hydractinia echinata*. *Int J Dev Biol*, 47(6): 439-450.

Powell, A.E., Nicotra, M.L., Moreno, M.A., Lakkis, F.G., Dellaporta, S.L., Buss, L.W. (2007). Differential effect of allorecognition loci on phenotype in Hydractinia symbiolongicarpus. *Genetics*, 177 (4): 2101-2107.

Price, D.A., and Greenberg M.J. (1977). Purification and characterization of a cardioexcitatory neuropeptide from the central ganglia of a bivalve mollusk. *Prep Biochem,* 7: 261–281.

Price, D.A., and Greenberg, M.J. (1989). Structure of a molluscan cardioexcitatory neuropeptide. *Science*, 97: 670–671.

Price, D.A., and Greenberg, M.J. (1989). The hunting of the FaRPs: The distribution of FMRFamide-related peptides. *Biol Bull,* 177: 198–205.

Putnam, N.H., Srivastava, M., Hellsten, U., Dirks, B., Chapman, J., Salamov, A., Terry, A., Shapiro, H., Lindquist, E., Kapitonov, V.V., Jurka, J., Genikhovich, G., Grigoriev, I.V., Lucas, S.M., Steele, R.E., Finnerty, J.R., Technau, U., Martindale, M.Q., Rokhsar, D.S. (2007). Sea anemone genome reveals ancestral eumetazoan gene repertoire and genomic organization. *Science,* 317: 86-94.

Quan, X.J. and Hassan, B.A. (2005). From skin to nerve: flies, vertebrates and the first helix. *Cell Mol Life Sci*, 62: 2036-2049.

Quiroga Artigas, G., Lapebie, P., Leclere, L., Takeda, N., Deguchi, R., Jekely, G., Momose, T., Houliston, E. (2018). A gonad-expressed opsin mediates light-induced spawning in jellyfish *Clytia*. *Elife,* 7: e29555.

Raina, A.K., Jaffe, H., Kempe, T.G., Keim, P., Blacher, R.W., Fales, H.M., Riley, C.T., Klum, J.A., Ridgway, R.L., Haves, D.K. (1989). Identification of a neuropeptide hormone that regulates sex pheromone production in female moths. *Science*, 244: 796–798.

Rebscher, N., Volk, C., Teo, R., Plickert, G. (2008). The germ plasm component *Vasa* allows tracing of the interstitial stem cells in the cnidarian *Hydractinia echinata*. *Dev Dyn*, 237: 1736-1745.

Reddien, P. W., and Sanchez Alvarado, A. (2004). Fundamentals of planarian regeneration. *Annu Rev Cell Dev Biol,* 20: 725-757.

Reiprich, S., and Wenger, M. (2015) From CNS stem cells to neurons and glia: Sox for everyone. *Cell Tissue Res*, 359: 111-124.

Reitzel, A.M., Burton, P.M., Krone, C., Finnerty, J.R. (2007). Comparison of developmental trajectories in the starlet sea anemone *Nematostella vectensis*: embryogenesis, regeneration, and two forms of asexual fission. *Invertebr Biol*, 126: 99-112.

Rentzsch, F., Anton, R., Saina, M., Hammerschmidt, M., Holstein, T.W., Technau, U. (2006) Asymmetric expression of the Bmp antagonists chordin and gremlin in the sea anemone *Nematostella vectensis*: implications for the evolution of axial patterning. *Dev Biol*, 296: 375–387.

Richards, G.S., Rentzsch, F. (2014) Transgenic analysis of a SoxB gene reveals neural progenitor cells in the cnidarian *Nematostella vectensis*. *Development,* 141: 4681–4689.

Richards, G.S. and Rentzsch, F. (2015). Regulation of *Nematostella* neural progenitors by SoxB, Notch and bHLH genes. *Development*, 142: 3332-3342.

Ross, K.G., Molinaro, A.M., Romero, C., Dockter, B., Cable, K.L., Gonzalez, K., Zhang, S., Collins, E.S., Pearson, B.J., Zayas, R.M. (2018) *SoxB1* Activity Regulates Sensory Neuron Regeneration, Maintenance, and Function in Planarians. *Dev Cell*, 47 (3): 331-347.

Ryan, J.F., Pang, K., Schnitzler, C.E., Nguyen, A.D., Moreland, R.T., Simmons, D.K., Koch, B.J., Francis, W.R., Havlak, P., Smith, S.A., Putnam, N.H., Haddock, S.H., Dunn, C.W., Wolfsberg, T.G., Mullikin, J.C., Martindale, M.Q., Baxevanis, A.D. (2013). NISC Comparative Sequencing Program: The genome of the ctenophore *Mnemiopsis leidyi* and its implications for cell type evolution. *Science,* 342: 1242592.

Salvini-Plawen, L.V. (1978). On the origin and evolution of the lower Metazoa. *Z Zool Syst Evolut Forsch*. 16: 40-88.

Sanchez Alvarado, A. (2000). Regeneration in the metazoans: why does it happen? *BioEssays,* 22: 578-590.

Sanchez Alvarado, A. and Tsonis, P.A. (2006). Bridging the regeneration gap: genetic insights from diverse animal models. *Nat Rev Genet*, 7 (11): 873-884.

Sanders, S.M., Ma, Z., Hughes, J.M., Riscoe, B.M., Gibson, G.A., Watson, A.M., Flici, H., Frank, U., Schnitzler, C.E., Baxevanis, A.D., Nicotra, M.L. (2018). CRISPR/Cas9-mediated gene knockin in the hydroid *Hydractinia symbiolongicarpus*. *BMC Genomics*, 19(1):649

Sarkar, A. and Hochedlinger, K. (2013). The Sox family of transcription factors: versatile regulators of stem and progenitor cell fate. *Cell Stem Cell*, 12 (1): 15-30.

Sasai, Y. (2001) Roles of Sox factors in neural determination: conserved signaling in evolution? *Int J Dev Biol*, 45: 321–326.

Savatier, P., Lapillonne, H., Jirmanova, L., Vitelli, L., Samarut, J. (2002). Analysis of the cell cycle in mouse embryonic stem cells. *Methods Mol Biol*, 185: 27-33.

Schepers, G., Teasdale, R., Koopman, P. (2002). Twenty pairs of sox: extent, homology, and nomenclature of the mouse and human sox transcription factor gene families. *Dev Cell,* 3: 167–170.

Schmich, J., Rudolf, R., Trepel, S., Leitz, T. (1998) Immunohistochemical studies of GLWamides in Cnidaria. *Cell Tissue Res*, 294: 169–177.

Schmich, J., Trepel, S., Leitz, T. (1998). The role of GLWamides in metamorphosis of *Hydractinia echinata*. *Dev Genes Evol,* 208: 267-273.

Schnitzler, C.E., Simmons, D.K., Pang, K., Martindale M.Q., Baxevanis A.D. (2014). Expression of multiple Sox genes through embryonic development in the ctenophore *Mnemiopsis leidyi* is spatially restricted to zones of cell proliferation. *EvoDevo*, 5:15.

Schuchert, P. (2011). *Podocoryn carnea* M. Sars, 1846. In: Schuchert, P. World Hydrozoa database. World Register of Marine Species. www.marinespecies.org/aphia.php?p=taxdetails&id=220573

Séguin, C.A., Draper, J.S., Nagy, A., Rossant, J. (2008). Establishment of endoderm progenitors by SOX transcription factor expression in human embryonic stem cells. *Cell Stem Cell*, 3: 182-195.

Seipp, S., Schmich, J., Leitz, T. (2001). Apoptosis: A death-inducing mechanism tightly linked with morphogenesis in *Hydractinia echinata* (Cnidaria, Hydrozoa). *Development*, 128: 4891-4898.

Seipp, S., Schmich, J., Will, B., Schetter, E., Plickert, G., Leitz T. (2010). Neuronal cell death during metamorphosis of *Hydractinia echinata* (Cnidaria, Hydrozoa). *Invertebr. Neurosci*. 10: 77-91.

Sekine, K., Furusawa, T, Hatakeyama, M. (2015). The boule gene is essential for spermatogenesis of haploid insect male. *Dev Biol*, 339 (1): 154-163.

Shenk, M.A. (1991) Allorecognition in the colonial marine hydroid *Hydractinia* (Cnidaria/Hydrozoa), *Amer Zool*, 31:549-557.

Shinzato, C., Iguchi, A., Hayward, D.C., Technau, U., Ball, E.E., Miller, D.J. (2008). Sox genes in the coral *Acropora millepora*: divergent expression patterns reflect differences in developmental mechanisms within the Anthozoa. *BMC Evol Biol*, 8: 311.

Shinzato, C., Shoguchi, E., Kawashima, T., Hamada, M., Hisata, K., Tanaka, M., Fujie, M., Fujiwara, M., Koyanagi, R., Ikuta, T., Fujiyama, A., Miller, D.J., Satoh, N. (2011) Using the *Acropora digitifera* genome to understand coral responses to environmental change. *Nature,* 476:320–323.

Siebert, S., Anton-Erxleben, F., Bosch, T.C. (2008). Cell type complexity in the basal metazoan *Hydra* is maintained by both stem cell-based mechanisms and transdifferentiation. *Dev Biol*. 313: 13–24.

Siggs, O.M. and Beutler, B. (2012). The BTB-ZF transcription factors. *Cell Cycle*, 11 (18): 3358-3369.

Sinclair, A., Berta, P., Palmer, M., Hawkins, J., Griffiths, B., Smith, M., Foster, J., Frischauf, A., Lovell-Badge, R., Goodfellow, P. (1990). A gene from the human sex-determining region encodes a protein with homology to a conserved DNA-binding motif. *Nature,* 346:240–244.

Simon, F., Ramat, A., Louvet-Vallee, S., Lacoste, J., Burg, A., Audibert, A., Gho, M. (2019). Shaping of *Drosophila* Neural Cell Lineages Through Coordination of Cell Proliferation and Cell Fate by the BTB-ZF Transcription Factor Tramtrack-69. *Genetics*, 212 (3): 773-788.

Slavotinek, A. (2018). Genetics of anophthalmia and microphthalmia. Part 2: syndromes associated with anophthalmia-microphthalmia. *Hum. Genet,* 138(8-9):831-846.

Soza-Ried, J., Hotz-Wagenblatt, A., Glatting, K.H., Del Val, C., Fel-Lenberg, K., Bode, H.R., Frank, U., Hoheisel, J.D., Frohme, M. (2010). The transcriptome of the colonial marine hydroid *Hydractinia echinata*. *FEBS J*, 277: 197-209.

Steinmetz, P., Aman, A., Kraus, J., Technau, U. (2017). Gut-like ectodermal tissue in a sea anemone challenges germ layer homology. *Nat Ecol Evol*, 1 (10): 1535-1542.

Tajan, M., Paccoud, R., Branka, S., Edouard, T., Yart, A. (2018). The RASopathy family: consequences of germline activation of the RAS/MAPK pathway. *Endocr Rev*, 39: 676-700.

Takahashi, K. and Yamanaka, S. (2006). Induction of pluripotent stem cells from mouse embryonic and adult fibroblast cultures by defined factors. *Cell*, 126 (4): 663-676.

Takahashi, T., Koizumi, O., Ariura, Y., Romanovitch, A., Bosch, T.C.G., Kobayakawa, Y., Mohri, S., Bode, H.R., Yum, S., Hatta, M., Fujisawa, T. (2000). A novel neuropeptide, Hym-355, positively regulates neuron differentiation in *Hydra*. *Development*, 127: 997–1005.

Takahashi, T., Nowakowski, R.S. and Caviness, V.S. (1995). The cell cycle of the pseudostratified ventricular epithelium of the embryonic murine cerebral wall. *J Neurosci,* 15, 6046-6057.

Takahashi, T., and Takeda, N. (2015). Insight into the molecular and functional diversity of cnidarian neuropeptides. *Int J Mol Sci*, 16 (2): 2610-2625.

Takemoto, T., Uchikawa, M., Yoshida, M., Bell, D., Lovell-Badge, R., Papaioannou, V., Kondoh, H. (2011) Tbx6- dependent Sox2 regulation determines neural or mesodermal fate in axial stem cells. *Nature*, 470: 394–402.

Tanaka, E., M. and Ferretti, P. (2009). Considering the evolution of regeneration in the central nervous system. *Nat. Rev. Neurosci*, 10: 713–723.

Tanaka, E.M. and Reddien, P.W. (2011). The cellular basis for animal regeneration. *Dev Cell*, 21: 172-185.

Tardent, P. and Holstein, T. (1982). Morphology and morphodynamics of the stenotele nematocyst of *Hydra* attenuate Pall. (Hydrozoa, Cnidaria). *Cell Tissue Res*, 224: 269-290.

Technau, U., Miller, M.A., Bridge, D., Steele, R.E. (2003). Arrested apoptosis of nurse cells during *Hydra* oogenesis and embryogenesis. *Dev. Biol*, 260: 191-206.

Technau, U. and Steele, R.E. (2011). Evolutionary crossroads in developmental biology: Cnidaria. *Development*, 138(8): 1447-1458.

Tomioka, M., Nishimoto, M., Miyagi, S., Katayanagi, T., Fukui, N., Niwa, H., Muramatsu, M., Okuda, A. (2002). Identification of Sox-2 regulatory region which is under the control of Oct-3/4-Sox-2 complex. *Nucleic acids res*, 30: 3202–3215.

Trembley, A. (1744). Mémoires pour servir à l'histoire d'un genre de polypes d'eau douce. Leide: Jean and Herman Verbeek.

Trevino, M., Stefanik, D.J., Rodriguez, R., Harmon, S., Burton, P.M. (2011). Induction of canonical Wnt signaling by alsterpaullone is sufficient for oral tissue fate during regeneration and embryogenesis in *Nematostella vectensis*. *Dev Dyn*, 240: 2673-2679.

Truman, J.W. (1992). The eclosion hormone synthesis of insects. *Prog Brain Res*, 92: 361–374.

Van Wolfswinkel, J.C., Wagner, D.E., Reddien, P.W. (2014). Single-cell analysis reveals functionally distinct classes within the planarian stem cell compartment. *Cell Stem Cell*, 15: 326-39.

Warner, J.F., Amiel, A.R., Johnston, H., Rottinger, E. (2019). Regeneration is a partial redeployment of the embryonic gene network, *BioRxiv*, doi.org/10.1101/658930.

Watanabe, H., Fujisawa, T., Holstein, T.W. (2009) Cnidarians and the evolutionary origin of the nervous system. *Develop Growth Differ*, 51: 167-183.

Watanabe, H., Kuhn, A., Fushiki, M., Agata, K., Ozbek, S., Fujisawa T., Holstein, T.W. (2014). Sequential actions of β-catenin and Bmp pattern the oral nerve net in *Nematostella vectensis*. *Nat Comm*, 5: 5536.

Weber, C. (1989). Smooth muscle fibers of *Podocoryne carnea* (Hydrozoa) demonstrated by a specific monoclonal antibody and their association with neurons showing FMRFamide-like immunoreactivity. *Cell Tissue Res*, 255: 275-282.

Wegner M. (2010). All-purpose Sox: The many roles of Sox proteins in gene expression. *Int J Biochem Cell Biol*, 42:381–471.

Weismann, A. (1883). The origin of the sexual cells in hydromedusae. Jena. Gustav Fischer

Westfall, J.A. (1973) Ultrastructural evidence for a granule containing sensory-motor-interneuron in Hydra littoralis. *J Ultrastruct Res*, 42: 268–282.

Westfall, J.A. (1987) Ultrastructure of invertebrate synapses. Nervous Systems in Invertebrates (ed. M. A. Ali), pp. 3–28. Plenum Press, New York.

Wilkerson MJ. (2012). Principles and applications of flow cytometry and cell sorting in companion animal medicine. *Vet Clin North Am Small Anim Pract*, 42, 53–71.

Wittlieb, J., Khalturin, K., Lohmann, J.U., Anton-Erxleben, F., Bosch, T.C. (2006). Transgenic *Hydra* allow in vivo tracking of individual stem cells during morphogenesis. *Proc Natl Acad Sci USA*, 103: 6208–6211.

Yaross, M.S., Westerfield, J., Javois, L.C., Bode, H.R. (1986). Nerve cells in *Hydra*. Monoclonal antibodies identify two lineages with distinct mechanisms for their incorporation into head tissue. *Dev. Biol*, 114: 225-237.

Zapata, F., Goetz, F.E., Smith, S.A., Howison, M., Siebert, S., Church, S. H., Sanders, S.M., Ames, C.L., Mcfadden, C.S., France, S.C. (2015). Phylogenomic analyses support traditional relationships within Cnidaria. *PloS One*, 10: e0139068.

Zenkert, C., Takahashi, T., Diesner, M.O., Ozbek, S. (2011). Morphological and molecular analysis of the *Nematostella vectensis cnidom. Plos One*, 6 (7): e22725.

Zhang, S. and Cui, W. (2014) Sox2, a key factor in the regulation of pluripotency and neural differentiation. *World J Stem Cells*, 6: 305-311.

Zupanc, G.K. and Clint S.C. (2003). Potential role of radial glia in adult neurogenesis of teleost fish. *Glia*, 43: 77–86.

Appendix A

Primers used in this project:

	Primer name	*Primer sequence*
SoxB1 reporter line	SoxBIII 5'UTRFwd	CCGATTACAAAGAGTTAGCCTG
	SoxBIII 5'UTRRvs	ATTTTTATGTAGTATAGCTAAGTATATATATAATATTTATTCATTCAAAACACTGTTTG
	SoxBIII 3'UTRFwd	TATTATTCTTTATATTATTAAGGTATAAATCTTTTAGGGTTGTAC
	SoxBIII 3'UTRRvs	CCTCTTCCCTTTCTGAACTACAC
	SoxBIIItdTFwd+endof5UTR	GCTATACTACATAAAAATATGACTTCCAAA GGTG
	SoxBIIItdTRvs+begof3UTR	TTATTTGTACAGTTCGTCCATTCCCCTTAA TAATATAAAGAATAATA
	SoxBIIIFwdBb+endof3UTR	GCGTCCACTAAGAATGTTTTACCGTACGGG CCCTTTCG
	SoxBIIIRvsBb+begof5UTR	ACTGGCCGTCGTTTTACCAGGCTAACTCTT TGTAATCGG
	SoxBIII5UTRFusFwd	CACATGACGCCAATCGC
	SoxBIII3UTRFusRvs	GAGCACTGTGGCTTAGC
	tdTomSeqFusRvs	CCAAGCAAATGGCAGTGGAC
	tdTomatoFwd+endof5'UTR	GCTATACTACATAAAAATATGACTTCCAAAGGTG
	tdTomatoRvs+begof3'UTR	TTATTTGTACAGTTCGTCCATTCCGTACAACCCTAAAAGATTTATACC
	tdTomatoRvs+begof3'UTR	TTATTTGTACAGTTCGTCCATTCCCCTTAATAATATAAAGAATAATA
SoxB2 reporter line	SoxBIpromoterfwdBamH1	aaaaaa ggatccCGAGTTTCGAGTTGTTTGAAATTTGATATC
	SoxBIpromoterrevNot1	aaaaaagcggccgcACTAAAACAATAGAACACGTTCTATTTTTC
	SoxBIATGrev Not1	aaaaaagcggccgcCTCAGTCTAGCTAGAAGATAAAAACAAAC
	SoxBI3fwd Sac1	aaaaaagagctcTGAATTAATACTACAATTAGGAAACAACATATATTTATTTTTATAG
	SoxBI3'revPac1	aaaaaattaattaaCGGGCCATTTGATGATTTCATAATC
	GFPseqFusRvs	TTGCATCACCTTCACCCTCTCC
SoxB3 reporter line	SoxBII 5'UTRFwd	CTTGTGTATTCCGTAACGATTCG
	SoxBII 5'UTRRvs	TCTTGTCCTTTTTGCTACAGG
	SoxBII 3'UTRFwd	CGATTTTGAAAGTAAACTTTGTTAATGTGGTG
	SoxBII 3'UTRRvs	TGAAATAAATCAGGTTTGACCC
	SoxBIIbbFwdBamHI	AAAAAAGGATCCCGTACGGGCCCTTTCG
	SoxBIIbbRvsPacI	AAAAAATTAATTAAACTGGCCGTCGTTTTA CAAC
	SoxBII5UTRfwdBamHI	AAAAAAGGATCCCATCTAAGAAGAAGGAAG TTTACGCC
	SoxBII3UTRrvsPacI	AAAAAATTAATTAATGAAATAAATCAGGTT TGACCC
	SoxBII5UTRFusedFwd	GCTACTGTTTATGTTGTAATAATTTGTTG
	SoxBII3UTRFusedRvs	ACTGACGCTCTTCTGAAC
	GFPseqFusRvs	TTGCATCACCTTCACCCTCTCC

	SoxBIIGFPFwd+endof5UTR	GTAGCAAAAAGGACAAGAATGAGTAAAGGA G
	SoxBIIGFPRvs+begof3UTR	CTATTTGTATAGTTCATCCCAAAGTTTACT TTCAAAATCG
	SoxBIIFwdBb+endof3UTR	GGGTCAAACCTGATTTATTTCACGTACGGG CCCTTTCG
	SoxBIIRvsBb+begof5UTR	ACTGGCCGTCGTTTTACCTTCCTTCTTCTT AGATG
	SoxB3fwd5UTRnewBamHI	aaaaaggatccGACTGTCAGTATCCATGTAC
	SoxB3rvs5UTRnewNotI	aaaaagcggccgcTCTTGTCCTTTTCGCTACAGG
	SoxB3fwd3UTRnewSacI	aaaaagagctcCGATTTTGAAAGTCAACTTTGTTAATGTTGTG
	SoxB3rvs3UTRnewPacI	aaaaattaattaaATAGTTGAAGTACTGATATTGATAAAAAC
	BBfwdPacI	aaaaattaattaaCGTACGGGCCCTTTCG
	BBrvsBamHI	aaaaaggatccACTGGCCGTCGTTTTAC
SoxB1 antibody	SoxBIII_fwd	AAAAAACATATGCACCATCACCATCACCACATGATTGGTGCAGATGGTAAACAAAT
	SoxBIII_rev	ttatatGGATCCTCATGAATTCTGTTGCACAGAAGTATT
FISH probes	SoxB1ISHFwd	ATGACAACTACAGCTGAAGTTATTTCACAAACAGC
	SoxB1ISHRvs	CTCAGACACTGCCAGAACAGGTGAATTCTG
SABER FISH SoxB1 probes	SoxB1.1	GCAGTTGCTGTTTGTGAAATAACTTCAGCTGTAGTTGTCATTTTCATCATCAT
	SoxB1.2	AGTTGCAGACATTGTCATTGGGAGAATATGATGAGTTGGATTTTCATCATCAT
	SoxB1.3	GCCTCTTGAGACATCAGATGAGAAATGTTGGAAGTTTGCATTTTCATCATCAT
	SoxB1.6	GTCGATACTTGTAATCTGGATGGGACTTCATGTGCTCTGTTTCATCATCAT
	SoxB1.7	ACCATCTGCACCAATTACAGCAGTAGGCATAGCAATTTTATTTTCATCATCAT
	SoxB1.8	ACCACTGGCAATTGCATAAGGATATTGTGCTGACATAAAGATTTCATCATCAT
	SoxB1.9	CCAGCATGATAAGCTTCATGTCCATTAACTAAGGCTGACATTTTCATCATCAT
	SoxB1.11	ACTAGATGAAGTAGTTGATTGTGGTAAGCTTGCAACTGCTTTTCATCATCAT
	SoxB1.13	ACGAAAATGGGCTATACATATATGTAGTCCCACCAGGAACATTTCATCATCAT
	SoxB1.14	GCTTGAGCACTATAGGCACTCATTGTAGCACCATTTAAGTATTTCATCATCAT
	SoxB1.16	TCTGTTGCTGTGGTAGTAACAGCTGCCTCATGCTTGTTTCATCATCAT
	SoxB1.18	TGACTTGGTAATGCAGTTGCTGTAGTAGTTGTACTAGTTGCTTTCATCATCAT
	SoxB1.19	CAACTGCTGTGGGATACATTCCACCGATTGGATAGTAATTTCATCATCAT
	SoxB1.22	ACAGAAGTATTCATGCTTCGAGCTGGACTCTGTGAATTTTCATCATCAT
	SoxB1.23	CACTCAGACACTGCCAGAACAGGTGAATTCTGTTGCTTTCATCATCAT
SABER FISH SoxB2 probes	SoxB2.1	ACACGTCTTGCTTGACTTGTGCAACCATGTTATTCATTTTAATACTCTC
	SoxB2.4	GCGGTTGAGCGGTTTGAGTAAGTTGTGGAATATGTGTTATTTAATACTCTC
	SoxB2.5	TAACCCCATGAAGCGTGGTGGTGGCTGGTATGGAAGTTTAATACTCTC
	SoxB2.12	GCTTTGAAATCTCCGAATTATGCATGCGAGGGTTTTCTTGTTTAATACTCTC
	SoxB2.13	CTTCTCGACCTGCGTTAAGCACTTCCACTCTGCCCCTTTAATACTCTC
	SoxB2.18	TTTGTACTTGTAGTCGGGGTGCTCTTGGATGTGTACTTTAATACTCTC

	SoxB2.22	TTGGTAGGCCATGCTGCCGTACTTAGGATCTATACCTTTAATACTCTC
	SoxB2.25	CTGGGTAACCATAGCCGGGACTCATTTTGCTGTACATTTAATACTCTC
	SoxB2.29	CAGCGGTCGGAGAAGGGGTCATGCTACTCAAACTGTTTTAATACTCTC
	SoxB2.34	TGGCGTTGCTGTCCGTCATAACAGGTGTTCCATTGGTTTAATACTCTC
	SoxB2.37	CGGGGCTGTATTGACTAGTGACGTTGCTATAGTAACTCTTTTAATACTCTC
	SoxB2.39	GGTATCTGGCCTGTGAATGAACCTGAGGGGCACTGGTTTAATACTCTC
	SoxB2.41	AGACTTGCGTTGAGTGGCGATTTTCGTCAGGGGAAGTTTAATACTCTC
	SoxB2.46	ACGTGTTGTGTTTTCCGACGAATAAGTAGGTGGCGTTTTAATACTCTC
	SoxB2.48	GGATAAATCTGATTGTTGCGTTGTTTGCGGCCAATGTTTAATACTCTC
SABER FISH SoxB3 probes	SoxB3.2	TTGGCTTCGCTAATTTTCTTTCGTTCCAAGCGGGACTTTCATCATCAT
	SoxB3.3	TCTTCCGTTAAAAGTTTCCATGAAGCACCAAGACGTTTAGATTTCATCATCAT
	SoxB3.5	TCGGACGATATTTATACTCGGGGTGTTCCTCCATATGTTTTCATCATCAT
	SoxB3.7	CAGTTCCGGACCTTTGCTTTGAATACTCTGGAATAGACATTTTCATCATCAT
	SoxB3.9	CTGGTAAATTGACAACACGTGGATGCCCAACATATTGATTTTCATCATCAT
	SoxB3.10	ATAGCGCGATGACGGGTAATGGATCGTGGTGACACCTTTCATCATCAT
	SoxB3.12	CTGTGACGGCGGAAGTCTCTGTCAAAGGGACTACGATTTCATCATCAT
	SoxB3.13	CCTCTAAATGAGTGGTGTTCTTGTGGACTTATCGGGTGATATTTCATCATCAT
	SoxB3.15	TTGCTTTGAGGTTTACTATGTGGTGCCACTGGTGAGTTTCATCATCAT
	SoxB3.17	CCTTTTCGTTTATTGCGTTGAGAATTCTTGCGATCTGTTGTTTTCATCATCAT
	SoxB3.19	ACTCCGATACGCAATAGGACTTCTCTCATTGTATCGTACAATTTCATCATCAT
	SoxB3.21	GCATACATCGGGCGACATATGAGAACTTCTTGGCTGTTTCATCATCAT
	SoxB3.23	GCGCACACTGTGGCGAGGTATGTACTTATTATGATATTTCATTTCATCATCAT
	SoxB3.25	CGTAGAATTGTCTGTGTGCACCTTCTTCACAATCTGAACAATTTCATCATCAT
	SoxB3.27	CGGTCTTTACTTCTTGGAGGACGACCACTTGTACTGTTTCATCATCAT
SoxB1 OE	SoxB1OEfwdNotI	AAAGCGGCCGCGGTGGAGGTGGATCTGAAAAAATGACAACTACAGCTG
	SoxB1OErvsEcoRV	AAAGATATCCTCAGACACTGCCAGAACAGGTG
	SoxB1CSfwd	TTATAGATGAAGCGAAACGTCTCCG
	SoxB1CSrvs	TCATAATAGAACTGGCACGTACGCAACC
	GFPSacIrvs	GAGCTCCTATTTGTATAGTTCATCCATGC
shRNAi	shSoxB1Fwd (GG)	TAATACGACTCACTATAGGTCATATGTGAGCCCTAGTTATTTACTAACTAAGGCTGACATATAACCTT
	shSoxB1Rvs (GG)	AAGGTTATATGTCAGCCTTAGTTAGTAAATAACTAGGGCTCACATATGACCTATAGTGAGTCGTATTA
	shSoxB2Fwd (GG)	TAATACGACTCACTATAGGAATAATGCAAGGTACAGATATTTACTATCTATACCTGGCATCATTCCTT
	shSoxB2Rvs (GG)	AAGGAATGATGCCAGGTATAGATAGTAAATATCTGTACCTTGCATTATTCCTATAGTGAGTCGTATTA

shSoxB3Fwd (GG)	TAATACGACTCACTATAGGAGAAACACACCGAGCATAAATTTACTTTATACTCGGGGTGTTCCTCCTT
shSoxB3Rvs (GG)	AAGGAGGAACACCCCGAGTATAAAGTAAATTTATGCTCGGTGTGTTTCTCCTATAGTGAGTCGTATTA
shGFPFwd	TAATACGACTCACTATAGGATGACGCGATCTGCAAGACAATTTACTTGTCTTGTAGTTCCCGTCATCTT
shGFPRvs	AAGATGACGGGAACTACAAGACAAGTAAATTGTCTTGCAGATCGCGTCATCCTATAGTGAGTCGTATTA
shGFPcontrolFwd	TAATACGACTCACTATAGGATGACGGGAGCTACAAGACAATTTACTTGTCTTGTAGCTCCCGTCATCTT
shGFPcontrolRvs	AAGATGACGGGAGCTACAAGACAAGTAAATTGTCTTGTAGCTCCCGTCATCCTATAGTGAGTCGTATTA
shPiwi1fwd	TAATACGACTCACTATAGGTAACACATGCAGAGTGGTAATTTACT
shPiwi1rvs	AAGGTAACACGTCCAGAGTGGTAAGTAAATTACCACTCTGCATG
shPiwi2fwd	TAATACGACTCACTATAGGAATCTTACATTCCTGCTATATTTACT
shPiwi2rvs	AAGGAATCTTACCTGCGTGCTATAGTAAATATAGCAGGAATG

Appendix B

Sequence of SoxB1 reporter line vector. Purple – SoxB1 promoter, Dark red – tdTomato, Green – SoxB1 terminator, Black – pBluescript backbone, Blue – B-lactamase-AMPr, Red – Restriction sites.

GGATCCGGTTATTCTTAACTCGTCTACCTTAAAAAAGTGAGCACGCACCATAAGAACTAAAAAAGAAAACAAAATGCATTTTCCG
CCAATTTTGACACCCTAAAATCACAAATCCCTACAGCGACAACAATGGGGACACCTCCTGGGACTATACTATACCAATTAGTGAA
ATATTAGCGAAGTAATTATGATACAAAAATTTGAACACTGAATATTTTAACAGCTACTCAAACAAAAAAATCTTATATAGCTATA
TATATCTGTTGTTTGTGATTTTCAACTCTATGATCATGCCATGCACAGCTCTTGTATTAAGTGCTCCAGTATAGATCAAACTTGA
GCGAACCTACAAGCATCAATGAATCTTTGAGAATAAAGAATTGCTTTCACAAATTTAGTCCCTGTGTACATTATATTAACACTCC
TAAAAAATCATACTTAGCTGGCTTAGCTAGCTACTGGAGAGACAAATGCTTAAAATTGACAAAACAGAAATAAAGAGAAAAATGA
AGTTAAAAAATAATTTCAGTGTCTTTCCCATCTTGTGTTGTCAGAACTATTAGTTACATTGTATAATAGCTATTTTACTTTAGAG
CTAGCTGCAGTTTTGCTTCTTTTTAGCTACAAGAGAATGTGCGCGCATTTACAAAAATCCGTAAACCTTGGTGAACTTTACTTTA
GTCATCTAGCTAGCTATCTATTAGCTGAAGAAACAGATGCATAATAAAAGGTAAGATGTATTATACTTTGATTCCCCGATTACAA
AGAGTTAGCCTGTTAATTCTCCAGCCCAGCTAATTAATTTAATGAGCTTTGGTAATAAAGGAAAACTAAAGAAAATTTTTAAAAA
CTACCTAAAACGCGAAAACAAGATAAATATTATGCTCAAGAGCAGCAAATCAATTTTACAGAACAACTCTCTGAGCAAGTGAGAG
GAAACATTCGGATTAGCCATTGTTTACCCAAAAGGTATACAGTCATTGATGACAATACTTATTCTAAAATTTCTAAGACTGTGCG
TGTGATATATGGTAAAATATAAATATACAAATAAAAAAGGTTTTCAAATATCAAAACTTGAACCCCCGGAAAATATTGTTTAATA
GATAATTATAGTCTTTTCACATGACGCCAATCGCTGAATGAGCCTTTTGTTTTTTTGGTTAATAAGCTATTGTTGATGCTTTGTT
CAATATTCAACAAACTGTGAAGCGAATCAAAATAGCATAACATGTACCCTGGTACTTACTCCTTCTAAGTTTTGTTTATGTGTTT
TAAAAAGACCCGAGGCCGAAGTGCTGAAAGCGTCATTGTGATTGGTTAATAAGTTGTCAATCAAACTTTTATGTGTGATTACAAC
TAGACAATATGTTCATCACAATATTTGATTCGAACCAACGTGTGTGTTGTTCTCTAGAGACGTATTCTGAATAGGTTGCTATTAT
TCGCTTTTTTTATTCAGAAATTATTACGGTTGTTCTGCTTTTGTTTGAAAGAGATACAGAACAGAGGTTTTAGTACAAGGCTAATA
AAGAAACTCAAGAAGTTCTTGGAAATTGTGAAACAAAAAGTGGATCGAGATTAAATGAAATCAAACAGTGTTTTGAATGAATAAA
TATTATATATATACTTAGCTATACTACATAAAAATGCGGCCGCATGACTTCCAAAGGTGAAGAGGTTATCAAAGAATTTATGCGT
TTCAAAGTTCGAATGGAAGGGAGTATGAATGGACATGAGTTTGAGATAGAAGGAGAAGGGGAAGGTAGACCCTATGAAGGCACTC
AAACGGCTAAGTTAAAAGTTACAAAGGGAGGTCCACTGCCATTTGCTTGGGATATTTTGTCTCCTCAATTCATGTATGGTTCGAA
AGCATACGTTAAACACCCTGCAGATATTCCGGACTATAAGAAGTTATCGTTTCCAGAAGGTTTTAAATGGGAACGCGTTATGAAC
TTCGAAGATGGTGGGTTAGTAACAGTAACACAGGATAGCAGCTTGCAAGATGGTACGTTAATCTACAAAGTGAAAATGAGAGGCA
CCAATTTTCCACCAGATGGACCAGTCATGCAGAAGAAAACTATGGGCTGGGAAGCAAGCACCGAAAGGCTATATCCTAGGGATGG
TGTTTTAAAAGGAGAGATCCATCAAGCTTTGAAACTAAAAGACGGTGGCCACTATTTGGTGGAATTTAAGACCATATACATGGCT
AAGAAACCGGTACAGTTACCGGGATATTATTACGTGGATACTAAGCTAGATATAACATCTCACAACGAGGACTACACAATTGTGG
AACAATATGAAAGATCAGAAGGCCGTCATCATTTGTTTCTTGGCCATGGCACTGGTTCCACCGGTAGTGGATCATCAGGTACTGC
TTCAAGTGAGGACAACAACATGGCGGTGATAAAAGAGTTCATGAGATTTAAAGTGCGAATGGAGGGCTCAATGAATGGACACGAA
TTTGAAATTGAAGGGGAGGGTGAAGGACGACCGTACGAAGGAACACAAACAGCCAAATTGAAAGTAACTAAGGGAGGTCCTCTTC
CTTTTGCATGGGACATCTTATCTCCACAATTTATGTACGGATCTAAAGCCTATGTCAAACATCCAGCTGATATTCCCGATTACAA
GAAACTTAGCTTTCCAGAGGGATTCAAATGGGAACGTGTGATGAATTTCGAAGATGGAGGTTTAGTTACAGTAACCCAAGACAGT
TCTTTACAAGATGGAACTTTGATCTATAAAGTCAAAATGAGAGGAACAAATTTCCCACCAGATGGGCCTGTTATGCAAAAGAAAA
CGATGGGTTGGGAGGCATCAACTGAGAGATTGTATCCACGTGACGGAGTCTTGAAAGGGGAGATACATCAAGCCCTAAAGCTTAA
AGATGGTGGCCATTATCTGGTAGAATTTAAAACCATTTATATGGCGAAAAAACCTGTCCAGTTACCAGGCTACTACTACGTTGAC
ACAAAGTTAGATATTACAAGTCACAATGAAGATTACACTATTGTTGAACAGTATGAACGCTCTGAAGGTAGACACCACTTATTTC
TTTACGGAATGGACGAACTGTACAAATAAGAGCTCTGAATTAATACTACAATTAGGAAACAACATATATTTATTTTTATAGAGGC
CACCCTTTGAGAGTGTTTTTATCATTTTTGTGTTTTTTTCCATCTTGCGATAATCAAACTTATGTTACGAAAGGGAAATCAGATT
TGCGTTACGAAGAAGTTCGTACTTTTTTTTACCCCCCTTGCTTCCATTTTTTTTGCTTTGTGTCAGATAAACAGGATAGTACAGA
GGAGAAATTCTCGCCCAAGGTGTCAATTTTAGCACGGGAAAGAAAAAGAAACATCGATGAATCGTTTCCCTCGATAATGTGAAAA
ACATTCTCTCTTAACAAGAAATGTTTTGCGTTAAACGTAAAGTCCAGGTTATACTACATAATAAATGTCCCAATAATACTGTGGT
TGCTTTAAATTATTAAAAAGAAACAACCCTATATAAATGAGGCCTTATTTTTGTTGTTCAAGAATACTTTTTTTTGCAAGTAACT
TTTATCGATTAAAACGTGGTGTACACGAGTGTTGCGTTTTACTTGTTACCATGGCAATCTCCACGTCATTTTGTCATTTCGTATT
CACATTTCACCTTTGATTTAATTTTCAAAATTTATCTTCGTTGAAACGAAGAAAGGTATAGAGATATGTTAGTGTCATTGAGATA
CGATTATTTAACAAAGTATAACTCCGTGTAATATATTCTCATCTTGTTCAATTTAGACAAACCGATAAAATAGGATAAATATGAG
TAATAAAACAATGTTATATTTAATAACATCAACTTTTCTTTCATGAAAAGGATCAACCTAGAATATTTTTGTGTGTTGCAAATAC
GGCTTCGTGTAACTCAAACCTGTCTTCATTACGGTCAAACATGCTAATGAAAATAGGAGCCTTGCGCATTTTGTCAACGTTAGTA
TGACCATTCTAATTATAGTTTGTTTTTTTGTATTTATACTTAAAGAAGATTTATATAAATATTCACGATTGCTTTTGCAGGGATC
ATCATACGCGAATAAAATAGTTCGCCTAAGCACCCCTTGCTTTTTATGGAAATCGTATTCAGGTTTCTATAAAAAAACAGAGACC
TGGGCAAGAGAATGAGTTTTTAATTGTCGATAATGAGGCTATTAAAAGCATGGCGGTTGACACGCCTAAAGAAGCATTTATTAAC
ACCATGCAAATTCTTCCCTAATTTGTTATTTATCGGCTTCACTCAATGAAAAGTATTAACAAACAGAAAAATTCAATATTTGTTT
ACACCATCTGTTTGGTTAAGCAAGCAAACGTACATTTATTTGTCTTCCCTTGTGCACGTGGTATTTGACAAGTCGAAACGAAAAC
ACATGTGTAACACCTGATCAATGCGTTGTAACAATGTGTCAAATCACTTTTATAGGACGTGAGAACGCGGTATATCACAACACTG
TGTCATTGGCCGCATGTGAAATATGTGAGACATTTTAAATCTTGGTGGAAAGTATTATGTAGAAAGCCCAATAAAATAAACAAGG
ATAAACAAATAAAAACTAATTTAACGAGAAAAGGATAACATCAAGGTTAGAAATATTAATCTGGTAAAATCGCAAACCTAGGGTC
TAATACCCAAAATTGTGTATTTAGGTTTAAGATTTCCCAAACCACTGAGTTTTACAGAGGTGATGTAAAGGAAAAAATACAAGTA
AAAATAGCGTTTCCGAATGGATATTTCTAAGCTAAAAAAAAATTCGTGATATTTATTAATTTTTCTAATTTTTTGAACCACGGGG

AAGCATTAAAATTGCAGGTGCTCTTCATTTTCTTATATCAAATTGGTTTACACGAAAAATTAATAATTTTGGTGTAAAAGAAGGT
ACAGATGTAGTTTTTGTATAATTTTGGTGTAAAAGAAGGTACAGATGTAGTTTTTGTATTATTGGTTCAGTTATGTACAAAATAT
AGCTATTTCAAAATGATGAAAAAAATTAACAATTTTGGTTCACATTTCATGTAATCTTTGACAGAAAGGAAATACTTTAACTAGC
CAGTACGTGAAATATGTTTAAAGTATCCCCCCCCCCCCCTTCTCTCGCCAAAACGATGTACAAAAAAACTGCTCTTCACATCACT
GGAAGACTGTCATTGCAACTTCGTCCCCAGGGCTCTTTTCACTTTTTGATATCGGGATGGCAGTGAAAAAAAAAACAGGGCACGA
GATTGTCCCTAACGTGTCCTTTATTCCTTTATGTCCAAAATTTGCCTGTTCGTTGATCGTCTTTTTAAAATAGAGAATAAATATT
GAATGACTAAAATAGTGTCAAAACTGAAATTTATGTCCATGAATTTCCCTAAAAATCCATTTACTTGTGAAGAAACTTCGATGAC
TAATTATTTTTATATATGCAACTTATCCCACACTTTTTGGGTTGTAACCGCGTTTACTTTTATTTTATATTATACAGTTTTTTAC
GACCAATAGTGTATGTTTCTCTATAGACTAAATTATTTATTGCATTGATAAAACTAAAAAAATAGAAAAGTAATTCGAGCAGACG
TAGATAAAACATAACGTGTGAAATTTTTTTCCAACATTAAGCCAAGTAACAATAGGAACGGAAGCAATTAGCGCGCTAATGTGCC
TGCTAATGTGTTTTAATTTCAGTAAACGTCAAATATTGACACTTGCACTTGTGAACTGTTGAAATGTGAGATGAAAAAATGTTTT
TATATACGCGACAATATAAAACTTGCATTCTTCCTGGTACGAGTGTTATAGCTATTATCTACTTTGTTGAAACTATTATCGGCCT
TATTTACTCAAGTTATCTACTTTGTTAAGCAAACCAACCTAAGGTTGAATGCTTTTGTCTCTCAAACAAAAATGGATTATGAAAT
CATCAAATGGCCCGTTAATTAACGTACGGGCCCTTTCGTCTCGCGCGTTTCGGTGATGACGGTGAAAACCTCTGACACATGCAGC
TCCCGGAGACGGTCACAGCTTGTCTGTAAGCGGATGCCGGGAGCAGACAAGCCCGTCAGGGCGCGTCAGCGGGTGTTGGCGGGTG
TCGGGGCTGGCTTAACTATGCGGCATCAGAGCAGATTGTACTGAGAGTGCACCATATGCGGTGTGAAATACCGCACAGATGCGTA
AGGAGAAAATACCGCATCAGGCGGCCTTAAGGGCCTCGTGATACGCCTATTTTTATAGGTTAATGTCATGATAATAATGGTTTCT
TAGACGTCAGGTGGCACTTTTCGGGGAAATGTGCGCGGAACCCCTATTTGTTTATTTTTCTAAATACATTCAAATATGTATCCGC
TCATGAGACAATAACCCTGATAAATGCTTCAATAATATTGAAAAAGGAAGAGTATGAGTATTCAACATTTCCGTGTCGCCCTTAT
TCCCTTTTTTGCGGCATTTTGCCTTCCTGTTTTTGCTCACCCAGAAACGCTGGTGAAAGTAAAAGATGCTGAAGATCAGTTGGGT
GCACGAGTGGGTTACATCGAACTGGATCTCAACAGCGGTAAGATCCTTGAGAGTTTTCGCCCCGAAGAACGTTTTCCAATGATGA
GCACTTTTAAAGTTCTGCTATGTGGCGCGGTATTATCCCGTATTGACGCCGGGCAAGAGCAACTCGGTCGCCGCATACACTATTC
TCAGAATGACTTGGTTGAGTACTCACCAGTCACAGAAAAGCATCTTACGGATGGCATGACAGTAAGAGAATTATGCAGTGCTGCC
ATAACCATGAGTGATAACACTGCGGCCAACTTACTTCTGACAACGATCGGAGGACCGAAGGAGCTAACCGCTTTTTTGCACAACA
TGGGGGATCATGTAACTCGCCTTGATCGTTGGGAACCGGAGCTGAATGAAGCCATACCAAACGACGAGCGTGACACCACGATGCC
TGTAGCAATGGCAACAACGTTGCGCAAACTATTAACTGGCGAACTACTTACTCTAGCTTCCCGGCAACAATTAATAGACTGGATG
GAGGCGGATAAAGTTGCAGGACCACTTCTGCGCTCGGCCCTTCCGGCTGGCTGGTTTATTGCTGATAAATCTGGAGCCGGTGAGC
GTGGGTCTCGCGGTATCATTGCAGCACTGGGGCCAGATGGTAAGCCCTCCCGTATCGTAGTTATCTACACGACGGGGAGTCAGGC
AACTATGGATGAACGAAATAGACAGATCGCTGAGATAGGTGCCTCACTGATTAAGCATTGGTAACTGTCAGACCAAGTTTACTCA
TATATACTTTAGATTGATTTAAAACTTCATTTTTAATTTAAAAGGATCTAGGTGAAGATCCTTTTTGATAATCTCATGACCAAAA
TCCCTTAACGTGAGTTTTCGTTCCACTGAGCGTCAGACCCCGTAGAAAAGATCAAAGGATCTTCTTGAGATCCTTTTTTTCTGCG
CGTAATCTGCTGCTTGCAAACAAAAAAACCACCGCTACCAGCGGTGGTTTGTTTGCCGGATCAAGAGCTACCAACTCTTTTTCCG
AAGGTAACTGGCTTCAGCAGAGCGCAGATACCAAATACTGTCCTTCTAGTGTAGCCGTAGTTAGGCCACCACTTCAAGAACTCTG
TAGCACCGCCTACATACCTCGCTCTGCTAATCCTGTTACCAGTGGCTGCTGCCAGTGGCGATAAGTCGTGTCTTACCGGGTTGGA
CTCAAGACGATAGTTACCGGATAAGGCGCAGCGGTCGGGCTGAACGGGGGGTTCGTGCACACAGCCCAGCTTGGAGCGAACGACC
TACACCGAACTGAGATACCTACAGCGTGAGCTATGAGAAAGCGCCACGCTTCCCGAAGGGAGAAAGGCGGACAGGTATCCGGTAA
GCGGCAGGGTCGGAACAGGAGAGCGCACGAGGGAGCTTCCAGGGGGAAACGCCTGGTATCTTTATAGTCCTGTCGGGTTTCGCCA
CCTCTGACTTGAGCGTCGATTTTTGTGATGCTCGTCAGGGGGGCGGAGCCTATGGAAAAACGCCAGCAACGCGGCCTTTTTACGG
TTCCTGGCCTTTTGCTGGCCTTTTGCTCACATGTTCTTTCCTGCGTTATCCCCTGATTCTGTGGATAACCGTATTACCGCCTTTG
AGTGAGCTGATACCGCTCGCCGCAGCCGAACGACCGAGCGCAGCGAGTCAGTGAGCGAGGAAGCGGAAGAGCGCCCAATACGCAA
ACCGCCTCTCCCCGCGCGTTGGCCGATTCATTAATGCAGCTGGCACGACAGGTTTCCCGACTGGAAAGCGGGCAGTGAGCGCAAC
GCAATTAATGTGAGTTAGCTCACTCATTAGGCACCCCAGGCTTTACACTTTATGCTTCCGGCTCGTATGTTGTGTGGAATTGTGA
GCGGATAACAATTTCACACAGGAAACAGCTATGACCATGATTACGCCAAGCTTGTTGTAAAACGACGGCCAGT

Sequence of SoxB2 reporter line vector. Purple – SoxB2 promoter, Green – GFP, Orange – SoxB2 terminator, Black – pBluescript backbone, Blue – B-lactamase-AMPr, Yellow – Restriction sites.

CGAGTTTCGAGTTGTTTGAAATTTGATATCTTGTTCAATGATGACATAAAACCTGACTAAAATGTTAAAAACGGAAAAAGCAACT
TCCTCTCCACTATTTTGACACCATAACACCCGAGTTAAAAATAAACAACGTGCTATTTTTAGACAGTGTTCGGAAAGTCTTTCCA
AAATAAGACTAGAATGATAATCCTTATATGACTTCTCCTTGACAACCCTAAAACCCTAGAACAATTTAATAAAGTCGTATAGTTT
TGTCTCTACTACACGTTTCTAGCAAGAAGAAACGATAAAAACTGTACGCTTAAACGCTTCACATGACTCTGTCTACGTTTNNNNN
NNNNNNNNNNNNNNNNNNNNNNNNNNNNNNNNNNNNNNNNNNNNNNNNNNNATTAAATTGACATTTCACCAGATCATTTTCTTTTCCC
TCTGAATTGAACTGAAGGGATGTAAATAATTTTATAAATGGCGCCCTTTTTTGTATTTTTAAAAACGAAAAAATAAGCTCATGTG
GTTCCAAAAGAACGTTACTAAAAGTGATGCATGGAATATGGAAGAAATCAAAATAAAATGTGAATTTATATGAATAAAACATAAC
AAATCACAAGTATACTTGAGATTATAGCACAGTCAAAAATATCACAAAAGCAATGTGTTACATCAAAAGTTTCCAGCTACACCCG
TTGAAAAATCCTAAAATTTTCACTCAATTTTCATTCTAAAAGTAAGATAATGAATCAAGTTAGGGTTAAATTTTGTTTCACATCT
GTTATTTCACAGACTGTAAATGATTGAAATATACAAAGTGCGCGGTAGATCATAATGTTTTATTATTTATGACTTCCCTCTTTGA
AAACTGCATCCGAAACACCCAAAAGCGTGAAGATTTGATTAGACGGGAATTGCATATGTGCAAGAAATAAAATGGCATCTGTTCC
AAAGTTAAAAAACAAAATTAAAAAATTAAAATATACTAATTATATTGACATGCTGTTTTTATTTCAGTTTCACACTTTGAATCAG
GCATGTGGCCACCTTGCATTTGGGGAGAAAGTCAATATAATTTTAGAATTGTATGATTTATCAAAAATTCTATAAAATTTGCACT
GCTATGTTTGGCAGTCTTTTGTGATGGATAGCATATGAGTCACGGCATCTTGACTTTTAAATTGTATTCGTATTCGCGCATCCGT
CTTACTTATAAAAATCAACAGAATTATTTATTTACTAAGCAAATTGGAGCTATTGTTTCACGACCTTCAATAACAATACTCTACA
TCAACAAGTTTTTCTTAGCCTGCAAGTATAAATCCTTAATTTGATATGTGTGTTAAAAAAATCCCAATAAAAAATTAAACTTCTT
TTTTTCTGGAAAATGTTACAATTTTAATTACATATTTAGTTATGCTATTATCCACATCAACCGCATATATTAACATAATTAATTT
AAGAAAAATAGAACGTGTTCTATTGTTTTAGTGTTAATTATGCGTATTTACGTCAAAACATGATAATAATGTAATGTTTACTAGT
GCGTGAATAGCAAAAAGTTAAATAGACAGGCGGGATTTTAAAAGTCATTTACTTAGCGGTAATATAACAGCAACGGGGCTGTCAA
TAAAGGAAATATAATAAAAAACGCGCTCGAAATCGATAACACATTGTTTTCATGAATGGATATTCCATTAGAGCATAAAAAAGAT
CAGTAACGATATATAGTTTCATAAGAAAGAAGTTAAAAGCTCCAACTAACACTTGCTCATAAAGAAAGGTAAAGATTTTTATATT
GCATTGAAATAATAATGTCATGTTATTGTAAGTGGTTTTAAAGAAAATAATGTTTTTTTAAGTTGTAATTATTATAAAGTCCCTT
TTGTAAAAAATCTACCTTTTGTGATGTTTTTTTATCTCTAAAGATTCTCTATTTTAATTGTAAGATTTTAAAACAAAAAAACTTC
TCAGAAAAAGCTTTCTTTTATGCGTGTCTTTTATTTTTTATATACAATATTTTATTTTAGATAATGTTATTTCATTTCTTTGTTC
AGGAAAAATGTCTCACAAGATGTTCTTTCGTTTTTACTTTTATTTTACGGATATAAGGTTTTTCTAACCTTATATTTTTAACAAG
ATTTTTGATTTTTTTTTCCGCACAGGCTGTACAAAACTTTTATATATAGAAAAAATATCGAAAATTTTGATTTTCTTCTAACAAG
ATAGCCCAAAAGATCTTCGTCACAACACGACTGCCATTTAAGGAACAAATATTTTGTTTGTAGGAAGGATTTTCGGTATTCGTTA
AAATTAAATTAAAAAAAGAAAAAAAGGATGAGAAATCAACTAATAAATAAATAAGTGAATAAAGTTTACGCGCGTGTAGGAAGGA
AAATCACGAAGGCTGAACTTTTCAAGTGGACGGACACACTTCTCACATGTTATAGCGACGTGTTTGAAAGAGGAGGAGTTCACGC
ACTTTTTTTCATCGCTAGCACCGCCATTTTATCGTAAGATAGTCACAAAAATATAGAAGAGATACGAAAAATCTGCCACTTCAAT
TCCTTTACTCTTGTTCGAAATCGTGGATAGAAATAATGGCGGGAACCTAAAATTCAAAATTCAAAAATCGTCTGCATTTTGGTTG
TTGAAACATGAAACCATGTGTTTTGTTTGGCATATTGTTACTGTCATAAAGTCAAGTCTTCGGAAAAAACCTGCAAAACATCAAG
CCTGTCACGAGTGAAACTTTTGTTTTCATCGTTAATAATTAGTGATGCAATTTTATGATGAGGGAGATATATTTCTCCACTCTCG
ATAGCGAAAGAAAAACTCATTTCCTACTAATTACGCGCCATATTAACTATATATCGAAAACACCTTACCGCGGAGAGATCTAACA
AATTCAAAGTTAAAAAAAAAAAACGTTTAGTTATCATAAAGTTATCCATCGCAAAGTGGATACTCCAATTCTATTTCCATCCGCT
GTTCAATCTTTAATTTCTGCCAGTTTGTTTTTATCTTCTAGCTAGACTGAG**GCGGCCGCTGCAGCCCCGGTAGAAAAAATGAGTA**
AAGGAGAAGAACTTTTCACTGGAGTTGTCCCAATTCTTGTTGAATTAGATGGTGATGTTAATGGGCACAAATTTTCTGTCAGTGG
AGAGGGTGAAGGTGATGCAACATACGGAAAACTTACCCTTAAATTTATTTGCACTACTGGAAAACTACCTGTTCCATGGCCAACA
CTTGTCACTACTTTCTGTTATGGTGTTCAATGCTTTTCAAGATACCCAGATCATATGAAACGGCATGACTTTTTCAAGAGTGCCA
TGCCCGAAGGTTATGTACAGGAAAGAACTATATTTTTCAAAGATGACGGGAACTACAAGACACGTGCTGAAGTCAAGTTTGAAGG
TGATACCCTTGTTAATAGAATCGAGTTAAAAGGTATTGATTTTAAAGAAGATGGAAACATTCTTGGACACAAATTGGAATACAAC
TATAACTCACACAATGTATACATCATGGCAGACAAACAAAAGAATGGAATCAAAGTTAACTTCAAAATTAGACACAACATTGAAG
ATGGAAGCGTTCAACTAGCAGACCATTATCAACAAAATACTCCAATTGGCGATGGCCCTGTCCTTTTACCAGACAACCATTACCT
GTCCACACAATCTGCCCTTTCGAAAGATCCCAACGAAAAGAGAGACCACATGGTCCTTCTTGAGTTTGTAACAGCTGCTGGGATT
ACACATGGCATGGATGAACTATACAAATAGGAGCTCTGAATTAATACTACAATTAGGAAACAACATATATTTATTTTTATAGAGG
CCACCCTTTGAGAGTGTTTTTATCATTTTTGTGTTTTTTTCCATCTTGCGATAATCAAACTTATGTTACGAAAGGGAAATCAGAT
TTGCGTTACGAAGAAGTTCGTACTTTTTTTTACCCCCCTTGCTTCCATTTTTTTTTGCTTTGTGTCAGATAAACAGGATAGTACAG
AGGAGAAATTCTCGCCCAAGGTGTCAATTTTAGCACGGGAAAGAAAAAGAAACATCGATGAATCGTTTCCCTCGATAATGTGAAA
AACATTCTCTCTTAACAAGAAATGTTTTGCGTTAAACGTAAAGTCCAGGTTATACTACATAATAAATGTCCCAATAATACTGTGG
TTGCTTTAAATTATTAAAAAGAAACAACCCTATATAAATGAGGCCTTATTTTTGTTGTTCAAGAATACTTTTTTTTGCAAGTAAC
TTTTATCGATTAAAACGTGGTGTACACGAGTGTTGCGTTTTACTTGTTACCATGGCAATCTCCACGTCATTTTGTCATTTCGTAT
TCACATTTCACCTTTGATTTAATTTTCAAAATTTATCTTCGTTGAAACGAAGAAAGGTATAGAGATATGTTAGTGTCATTGAGAT
ACGATTATTTAACAAAGTATAACTCCGTGTAATATATTCTCATCTTGTTCAATTTAGACAAACCGATAAAATAGGATAAATATGA
GTAATAAAACAATGTTATATTTAATAACATCAACTTTTCTTTCATGAAAAGGATCAACCTAGAATATTTTTGTGTGTTGCAAATA
CGGCTTCGTGTAACTCAAACCTGTCTTCATTACGGTCAAACATGCTAATGAAAATAGGAGCCTTGCGCATTTTGTCAACGTTAGT
ATGACCATTCTAATTATAGTTTGTTTTTTTGTATTTATACTTAAAGAAGATTTATATAAATATTCACGATTGCTTTTGCAGGGAT
CATCATACGCGAATAAAATAGTTCGCCTAAGCACCCCTTGCTTTTTATGGAAATCGTATTCAGGTTTCTATAAAAAAACAGAGAC
CTGGGCAAGAGAATGAGTTTTTAATTGTCGATAATGAGGCTATTAAAAGCATGGCGGTTGACACGCCTAAAGAAGCATTTATTAA
CACCATGCAAATTCTTCCCTAATTTGTTATTTATCGGCTTCACTCAATGAAAAGTATTAACAAACAGAAAAATTCAATATTTGTT
TACACCATCTGTTTGGTTAAGCAAGCAAACGTACATTTATTTGTCTTCCCTTGTGCACGTGGTATTTGACAAGTCGAAACGAAAA
CACATGTGTAACACCTGATCAATGCGTTGTAACAATGTGTCAAATCACTTTTATAGGACGTGAGAACGCGGTATATCACAACACT
GTGTCATTGGCCGCATGTGAAATATGTGAGACATTTTAAATCTTGGTGGAAAGTATTATGTAGAAAGCCCAATAAAATAAACAAG
GATAAACAAATAAAAACTAATTTAACGAGAAAAGGATAACATCAAGGTTAGAAATATTAATCTGGTAAAATCGCAAACCTAGGGT
CTAATACCCAAAATTGTGTATTTAGGTTTAAGATTTCCCAAACCACTGAGTTTTACAGAGGTGATGTAAAGGAAAAAATACAAGT
AAAAATAGCGTTTCCGAATGGATATTTCTAAGCTAAAAAAAAATTCGTGATATTTATTAATTTTTCTAATTTTTTGAACCACGGG
GAAGCATTAAAATTGCAGGTGCTCTTCATTTTCTTATATCAAATTGGTTTACACGAAAAATTAATAATTTTGGTGTAAAAGAAGG
TACAGATGTAGTTTTTGTATAATTTTGGTGTAAAAGAAGGTACAGATGTAGTTTTTGTATTATTGGTTCAGTTATGTACAAAATA

TAGCTATTTCAAAATGATGAAAAAAATTAACAATTTTGGTTCACATTTCATGTAATCTTTGACAGAAAGGAAATACTTTAACTAG
CCAGTACGTGAAATATGTTTAAAGTATCCCCCCCCCCCCCTTCTCTCGCCAAAACGATGTACAAAAAAACTGCTCTTCACATCAC
TGGAAGACTGTCATTGCAACTTCGTCCCCAGGGCTCTTTTCACTTTTTGATATCGGGATGGCAGTGAAAAAAAAAACAGGGCACG
AGATTGTCCCTAACGTGTCCTTTATTCCTTTATGTCCAAAATTTGCCTGTTCGTTGATCGTCTTTTTAAAATAGAGAATAAATAT
TGAATGACTAAAATAGTGTCAAAACTGAAATTTATGTCCATGAATTTCCCTAAAAATCCATTTACTTGTGAAGAAACTTCGATGA
CTAATTATTTTTATATATGCAACTTATCCCACACTTTTTGGGTTGTAACCGCGTTTACTTTTATTTTATATTATACAGTTTTTTA
CGACCAATAGTGTATGTTTCTCTATAGACTAAATTATTTATTGCATTGATAAAACTAAAAAAATAGAAAAGTAATTCGAGCAGAC
GTAGATAAAACATAACGTGTGAAATTTTTTTCCAACATTAAGCCAAGTAACAATAGGAACGGAAGCAATTAGCGCGCTAATGTGC
CTGCTAATGTGTTTTAATTTCAGTAAACGTCAAATATTGACACTTGCACTTGTGAACTGTTGAAATGTGAGATGAAAAAATGTTT
TTATATACGCGACAATATAAAACTTGCATTCTTCCTGGTACGAGTGTTATAGCTATTATCTACTTTGTTGAAACTATTATCGGCC
TTATTTACTCAAGTTATCTACTTTGTTAAGCAAACCAACCTAAGGTTGAATGCTTTTGTCTCTCAAACAAAAATGGATTATGAAA
TCATCAAATGGCCCG**TTAATTAA**CGTACGGGCCCTTTCGTCTCGCGCGTTTCGGTGATGACGGTGAAAACCTCTGACACATGCAG
CTCCCGGAGACGGTCACAGCTTGTCTGTAAGCGGATGCCGGGAGCAGACAAGCCCGTCAGGGCGCGTCAGCGGGTGTTGGCGGGT
GTCGGGGCTGGCTTAACTATGCGGCATCAGAGCAGATTGTACTGAGAGTGCACCATATGCGGTGTGAAATACCGCACAGATGCGT
AAGGAGAAAATACCGCATCAGGCGGCCTTAAGGGCCTCGTGATACGCCTATTTTTATAGGTTAATGTCATGATAATAATGGTTTC
TTAGACGTCAGGTGGCACTTTTCGGGGAAATGTGCGCGGAACCCCTATTTGTTTATTTTTCTAAATACATTCAAATATGTATCCG
CTCATGAGACAATAACCCTGATAAATGCTTCAATAATATTGAAAAAGGAAGAGTATGAGTATTCAACATTTCCGTGTCGCCCTTA
TTCCCTTTTTTGCGGCATTTTGCCTTCCTGTTTTTGCTCACCCAGAAACGCTGGTGAAAGTAAAAGATGCTGAAGATCAGTTGGG
TGCACGAGTGGGTTACATCGAACTGGATCTCAACAGCGGTAAGATCCTTGAGAGTTTTCGCCCCGAAGAACGTTTTCCAATGATG
AGCACTTTTAAAGTTCTGCTATGTGGCGCGGTATTATCCCGTATTGACGCCGGGCAAGAGCAACTCGGTCGCCGCATACACTATT
CTCAGAATGACTTGGTTGAGTACTCACCAGTCACAGAAAAGCATCTTACGGATGGCATGACAGTAAGAGAATTATGCAGTGCTGC
CATAACCATGAGTGATAACACTGCGGCCAACTTACTTCTGACAACGATCGGAGGACCGAAGGAGCTAACCGCTTTTTTGCACAAC
ATGGGGGATCATGTAACTCGCCTTGATCGTTGGGAACCGGAGCTGAATGAAGCCATACCAAACGACGAGCGTGACACCACGATGC
CTGTAGCAATGGCAACAACGTTGCGCAAACTATTAACTGGCGAACTACTTACTCTAGCTTCCCGGCAACAATTAATAGACTGGAT
GGAGGCGGATAAAGTTGCAGGACCACTTCTGCGCTCGGCCCTTCCGGCTGGCTGGTTTATTGCTGATAAATCTGGAGCCGGTGAG
CGTGGGTCTCGCGGTATCATTGCAGCACTGGGGCCAGATGGTAAGCCCTCCCGTATCGTAGTTATCTACACGACGGGGAGTCAGG
CAACTATGGATGAACGAAATAGACAGATCGCTGAGATAGGTGCCTCACTGATTAAGCATTGGTAACTGTCAGACCAAGTTTACTC
ATATATACTTTAGATTGATTTAAAACTTCATTTTTAATTTAAAAGGATCTAGGTGAAGATCCTTTTTGATAATCTCATGACCAAA
ATCCCTTAACGTGAGTTTTCGTTCCACTGAGCGTCAGACCCCGTAGAAAAGATCAAAGGATCTTCTTGAGATCCTTTTTTTCTGC
GCGTAATCTGCTGCTTGCAAACAAAAAAACCACCGCTACCAGCGGTGGTTTGTTTGCCGGATCAAGAGCTACCAACTCTTTTTCC
GAAGGTAACTGGCTTCAGCAGAGCGCAGATACCAAATACTGTCCTTCTAGTGTAGCCGTAGTTAGGCCACCACTTCAAGAACTCT
GTAGCACCGCCTACATACCTCGCTCTGCTAATCCTGTTACCAGTGGCTGCTGCCAGTGGCGATAAGTCGTGTCTTACCGGGTTGG
ACTCAAGACGATAGTTACCGGATAAGGCGCAGCGGTCGGGCTGAACGGGGGGTTCGTGCACACAGCCCAGCTTGGAGCGAACGAC
CTACACCGAACTGAGATACCTACAGCGTGAGCTATGAGAAAGCGCCACGCTTCCCGAAGGGAGAAAGGCGGACAGGTATCCGGTA
AGCGGCAGGGTCGGAACAGGAGAGCGCACGAGGGAGCTTCCAGGGGGAAACGCCTGGTATCTTTATAGTCCTGTCGGGTTTCGCC
ACCTCTGACTTGAGCGTCGATTTTTGTGATGCTCGTCAGGGGGGCGGAGCCTATGGAAAAACGCCAGCAACGCGGCCTTTTTACG
GTTCCTGGCCTTTTGCTGGCCTTTTGCTCACATGTTCTTTCCTGCGTTATCCCCTGATTCTGTGGATAACCGTATTACCGCCTTT
GAGTGAGCTGATACCGCTCGCCGCAGCCGAACGACCGAGCGCAGCGAGTCAGTGAGCGAGGAAGCGGAAGAGCGCCCAATACGCA
AACCGCCTCTCCCCGCGCGTTGGCCGATTCATTAATGCAGCTGGCACGACAGGTTTCCCGACTGGAAAGCGGGCAGTGAGCGCAA
CGCAATTAATGTGAGTTAGCTCACTCATTAGGCACCCCAGGCTTTACACTTTATGCTTCCGGCTCGTATGTTGTGTGGAATTGTG
AGCGGATAACAATTTCACACAGGAAACAGCTATGACCATGATTACGCCAAGCTTGTTGTAAAACGACGGCCAGTggattcc

Sequence of SoxB3 reporter line vector. Purple – SoxB3 promoter, Green – GFP, Orange – SoxB3 terminator, Black – pBluescript backbone, Blue – B-lactamase-AMPr.

CATCTAAGAAGAAGGAAGTTTACGCCTACTGTTTTATTTTCTTGAAAGGGCTGTAATATCACTCCTGCGATTTTTAAATAAGTAT
AATTATTTACAATAACTTTGTCGTGATTTTCTTATAAGATTTGTACAAAAATTCTACCAAGTCCTTTACCAAGGCGATGCGCGAT
TCTCCGATACTGCTTGCATGCAGTGCATGTGCAATGCATTATTGTCTATATGCTATTCTACATTTAAAAATGCACGGTACTGGGC
TCATTGCGATCTTGATTATATTTTAACACAGAAAACCACCTGTATGTAAATCTGAATTACGAGTCCGATTTCCTTGATGTGGATG
AACTTCCACCGAATATTATGCTTGAAGGTGAACGCGTGTAAATAAGTAGGCTAAGTCGATTCATTTTTTTAGGAAATATGCCAAA
TATACTAAAACAAACTTCATAAAGCTTAGAAATAAATTCCGAGAAAGGACAATATATATTTTATCGTGATTTTCTGATAACATTT
GTATATTTAGGGAGAGCTAAAAAAACAGCCAAAAAATAGAATGAGTTCTACGCATGATTTCGTATCTAAAAAAATTAATCACAAA
ATGAAGGCTCGTGTGGTTGTTATTACTTTTGTGTTGTAGAATGCGAAAAATTGAGTACCTGCCAAGATTAACGTACGTAATTCCA
AATTTTTATTAGTTAGCGCTCGTAGGGAAGCTTTCTTTGTCAAGAATCTATTTTCATTTATATTCGAAGTTTGCATAAAGGAAAC
TGCGAATGATTGTTTTCGAATAGAAATTTTGTTGTTCTGCTGTGTTCGCTCAGTTTAATCATGATTATTTTAGTGAATAGTTGAA
GTTTGGTGGTTGTATAAATATGTGAAAGCTTGAATGGGTTTGAATACAATAGAATGATTTGATGAATACAGCGTACCTGACGGGT
AGTTGAATATCTCAATACAACCACCAACAATGCTTCTATTCACAATGAGCAGTTATGAATGAAGGCTTTTATTTATTGTATTGTT
ATTTAAACAATAGGCTAACAATATAAAAAGGTTTAACAATAGGTAGCTAGTGAATTTTGCGAGTTTTAAAAACGAGTATTGAATA
GAAAAAACATTATTTCTGCGTCGGTTTTATGTGAGCAAAGCAATTTGGTTAGCAAGCATTGATCGGTGACCAGGTAAGTCAAACT
TCCATTTTTTTCTTTGCTACTGTTTATGTTGTAATAATTTGTTGTTGTTTCGTTCTGTAGTACAAAAGCACAACATGTTATTAGT
CAATACAAAACACAAAAAAGCTAACTTAGCACAAAAGATTGTTTTTCGAAAGCTTTTTTCACCCATTTTTAAAATGTTGACCTTC
GCTTTTGTTATTTAAGCTGTCGGCTCTTTCCATAACAAAAGCTTAATATTGAAATCTGACAGCTAGATAAAGATTTTGTTGTCTT
TTAACGGTGCTTTTAAAATTAAATTTATTTTTTACTGTATATTATTATGATCAGTAAGTACGGCAAAACAAATTGAAATTTGAGG
TAAGACTCCTACAGTCGACACACACGACTTTTTTTCTCACCAAGTTACATTTCACATCGTGCGTTCTTTTCACGTGGTGGTAAAA
CTATGCCGATTTTATTTTTTGTGCATATTCGGCATTGTTAAACAACATGGTAGATTAGCTTTGATTTATGTTAACTTTTTTATTT
TATTATTTGAGTCATAGTACGGTTGACTTTTTTTTCACTCATTTTATATTCATTTAAAATGTCTTTGTCTTTAATGTACTTCGCT
ATTATTCTACTCTGTTGTTATTCTAATCCTGAGGTTAATAAATACTTCCCATCACAATAGAAAAGACTCAATCCTATTTAAATCC
AAACTCAGTATTGTGCTATTATTTGTCTTTGTTTTACTTTGTTTATCGTTGACTAAGATTTACTGTGGATTTATAACAACTTTTT
TCACCTATTACTACTCTACAAGCTGCGTTGATCACATTTATATTTAGACATTGCAATAAATTGTATAGTGCACGACATACTGTCG
TGCGGGTTTTATTTCTGCTGAATTTTCTGTACTGTTGTCCTTTCTCTTATTGCTCATATTAAATTTTATTCCTGTAGCAAAAAGG
ACAAGA**ATGAGTAAAGGAG**AAGAACTTTTCACTGGAGTTGTCCCAATTCTTGTTGAATTAGATGGTGATGTTAATGGGCACAAAT
TTTCTGTCAGTGGAGAGGGTGAAGGTGATGCAACATACGGAAAACTTACCCTTAAATTTATTTGCACTACTGGAAAACTACCTGT
TCCATGGCCAACACTTGTCACTACTTTCTGTTATGGTGTTCAATGCTTTTCAAGATACCCAGATCATATGAAACGGCATGACTTT
TTCAAGAGTGCCATGCCCGAAGGTTATGTACAGGAAAGAACTATATTTTTCAAAGATGACGGGAACTACAAGACACGTGCTGAAG
TCAAGTTTGAAGGTGATACCCTTGTTAATAGAATCGAGTTAAAAGGTATTGATTTTAAAGAAGATGGAAACATTCTTGGACACAA
ATTGGAATACAACTATAACTCACACAATGTATACATCATGGCAGACAAACAAAAGAATGGAATCAAAGTTAACTTCAAAATTAGA
CACAACATTGAAGATGGAAGCGTTCAACTAGCAGACCATTATCAACAAAATACTCCAATTGGCGATGGCCCTGTCCTTTTACCAG
ACAACCATTACCTGTCCACACAATCTGCCCTTTCGAAAGATCCCAACGAAAAGAGAGACCACATGGTCCTTCTTGAGTTTGTAAC
AGCTGCTGGGATTACACATGGCATGGATGAACTATACAAATAGCGATTTTGAAAGTAAACTTTGTTAATGTGGTGTAAATATTTC
GTTTGTGTAAATGACAGGATCTATCATAAAACTAATTTGGCCCTTCTTATACCAGGCTTCTACAGCCAACTTCTTTATTCTTATA
CTAGACTTCTGCAGCCTAGTGGTAGAGCGTTCGCTTACAGTGCGGGAGCTTTTGGGTTCAAACCCCGGTCGAGCCATGCCAGAGA
CTATAAAAGTGTGATTCTATCCTTCTGCTTAGCGTTCAGCATGAGAATAGGATTGGTATCTACGGTTGTCTAGTTGAGGCATTGC
TGTACTGTACACGACTTTGGTAGCTTAAGTGGGTTAAATGCACTAGGACCTCCTTCGCAGGACCCTTTGTTAGCAGTACCAATAG
GAACTGAAAAGGCTATTCTGGGTAAACAAATTTCAATAATAATAATAATAATAATAATAATCCCGTTATCCACATTCAATAGAGC
TGGCGTGTCGTTGCTGACACCATCGATATATTTAAGTAAAATATTTTACTTGTCGCTTTATGACTAAGTGAACTTTGCTAATTTA
CTGGTTACCGTTAAAATTGTTACTAGTTGTGCTCTTTTTCCAAAGATTTCTTTTATGACGTATTTTTTTGTGCCGTAGAATTACT
TTTTTCGGGACACGAAATAATAAATTTTCGAGTTTTAATATCTCTCAGGTGAGAAAAGTTCAGAAGAGCGTCAGTCACTCATCAT
TTTCTTAACAATTGTTGTGTGGCAATAAACATTGGTCAATATTCTGTTTCCTATGTGATGATTTTCTTTTGTCGTGGATTTCGTT
TTGCGTTGTGACACTTGAAGGTTAGGACTCTTTTTAAGAGAAAAAAAAATTTAGCCGATCTTCCGACCACCTTTTAACCGATAAA
TTACCATGACAACAGACGTGATGTCACACCAAAAATATTCCGACTAACCCGAAGCTAACTAATGATGAAAAGTCAAAAATTTCAA
TAAAGCCCCTACTCTTCGGCCCGAATAGTACAGAAGCCGAACAGGGTCAAACCTGATTTATTTCA**CGTACGGGCCCTTTCGTCTC**
GCGCGTTTCGGTGATGACGGTGAAAACCTCTGACACATGCAGCTCCCGGAGACGGTCACAGCTTGTCTGTAAGCGGATGCCGGGA
GCAGACAAGCCCGTCAGGGCGCGTCAGCGGGTGTTGGCGGGTGTCGGGGCTGGCTTAACTATGCGGCATCAGAGCAGATTGTACT
GAGAGTGCACCATATGCGGTGTGAAATACCGCACAGATGCGTAAGGAGAAAATACCGCATCAGGCGGCCTTAAGGGCCTCGTGAT
ACGCCTATTTTTATAGGTTAATGTCATGATAATAATGGTTTCTTAGACGTCAGGTGGCACTTTTCGGGGAAATGTGCGCGGAACC
CCTATTTGTTTATTTTTCTAAATACATTCAAATATGTATCCGCTCATGAGACAATAACCCTGATAAATGCTTCAATAATATTGAA
AAAGGAAGAGTATGAGTATTCAACATTTCCGTGTCGCCCTTATTCCCTTTTTTGCGGCATTTTGCCTTCCTGTTTTTGCTCACCC
AGAAACGCTGGTGAAAGTAAAAGATGCTGAAGATCAGTTGGGTGCACGAGTGGGTTACATCGAACTGGATCTCAACAGCGGTAAG
ATCCTTGAGAGTTTTCGCCCCGAAGAACGTTTTCCAATGATGAGCACTTTTAAAGTTCTGCTATGTGGCGCGGTATTATCCCGTA
TTGACGCCGGGCAAGAGCAACTCGGTCGCCGCATACACTATTCTCAGAATGACTTGGTTGAGTACTCACCAGTCACAGAAAAGCA
TCTTACGGATGGCATGACAGTAAGAGAATTATGCAGTGCTGCCATAACCATGAGTGATAACACTGCGGCCAACTTACTTCTGACA
ACGATCGGAGGACCGAAGGAGCTAACCGCTTTTTTGCACAACATGGGGGATCATGTAACTCGCCTTGATCGTTGGGAACCGGAGC
TGAATGAAGCCATACCAAACGACGAGCGTGACACCACGATGCCTGTAGCAATGGCAACAACGTTGCGCAAACTATTAACTGGCGA
ACTACTTACTCTAGCTTCCCGGCAACAATTAATAGACTGGATGGAGGCGGATAAAGTTGCAGGACCACTTCTGCGCTCGGCCCTT
CCGGCTGGCTGGTTTATTGCTGATAAATCTGGAGCCGGTGAGCGTGGGTCTCGCGGTATCATTGCAGCACTGGGGCCAGATGGTA
AGCCCTCCCGTATCGTAGTTATCTACACGACGGGGAGTCAGGCAACTATGGATGAACGAAATAGACAGATCGCTGAGATAGGTGC
CTCACTGATTAAGCATTGGTAA**CTGTCAGACCAAGTTTACTCATATATACTTTAGATTGATTTAAAACTTCATTTTTAATTTAAA**

AGGATCTAGGTGAAGATCCTTTTTGATAATCTCATGACCAAAATCCCTTAACGTGAGTTTTCGTTCCACTGAGCGTCAGACCCCG
TAGAAAAGATCAAAGGATCTTCTTGAGATCCTTTTTTTTCTGCGCGTAATCTGCTGCTTGCAAACAAAAAAACCACCGCTACCAGC
GGTGGTTTGTTTGCCGGATCAAGAGCTACCAACTCTTTTTCCGAAGGTAACTGGCTTCAGCAGAGCGCAGATACCAAATACTGTC
CTTCTAGTGTAGCCGTAGTTAGGCCACCACTTCAAGAACTCTGTAGCACCGCCTACATACCTCGCTCTGCTAATCCTGTTACCAG
TGGCTGCTGCCAGTGGCGATAAGTCGTGTCTTACCGGGTTGGACTCAAGACGATAGTTACCGGATAAGGCGCAGCGGTCGGGCTG
AACGGGGGGTTCGTGCACACAGCCCAGCTTGGAGCGAACGACCTACACCGAACTGAGATACCTACAGCGTGAGCTATGAGAAAGC
GCCACGCTTCCCGAAGGGAGAAAGGCGGACAGGTATCCGGTAAGCGGCAGGGTCGGAACAGGAGAGCGCACGAGGGAGCTTCCAG
GGGGAAACGCCTGGTATCTTTATAGTCCTGTCGGGTTTCGCCACCTCTGACTTGAGCGTCGATTTTTGTGATGCTCGTCAGGGGG
GCGGAGCCTATGGAAAAACGCCAGCAACGCGGCCTTTTTACGGTTCCTGGCCTTTTGCTGGCCTTTTGCTCACATGTTCTTTCCT
GCGTTATCCCCTGATTCTGTGGATAACCGTATTACCGCCTTTGAGTGAGCTGATACCGCTCGCCGCAGCCGAACGACCGAGCGCA
GCGAGTCAGTGAGCGAGGAAGCGGAAGAGCGCCCAATACGCAAACCGCCTCTCCCCGCGCGTTGGCCGATTCATTAATGCAGCTG
GCACGACAGGTTTCCCGACTGGAAAGCGGGCAGTGAGCGCAACGCAATTAATGTGAGTTAGCTCACTCATTAGGCACCCCAGGCT
TTACACTTTATGCTTCCGGCTCGTATGTTGTGTGGAATTGTGAGCGGATAACAATTTCACACAGGAAACAGCTATGACCATGATT
ACGCCAAGCTTGTTGTAAAACGACGGCCAGT

Appendix C

The Differential Analysis gene lists from can be found in the electronic version of the thesis.